Initiation and termination of cAMP signalling in PANC-1 cells: interplay between cAMP and Ca^{2+} signalling cascades.

Thesis submitted in accordance with the requirements of the University of Liverpool for the degree of Doctor in Philosophy

By

Tony Parker

January, 2015

TABLE OF CONTENTS

Abstract

Pancreatic ductal adenocarcinoma (PDAC) is noted for its resistance to therapy and poor prognosis. PDAC is characterised by extensive local invasion and metastases at distant organs. Having previously shown that the cAMP cascade had regulatory effects on cell migration/invasion in PDAC cells, which are vital processes in metastasis formation, we decided to characterise the cAMP signalling machinery in PANC-1 cells. In this study we adopted a live-cell imaging approach taking advantage of genetically engineered probes that use Förster resonance energy transfer (FRET) to reveal cAMP concentration and PKA activity at a single cell level. Using the Epac-based cAMP sensor H134 we found that PDE3 and PDE4 are the principal cAMP destroyers, whereas β-adrenoceptors are the main physiological cAMP-cascade activators, in PANC-1 cells. Downstream, using Boyden chamber assays we found that PDE3 has the biggest role in cell migration under 'basal' conditions, whereas PDE4 has a bigger role in the presence of isoproterenol. However, isoproterenol on its own did not influence PANC-1 cell migration despite having the ability to increase cAMP concentration inside the cell. This part of the study puts forward PDE3 and PDE4 as potential targets for reducing migration/invasion of PDAC. In the second part of the study, we found that these cells have an efficient Ca^{2+} signalling system; in which ORAI1 is the main mediator of store-operated Ca^{2+} entry (SOCE) in PANC-1 cells. To explore the possibility of a Ca^{2+}-cAMP crosstalk in PANC-1 cells, we used the AKAR4 probe to measure PKA activity during Ca^{2+} responses. The application of neurotensin (NT), a well-known IP_3-producing agonist in this cell type, induced a Ca^{2+} response which was accompanied by an increase in PKA activity. SOCE is likely to play an important role in this process since the activation of SOCE by thapsigargin-mediated store depletion consistently and robustly increased PKA activity. To further investigate the downstream roles of PKA signalling in PANC-1 cells we utilised immunofluorescence to visualise the distribution of PKA activity. Using antibodies specific for phosphorylated PKA substrates, we found that phosphorylated PKA substrates are preferentially concentrated in the nucleus; and notably at the leading edges of PANC-1 cells displaying a migratory phenotype. At the leading edges phosphorylated PKA substrates colocalised with actin-rich ruffles. Interestingly, utilising the rapamycin-inducible heterodimerisation system to reveal endogenous ER-PM junctions in migrating PANC-1 cells, we found that ER-PM junctions are also situated in close proximity to the leading edge. These results suggest that SOCE activates PKA responses in the region strategically important for PDAC cell migration.

Acknowledgements

First and foremost I would like to thank Alexei Tepikin for his contant support and guidance throughout the development of my PhD project, and especially for his patience with me in the numerous times in which my experiments were not working. I have greatly enjoyed the environment and the self-motivating atmosphere that he created during my time here, and facilitated my improvement as a junior scientist.

Further I would like to thank my secondary supervisors Eithne Costello, David Criddle and Robert Sutton for their invaluable ideas that helped shape my project.

I would also like to show my gratitude to Emmanuel Okeke, Alex Burdyga, Hayley Dingsdale, Misha Chvanov and Svetlana Voronina and the rest of Blue Block for providing me with their expertise on biochemical and microscopic techniques.

I'm eternally grateful to external collaborators Kees Jalink, Manuela Zaccolo and Jin Zhang for generously providing me with the genetically encoded cAMP and PKA constructs, without which my project would never succeed.

Finally I would like to thank all my friends, especially those who came to this department the same year as I did: Amos Liang, Anna Newylacyl, and Nicole Cash for sharing my pain during the rough patches of my project.

This project was funded by the Wellcome Trust.

Abbreviations

2-APB	2-Aminoethoxydiphenyl borate
8-mm-IBMX	8-methoxymethyl-3-isobutyl-1-methylxanthine
AC	Adenylyl cyclase
ADP	Adenosine diphosphate
AKAP	A-kinase anchoring proteins
AKAR4	A-kinase activity reporter 4
AOBS	Acousto-optical beam splitter
Arp2/3	actin-related proteins 2 and 3
ATP	Adenosine triphosphate
BSA	Bovine serum albumin
Btk	Bruton's tyrosin kinase
CaM	Calmodulin
CaMKII	Calmodulin-dependent kinase II
cAMP	3'-5'-cyclic adenosine monophosphate
CaN	Calcineurin
CARMIL	Capping protein, arp2/3 and myosin I linker
CC	Coiled coil
CDC42	Cell division control protein 42 homolog
CDI	Ca^{2+}-dependent inactivation
CFP	Cyan fluorescent protein
cGMP	Cyclic guanosine monophosphate
CICR	Ca^{2+}-induced Ca^{2+} release
CIN	Chronophin
CIRB	Calmodulin and IP_3R binding
CLZ	Cilostazol
CNB domain	Cyclic-nucleotide binding domain
CNG	Cyclic nucleotide-gated ion channel
CNS	Central nervous system
COX-2	Cyclooxygenase-2
CP	Capping protein
CREB	cAMP response element binding protein
D/D	Docking and dimerisation domain
DAG	Diacylglycerol
DEP domain	Dishevelled, Egl-10, and Pleckstrin domain
DMEM	Dulbecco's modified Eagle medium
DMSO	Dimethyl sulfoxide
ECM	Extracellular matrix
EDTA	Ethylenediaminetetraacetic acid
EGF	Epidermal growth factor
EGFR	Epidermal growth factor receptor
EHNA	erythro-9-(2-hydroxy-3-nonyl)adenine
EMT	Epithelial to mesenchymal transition
ENA/VASP	Vasodilator-stimulated phosphoprotein
EPAC	Exchange protein activated by cAMP

ER	Endoplasmic reticulum
ERK	Extracellular signal-related kinase
ERM	Erzin-moesin-radixin domain
FAK	Focal adhesion kinase
FBS	Foetal bovine serum
FKBP	FK506 binding protein
FRET	Forster resonance energy transfer
FRB	FKBP-rapamycin binding domain of FKBP-rapamycin-associated protein
GABA	γ-Aminobutyric acid
GAF domain	cGMP-specific phosphodiesterases, adenylyl cyclases and FhlA domain
GAP	GTPase activating protein
Gd	Gadolinium
GDP	Guanosine diphosphate
GEF	Guanine nucleotide-exchange factor
GFP	Green fluorescent protein
GLP	Glucagon-like peptide
GPCR	G-protein coupled receptor
GTP	Guanosine triphosphate
HCN	Hyperpolarization-activated cyclic nucleotide-gated (HCN) channels
HDAC	Histone deacetylase
HEK293	Human embryonic kidney 293 cells
HEPES	4-(2-Hydroxyethyl)piperazine-1-ethanesulfonic acid
IBMX	3-isobutyl-1-methylxanthine
IGF	Insulin-like growth factor
IKK-β	Inhibitor of nuclear factor kappa-B kinase subunit-β
ILK	Integrin-linked Kinase
IP_3	inositol 1,4,5-trisphosphate
JMY	Junction-mediating and regulatory protein
KO	Knock out
KRAS	V-Ki-ras2 Kirsten rat sarcoma viral oncogene homolog
LIM kinase	Lin11, Isl-1 and Mec-3 kinase
LPA	Lysophosphatidic acid
LSCM	Laser scanning confocal microscope
mDia	Mammalian diaphanous
MEK	MAPK/ERK kinase
MEKK	MAPK/ERK kinase kinase
MLC	Myosin light chain
MLCK	Myosin light chain kinase
MLCP	Myosin light chain phosphatase
MMP	Matrix metalloproteinase
mRFP	Monomer red fluorescent protein
mTOR	Mammalian target of rapamycin
NA	Numerical aperture
NCKX	Na^+/Ca^{2+}-K^+ exchangers
NCX	Na^+-Ca^{2+} exchanger
NFAT	Nuclear factor of activated T-cells

NF-kB	Nuclear factor kappa-light-chain-enhancer of activated B cells
NGF	Nerve growth factor
NHERF	Na^+/H^+ Exchanger Regulatory Factor
Nrf2	Nuclear factor (erythroid-derived 2)-like 2
NT	Neuortensin
PAK	P21-activated kinase
PanIN	Pancreatic intraepithelial neoplasia
PAS domain	Per-Arnt-Sim domain
PBS	Phosphate buffered saline
PDAC	Pancreatic ductal adenocarcinoma
PDE	Phosphodiesterase
PI3K	Phosphatidylinositol-4,5-bisphosphate 3-kinase
PIP_2	Phosphatidylinositol 4,5-bisphosphate
PIX	PAK-interacting exchange factor
PKA	Protein kinase A
PKB	Protein kinase B
PKC	Protein kinase C
PKG	Protein kinase G
PLC	Phospholipase C
PLD	Phospholipase D
PM	Plasma membrane
PMCA	Plasme membrane Ca^{2+} ATPase
PP2A	Protein phosphatase 2A
PSG	Penicillin-Streptomycin-Glutamine
Rac	Ras-related C3 botulinum toxin substrate
REC domain	CheY-like phosphoacceptor (or receiver) domain
RGS	Regulators of G-protein signalling
RhoGDI	Rho GDP-dissociation factor
ROCK	Rho-associated kinase
ROS	Reactive oxygen species
RTK	Receptor tyrosine kinase
RyR	Ryanodine receptor
sAC	Soluble adenylyl cyclase
SAM	Sterile-α-motif
SERCA	Sarcoplasmic/Endoplasmic reticulum Ca^{2+} ATPase
SHIP2	Phosphatidylinositol-3,4,5-trisphosphate 5-phosphatase
SOAR	STIM-ORAI activating region
SOCE	Store-operated Ca^{2+} entry
SSH1	Slingshot
STIM1	Stromal interaction molecule 1
TG	Thapsigargin
TGFβ	Transforming growth factor β
TM	Transmembrane
TRPC	Canonical transient receptor potential channels
UCR	Upstream conserved region

VEGF	Vascular endothelial growth factor
VGCC	Voltage-gated Ca^{2+} channels
VIP	Vasoactive intestinal peptide
VSMC	Vascular smooth muscle cell
WASP	Wiskott-Aldrich syndrome protein
WAVE	WASP family verprolin homologous protein
YFP	Yellow fluorescent protein
β-AR	β-adrenergic receptor

Chapter 1 – Introduction

Chapter 1: Introduction

1.1. Pancreatic ductal adenocarcinoma (PDAC)

Pancreatic ductal adenocarcinoma is the cancer of the exocrine pancreas, representing 95% of all pancreatic cancers (the other being insulinoma, cancer of the endocrine pancreas). The development process from the exocrine pancreas into PDAC is complex, but a few critical stages are known. The first critical stage is the activating mutation of the Kras protein (G12D), resulting in a constitutively active KRAS pathway (Shi et al., 2013, Kruger et al., 2014). This likely provides a driving force for the creation of a series of lesions, known as pancreatic intraepithelial neoplasia (PanINs1-3, graded by the severity of the lesions) (Maitra et al., 2005, Hruban et al., 2001, Kopp et al., 2012); and the mutated cells in the lesions start to remodel its surrounding environment, especially the stroma (Pylayeva-Gupta et al., 2012, Chu et al., 2007). Moreover, EGF has also been shown to accelerate the PanIN1-3 → PDAC progression parallel and independent of Kras signalling; implying that EGFR signalling is also involved (Navas et al., 2012). The second stage is the loss of the tumour suppressor gene p16, also early in the PanIN development either by promoter deletion or homozygous deletion (Deer et al., 2010, Cowgill and Muscarella, 2003). As the lesions amplify, they are also reported to extensively remodel their stroma and induce an inflammatory, immunosuppressive environment to avoid detection from the immune system (Pylayeva-Gupta et al., 2012). The final critical stage appears to be the loss of the tumour suppressor gene TP53, occurring in the final stages of the transformation from PanIN into PDAC (Moore et al., 2003). The loss of another tumour suppressor SMAD4 is also commonly reported in about 50% of invasive PDACs (Deer et al., 2010, Kruger et al., 2014).

It was traditionally assumed that PDAC is derived from pancreatic ductal epithelial cells. However, recently evidence is accumulating suggesting that this cancer may instead arise from differentiated acinar cells being 'forced' into a more ductal-like phenotype in a Kras-dependent manner, in a process known as acinar-ductal metaplasia (Shi et al., 2013, Kopp et al., 2012). Nevertheless, ambiguity remains on the origin of PDAC and more study is required.

Statistically PDAC is currently the 5th most common cause of cancer-related deaths in the UK and 4th in the USA, but has the worst survival rate of all cancers; with a median survival period of just 6 months and a 97% mortality rate within 5 years (Pylayeva-Gupta et al., 2012, Kern et al., 2011, Maitra and Hruban, 2008). This is mainly due to the disease being asymptomatic until presentation, by which point the cancer had already reached an advanced stage, making this cancer resistant to chemotherapy (Schuller and Al-Wadei, 2010). The best possible treatment for this disease, pancreatectomy, is still relatively ineffective due to the aggressive and invasive nature of PDAC (Rissel et al., 2003). Like many other cancers, the main cause of death from PDAC is metastatic disease, and advanced stage PDAC clinically forms extensive secondary tumours; especially in the liver, lymphatic system and central nervous system (Rhim et al., 2012, Delcore et al., 1996). Therefore, information on the intracellular signalling pathways that contribute to their aggressive physiology is urgently needed to help reduce the mortality rate.

1.2. G-protein coupled receptors (GPCR) system

The GPCR is a massive family of seven-pass membrane receptors for first messengers, consisting of over 1000 different types and their genes comprises 1% of the genome

(Hermans, 2003). There are 3 different groups of GPCRs – Group A, consisting of receptors for classical neurotransmitters, prostaglandins, odour and rhodopsin; group B, including receptors for most hormones; and group C, which contains receptors for glutamate, GABA and Ca^{2+} ions (Wess, 1998). The GPCR complex is composed of four components: the receptor, which contains 7 transmembrane domains with the intracellular loops forming the GTP and GDP binding domain, hence its name (Kobilka, 2007). There, the receptor is coupled to a heterotrimeric G protein consisting of the Gα subunit and a Gβγ dimer (Neves et al., 2002, Hamm, 1998).

There are 16 different genes encoding for Gα, 5 for Gβ and 12 for Gγ (Hamm, 1998, Neves et al., 2002, Cabrera-Vera et al., 2003); which contributes to the diversity of this receptor type and subsequent function. Gα is a GTPase that is structurally not dissimilar to the cytosolic small G-proteins like Ras and Rac (Cabrera-Vera et al., 2003). It contains a GTPase region, which mediates the hydrolysis of GTP into GDP; and a helical domain, important for keeping GTP in its binding pocket (Cabrera-Vera et al., 2003, Hamm, 1998). Gβ consists of a 7-blade β-propeller, and complexes strongly with the Gγ subunit via the coiled coil domain in the latter, and then all along the base of the Gβ-subunit (Cabrera-Vera et al., 2003, Hamm, 1998). When the receptor is inactive, Gα is bound with GDP and is locked together with Gβγ; on ligand binding, a conformational change ensues in Gα causing an exchange of GTP for GDP and its resultant dissociation from the Gβγ subunits (Sprang, 1997, Hamm, 1998, Cabrera-Vera et al., 2003).

Unbound Gα-GTP can mediate a wide range of functions in different cells. There are 4 main classes of Gα subunits grouped by the homology of their amino acid sequences (Suzuki et

al., 2009): Gαs, Gαi/o, Gαq/11, and Gα12/13, each further divided into subclasses (Cabrera-Vera et al., 2003, Hermans, 2003, Neves et al., 2002) and carry out unique downstream effects. Gαs is possibly the best characterised subunit of this family, and it activates all membrane isoforms of adenylyl cyclases (AC) to produce cAMP in cells (Neves et al., 2002), of which β_2-adrenergic receptors in cardiomyocytes (Mongillo and Zaccolo, 2006) and glucagon-like peptide (GLP) receptors in pancreatic β-cells (Tian et al., 2011a) are the best examples. Gαi, although initially found as the adenylyl cyclase inhibiting subunit (e.g. calcium sensing receptors and groups II and III metabotropic glutamate receptors in the brain) (Riccardi and Kemp, 2012, Moussawi and Kalivas, 2010, Neves et al., 2002), understanding in its roles has since diversified into the regulation of Ca^{2+} and K^+ (also called Gαz) (Jeong and Ikeda, 1998) and the activation of PDE6 (transducin, Gαt) (Stryer, 1983) to name a few. Gαq is classically known to be PLCβ activators to trigger the IP_3 signalling pathway; examples include the cholecystokinin receptor in pancreatic acinar cells (Murphy et al., 2008). The functions of Gα12/13, compared to others, is still not completely understood (Neves et al., 2002). Examples of this receptor type includes the thrombin and LPA receptor, and there is accumulating evidence that p115RhoGEF can be activated by this Gα subtype, resulting in the induction of the RhoA signalling cascade (Suzuki et al., 2009). The importance of Gα12/13 is the observation that Gα13 KO mice is embryonically lethal (Offermanns et al., 1997, Suzuki et al., 2009). Finally, it is important to mention here that crosstalk exists between the receptors coupled with different classes of Gα subunits; converging their signalling onto the same intracellular target; with the convergence of Gαq and Gα12/13 onto Rho being one such example (Hermans, 2003, Gu et al., 2002, Suzuki et al., 2009). Conversely, in many cases the receptor-Gα coupling is not rigid; meaning that a single GPCR can couple to multiple Gα isoforms in the same cell. For example, in the heart

β2-adrenergic receptors, mentioned above to conventionally couple to Gαs, was found to also couple to the AC- inhibitory Gαi/o subunits (Kilts et al., 2000). Furthermore, in the rat gonadotroph, gonadotrophin-releasing hormone (GnRH) receptors was found to couple with Gαq, Gαi and Gαs (Stanislaus et al., 1998)

Independent of Gα, the Gβγ subunit can also activate signalling pathways by the virtue that it interacts with a wide range of proteins (Hermans, 2003, Cabrera-Vera et al., 2003). One of the more established functions of the Gβγ subunit is the activation of phospholipase Cβ (PLCβ), phospholipase D (PLD), Bruton's tyrosine kinase (Btk). Additionally, the Gβγ subunit has been known to modulate the activity of ACs (Khan et al., 2013, Cabrera-Vera et al., 2003); as it has been known to further potentiate the actions of the Gαs subunit on ACII, IV and VII, but inhibit that of ACI (Willoughby and Cooper, 2007). Hence, it is possible that after activation of a single GPCR, Gα and Gβγ can each deliver independent downstream signals; such as the inhibition of AC by Gαi/o and activation of PLC by Gβγ (Hermans, 2003).

When GPCR signalling is no longer required it is turned off by the hydrolysis of GTP in the Gα-subunit, resulting in the re-stabilisation of interactions with the Gβγ subunit (Cabrera-Vera et al., 2003, Hamm, 1998). This process can be accelerated by GTPase activating proteins (GAPs) such as regulators of G-protein signalling (RGS) proteins (Suzuki et al., 2009). In addition, chronic GPCR activation also results in β-arrestin mediated endocytosis of the receptors, resulting in its sequestration into the cell where they are mostly degraded; but evidence exists that they can carry on signalling in vesicles deep inside the cell (Irannejad and von Zastrow, 2014).

1.3. The Ca^{2+} signalling system

In a typical mammalian system the intracellular concentration of free Ca^{2+} ($[Ca^{2+}]_{cyt}$) is kept at approximately 100nM in the cytosol, whereas in the extracellular fluid it stands at about 5mM (Clapham, 2007). This creates a massive concentration gradient across the plasma membrane. Cells have taken advantage of this gradient to create specialised channels to allow Ca^{2+} entry into the cytosol at appropriate moments. Due to the steep gradient, Ca^{2+} will rush into the cell almost immediately upon channel opening, increasing $[Ca^{2+}]_{cyt}$ by around 10 fold (Clapham, 2007). High $[Ca^{2+}]_{cyt}$ is toxic to the cell, so intracellular Ca^{2+} homeostasis has to be tightly controlled by efficient Ca^{2+} extruding mechanisms, namely Ca^{2+} pumps and Na^{+}/Ca^{2+} exchangers at the plasma membrane to prevent the overload of this ion in physiological conditions (Kass and Orrenius, 1999, Nicotera et al., 1992, Pozzan et al., 1994). More importantly, inside the cell the mitochondria (Williams et al., 2013) and endoplasmic reticulum (ER) require elevated $[Ca^{2+}]$ for effective function, with $[Ca^{2+}]_{ER}$ at approximately 400µM (Samtleben et al., 2013, LaFerla, 2002); so they act as intracellular Ca^{2+} stores. Therefore, cells have also evolved channels and pumps onto these organelles to maintain their own $[Ca^{2+}]$ and modulate $[Ca^{2+}]_{cyt}$. This flux of Ca^{2+} into and out of cytosol from outside the cell and intracellular stores forms the basis of Ca^{2+} signalling in cells (Clapham, 2007).

There are two types of cellular Ca^{2+} signalling: signalling in excitable and non-excitable cells. Excitable cells are cells that base their Ca^{2+} signalling on the charge difference across the plasma membrane (also known as the membrane potential). Ca^{2+} entry into excitable cells is mediated by voltage-sensitive channels on the PM such as the L-type Ca^{2+} channels that open in response to depolarisation. Examples of excitable cells include neurones and

pancreatic β-cells, which couples increases of [Ca^{2+}] to vesiclular fusion and excretion of first messengers (Idevall-Hagren et al., 2010, Braun et al., 2008). Non-excitable cells, on the other hand, rely on the mobilisation of intracellular Ca^{2+} stores, predominantly from the ER, in response to extracellular first messengers followed by second messenger signalling (Van Den Brink et al., 1999). Examples of non-excitable cells include most epithelial cells including exocrine cells from the digestive system such as pancreatic acinar cells.

Focusing on non-excitable cells, activation of the Ca^{2+} signalling cascade involve the binding of first messengers to receptors on the PM, most commonly GPCRs or receptor tyrosine kinases (RTKs) (Pannekoek et al.), resulting in the intracellular activation of phospholipase Cβ (PLCβ) or PLCγ respectively. PLC then cleaves phosphatidylinositol-4, 5-bisphosphate (PIP_2), a component of the PM, into diacylglycerol (DAG) and inositol-3-trisphosphate (IP_3), resulting in the latter being released into the cytosol, where it docks onto its receptor (IP_3 receptors, or IP_3R) on the ER; ending in the release of calcium into the cytosol. IP_3Rs are specialised, six-transmembrane spanning, tetrameric intracellular Ca^{2+} channels on the ER that open on IP_3 binding and allow Ca^{2+} to flow into the cytosol down the gradient (Clapham, 2007, Taylor and Tovey, 2010). In addition, also resident on the ER are ryanodine receptors (RyR), which have the same end-point function as IP_3R but are activated directly by Ca^{2+}, facilitating a process called Ca^{2+}-induced Ca^{2+} release (CICR) (Clapham, 2007).

1.3.1. Store operated calcium entry (SOCE)

In stimulated non-excitable cells, cytosolic Ca^{2+} transients develop as a result of Ca^{2+} release from the ER; meaning that after multiple stimulations, ER Ca^{2+} stores would be cumulatively depleted in the long term, and would render the cell incapable of sustaining medium to

long-term Ca^{2+} signals. Furthermore, chronic Ca^{2+} depletion from the ER impedes its primary function of facilitating protein folding, resulting in ER stress (Rasheva and Domingos, 2009, Austin, 2009). Therefore, cells need mechanisms by which to replenish ER Ca^{2+} stores. This is carried out in a process known as store operated Ca^{2+} entry (SOCE), which causes the influx of Ca^{2+} into the cytosol, where sarcoplasmic/endoplasmic reticulum Ca^{2+} ATPase (SERCA) on the ER membrane pumps 2 Ca^{2+} ions back into the lumen in exchange for 1 molecule of ATP hydrolysed (Clapham, 2007). SOCE is mediated mainly by two components: Stromal interaction molecule on the ER, and ORAI proteins on the PM (Cahalan, 2009). The principal role of SOCE appears to be sustaining long-term Ca^{2+} signalling regulation of gene transcription, as reported in mast and leukaemia cells (Kar et al., 2012). The importance of SOCE is undisputed (the pathophysiological effects of the lack of SOCE are listed in Soboloff et al., 2012), but it is best exemplified in the immune system, where ORAI1 KO mice has impaired adaptive immune responses (Feske et al., 2012).

1.3.1.1. Stromal interaction molecule (STIM)

STIM is a type 1A single span multi-domain membrane protein that mainly populates the ER, although 10% of the molecules also localise to the PM. The N-terminal region of each monomer contains two EF-hand domains, followed by a sterile-α-motif (SAM); and these two domains are resident in the ER lumen (Soboloff et al., 2011). The N-terminus of the cytoplasmic region of STIM immediately after the transmembrane domain are made of 3 coiled-coil (from N-terminal side, CC1, CC2 and CC3) regions formed mainly of α-helices (Soboloff et al., 2012, Cole et al., 2008). The combined CC2 and CC3 regions are also known as the STIM-ORAI activating region (SOAR) (Yuan et al., 2009). After CC3, towards the C-

terminus comes the inhibitory domain (ID) followed by the Pro/Ser rich (PS) domain, before reaching the Lys-rich domain at the C-terminus (Soboloff et al., 2012, Lee et al., 2014). There are 2 different isoforms of STIM - STIM1 and STIM2, with the main difference being the properties of the luminal EF hand. The EF hand of STIM2 (K_d = 400μM) has a half the Ca^{2+} affinity of that in STIM1 (K_d = 200μM) (Soboloff et al., 2012, Fahrner et al., 2013, Fahrner et al., 2009), lowering its SOCE activation threshold and hence activates at higher $[Ca^{2+}]_{ER}$ (Parvez et al., 2008, Zhou et al., 2009). However, STIM2 are poor activators of ORAI channels due to the conformational change in the luminal domain being more sluggish after store depletion (Soboloff et al., 2012, Zhou et al., 2009, Parvez et al., 2008). A recent report suggests STIM2 to have a 'housekeeping' function to maintain a constant basal $[Ca^{2+}]_{ER}$, and is important for maintaining long term Ca^{2+} oscillations to regulate transcription (Kar et al., 2012).

At resting $[Ca^{2+}]_{ER}$, STIM normally exists as a dimer that is distributed throughout the ER (Soboloff et al., 2012). The dimerization interface is proposed to be at the CC regions in the cytoplasmic domain (Muik et al., 2009), where CC1 and the SOAR region from each monomer mutually interact with the former sterically inhibiting the latter (Yang et al., 2012). In the ER lumen, only one N-terminal EF-hand binds Ca^{2+}, which serves as a sensor for this ion; whereas the other remains hidden (Soboloff et al., 2012). After store depletion, Ca^{2+} detaches from the EF-hand, inducing a conformational change in the EF hand and SAM domains in such a way that favours their interaction within the dimer, resulting in the oligomerisation of STIM molecules (Covington et al., 2010, Muik et al., 2009). This clustering of EF-hand and SAM domains between dimers also translates a conformational change into the cytosolic domain, where CC1 would partially unfold into a 'straightened' configuration;

in the process releasing the autoinhibitory mechanism on the SOAR region (Soboloff et al., 2012, Muik et al., 2011). This activated STIM oligomer then proceeds to localise to the PM, where it (SOAR regions of STIM oligomers) interacts with the cytoplasmic coiled-coil domain of ORAI channels to activate SOCE (Calloway et al., 2010). The stoichiometry of a STIM-ORAI complex is reported to be 2 STIM dimers for every ORAI subunit (Hoover and Lewis, 2011, Rothberg et al., 2013). It should be noted here, however, aside from ORAI, the transient receptor potential cation channel (TRPC) family of channels has also been touted to be mediators of SOCE in some cells, though this hypothesis is still debated (Salido et al., 2009, Ramsey et al., 2006). SOCE is turned off by one rapid and one slow process – Ca^{2+}-dependent inactivation (CDI), the rapid phase of inhibition, is caused by the increase of local [Ca^{2+}] in the immediate vicinity of the intracellular side of ORAI, which prevents further Ca^{2+} entry (Zweifach and Lewis, 1995, Derler et al., 2009). CDI is also partly facilitated by calmodulin binding to ID region on the STIM C-terminus (Litjens et al., 2004). The slow phase is the dissociation of STIM clusters from ORAI as Ca^{2+} returns into the EF hand in the ER lumen (Shen et al., 2011).

1.3.1.2. CRAC channels – ORAI subunits

The full structure of the CRAC channel formed by ORAI is still not fully clear, as it has no homology to other Ca^{2+} channels (Fahrner et al., 2013). The conventional view was that the CRAC channel is a tetrameric structure, due to an overwhelming amount of evidence stockpiled. However, a recent crystallographic structure of a drosophila ORAI channel shows that the subunits of ORAI actually arrange themselves into a hexameric configuration around the pore, formed by three pairs of dimers, potentially making it a hexamer (Hou et al., 2012). Thankfully, more is known about the key structural elements of the ORAI

subunits. Each subunit contain 4 transmembrane domains (from the N-terminal, termed M1, M2, M3 and M4), with both termini in the cytoplasm (Fahrner et al., 2013, Fahrner et al., 2009). M1 of each subunit contributes to the pore, with both M1 and M4 containing extensions that protrude into the cytoplasm. The N-terminus contains proline/arginine rich regions and a polybasic motif, whereas the C-terminus contains a basic coiled-coil domain (Fahrner et al., 2009). The pore is impermeable to monovalent ions when other divalent ions are present, but is very selective for Ca^{2+} ions (Rothberg et al., 2013); this is mainly due to a ring of glutamate residues on the pore entrance, which acts as an ion filter. Beyond the entrance, the pore cavity is relatively hydrophobic, with the intracellular portion being positively charged contributed by the M1 extension, which may act as an electrostatic barrier at rest (Rothberg et al., 2013, McNally et al., 2012). At resting conditions, ORAI1 display very low conductance, requiring millimolar concentrations of the ion for entry and only increasing on contact with STIM clusters (Hoth and Penner, 1993). This corresponds well to its physiological function as it makes sure that no Ca^{2+} enters the cell before STIM is activated.

The electrophysiological property of this channel is defined by the small, inwardly rectifying current, termed I_{CRAC}, it occurs following store depletion (Hoth and Penner, 1992). The exact manner in which STIM1 binds ORAI is still to be fully elucidated. However, there is substantial evidence that the CC2 basic region of the STIM SOAR domain interacts with the acidic C-terminal cytoplasmic tail of ORAI via electrostatic interactions (Park et al., 2009, Frischauf et al., 2008, Soboloff et al., 2012). STIM1 also interacts weakly with the N-terminal region of ORAI, thereby forming a bridge between the N and C-terminal ends (Frischauf et al., 2008, Soboloff et al., 2012, Park et al., 2009). A recent model suggests that STIM1

activates ORAI1 by widening the pore, thereby removing the electrostatic barrier formed by the M1 helices to allow full Ca^{2+} entry (Rothberg et al., 2013). This arrangement is further stabilised by the interaction between the STIM1 C-terminal Lys-rich motif and the plasma membrane, though it is not essential (Park et al., 2009).

There are 3 different isoforms of ORAI - 1-3, with ORAI2 and 3 lacking the proline/arginine rich motifs on the N-terminus but carrying a more stable and extensive coiled-coil region than ORAI1 (Fahrner et al., 2013). All three isoforms exhibit the same functions in that they all bind STIM1 to mediate SOCE, but have different activation/inhibition, expression and pharmacological profiles (Fahrner et al., 2009, Lis et al., 2007, DeHaven et al., 2007). For example, ORAI3 has a much lower store-operated Ca^{2+} current but a much faster negative-feedback mechanism (Shuttleworth, 2012a, Shuttleworth, 2012b); moreover, the well-known SOCE inhibitor 2-APB potently inhibits ORAI1 but activates ORAI3 when applied at high concentrations (Shuttleworth, 2012b, Shuttleworth, 2012a). ORAI3 has also been implicated in some diseases, most notably in breast cancer, where a switch from ORAI1 to ORAI3 takes place on transformation from normal breast cells to malignancy (Motiani et al., 2013a, Motiani et al., 2013b).

1.3.1.3. Canonical Transient receptor potential channels (TRPC)

TRPC channels are part of a wider group of Ca^{2+} channels that form a big family of TRP channels; when combined with TRPL, TRPP, TRPV, TRPM, TRPN and TRPA (Venkatachalam and Montell, 2007, Ramsey et al., 2006). The TRPC channel subfamily itself has 7 different isoforms, with TRPC2 not expressed in humans but present in rodents. They are further subdivided into four subsets based on biochemical and structural properties to TRPC1, TRPC

2, TRPC3/6/7, and TRPC4/5, each with differential expression in tissues (Venkatachalam and Montell, 2007). This diversity can be increased via heterodimerisation of different TRPC subunits (Cheng et al., 2013). The common property of these channels is that all isoforms can be activated by the PLC pathway, as they can all interact with IP_3R (Ramsey et al., 2006). The best characterised function of TRPC channels is probably in the CNS, where different isoforms of TRPC channels work in tandem to assist in the homing of neuronal growth cones to extracellular cues (Ramsey et al., 2006). Unlike ORAI channels, they are not selective for Ca^{2+} as they are also permeable to other mono- and divalent ions, resulting in different current/voltage profiles (Cheng et al., 2013, Ramsey et al., 2006).

Each monomer of TRPC channels contains six transmembrane domains, with the loop between TM5 and TM6 contributing to the pore (Vazquez et al., 2004). Both the N and C terminus protrude into the cytoplasm, forming extensive motifs and domains. The N-terminal domain contains 3-4 ankyrin repeats, a coiled coil region (CC) and a caveolin interaction region, whereas the C-terminus contains a TRP signature motif (EWKFAR), a proline-rich motif, a CIRB (calmodulin and IP_3R binding) region and a coiled coil domain (Vazquez et al., 2004, Ramsey et al., 2006). In TRPC4/5, the C-terminal has an extension; containing an extra PDZ domain, which may provide a link to PLCβ and the cytoskeletion via the adaptor protein NHERF (Vazquez et al., 2004). Although still ambiguous, each TRPC channel is likely formed by 4 subsunits (Clapham, 2007, Ramsey et al., 2006). The ankyrin repeats seem to be important for the trafficking of the channel to the PM, whereas the N-terminal CC domain takes part in dimerisation; implying that the N-terminal region is important for the correct localisation of the channel (Vazquez et al., 2004). The C-terminal appears more regulatory, as the CIRB domain serves as a binding site for IP3R and

calmodulin; the CC domain in this region also serves as a binding site for calmodulin, but only in TRPC1 (Vazquez et al., 2004). Finally, the proline rich motif is a binding site for the anchoring/adaptor protein Homer, and is important for its coupling to IP3R for regulation (Vazquez et al., 2004).

Despite the discovery that ORAI is the frontline mediator of SOCE, evidence for TRPC also contributing to this process still remains (Worley et al., 2007), with the most convincing isoform being TRPC1 (Kim et al., 2009). The KD of TRPC1 in HEK293 cells, Human submandibular gland cells, human lung epithelial and pulmonary smooth muscle cells all resulted in a reduction in SOCE (Vazquez et al., 2004, Cheng et al., 2013). Moreover, pancreatic acinar cells and salivary gland cells from $TRPC1^{-/-}$ mice had displayed impaired SOCE despite ORAI presence (Hong et al., 2011). Indeed, in various mammalian cell systems STIM1 is known to interact with the two aspartate residues on TRPCs in the C-terminal domain, specifically via the STIM N-terminal lys-rich motif (Zeng et al., 2008). Furthermore, the CC domains on both ends of TRPC subunits are putative interaction sites with STIM (Lee et al., 2014). Interestingly, for TRPC1 to mediate SOCE, ORAI must also be present; since it is required for the translocation of TRPC1-containing vesicles to the membrane (Cheng et al., 2011). This suggests that ORAI is indeed the principle SOCE mediator, with TRPC1 immediately recruited downstream as an 'assistant' to ORAI, playing a secondary role in sculpting the SOCE Ca^{2+} signalling signature (Cheng et al., 2011). Supporting this, it was proposed previously that ORAI is important for establishing Ca^{2+} oscillations, where TRPC1 alters the amplitude and the frequency; resulting in the dependency of NFAT activation on ORAI, while NF-κB depends on TRPC1 (Ong et al., 2012, Cheng et al., 2011).

1.3.2. Downstream and the end of Ca^{2+} signalling

Downstream, increases in $[Ca^{2+}]_{cyt}$ results in this ion being intercepted by cytosolic proteins that serve to relay this signal into physiological functions. Calmodulin (CaM) is the most common Ca^{2+} receptor immediately downstream of a rise in $[Ca^{2+}]_{cyt}$ (Heist and Schulman, 1998) which, when bound with 4 Ca^{2+} ions, binds to and activates a whole host of proteins. These include the CaM-dependent kinase family (CaMK), serine/threonine phosphatase calcineurin (CaN), myosin light chain kinases (MLCK) (Clapham, 2007), adenylyl cyclases (ACI and VIII), and phosphodiesterase 1 (PDE1) (Halls and Cooper, 2011, Willoughby and Cooper, 2007). Independent of CaM, Ca^{2+} signalling also activates the serine/threonine kinase protein kinase C (PKC). There are 11 families of PKC, split into 3 groups: conventional, consisting of PKCα, βI, βII, and γ; novel consisting of PKCδ, ε, θ, and η, and atypical, consisting of PKCλ, ι and ζ. Conventional PKCs require both Ca^{2+} binding and DAG for activation, whereas the novel varieties only need DAG for activation (Fan et al., 2014, Griner and Kazanietz, 2007). In contrast, atypical PKCs respond to neither, instead relying on other lipid derived second messengers for activation (Fan et al., 2014, Griner and Kazanietz, 2007). The differential expression patterns of the PKC isoforms in different cells have been implicated in a wide range of diseases including cancer, diabetes and heart failure (Fan et al., 2014, Griner and Kazanietz, 2007, Mochly-Rosen et al., 2012);. Together, these proteins can mediate both short term and long term effects depending on the cell type and desired function (Berridge et al., 2003). Examples of short term Ca^{2+} mediated processes include vesicle fusion for secretion (Ca^{2+})(Petersen and Ueda, 1976), MLCK mediated cell migration (CaM) (Chen et al., 2014b), the modulation of the cAMP pathways (Ca^{2+} and CaM), and the regulation of metabolism (PKC).

Long-term Ca^{2+} signalling, sustained by SOCE as mentioned earlier, results in the activation of transcription factors NFAT, which is activated by CaN-mediated dephosphorylation required for its translocation into the nucleus (Parekh, 2011). NF-κB, on the other hand, is activated by its dissociation from its inhibitory complex with IKK-β in a process dependent on PKC-induced phosphorylation (Chen and Greene, 2004). NFAT and NF-κB are utilised by a wide range of cellular systems, where they determine cellular outcomes. This is especially true in the adaptive immune system, where both NFAT and NF-κB activation are required for the activation and proliferation of T-lymphocytes.

Once signalling is complete, excess cytosolic Ca^{2+} is removed via the plasma membrane or transported into the ER (mentioned earlier). This is carried out by pumps and exchangers – plasma membrane Ca^{2+} ATPase (PMCA), the Na^{+}-Ca^{2+} exchanger (NCX), and the Na^{+}/Ca^{2+}-K^{+} exchangers (NCKX) (Clapham, 2007). The pumps carry out Ca^{2+} removal in exchange for ATP hydrolysis, whereas exchangers take advantage of the overwhelming out/in Na^{+} gradient to export Ca^{2+} ions. NCX exchanges one Ca^{2+} ion for 3 Na^{+} ions. NCKX exports 1 Ca^{2+} ion and 1 K^{+} ion in exchange for 4 Na^{+} ions (Clapham, 2007). Moreover, the mitochondrial Ca^{2+} uniporter also contributes to the removal of Ca^{2+} from the cytosol (Duchen, 2000).

1.4. The cAMP signalling system

cAMP is an ubiquitous, organic second messenger that is created by 10 different isoforms of adenylyl cyclases and destroyed by phosphodiesterases. Downstream, cAMP activates three main classes of proteins – protein kinase A, exchange protein activated by cAMP and cyclic nucleotide-gated channel family. This pathway is also under spatiotemporal regulation by A-

kinase adaptor proteins which anchor cAMP signalling components to specific areas of the cell where they mediate a wide range of functions.

1.4.1. Adenylyl cyclase (AC)

ACs is a family of enzymes that catalyse the cyclisation of ATP into a molecule of cAMP, with 2 Mg^{2+} ions also required as co-factor. So far 9 (AC1-9) membrane-bound isoforms and one soluble isoform (sAC) have been discovered, each with different modes of regulation and differential expression in tissues. It is normal for cells to express more than one AC isoforms at the same time to perform non-redundant functions. AC4, 6, 7 and 9 have a widespread expression profile, whereas AC1 is predominantly found in the brain, and AC2 is also expressed in the lung as well as the brain; AC3 is principally expressed in olfactory epithelium and pancreas; AC5 is mostly found in the heart, and AC8 is expressed in the brain and pancreas (Willoughby and Cooper, 2007, Halls and Cooper, 2011). Experiments carried out in AC knock-out mice underline their importance to mammals: AC1 knockout (KO) mice have reduced long term potentiation (Halls and Cooper, 2011, Wu et al., 1995), whereas a lack of AC8 results in altered stress-induced anxiety (Schaefer et al., 2000) and defective spatial memory (Zhang et al., 2008b). AC5 KO mice have decreased left ventricular functions, but a longer lifespan and higher stress endurance (Yan et al., 2007, Vatner et al., 2009, Vatner et al., 2013, Okumura et al., 2003), and the KO of the similar AC6 resulted in similar effects in the heart but also have independent effects to AC5 (Tang et al., 2008). AC3 KO mice have attenuated responses to pheromones, resulting in the lack of behaviour towards other males as well as a striking obese phenotype (Wang et al., 2009). Lastly, sAC has been found to be vital for sperm motility in mice (Esposito et al., 2004).

Inside each cell, nearly all AC isoforms are localised on the plasma membrane and can form functional inter-isoform dimers (Willoughby and Cooper, 2007, Cooper and Tabbasum, 2014, Halls and Cooper, 2011). The major exception from this is sAC, which has a cytosolic distribution and is activated by bicarbonate ions (Steegborn, 2014, Lefkimmiatis et al., 2013). AC is a monomer consisting of 2 transmembrane clusters (TM1 and TM2 domains), with each cluster containing 6 transmembrane helices (Zhang et al., 1997). The two clusters are connected by an intracellular loop, which is split into C1a and C1b region (Tesmer and Sprang, 1998, Zhang et al., 1997). After TM2, the C-terminal tail is an intracellular tail, similarly spilt into the C2a and C2b region (Zhang et al., 1997). The ATP binding active site is formed by the association of C1a and C2a regions; and for that reason these two regions are the most conserved section of the enzyme (Tesmer and Sprang, 1998, Zhang et al., 1997).

Physiologically, every isoform (except sAC) can be activated by GPCRs coupled to the Gαs subunit to produce cAMP, with Gαs-GTP binding to the N-terminal side of C1a in the C1a/C2a interface (Tang and Hurley, 1998). Aside from GPCRs, ACs is also the subject of stimulatory and inhibitory modulations from a whole host of elements of the cell including PKA (inhibits AC5/6), Gαi (inhibits all apart from AC2/4/7), Gβγ (mentioned earlier), and most notably the Ca^{2+} pathway which has already been described extensively (Cooper and Tabbasum, 2014, Halls and Cooper, 2011, Willoughby and Cooper, 2007). Intriguingly, all AC isoforms are sensitive to the Ca^{2+} signalling pathway, whether directly or by downstream effectors. For example, AC1 and AC8 are activated by Ca^{2+} via a calmodulin-dependent mechanism. AC8 is activated by the removal of the attached autoinhibitory calmodulin, whereas AC1 is activated by Ca^{2+}-calmodulin binding, both via the C1b domain (Masada et al., 2009). In contrast, AC5 and AC6 are directly inhibited by submicromolar concentrations

of the Ca^{2+} ion itself by competing with Mg^{2+} (Mou et al., 2009). The rest of isoforms i.e. AC2, 3, 4 and 7, are not directly activated by Ca^{2+}; but are instead effected by downstream mediators: AC2, 4 and 7 are activated by PKC, whereas AC3 and AC9 are inhibited by CaMKII and CaN repectively. Interestingly, ACs1, 5, 6, and 8 are preferentially activated by Ca^{2+} signals generated by store operated calcium entry, whilst being insensitive to global Ca^{2+} increases induced by ionophores such as ionomycin (Willoughby and Cooper, 2007, Cooper and Tabbasum, 2014). Thanks to the work of the Dermot Cooper lab, we now understand that this phenomenon is due to the localisation of Ca^{2+} sensitive ACs to specialised, cholesterol and sphingolipid-rich domains of the plasma membrane, called lipid rafts, where they interact with SOCE-mediating channels ORAI1 (in non-excitable cells) and L-type Ca^{2+} channels (in excitable cells) (Cooper and Tabbasum, 2014). Also, in a more recent account, the depletion of Ca^{2+} stores in the ER alone, and not SOCE, can increase cAMP levels in certain cell systems such as colonic crypt and airway epithelial cells; thought to be mediated by AC3 in a STIM1 dependent manner but not involving ORAI (Maiellaro et al., 2012, Lefkimmiatis et al., 2009). This effect had been called store operated cAMP signalling (SOcAMP), which can potentially provide a link between the status of the ER and cAMP signalling.

ACs is under the control of protein components from different pathways at the same time. Therefore, although AC isoform-specific knock-out studies have been made in mice producing definitive phenotypes, very little is actually known as to the physiological outcome of Ca^{2+}-induced cAMP production (Halls and Cooper, 2011). Studies on MIN6 pancreatic β-cells suggests that Ca^{2+} is likely a fine-tuner tool for cAMP signalling, as it produced oscillations that synchronised with Ca^{2+} and downstream PKA activity to exert

temporal control on downstream proteins (Ni et al., 2011, Dyachok et al., 2006, Landa et al., 2005).

1.4.2. Phosphodiesterase (PDEs)

PDEs is a group of enzymes that catalyses the conversion of cAMP into 5'-AMP, which effectively 'switches off' the pathway (Francis et al., 2011). However, in more complex terms their role is actually to confine cAMP signalling to specific areas of the cell. In a singular cell, it is quite common that multiple cAMP 'clouds' exist in segregated compartments maintained by PDEs, resulting in distinct outcomes in different parts of the cell (Lefkimmiatis and Zaccolo, 2014). This occurrence is best exemplified in the heart, where various PDE isoforms operate in conjunction with AKAPs at different locations of the same cell can simultaneously regulate hypertrophy and excitation-contraction coupling mechanisms (Stangherlin and Zaccolo, 2012). So far 11 isoforms have been discovered, each categorised by their substrate specificities and their modes of regulation. In reality, each isoform consists of at least 2 splice variants with distinct properties and expression profiles, which diversifies the number of potentially different PDEs to well over 100 in mammals (Bender and Beavo, 2006).

Physiologically, PDEs principally operate as dimers, with each monomer containing an N-terminal regulatory region and the catalytic core in the C-terminal region (Francis et al., 2011). Unsurprisingly the catalytic core is well conserved across all 11 families, whereas the regulatory region is very diverse (Bender and Beavo, 2006, Francis et al., 2011). A comprehensive expression profile of all PDE splice variants with their KO phenotypes in mice has already been discussed elsewhere (Bender and Beavo, 2006, Keravis and Lugnier, 2012,

Maurice et al., 2014); so in this account only a brief overview for each isoform will be provided. In general, despite the quantitative differences, all PDE isoforms display widespread expression profiles except for 6 (eye, lung and pineal gland), 10 (brain and testes) and 11 (male reproductive system, salivary and pituitary gland).

PDE1 is a Ca^{2+} sensitive PDE, as the binding of two CaM molecules per monomer increases the V_{max} by 10 fold (Kincaid et al., 1985), possibly by the removal of autoinhbition (Francis et al., 2011). Unlike other isoforms, functional PDE1 normally exist as hetereotetramers (Francis et al., 2011). Three splice variants exist – PDE1A, PDE1B and PDE1C, of which A and B prefer cGMP as the substrate and C has equal preference for both cGMP and cAMP (Goraya et al., 2008). They are the subject of PKA and CaMKII phosphorylation, which results in PDE1 inhibition (Hashimoto et al., 1989, Ang and Antoni, 2002). PDE1B may have a role in learning and memory in mice, whereas PDE1C may regulate smooth muscle proliferation and olfaction (Siuciak et al., 2007, Cygnar and Zhao, 2009).

PDE2 is a dual specificity enzyme, consisting of splice variants PDE2A1-3. They contain two GAF domains on the N-terminal domain – termed GAF-A and GAF-B, which facilitate its dimerization and allosteric activation (Francis et al., 2011). The binding of cGMP to GAF-B results in a 30-fold increase in cAMP hydrolysis; making it a cGMP-activated enzyme and provides a node in which cGMP-cAMP crosstalk can take place (Keravis and Lugnier, 2012). Due to its broad expression profile, PDE2 has been reported to affect numerous processes throughout the body; the most characterised of which being the regulation of the L-type Ca^{2+} current in cardiomyocytes (Fischmeister et al., 2005). Moreover, PDE2A KO in mice is embryonically lethal (Maurice et al., 2014).

PDE3 is also a dual specific enzyme, with the active site containing higher affinity for cAMP than cGMP, typified by the 10x higher V_{max} for cAMP. Therefore, cGMP acts as a competitive inhibitor of PDE3 (Francis et al., 2011). Two different splice variants are known – PDE3A and PDE3B. They can be found anchored to membranes due to the membrane-associated domain(s) on its N-terminus (Shakur et al., 2001). PKA, Akt and PKC can all phosphorylate PDE3, resulting the activation of the enzyme; and facilitates binding to 14-3-3 adaptor proteins (Okumura et al., 2003, Shakur et al., 2001, Perino et al., 2011). PDE3A is vital for platelet aggregation and oocyte maturation (Conti et al., 2002, Masciarelli et al., 2004); whereas PDE3B regulates cardiac and vascular smooth muscle contractility (Patrucco et al., 2004, Maurice et al., 2003) as well as playing a large role in regulating energy homeostasis (Guirguis et al., 2013, Degerman et al., 2011).

PDE4 is a cAMP specific enzyme and contains four splice variants – PDE4A-D, each originating from different promoters and playing non-redundant roles (Keravis and Lugnier, 2012). PDE4 has the largest group of splice variants within the PDE family, with that number exceeding 25 (Bender and Beavo, 2006). In the general structure, the N-terminal regions contain two upstream conserved regions (UCR1 and UCR2) (Francis et al., 2011). UCR1 can be phosphorylated by PKA resulting in activation (Sette and Conti, 1996, Beard et al., 2000); whereas UCR2 plays an autoinhibitory role for the enzyme, either directly or by binding to anchoring proteins such as XAP2 and DISC2 (Francis et al., 2011). This large family is further branched into 3 categories: the long form, which is the only PDE4 subtype to dimerise; the short form, which contains only UCR1; and the super short form, which contain only half of UCR2 (Keravis and Lugnier, 2012, Francis et al., 2011). The C-terminal end of the catalytic region is also the subject of phosphorylation by ERK, which activates the short forms of

PDE4 but inhibits the long forms (Houslay and Adams, 2003, Baillie et al., 2000). PDE4D KO appeared to result in drastic phenotype changes in terms of disease, as PDE4D KO mice displayed stunted growth and impaired muscarinic cholinergic stimulation (Hansen et al., 2000); whereas PDE4B plays a significant role in initiating the inflammatory response in monocytes (Jin and Conti, 2002).

PDE5 is a cGMP-specific enzyme, allosterically activated by cGMP binding in a negative-feedback mechanism (Francis et al., 2011). Three variants are known – PDE5A1-3. PDE5 contains two GAF domains (GAF-A and GAF-B); cGMP binds only to GAF-A, while GAF-B serves as an autoinhibitory domain (Zoraghi et al., 2005); this, combined with its phosphorylation by PKG, a downstream effector of cGMP, increases the V_{max} and cGMP affinity in the active site (Francis et al., 2011, Corbin et al., 2000, McAllister-Lucas et al., 1995). Like PDE1-4, PDE5 also has a broad expression profile, with its most notable role the regulation of vascular smooth muscle contraction, especially in the lung and penis (Conti and Beavo, 2007).

PDE6 is specialised enzyme that is specific for cGMP, with its expression exclusively limited to the eye, though trace amounts have also been found in the lung (Bender and Beavo, 2006). Their tertiary structure consists of two large catalytic subunits (PDE6A, B, C or D) attached to two small inhibitory subunits (PDE6G or PDE6H)(Keravis and Lugnier, 2012). Each catalytic subunit contains two GAF domains, to which cGMP must bind for full activation. They are important for the signal transduction of rhodopsin to CNG in rod and cone cells in vision (Conti and Beavo, 2007, Bender and Beavo, 2006).

PDE7 is a cAMP specific enzyme, consisting of splice variants PDE7A and PDE7B. Its V_{max} is among the lowest of all PDE families (Bender and Beavo, 2006). The mode of regulation for PDE7 is still not clear, due to its N-terminus containing no recognisable domains. However, what is known of that region is that it can bind to, and inhibit, the catalytic subunit of PKA with high affinity (Keravis and Lugnier, 2012). This PDE isoform is mainly found in the striatal neurones, cardiac and skeletal muscle, and cells of the immune system, in particular in T lymphocytes, where they have been implicated to play a role in T-cell activation and in chronic lymphocytic leukaemia (CLL) (Lee et al., 2002, Zhang et al., 2008a, Bender and Beavo, 2006).

PDE8 is also a cAMP specific enzyme, and has the highest affinity for cAMP out of all enzymes (Gamanuma et al., 2003, Fisher et al., 1998a). Two variants are known, A and B. Though the consequence of which is unknown, the N-terminal regulatory region contains a REC (analogous to bacterial receiver domains)(Galperin et al., 2001) and PAS (involved in the regulation of circadian rhythms in bacteria) domain (Gilles-Gonzalez and Gonzalez, 2004), but they do have proposed PKA and PKG phosphorylation sites between the PAS and catalytic domain(Keravis and Lugnier, 2012). Although differential amounts of expression have been found elsewhere in the body, their main location of expression is in the testis, where they have been shown to take part in cholesterol synthesis (Bender and Beavo, 2006, Tsai and Beavo, 2012).

PDE9 has the highest affinity for cGMP of all PDE classes; and is predominantly expressed in the immune tissues and the brain; and consists of splice variants PDE9A1-20 (Conti and Beavo, 2007, Fisher et al., 1998b). KO studies in mice have shown it to be important in

regulating insulin-related metabolism, as PDE9$^{-/-}$ mice appeared to have improved insulin response and have less fat content (Deninno et al., 2009).

PDE10 in many aspects is the exact opposite of PDE3, in that it has a higher affinity to cGMP than cAMP, and consequently inhibited by cAMP in the same manner as cGMP for PDE3 (Francis et al., 2011, Bender and Beavo, 2006). Strangely, it contains two GAF domains in its N-terminus that only binds cAMP (Francis et al., 2011). PDE10 may be involved in long-term potentiation, and are mainly expressed in the testes and the brain,(Conti and Beavo, 2007). PDE10A$^{-/-}$ mice displayed altered behaviour, appearing more 'lethargic' and having a delayed acquisition of conditioned avoidance (Piccart et al., 2011).

PDE11 is another GAF containing dual specificity enzyme. Four variants are known – PDE11A1-4, each segregated by the differences in the architecture of the GAF domain (Yuasa et al., 2000, Bender and Beavo, 2006, Conti and Beavo, 2007). The role of this GAF domain is unknown; in fact, not too much is known about PDE11. They are mainly expressed in the prostate, testes and the pituitary gland, where they may have a hand in regulating sperm viability and movement (Wayman et al., 2005). However, a recent report using PDE11A-/- mice showed that it is also expressed in the brain, where the lack of this PDE isoform leads to mild psychological disorders (Kelly et al., 2010).

1.4.3. Downstream cAMP effectors

1.4.3.1. Protein Kinase A (PKA)

PKA is a serine/threonine kinase that belongs to the greater AGC family of kinases, which also includes PKG, PKC and Akt (Taylor et al., 2012). It catalyses the transfer of a phosphate

onto a target substrate with the consensus sequence of RRXS/T, RKXS/T, KRXS/T and KKXR/T (i.e. positive residues near the substrate site) in response to cAMP binding (Shabb, 2001).

Structurally in its inactive form PKA consists of a homodimer of two regulatory subunits (R subunits) each bound with a catalytic subunit (C subunit) bound, forming a R_2C_2 stoichiometry (Taylor et al., 2008). Four different isoforms are known for C subunits in mammals (Prkx, Cα, Cβ, and Cγ), which are well conserved among its family members (Skalhegg and Tasken, 2000). It consists of a small N lobe and a larger C lobe, flanked by cis-regulatory N and C tails; with the active site situated in between the two lobes, where the ATP and the substrate bind (Taylor et al., 2012, Taylor et al., 2013). In physiological conditions, C subunits are already pre-phosphorylated and active at assembly, with the R subunit being its sole inhibitor (Taylor et al., 2005). The R subunit is more diverse, of which four isoforms are known (RIα and RIβ, also called type I PKA; and RIIα, and RIIβ, also known as type II PKA) (Taylor et al., 2008, Taylor et al., 2012). From the N-terminus towards the C-terminus, it contains a docking and dimerisation domain (D/D), followed by a disordered linker region which includes an inhibitor sequence (Taylor et al., 2005, Taylor et al., 2012); with two cyclic nucleotide binding domains (CNBD) in tandem, named CNBA and CNBB, at the C-terminus (Taylor et al., 2004). There is significant homology between the D/D domain and the CNB domains across the four R subunits, with the linker region being the most diverse (Vigil et al., 2004). The R subunits bind to and inhibit the kinase activity of C subunits by directly docking its inhibitor sequence onto the active site cleft, effectively acting as a pseudosubstrate (Taylor et al., 2012). On RII but not RI subunits, this inhibitory sequence can be autophosphorylated by the catalytic subunit (Taylor et al., 2012). In RI subunits, Mg_2ATP is required for binding and hence inhibition of the C subunit, whereas this does not

apply for RII subunits (Taylor et al., 2008, Taylor et al., 2013). The D/D domain is where R subunits interact to form homodimers. PKA is activated in an allosteric manner; where cAMP initially binds to the CNBB, which causes a change in conformation that exposes the CNBA for the binding of the second cAMP molecule to induce a second change in conformation to weaken the R/C subunit interface (Taylor et al., 2008). Consequently, each PKA R_2C_2 complex requires 4 cAMP molecules for complete C subunit release, with RI having four times higher affinity for cAMP than RII; the activation constant being 50-100nM and 200-400nM respectively (Dostmann and Taylor, 1991, Pidoux and Tasken, 2010, Gamm et al., 1996).

Downstream of PKA, three well-known substrates of this kinase are the transcription factor cAMP reponse element binding protein (CREB), which mediates PKA-induced genomic effects; and PDEs 3 and 4, which destroy cAMP, providing a negative feedback loop of the cAMP pathway. In reality, however, such is the ubiquitous nature of PKA, that processes such as ion channel and cell receptor dynamics (Martin et al., 2004, Howe, 2004) cell migration (Howe, 2004), mitochondrial function (Lefkimmiatis et al., 2013, Di Benedetto et al., 2014) metabolism (Luu et al., 2013), with this list not being exhaustive, are regulated by PKA. In fact, most processes in a mammalian cell have at least one component that is reportedly modulated by PKA, no matter which organ it was derived from.

One way of regulating PKA is via differential expression of RI and RII isoforms in tissues. Even when both are expressed in the same cell, they can play non-redundant roles; with AKAPs further segregating their downstream functions (Skalhegg and Tasken, 2000). RIα and RIα are expressed everywhere (Lee et al., 1983, Scott et al., 1987), as their importance

underlined in the finding that RIα KO is embryonically lethal (Amieux et al., 1997, Amieux and McKnight, 2002); whereas RIIα KO is actually beneficial in mice, as they displayed resistance to obesity and conveyed intolerance to glucose (London et al., 2014). RIβ is mainly present in brain (Cadd and McKnight, 1989) where a knock-out in mice results in impaired hippocampal function (Gronholm et al., 2003); and RIIβ is expressed in the endocrine and reproductive system (Jahnsen et al., 1986), dominating in adipose tissues (Amieux et al., 1997), and the visual cortex where RIIβ play a pivotal role in long-term depression (Fischer et al., 2004). Moreover, it has been known for more than 20 years that the RI/RII ratio is an indicator for directing cellular growth, or growth inhibition and differentiation; where RI favours growth and RII favours inhibition (Cho-Chung, 1990). As such, alteration of the RI/RII ratio has been observed to affect a number of processes, most notably in carcinogenesis. Breast, prostate, colon and ovarian cancers, all have been documented to display elevated RI expression (Nesterova et al., 2000).

Another additional level of PKA regulation can be achieved by sequestering it to defined microdomains to restrict their activity area (Lefkimmiatis and Zaccolo, 2014, Gold et al., 2013, Stangherlin and Zaccolo, 2012, Jarnaess and Tasken, 2007). Curiously, RI has a generally diffused localisation in the cytosol, whereas RII is usually found anchored to the plasma membrane or other cellular structures (Colledge and Scott, 1999, Di Benedetto et al., 2008). PKA can be anchored to a specific cellular locations via interaction with A-kinase adaptor proteins (AKAPs), which is a scaffolding protein that bind to the D/D domain of the R subunit dimer (Taylor et al., 2004, Taylor et al., 2008). More than 50 types of AKAPs have now been discovered, each having their unique designated cellular locations and different affinities to RI and RII subunits (Tasken and Aandahl, 2004, Jarnaess and Tasken, 2007). Not

surprisingly, all of them are known to bind to type II PKA; although AKAPs that anchor type I PKA and those with dual specificity have also been documented (Huang et al., 1997, Colledge and Scott, 1999). In addition to regulating the location of PKA signalling, AKAPs also serve to accelerate the relay of signalling by tethering this kinase to other proteins such as PKA activators, substrates and antagonists (i.e. ACs, PDEs and phosphatases); bringing them in proximity with each other in macromolecular complexes to minimise the limiting factor of diffusion (Willoughby and Cooper, 2007). As a result, AKAP tethered PKAs can give rise to highly efficient, functionally distinct, spatially restricted signals (Stangherlin and Zaccolo, 2012, Pidoux and Tasken, 2010). This phenomenon is widely accepted to play crucial roles in most systems, especially in cardiac (Taglieri et al., 2014, Soni et al., 2014) and neuronal signalling (Hoshi et al., 2010, Murphy et al., 2014, Dittmer et al., 2014) where a rapid relay of signalling is required.

1.4.3.2. Exchange protein activated by cAMP (EPAC)

EPAC is the most recently discovered of the downstream effectors of cAMP signalling. It is a cAMP-activated guanine nucleotide exchange factor (GEF) that activates Rap, which belongs to the Ras family of small G-proteins, by exchanging the bound GDP for GTP (Gloerich and Bos, 2010). There are two main isoforms of Epac discovered thus far - Epac1 and Epac2; with Epac2 having three splice variants (Epac2A, Epac2B and Epac2C) (Ueno et al., 2001, Niimura et al., 2009). Epac1 and Epac2 generally have broad but specific expression profiles; with Epac1 expression dominating all immune and blood cells as well as the kidney, the vascular system, heart, adipose tissue, and the female reproductive system (Grandoch et al., 2010, Schmidt et al., 2013); whereas Epac2 is mainly present in the pancreas and adrenal gland (Kawasaki et al., 1998). Epac2C is a specialised isoform that is only present in the liver (Fu et

al., 2011). The central nervous system is an exception in that it expresses both Epac1 and Epac2.

In terms of its structure, both isoforms of Epac exist as monomers, with various domains that define their function. At the N-terminus of Epac1, there is a dishevelled-egl-10-pleckstrin (DEP) domain linked to a CNB domain (cAMP-B) not dissimilar to that of PKA, which forms the regulatory region (de Rooij et al., 2000); after which comes the catalytic region, which contains a Ras-exchange motif (REM) connected to CDC25-homology domain (CDC25HD) at the C-terminus via a RA domain (Bos, 2006). Epac2 is largely identical to Epac1 but contains a second CNB domain (cAMP-A) at the N-terminus before the DEP domain; Epac2C is truncated even further, lacking the DEP and the extra CNBC (Rehmann, 2013). REM binds to and stabilises CDC25HD to form a minicomplex, which carries out the GDP → GTP exchange. Elsewhere, the DEP domain, as well as the extra CNBD on Epac2, is important in directing Epac to appropriate compartments of the cell (Ponsioen et al., 2009, Li et al., 2011); while the common CNBD provides an autoinhibitory function on the active site (Rehmann et al., 2006). Inhibition is by the N-terminal common CNBD (cAMP-B) 'latching' onto the C-terminal catalytic region via an ionic bridge, obscuring CDC25HD from its targets (Rehmann et al., 2007); on binding of cAMP onto the CNBD, a conformational change takes place, breaking this ionic interaction and exposing the active site (Das et al., 2008). Compared to PKA, although the cAMP affinity is approximately the same for both proteins in vitro, physiologically Epac requires 30 times higher concentration of cAMP for activation due to a lack of allosteric cooperation between domains (Dao et al., 2006).

Much like PKA, Epac is also spatiotemporally regulated via interactions with other cellular modules via AKAP binding. In fact, it is actually quite common for PKA and Epac to be in the

same AKAP complex, with a good example being the mAKAP signalosome in cardiomyocytes. There, this mAKAP complex containing PKA, PDE4D3 and Epac1 inhibits ERK5-mediated cardiac hypertrophy (Dodge-Kafka et al., 2005). However, localisation of Epac can also be modulated independently of AKAPs thanks to the DEP domain (Schmidt et al., 2013). The DEP domain allows the anchoring of Epac onto phosphatidic acid (PA) and ezrin-moesin-radixin (ERM) proteins on the plasma membrane to relay signals from cell-surface receptors such as β_1-adrenergic receptors (Consonni et al., 2012). Interestingly, Epac1 has been found at the nuclear pore complex, where it interacts with RanBP and Ran-GTP via its RA domain to regulate the export of nuclear proteins such as histone deacetylase 4/5 (HDAC4/5) and DNA damage responsive DNA kinases (Huston et al., 2008, Liu et al., 2010, Metrich et al., 2010). There, its GTP exchange activity towards Rap is inhibited by RanBP, but is accelerated by binding to microtubules of the nucleoskeleton (Gupta and Yarwood, 2005).

The most well-known downstream effector of Epac signalling is Rap1 and Rap2 (Gloerich and Bos, 2010). When this pathway was first discovered, their central function was the maintenance of cell polarity, cell-cell interactions and cytoskeletal turnover (Raaijmakers and Bos, 2009, Pannekoek et al., 2009). This is done via interactions of Rap with other scaffolding proteins. For example, binding to AF-6 stabilises adherens junctions by preventing E-cadherin internalisation (Hoshino et al., 2005), whereas Rap binding to Riam and RapL facilitates focal adhesion formation in T cells (Lafuente et al., 2004, Katagiri et al., 2006). Moreover, Rap interactions with Krit1 tightens endothelial cell-cell junctions (Glading et al., 2007), interactions with RacGEFs vav2 and Tiam1 delivers Rac signalling to cell-cell contacts (Arthur et al., 2004), and actin dynamics can be regulated by Rap1-IQGAP1

complexes (Jeong et al., 2007). However, the understanding of the roles of Rap proteins has diversified since these findings; in particular, the Rap-PLCε-PKCε/CaMKII axis seems to be a common Epac-induced pathway in various cell-types (Schmidt et al., 2013). In pancreatic β cells, Epac2-Rap-PLCε is known to modulate K_{ATP} channel activity as well as potentiating the release of insulin via Ca^{2+} modulation (Hashiguchi et al., 2006, Ozaki et al., 2000, Eliasson et al., 2003). In cardiomyocytes, a similar signalling axis is known to control excitation-contraction coupling via phosphorylation of myofilament proteins (Oestreich et al., 2009), and the inhibition of ERK5 mediated hypertrophy (Dodge-Kafka et al., 2005).

1.4.3.3. Cyclic nucleotide-regulated ion channels

Cyclic nucleotide-regulated ion channels belong to the same superfamily as the voltage gated K^+ channel superfamily (Podda and Grassi, 2014). There are two types of ion channels that are directly regulated by cAMP – hyperpolarisation-activated cyclic nucleotide channel (HCN) and cyclic nucleotide gated channel (CNG) (Schunke and Stoldt, 2013). cAMP can directly bind to and activate both HCN and CNG without any intermediaries due to their structural setup, but with different activation profiles (Schunke and Stoldt, 2013).

Structurally, each channel exists as tetramer, with each monomer containing a cytosolic N-terminal region, the central transmembrane region, and the C-terminus (Long et al., 2005, Craven and Zagotta, 2006, Biel et al., 2009). The central transmembrane region consists of 6 helices (S1-S6) that traverses the membrane, with each subunit contributing two helices (S5-S6) to the tetramer to form the channel, with the positively charged S4 acting as the voltage sensor (Biel et al., 2009, Flynn et al., 2001, Craven and Zagotta, 2006). S5 and S6 are connected by a pore loop, which acts as a selectivity filter (Craven and Zagotta, 2006, Podda

and Grassi, 2014, Biel et al., 2009). The C-terminal domain on each monomer contains a cyclic nucleotide binding domain (CNBD), which acts as an autoinhibitory domain (Craven and Zagotta, 2006, Podda and Grassi, 2014, Benarroch, 2013). cAMP and/or cGMP activates the channel by binding to the CNBD, relaying a conformational change to the pore via a C-terminal linker connecting the CNBD to S6 (Craven and Zagotta, 2006, Biel et al., 2009).

HCN channels are mainly distributed in the nervous system and the heart, where they directly relay information mainly from cAMP, to control resting potentials and membrane resistance (Benarroch, 2013). Thus far, four isoforms are known (HCN1-4), each with slightly different properties and activation kinetics (Roubille and Tardif, 2013, Benarroch, 2013); however, the common characteristics between all 4 isoforms is that they are constitutively active at resting potentials, permeable to both Na^+ and K^+ ions conducting a cation I_h current (Biel et al., 2009, Kase and Imoto, 2012). The binding of cAMP results in the activation conditions shifted to more positive potentials; thus modulating the parameters of action potential generation (Biel et al., 2009, Benarroch, 2013). One example of HCN function is that in the heart sinoatrial node (SA), where I_h from HCN2 and HCN4 is known as the pacemaker current important in Ca^{2+} channel activation after repolarisation in diastole (Wahl-Schott and Biel, 2009, Postea and Biel, 2011, Roubille and Tardif, 2013). Moreover, HCN have also been shown to take part in learning, memory and motor coordination in the hippocampus and the cerebellum (Nolan et al., 2003, Nolan et al., 2004), and regulation of oscillations in thalamocortical neurones (Santoro and Baram, 2003); as mice missing certain types of HCN have been reported to cause symptoms of absence epilepsy and sinus dysrhythmia (Ludwig et al., 2003).

CNG channels consists of two types of subunits– A and B, of which four different isoforms of A (CNGA1-4) and 2 different isoforms of B (CNGB1 and CNGB3) are known in mammals (Bradley et al., 2001). The CNGA family are considered pore forming, while the CNGB family are modulatory as they cannot form pores when expressed on their own (Hofmann et al., 2005). Unlike HCN channels however, CNG is voltage-independent; as they will only conduct Na^+ and Ca^{2+} ions as a result of ligand binding, and tend to use cGMP more than cAMP as ligand; although in olfactory neurones CNG reacts to both cGMP and cAMP (Kaupp and Seifert, 2002). Much like HCN, they are prominently present in the nervous system, and are indispensable for sensory transduction in olfactory neurones and the eye (Podda and Grassi, 2014). In olfactory neurones, the cAMP generated by odour activated $G_{\alpha olf}$ - ACIII binds to CNG, causing an influx of Ca^{2+} ions to subsequently activate Ca^{2+} activated Cl^- channels, leading to depolarisation and the amplication of the signal (Antunes et al., 2014, Breer et al., 1990, Kleene, 2008). They are also reported to play a role in CNS development, synaptic plasticity and glial cell function (Podda and Grassi, 2014).

1.5. Cell migration

Cell migration is a physiologically important process that involves the translocation of a cell from its origin to another location to carry out its functions. It can take place over short distances, such as in wound healing and morphogenesis; or long distances such as in cancer metastasis and immune responses (Huttenlocher and Horwitz, 2011, Hoshino et al., 2013). Under normal circumstances this process takes place on the extracellular matrix (ECM), which is a mesh of structural proteins that serves as a supportive structure for its surrounding cells (Frantz et al., 2010). There are three general modes of cell migration - mesenchymal, amoeboid, and collective migration (Nurnberg et al., 2011). Amoeboid

migration is powered by hydrostatic pressure, which produces dynamic, non-apoptotic and intrusive blebs in areas of low cortical actin concentration; these 'bleb intrusions' are then consolidated by cortical actin polymerisation. This process is still poorly understood, but it is proposed to be downstream of Ezrin-radixin-moesin (ERM) and formin proteins (Nurnberg et al., 2011). Mesenchymal migration is perhaps the most studied and the best characterised form of cell migration, and involves the locomotion, or 'crawling', of a cell on a reasonably flat surface (Nurnberg et al., 2011). This is a highly coordinated process powered by the manipulation of intracellular actin cytoskeleton and the turnover of focal adhesions (Parsons et al., 2010). Lastly, collective migration is the plural form of mesenchymal migration, and is the movement of a cluster or sheet of cells that retain their cell-cell contacts on its substratum (Nurnberg et al., 2011). It is important to note that these three modes of cell migration are not mutually exclusive, and are instead rather part of a continuum. For example, a dendritic cell is capable of using a combination of amoeboid and mesenchymal type of migration to reach their destination, and non-mesenchymal cells can use mesenchymal migration for movement (Huttenlocher and Horwitz, 2011).

1.5.1. Actin – properties

Despite the differences in mechanism, what is beyond doubt is that the actin cytoskeleton is the central linchpin of all types of cell migration. Supporting this, both the inhibition of F-actin disassembly by jasplakinolide, and of G-actin polymerisation by cytochalasin D or latrunculin resulted in the obliteration of cell migration (Yarrow et al., 2004, Sayed et al., 2008, Zhang et al., 2012). Therefore, in order to understand this physiological process, it is important to consider the intrinsic properties of actin.

Actin is a ubiquitous, globular 42kDa protein that has the ability to bind and hydrolyse ATP. When bound with ATP, actin monomers (G-actin) can quickly associate with each other and polymerise into double helical filaments (F-actin, used interchangeably with actin filaments) (Nurnberg et al., 2011). Once incorporated into the filament, ATPase activity of each actin monomer increases; and the hydrolysis of ATP to ADP destabilises the actin filament, promoting depolymerisation (Nurnberg et al., 2011). Actin polymerisation normally consists of three phases - nucleation, elongation and steady state. Nucleation is the spontaneous formation of an ATP-actin trimer, also called the nucleus; this is the rate-limiting step of the process, due to the instability of this nucleus (Nurnberg et al., 2011, Krause and Gautreau, 2014). If the nucleus perseveres, then the elongation phase would take place rapidly, where ATP-actin monomers are added onto either side of the nucleus at an asymmetrical rate. During elongation, polymerisation occurs much more rapidly on one end (the '+', or the 'barbed' end) than the other (the '-' end) (Nurnberg et al., 2011). Lastly, the stabilisation phase is reached when equilibrium is reached between the addition of ATP-actin subunits at the barbed end and ATP hydrolysis-induced dissociation at the – end; such that the total length of the actin filament is not changed (Nurnberg et al., 2011). F-actin is a highly dynamic structure, constantly undergoing cycles of polymerisation and depolymerisation. Upon stabilisation, the actin filament has a tendency to 'move forward' in the direction of the barbed end whilst maintaining the same length as it polymerises at the barbed end while losing G-subunits at the – end; this is a process known as 'treadmilling'. It is this treadmilling property of F-actin that provides cells the necessary force to drive migration (Edwards et al., 2014).

1.5.1.1. Accessory proteins of actin

Under physiological conditions, spontaneous polymerisation and breakdown of actin filaments is far too slow to support the throughput required for migration; so a horde of proteins was developed by cells to make this process much more efficient. Profilin and β-thymosins act as buffers for G-actin monomers, where profilin 'prime' them again for polymerisation by catalysing the exchange of ADP for ATP and deliver them to the barbed ends of existing filaments; in contrast, the exact function of β-thymosins is still ambiguous, although it is thought to negatively regulate the amount of free actin monomers available for polymerisation, actin monomers can be readily exchanged between β-thymosin and profilin (Goldstein et al., 2005, Xue and Robinson, 2013). It is interesting to note that in migrating cells the concentration of free G-actin-ATP is maintained by profilin in such a way that F-actin formation is favoured under physiological conditions (Bravo-Cordero et al., 2013). This means that as soon as any short actin filaments become available, they are more likely to spontaneously elongate, skipping nucleation phase altogether. The major supplier of these short filaments in question is the F-actin-severing protein cofilin. Indeed, cofilin does technically take part in the disassembly of the actin cytoskeleton by breaking them up into fragments; however, in doing so this also creates ready-made nuclei for another round of assembly almost immediately (Bravo-Cordero et al., 2013). Nucleation can also be achieved de novo via Junction-mediating and regulatory protein (JMY), which bring actin monomers together in proximity to promote and stabilise oligomerisation; and SPIN90 proteins, which mimick the F-actin barbed end to 'lure' actin monomers into elongating against it (Krause and Gautreau, 2014, Nurnberg et al., 2011). Owing to the intracellular conditions, elongation can take place rapidly without assistance; however, to maximise this rate even further the barbed end of the filament, where actin polymerisation is occurring

the fastest, can be manipulated. For example, capping proteins (CPs) bind to the barbed end of the filament, preventing any further assembly of actin monomers and shifts the dynamics towards ATPase-mediated filament disassembly (Edwards et al., 2014). Counteracting this, the formin family of proteins, CARMIL proteins (capping protein, arp2/3 and myosin I linker) and ENA/VASP proteins compete with CPs for the barbed ends while recruiting competent profilin-G-actin complexes to encourage further filament assembly (Edwards et al., 2014, Krause and Gautreau, 2014). At the end of the actin cycle, cofilin makes its return, this time serving to remove any older actin filaments that are no longer contributing to force generation (e.g. at the back of the lamellipodia), with the resultant actin monomers or oligomers are turned back over to a location where they can be reused (Bravo-Cordero et al., 2013). Cooperating with cofilin, gelsolin is another severing protein that cuts actin filaments but remains attached to the barbed end of its product after cleavage as a capping protein, preventing it from becoming a nucleus for elongation (Sun et al., 1999). In reality however, in in vivo situations cofilin and gelsolin carry similar functions - to facilitate F-actin disassembly by severing actin filaments, while providing new polymerisation-competent oligomers to ensure the turnover of actin cytoskeleton.

1.5.2. Manipulation of actin in cell migration

During mesenchymal migration, cells are often flat and extended while exhibiting broad, protrusive and ruffling cell membranes that are densely packed with actin, called the lamellipodia, biased onto one side of the cell (called the leading edge) (Krause and Gautreau, 2014, Bravo-Cordero et al., 2013). Additionally, the area behind the lamellipodia protrusion of the cell is called the lamella, while the boundary between the lamellipodia and lamella is the ‘transition zone’ (Parsons et al., 2010, Nurnberg et al., 2011). This is the most

common morphology that competent cells employ for 2-dimensional movement; although other types of structural polarity exist. For example, filopodia are short, finger-like protrusions on the leading edge that are 'sharper' in appearance; but only support slower modes of migration (Howe, 2004). Occasionally, cells can migrate downwards into the ECM by degrading its structural framework in a specialised process known as invasion, using invadopodia and podosomes (Hoshino et al., 2013). This ability is prominent in cancer cells and immune cells such as leukocytes, where they can penetrate through the ECM and basement membranes to enter the bloodstream where they can travel long distances to enter other tissues (Hoshino et al., 2013). It is important to note here that these structures are highly dynamic and transient in nature; such that lamellipodia and filopodia are interchangeable, and can be rapidly created or disassembled when instructed by extracellular cues.

After an actin filament is made, the next level of complexity lies in the manipulation of the actin filaments so that they can be morphed into different tertiary structures. The lamellipodium, which takes part in mesenchymal migration, utilises a network of actin branches to generate a broad 'protrusive front' via the polymerisation of the barbed end tips pushing against the leading edge membrane (Nurnberg et al., 2011, Krause and Gautreau, 2014, Bravo-Cordero et al., 2013). This branching effect is thanks to the actin related protein 2 and 3 complex (Arp2/3), a protein that binds to an existing actin filament and facilitates the nucleation and elongation of another that branches off from the original; while this newly formed branch can also serve as the template from which another branch can be created by the virtue of another arp2/3 protein (Nurnberg et al., 2011, Krause and Gautreau, 2014). Cumulatively, these Arp2/3-F-actin branches significantly increases the

density of the lamellipodial actin network, and gives this structure its broad, spread-out appearance which maximises the surface area in which new focal adhesions can be formed for the next step. However, it must be emphasized here that these structures are highly dynamic and are constantly undergoing cycles of creation and destruction (Krause and Gautreau, 2014). Indeed, a balance is maintained between activities of proteins that make F-actin longer (JMY, SPIN90, profilin, CARMIL, formins and ENA/VASP) and of those that shorten or disassemble actin filaments (β-thymosins, capping proteins, cofilin, gelsolin and its own endogenous ATPase activity) within this compartment (Edwards et al., 2014, Krause and Gautreau, 2014, Nurnberg et al., 2011, Bravo-Cordero et al., 2013). This is done so that the actin branch network is constantly being turned over rapidly in order to maintain the force of protrusion against the leading edge while not overcrowding the lamellipodia with unproductive filaments (Krause and Gautreau, 2014, Bravo-Cordero et al., 2013). Supporting this, the density of actin branches correlates positively to the stability of the lamellipodia, but is inversely proportional to the speed of migration (Krause and Gautreau, 2014). This means that the more concentrated the branch network (more branches), the longer the lamellipodia will persist but in exchange of the slower migration; whereas less branches would mean faster cell migration but the lamellipodia becomes more prone to breakdown (Krause and Gautreau, 2014).

To enter the next stage of migration the leading edge protrusions must persist for long enough and provide enough mechanical force so that the lamellipodium can come into contact with part of the ECM that was previously in front of the cell (Bravo-Cordero et al., 2013). If successful, the contacts are then consolidated by integrin, forming a nascent focal adhesion. Integrins are heterodimeric transmembrane receptors that function to link the

ECM to the cytoskeleton while also relaying signalling to the cell (Bridgewater et al., 2012). Indeed, numerous isoforms of integrins are known, each with different binding affinities to ECM components, intracellular signalling and the phenotype they convey onto the cell (Bridgewater et al., 2012). While still in vesicles inside the cell, integrins are 'activated' by kindlin and talin binding, which serve to link the actin cytoskeleton to integrin, before being translocated to the PM (inside-out integrin signalling) (Bridgewater et al., 2012). At this stage, two outcomes are possible; either the intracellular integrin signalling complex fails to adequately make a connection with the actin cytoskeleton and disassemble, or it connects fully with the actin network and mature into a full focal adhesion as more integrin-ECM complexes accumulate in this concentrated area to stabilise this actin-integrin-ECM connection (Parsons et al., 2010, Huttenlocher and Horwitz, 2011). Integrin binding to the ECM then activates a wide range of signalling pathways that is translated into the rest of the cell (outside-in signalling) (Bridgewater et al., 2012).

In a polarised, migrating cell, behind the lamellipodia sits the lamella, which is rich in maturing, larger focal adhesions that anchor the cell to the ECM (Huttenlocher and Horwitz, 2011, Parsons et al., 2010). Here the actin filaments are not branched, but are instead arranged into a series of parallel bundles (called stress fibres) by myosin II and α-actinin into an extensive network of actomysosin bridges. In the transition zone (i.e. the lamellipodia-lamella border), actin filaments are either disassembled with the remnants transported back to the front of the lamellipodia or are remodelled into bundles (Parsons et al., 2010, Huttenlocher and Horwitz, 2011); while nascent adhesions undergo maturation into focal complexes, as components of the integrin signalling complex start to arrive (Shen et al., 2012, Huttenlocher and Horwitz, 2011). Outside-in integrin signalling activates a series of

actin-binding proteins – talin, vinculin and α-actinin, further promoting the bundling of the actin filaments while stabilising the focal adhesion (Parsons et al., 2010, Huttenlocher and Horwitz, 2011). To relay physiological effects downstream, the integrin signalosome also contains tyrosine kinases Src and focal adhesion kinase (FAK), and the adaptor protein paxillin to communicate the downstream effects of focal adhesion establishment (Shen et al., 2012, Huttenlocher and Horwitz, 2011). One of the most prominent effects is the activation of myosin II, resulting in the movement of antiparallel actin bundles past each other and cellular contraction (Shen et al., 2012, Huttenlocher and Horwitz, 2011, Parsons et al., 2010). During cell movement the force of lamellipodial protrusions is opposed by the resistance from the PM. Therefore, newly formed focal adhesions provide traction for the cell, from which the protrusions can be translated into forward movement whilst utilising actomyosin contraction to propel the rest of the cell forward in the direction of the lamellopodia to consolidate this event (Shen et al., 2012, Huttenlocher and Horwitz, 2011, Parsons et al., 2010). Moreover, this type of contraction also produces a force tension that is important for the full maturation and effective signalling of focal adhesions (Parsons et al., 2010).

It is thought that components of the integrin signalling machinery are constantly recycled around the central 'core' of the adhesion (Bravo-Cordero et al., 2013). In order for the cell to make a forward movement, it must release most of its focal adhesions at the rear of the cell. Actomysosin contraction provides tensional force that facilitates its detachment from the ECM (Parsons et al., 2010). However this is still not a completely understood process, though myosin IIA-mediated pulling of the integrin-linked actin bundles, the microtubule cytoskeleton and the protease activity of calpain to cleave protein components of the

integrin signalosome (talin, FAK and paxillin) are proposed to contribute to this process (Parsons et al., 2010).

1.5.3. Regulation of signalling in cell migration

Cell migration is a spatiotemporally regulated process that is carefully coordinated; during which the cell is constantly under the influence of a variety extracellular cues such as chemokines and ligands (chemotaxis), ECM density (haplotaxis), electric fields (electrotaxis), and the rigidity of the substratum (durotaxis) (Petrie et al., 2009). These cues are conveyed by surface receptors (RTKs and GPCRs) or 'sensors' and ion channels on the PM which are then relayed onto the regulators of actin dynamics by a complicated web of signalling pathways. Despite the differences in mechanisms of migration activation, Phosphoinositide -3-kinase (PI3K) signalling and subsequently the Rho family of GTPases, namely Rho, Rac and CDC42, appear to lie at the centre of this signalling hub (Parsons et al., 2010, Krause and Gautreau, 2014, Bravo-Cordero et al., 2013). Although there are notable exceptions (Shen et al., 2012), active Rac and CDC42 mainly populate the leading edge, where they facilitate the formation and maintenance of lamellipodia (Rac) and filopodia (CDC42) respectively (Howe, 2004); whereas the Rho family (including RhoA, RhoB and RhoC) predominantly operate from the lamella backwards where they mainly mediate actomyosin contraction and focal adhesion detachment (Ridley, 2013, Howe, 2004). Indeed, PtdIns(3,4)P_2 (PIP_2), a substrate of both PI3K and phospholipase C (PLC), is an important module for both the activity of cofilin and Rho GTPases (Bravo-Cordero et al., 2013, Krause and Gautreau, 2014). Rho GTPases act as molecular switches that are active when bound with GTP, but are inactivated when GDP-bound. Their regulation is by GTPase activating proteins (GAPs), which promote their endogenous GTPase activities to hydrolyse GTP to GDP to switch the protein off; and

guanine nucleotide exchange factors (GEFs), which activate the protein by exchanging the bound GDP with GTP (Shen et al., 2012). To enforce the protein in the inactive state, Rho guanine-nucleotide dissociation inhibitors (Rho-GDI) bind to RhoGDP to prevent GEF-mediated GTP exchange (Shen et al., 2012).

During the first protrusion step, the formation of lamellipodia requires Rac-GTP activity which, in collaboration with the Ras → ERK and Src →Abl kinase pathways, activates the SCAR/WAVE family verrolin-homologous protein (WAVE), a giant heteropentameric complex (400kDa) which acts as a signalling hub for direct effectors of actin dynamics (Chen et al., 2014a, Krause and Gautreau, 2014); and lamellipodin, which is important in defining the location and the speed of protrusion by modulating lamellipodial size and stability (Law et al., 2013), in a series of phosphorylations (Krause and Gautreau, 2014). Once activated, phosphorylated WAVE and lamellipodin translocate to the PM where they interact with the components that are regulated by PI_3K and SH2 domain-containing inositol 5'-phosphatase 2 (SHIP2), namely PIP_3 and PIP_2 (Krause and Gautreau, 2014). Interestingly, WAVE also requires PIP_3 binding on liposomes before recruitment to the PM in addition to RacGTP for full activation (Krause and Gautreau, 2014). While at the PM, activated WAVE and lamellipodin form a complex with each other and recruits arp2/3, an actin filament branching protein crucial in the creation lamellipodial protrusions; and ENA/VASP, an elongation factor important in the generation of forces behind the protrusions, to initiate the cell migration cycle. However, Rac also has inhibitory effects on actin dynamics by activating arpin, which switches off the arp2/3 at the edge of the lamellipodia (Dang et al., 2013). In reality, the leading edge usually consists of both lamellipodial and filopodial intrusions, as activities of Rac and cdc42 are oscillating between cycles of protrusion and

retraction as the cell is continuously probing the ECM (Krause and Gautreau, 2014). The movements of the leading edge requires careful spatial coordination between the activities of GEFs and GAPs to sculpt the architecture and the direction of the protrusion (Bos et al., 2007). Indeed, GEFs such as β-PIX (downstream of coronin1A), TRIO (downstream of CARMIL1), Tiam1 and Vav2; and GAPS such as SH3BP1 (downstream of exocyst) and SLIT-ROBO (SrGAP, as a potential negative feedback loop from lamellipodin and WAVE) have all been reported to provide positive and negative feedbacks for Rac in this compartment (Krause and Gautreau, 2014).

Cofilin, which is one of the central mediators of actin turnover, is also under the control of a range of signalling cascades, reviewed in detail previously (Bravo-Cordero et al., 2013). It is inactivated when bound to PIP_2 on the PM, and hence are activated by PLC, which releases cofilin into the cytoplasm. Once there, however, cofilin is also the subject of cytoplasmic control by phosphorylation such that when phosphorylated, cofilin activity is inhibited, and it translocates to the cytosol away from the leading edge. Therefore, the combined effects of PLC mediated PIP_2 cleavage and phosphatases are required for the full activation of cofilin. This process is also dependent on Rho-GTPases. For example, RAC2 activates the phosphatase CIN to activate cofilin, whereas phosphorylation by LIM kinase is considered inhibitory for the enzyme. It is interesting to note that Ca^{2+} signalling, which regulates gelsolin in actin disassembly, also plays a prominent role in cofilin activity, by regulating phosphatase slingshot1 (SSH) which, like CIN, serves to activate cofilin by dephosphorylation. SSH activity is inhibited when it is phosphorylated by CaMKII, which is opposed by calcineurin; meaning that cofilin is activated when calcineurin is dominating over CaMKII.

Nascent focal adhesions that were first formed in the lamellipodia gradually mature (i.e. more ECM-integrin-actin complexes are formed) as its cytosolic environment 'above' makes the transition from lamellipodia to lamella, and eventually to the trailing edge (Parsons et al., 2010). As such, the integrin signalosome undergoes constant remodelling at different stages of the migration cycle. Firstly, under the lamellipodia, integrin in nascent adhesions potentiates Rac activity by activating its specific GEFs DOCK180, hence feeding further into the generation of branched protrusions (Avraamides et al., 2008, Cote and Vuori, 2007). However, as some of the actin filaments coordinate with integrin there, they are also committed to the conversion from actin branches into bundles. Rac also appears to contribute to this by activating p21-activated kinase (PAK) to regulate myosin II-mediated contraction at the back-end of the lamellipodia and in the transition zone (lamellipodia-lamella interface) (Parsons et al., 2010, Brzeska et al., 2004, Riento and Ridley, 2003). Rho activity is generally suppressed in the lamellipodia by the activation of RhoGAPs (e.g. p190RhoGAP) as well as the inhibition of RhoGEFs (e.g. p115RhoGAP) in a concerted effort by Gα13, Src kinases, FAK-paxillin and Rac (Shen et al., 2012, Parsons et al., 2010). As the lamellipodia moves on, the signalling begins to change as the nascent adhesion matures into a focal complex and then into a full focal adhesion when the lamella arrives. From the transition zone backwards the balance begins to shift from Rac to Rho as RhoGEFs such as leukaemia-associated Rho-GEF (LARG) and GEF-H1 are activated, resulting in the activation of Rho-associated kinase (ROCK) to inhibit myosin light chain phosphatase (MLCP) (Kimura et al., 1996). This keeps MLC in an activated, phosphorylated state and maintains the tension produced by actomyosin bridges, hence aiding in the maturation of the focal adhesion and its signalling. This tension has also been proposed to switch off Rac by activating its GAP ARHGAP22, which provides one potential way that Rho can negate Rac

behind the leading edge (Sanz-Moreno et al., 2008). Activated Rho also couples to the formin mDia, which facilitates in the polymerisation of actin in the production of stress fibres (Huttenlocher and Horwitz, 2011, Parsons et al., 2010). Moreover, as mDia also interact with microtubules, it cannot be ruled out that this part of the cytoskeleton may also take part in the detachment of focal adhesions (Huttenlocher and Horwitz, 2011, Parsons et al., 2010). The reciprocal regulation of Rho and Rac activity during the cell motility cycle in a polarised cell is still poorly understood, as this role appears to be carried out by integrins and mediated by the similar upstream elements (i.e. FAK/paxillin/Src tyrosine kinases) (Shen et al., 2012). Therefore, it is likely that it is the spatiotemporal regulation of specific GEFs and GAP localisation around the core integrin signalosome that determines whether the signal they relay results in lamellipodial protrusion, cell contraction or tail retraction (Parsons et al., 2010, Shen et al., 2012).

1.5.4. Podosomes and invadopodia

Podosomes and invadopodia are actin-rich, integrin based complexes which have the ability to break down the ECM in order to migrate into it (Nurnberg et al., 2011). Compared to focal adhesions, which consists of ECM-integrin-actin bundles, actin molecules in podosomes and invadopodias are not arranged into bundles. Instead, the actin dynamics here is similar to that in the leading edge, where actin branches are formed by arp2/3 complexes allowing it to protrude into the ECM (Hoshino et al., 2013).

Podosomes are transient structures that are important for matrix remodelling, and are used by non-cancerous cells like dendritic cells, endothelial cells and osteoclasts (Huttenlocher and Horwitz, 2011, Hoshino et al., 2013). Their formation often start with the formation of actin protrusions, which is then enclosed by a ring of integrin complexes and the exocytosis

of metalloproteinase (MMP)-containing vesicles to enable degradation of the ECM (Weaver, 2006, Albiges-Rizo et al., 2009). On a cell, podosomes are able to arrange themselves into two rows at the cell periphery, called podosome belts, or into rings of podosome rosettes (Luxenburg et al., 2007). Invadopodia are similar in appearance to podosomes, but are generally more aggressive in terms of matrix degradation and protrude further into the ECM, as well as being more stable (Hoshino et al., 2013, Huttenlocher and Horwitz, 2011). Moreover, invadopodia don't often form higher order structures like podosomes unless in special circumstances. For example, in Src-transformed cells, belts and rosettes of invadopodia (termed 'invadosomes') are readily formed (Brabek et al., 2004).

Much like the formation of lamellipodia and filopodia, which involves the PI3K/SHP2 → Rac/cdc42 → WAVE pathway, the formation of invadopodia involves a similar mode of signalling. During the initiation phase of invadopodia formation, powered by the activation of growth factor receptors (e.g. EGF), PI3K signalling again coordinates with another Rho GTPase, CDC42, downstream to activate N-WASP (hence in an analogous PI3K/SHP2 → cdc42 → N-WASP pathway) (Nurnberg et al., 2011, Hoshino et al., 2013), which serves as the central signalling axis for the activation of actin nucleators such as arp2/3 and cortactin to mediate actin polymerisation and downward protrusion (Nurnberg et al., 2011). The next stage of invadopodia formation involves the enclosement of the actin rich regions by a ring of integrin-ECM complexes, which facilitates the degradation of the ECM beneath (Branch et al., 2012). Although components of the integrin signalosome mentioned earlier (i.e. paxillin, FAK, Cas/Crk, calpain and RhoA) have all been reported to contribute to invadopodial physiology, it is Src kinases and integrin-linked kinases (ILK) that appeared to play the least ambiguous roles (Huttenlocher and Horwitz, 2011, Hoshino et al., 2013). ILK, in association

with IQGAP1, the formin mDia and the exocyst complex, has been proposed to recruit the vesicle-bound MT-MMP1 to the PM to bring about ECM degradation (Sakurai-Yageta et al., 2008, Liu et al., 2009, Lizarraga et al., 2009). The activity of MT-MMP1 outside the cell has been shown to activate a range of signalling pathways such as TGFβ and VEGF (Hoshino et al., 2013).

1.6. Aims of this study

cAMP signalling has been reported to be important in the regulation of PDAC, especially that of cell migration (Burdyga et al., 2013, Zimmerman et al., 2013). However, the exact cAMP toolkit is poorly characterised in this cell type. Therefore, **the first aim of this study is to characterise the cAMP handling machinery in PDAC cells, using PANC-1 cells as the model cell-line. Specifically two main questions will be addressed: Which extracellular agonist can stimulate cAMP production? Which PDE isoform is predominantly active in PANC-1 cells?**

In light of the fact that Ca^{2+} signalling can influence cAMP signalling in many cell types**, the second aim of this study is to investigate the signalling crosstalk between Ca^{2+} and cAMP signalling cascades in PANC-1 cells, with emphasis on store-operated Ca^{2+} entry.**

Chapter 2 – Materials and methods

Chapter 2 – Materials and methods

2.1. Drugs and chemicals

Thapsigargin (TG) and rapamycin were obtained from Calbiochem (Nottingham, UK). PDE inhibitors i.e. 8-methoymethyl-IBMX (8-mm-IBMX), EHNA, T0156, rolipram, BRL-50487, BC11-38 and cilostazol, as well as forskolin, secretin, VIP, Iloprost, Isoproterenol, and H89 were purchased from Tocris biosciences (Abingdon, UK). IBMX, papaverine and neurotensin were purchased from Sigma-Aldrich (Gillingham, UK).

2.2. Plasmids and constructs

Lifeact-RFP construct was purchased from Ibidi (Martinsreid, Germany). TK-YFP-STIM1 and both constructs of the rapamycin-inducible linkers (PM-FKBP-mRFP and ER-FRB-CFP, (Varnai et al., 2007) were kind gifts from Dr. Tamas Balla (NIH, Maryland, USA). Genetically encoded probe for PKA activity, A-kinase activity reporter 4 (AKAR4), was a kind gift from Dr Jin Zhang (John Hopkins laboratory, USA) (Depry et al., 2011). Genetically encoded probe for cAMP concentration, mTurq2Del-EPAC(dDEPCD)Q270E-cp173Venus(d)-Venus(d) (H134), was a kind gift from Dr Kees Jalink (The Netherlands Cancer Institute, http://research.nki.nl/jalinklab/Constructs.htm) (Klarenbeek et al., 2011). On receiving the plasmids they were amplified using Qiagen Plasmid Maxi Prep HiSpeed kit (Manchester, UK) by the author of this thesis, according to manufacturer's instructions.

2.3. Cell Culture

Dulbecco's Eagle Medium (DMEM), Heat inactivated Foetal Bovine Serum (FBS), Penicillin-Streptomycin-Glutamine (PSG) and 0.05% trypsin-EDTA solution were all obtained from Life technologies (Paisley, UK). The incubator for cell culture (model Galaxy S) was purchased from Wolf Laboratories (York, UK). Cell culture flasks were purchased from Corning (Buckinghamshire, UK). Pre-made sterile phosphate-buffered saline was purchased from Lonza (Nottingham, UK). PANC-1 cells were obtained from ATCC and were constantly maintained at 5% CO_2 and 37^{o}C in sterile and humidified incubator, in DMEM supplemented with 10% FBS and 1% PSG. At each passage, cells at 90-110% confluency were quickly rinsed twice with sterile, phosphate buffered saline (PBS) solution before being treated with 800µl 0.05% trypsin-EDTA solution for approximately two minutes to detach the cells. Afterwards 5ml of fully supplemented DMEM was added to the cells suspension, which was subsequently centrifuged at 500rpm for 2 minutes. Finally the supernatant was removed and the pellet was suspended in 10ml of fully supplemented media; the cells were then diluted further in media so that 90% confluency could be attained again in 4 days.

2.4. Cell transfection

At the end of each passage, 2ml of cell containing solution was placed into 35mm MatTek glass-bottomed dishes (MatTek, USA) or regular plastic 35mm dishes (Corning, UK) with a small 18mm circular glass coverslip (VWR international, UK) for live cell imaging and immunofluorescence experiments respectively. Cell density was adjusted so that they would reach their corresponding confluence at the time of experiment (after 3 or 4 days): in studies examining fixed cells, the confluence would be 40%; whereas for live cell FRET

measurements it was closer to 80%. 24 hours prior to each experiment, plasmids were mixed with Promofectin reagent (Promokine, UK) with the ratio of 1.5µl promofectin per 1µg of plasmid per dish, which is made up in 50µl DMEM (not supplemented). This plasmid-promofectin mixture in DMEM was then left in sterile conditions at room temperature for 20 minutes for equilibration. 1ml media was removed from each dish before the addition of the plasmid-containing solution into the cells to attain the maximum possible transfection efficiency. Therefore, at the end of transfection each 35mm dish of cells should contain: 1ml of fully supplemented media, plus a transfection mixture containing 1.5µl promofectin + 1µg of plasmid made up in 50µl of unsupplemented DMEM. Note that in the case of co-transfections i.e. transfection of 2 plasmids simultaneously into the same dish of cells, 1µg of each plasmid (so that there are now 2µg of plasmid) was then mixed with 3µl of promofectin (so the concentration was correspondingly doubled) and made up in 50µl unsupplemented DMEM.

2.5. Cytosolic Ca^{2+} measurements in live cells

The ratiometric fluorescent Ca^{2+} dye Fura-2 was purchased from Life Technologies (Paisley, UK). On the day of the experiment the supplemented DMEM solution bathing the PANC-1 cells was removed and rinsed twice with a custom-made Na^{+}-HEPES based solution (composed of 140mM NaCl, 4.7mM KCl, 1.13mM $MgCl_2$, 10mM HEPES, 10mM Glucose, 1.8mM $CaCl_2$, all purchased from Sigma Aldrich, adjusted to pH 7.4; will be referred to as just HEPES solution hereafter) before being incubated in 5µM Fura-2 dissolved in HEPES solution for 1 hour at room temperature. After incubation the Fura-2 dye was removed by rinsing the cells twice with HEPES-based solution, before being placed into the perfusion chamber for live cell imaging. During each experiment cells were perfused with HEPES-

based solutions containing either 1.8mM Ca^{2+} or 'no Ca^{2+}' (nominally Ca^{2+} free solution), and various drugs defined in the description of specific experiments. DMSO, the vehicle used to dissolve most of the drugs in this study, was added to control solutions in experiments where concentrations of 0.1% or more were used.

2.6. FRET measurements in live cells

Before each experiment transfected cells were rinsed twice with HEPES-based solution to remove the DMEM media. All test solutions, including controls, were made using their corresponding HEPES-based solutions. After initial rinsing the dish containing the cells was attached to a custom-made metal insert, into which approximately 2mls of the baseline solution (HEPES-based solution, with or without added Ca^{2+}) was added. This insert was then placed in an enclosed chamber with the temperature set at 32^{o}C where the microscope resides. Once inside, the insert containing the cells was connected to a gravity-fed perfusion system, which accommodated an adaptor for a 6-way manifold on one side for solution entry and a vacuum line with a fluid trap for solution removal on the opposite side. The solutions were held in syringes, which were placed above the microscope stage. The nozzles of the syringes were equipped with two-way taps connected via silicone tubing to the manifold. This setup allows the cells to be under 2mls of solutions at all times with a perfusion rate of about 1ml/minute. To ensure that the solutions arriving in the chamber can reach the cells at the bottom as quickly as possible the entry point is situated at the bottom of the insert, whereas the vacuum suction is at the top of the insert. As with cytosolic Ca^{2+} measurements, DMSO was added to control solutions in experiments where concentrations of 0.1% or more were used .

The cell-containing chamber was mounted on the stage of an Olympus IX71 based inverted imaging system (Till Photonics GmbH, Germany). Excitation of fluorescence was provided by a 150W xenon high stability lamp and a polychrome V monochromator wavelength control (Till Photonics GmbH, Germany). Emission light was collected using band or high pass filters and sent to an iXon DV885 cooled EM CCD camera (Andor technology, UK). Camera binning was set to 2 both horizontally and vertically which provided a 502x502 pixel points per image. TillVision software (Till Photonics, Germany) was used to control the parameters of image acquisition and post-analysis, and allowed for the measurement of fluorescence while the experiment was in progress.

For Fura-2 experiments cells were sequentially excited by 340nm and 380nm light. Emission light was collected using a 510nm high pass filter. PANC-1 cells transfected with either AKAR4 or H134 were excited at 405nm, which is close to the excitation maximum of the donor, CFP. Emissions of both CFP and YFP fluorescence were measured simultaneously using specialised filters (Optical Insights Dual-View Filter cube with D480 $\pm$ 30m and D535 $\pm$ 40m Filter Sets, BioVision Technologies, USA) only allowing wavelengths of 480nm and 535nm to reach the camera. For both Ca^{2+} and FRET measurements, only spread out, flattened and not rounded up, were chosen to be imaged.

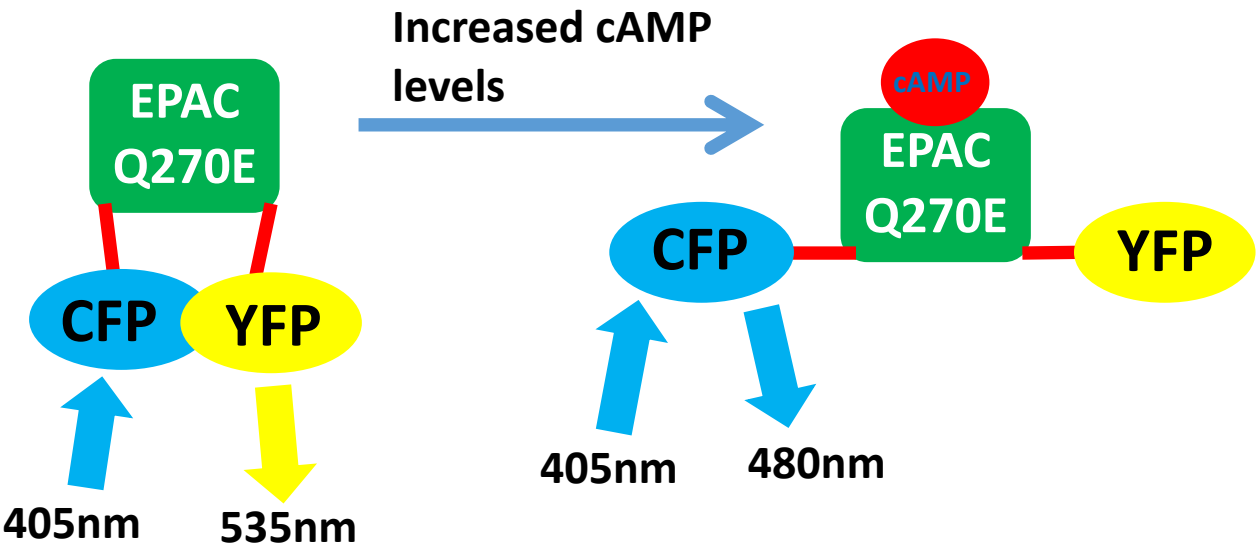

F_{CFP}/F_{YFP} ratio ∝ Relative cAMP concentration

Figure 2.1. H134 – structure and function.

A simplified schematic of cAMP induced changes in the H134 FRET signals. H134 (mTurqoise-EPAC-Q270E-VV) was made using Epac1-Q270E as backbone, with the Gln→Glu mutation induced to increase its binding affinity to cAMP. The Epac was flanked on its N-terminus by a CFP variant and YFP variants on its C-terminus. At resting levels the CFP and YFP are in close proximity, therefore FRET would be at its maximum; the binding of cAMP to its EPAC backbone leads to a conformational change that takes CFP away from YFP, dissipating FRET. An increase in cAMP concentration inside the cell increases the amount of cAMP-bound H134, resulting in a decreased overall F_{YFP}/F_{CFP} ratio or increased F_{CFP}/F_{YFP} ratio. It is via this mechanism that one can correlate relative cAMP concentration to the F_{CFP}/F_{YFP} ratio (Klarenbeek et al., 2011).

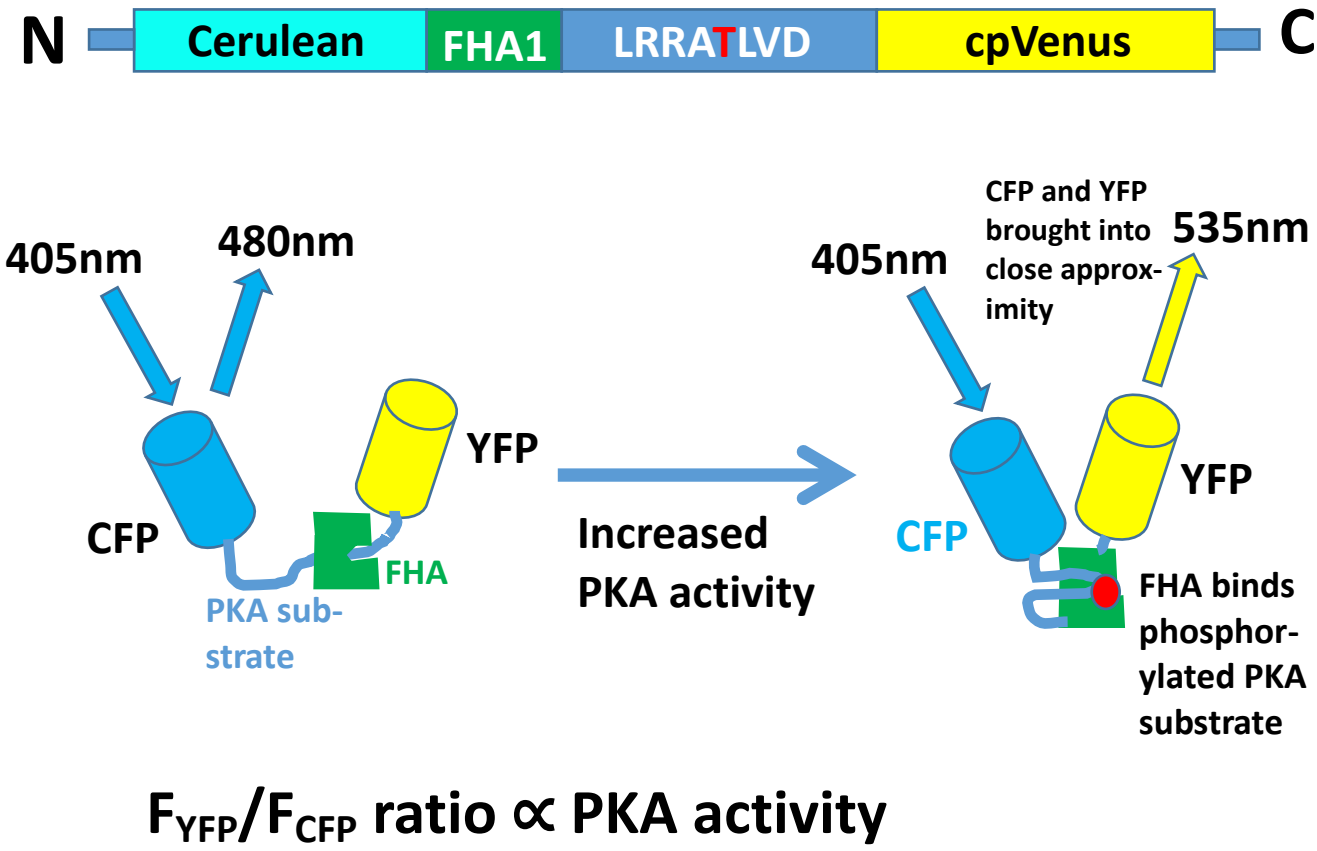

Figure 2.2. AKAR4 – structure and function.

A simplified schematic of the AKAR4 response to increased PKA activity. AKAR4 (A-Kinase activity reporter 4) is a biologically engineered probe flanked by CFP variant on the N-terminus and an YFP variant on the C-terminus. Between the two fluorescent proteins it contains a fork-head association domain followed by a consensus PKA substrate sequence. When PKA activity is increased inside the cell, PKA phosphorylates the threonine residue on the consensus sequence, creating a binding site for its neighbouring FHA1 domain. The binding of FHA1 to phospho-threonine brings CFP in proximity to YFP, increasing FRET. Hence, via this mechanism one can correlate increased PKA activity to increased F_{YFP}/F_{CFP} ratio (Depry et al., 2011).

2.7. Immunofluorescence

Anti-rabbit Phospho-PKA antibody was purchased from Cell Signalling technologies (Hitchin, UK). All secondary antibodies (mouse anti-rabbit Alexa488 and Alexa647), and Prolong Gold anti-fade medium were purchased from Life Technologies. All chemical components used to make up PBS (137mM NaCl, 2.7mM KCl, 10mM Na_2PO_4 and 1.8mM KH_2PO_4, adjusted to pH 7.4), as well as goat serum and bovine serum albumin (BSA) were all purchased from Sigma Aldrich. Paraformaldehyde (PFA) was purchased from Agar Scientific (Essex, UK).
In all immunofluorescence experiments the first step was always to remove existing media, which was done by rinsing the cells twice, and then replacing the cell maintenance solution with the HEPES solution supplemented with 1% FBS and 1.8mM Ca^{2+}. The cells were then incubated at 37^{o}C and 5% CO_2 for 30 minutes for acclimatisation.

In experiments concerning cells transfected with the PM-FKBP-mRFP and ER-FRB-CFP linkers, following acclimatisation the cells were treated with 100nM rapamycin dissolved in HEPES based solution for no more than 3 minutes. At the end of this treatment, cells were quickly rinsed twice with phosphate-buffered saline (PBS) before being fixed with 4% paraformaldehyde (PFA, made by diluting 16% PFA in PBS) for 30 minutes. All solutions hereafter were made up using PBS as base. Afterwards the PFA was removed by washing the cells three times for 5 minutes each with PBS on the rocker before the coverslips were then carefully dried and placed faced down onto a droplet of 20µl Prolong gold anti-fade medium on a microscopic slide (Fisher Scientific, UK). The fixed cells on the coverslip were kept at 4^{o}C in darkness for at least 24 hours to allow Prolong gold to harden.

In experiments involving cells transfected with Lifeact-RFP, following acclimatisation in HEPES-based solution supplemented with 1.8mM Ca^{2+} and 1% FBS at 37^{o}C and 5% CO_2 for

30-35 minutes; the cells were then rinsed twice with PBS before 30 minutes of fixation with 4% PFA at room temperature. Following the fixation procedure, the PFA was removed by rinsing the cells three times for 5 minutes on the rocker. The fixed cells were then treated with 0.2% Triton x-100 for 5 minutes. The three-time PBS rinse on the rocker was carried out again for the removal of Triton, before PBS supplemented with 10% Goat serum and 1% BSA were added to the fixed cells for 1 hour at room temperature to block any non-specific sites. After that the coverslip containing the cells was removed from the dish and placed face down onto a 100µl droplet containing the antibody against phospho-PKA substrate, diluted by a factor of 1/500 in PBS (supplemented with 5% Goat Serum and 0.1% BSA). The antibody containing solution and the coverslip were usually placed on the underside of the 35mm dish lid. The coverslips were then incubated like this for approximately 18 hours on the rocker at 4^{o}C. After this incubation the coverslips were rinsed 3 times with PBS for 5 minutes to remove excess primary antibody. The rabbit anti-mouse alexa488 secondary antibody diluted at 1:1000 in non-supplemented PBS, was then added to the cells via the same 'inverted coverslip onto a 100µl droplet' method and incubated for 30 minutes on the bench at room temperature. This was followed by another three-time 5-minute rinse with PBS on the rocker to remove excess secondary antibody. The coverslips were then carefully dried and placed faced down onto a droplet of 20µl Prolong gold solution on a microscopic slide. The microscopic slide containing the cells was stored at 4^{o}C in darkness.

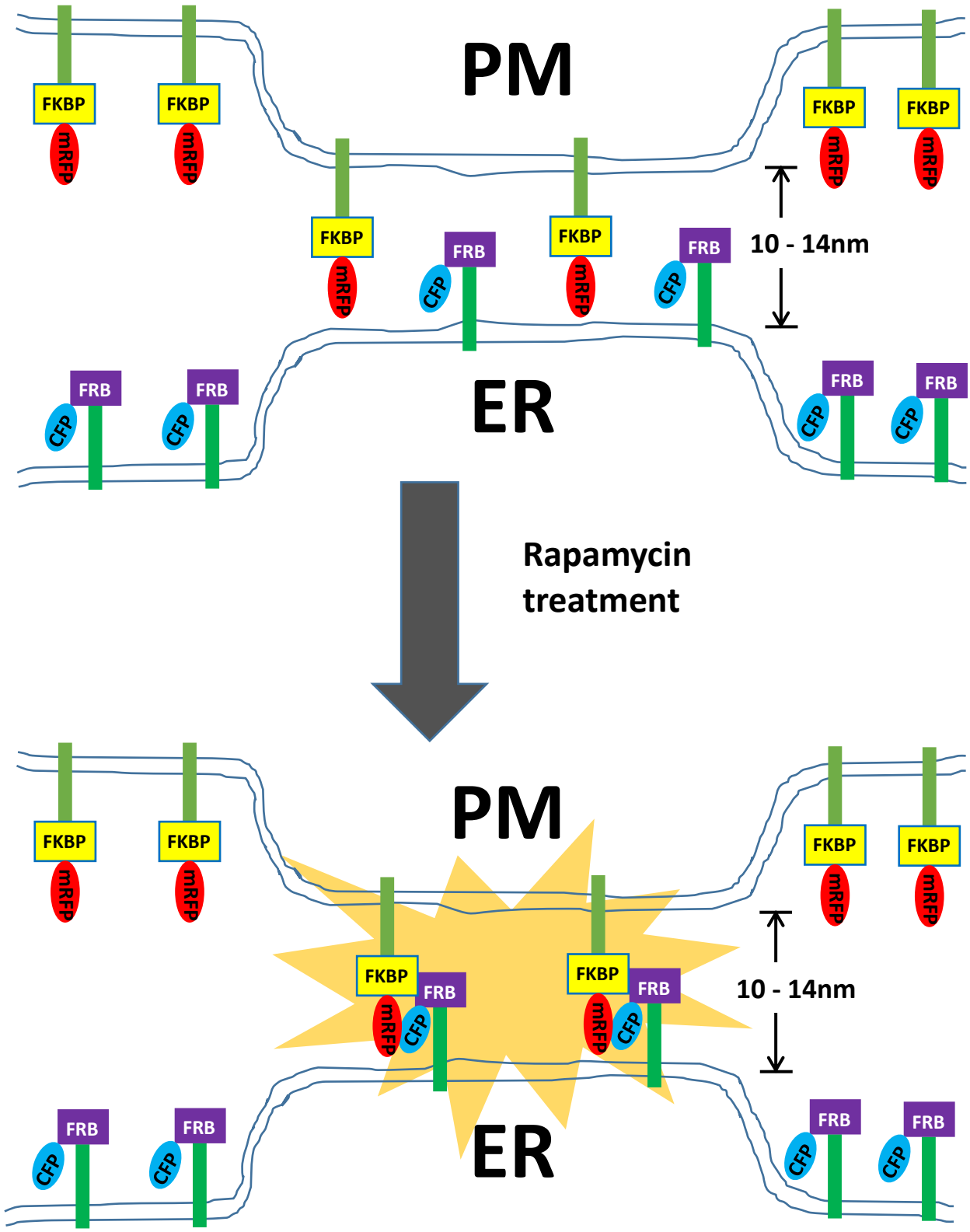
PM
FKBP
mRFP
FRB
CFP
10 - 14nm
ER
Rapamycin
treatment
PM
FKBP
mRFP
FRB
CFP
10 - 14nm
ER

Figure 2.3. ***FKBP-FRB heterodimerisation system – structure and function.***

PM targeted PM-FRB-CFP and the ER targeted ER-FKPB-mRFP. These two proteins were modelled on an mTOR backbone. When Rapamycin is added, a FKBP-FRB bridge is formed in areas where the distance between PM and ER is less than 14nm, resulting in the colocalisation of CFP and mRFP. By this mechanism, any close contacts between the PM and ER will be 'cross-linked' and the fluorescence of CFP and mRFP will be colocalised; enabling imaging of inter-organelle contacts (Varnai et al., 2007).

2.8. Confocal microscopy

All immunofluorescence coverslips were imaged using Leica TCS SP2 inverted laser scanning confocal microscopes (LSCM) fitted with an Acousto-Optical Beam Splitter (AOBS). All images were taken on a 63x oil immersion (NA=1.4) objective, using Leica confocal software for image acquisition. The XYZ mode of imaging with the airy unit set to 1 was used, which Z-scanned the focal plane from the bottom of the coverslip towards the top of the cell. A 512 x 512 pixel resolution was used in combination of 8 line averages to ensure that high quality of images with a high signal to noise ratio were taken.

During acquisition of images, Alexa488 was excited using the 488nm laser line with emission collected at 500-540nm, CFP was excited by the 405nm laser line and its emission was collected at 450-490nm; and mRFP was excited by the 594nm laser line with its emissions collected at 605-690nm.

In experiments involving linker constructs, CFP and mRFP were excited simultaneously for each confocal slice. However, imaging of cell samples transfected with the Lifeact-RFP constructs and Alexa488 were carried out sequentially (i.e. Lifeact-RFP was excited first, quickly followed by Alexa488) for each confocal slice to avoid spectral bleed through.

2.8.1. Analysis of confocal images

All colocalisation analyses were carried out using the ImageJ software (Schneider et al., 2012). For linker experiments i.e. where 2 fluorophores were imaged at once, colocalisationRGB plugin (developed by Sergio Caballero Jr, University of Florida, script can be found via http://rsb.info.nih.gov/ij/plugins/download/misc/ColocalizeRGB_.java) was used to first assess the localisation of mRFP and CFP via threshold analysis, with a map

showing spots in the cell where the two linkers colocalised (i.e. where mRFP and CFP localised at a particular pixel and passed a set fluorescence threshold) was obtained while 'masking' everything else.

Colocalisation of Lifeact-RFP and Alexa488 fluorescence (representing phosphor-PKA substrates) was performed using the Leica LAS AF Lite software.

2.9. Boyden chamber assays

The 24-well Fluoroblok chambers and their accompanying 24-well plates were purchased from BD biosciences (UK). 100% Methanol and RNase A were purchased from Sigma Aldrich. Propidium iodide was purchased from Life Technologies.

Random cell migration was assessed using 24-well Fluoroblok Boyden chambers with 8µm pore size. At the start of each experiment DMEM supplemented with 1% FBS and 1% PSG was added into the top and bottom well of the Boyden chamber. This solution would serve as the control to which test compounds would be added to in other conditions in the experiment. For measuring directional, chemotactic migration, the bottom well was supplemented with 5% FBS while the top well where the cells would be seeded was kept serum free so that at the time of seeding, cells were suspended in DMEM containing only 1% PSG but no serum. At the time of cell seeding, the bottom part contained 750µl of solution while the top section contained 350µl of solution in each chamber/well. Each chamber containing appropriate solutions in the top and bottom sections of the well was kept in the incubator at 37^{o}C and 5% CO_2 for 1 hr before the cells were seeded onto the top section. The seeding procedure is identical to the passaging protocol described in 2.3 until the pellet stage. Here the supernatant was removed, and the pellet was resuspended in 2ml

of DMEM containing 1% FBS in the case of random migration, and in serum-free DMEM in the case of chemotactic migration. 100µl of the solutions containing the resuspended cells were then seeded into the top section of each chamber before the chambers were returned into the incubator to commence the experiment. Each condition was carried out in duplicates and each experiment was repeated in at least 4 separate cell preparations.

After seeding, cells were allowed to migrate through the porous membrane during a 6-hour incubation period. Afterwards they were rapidly rinsed twice with PBS before being fixed with 100% methanol for 10 minutes at room temperature. The non-migrated cells were then removed from the top surface of the Boyden chamber membrane using a common cotton swab. The chambers were then incubated for 10 minutes in PBS to remove excess methanol, before being treated with PBS supplemented with 10µg/ml RNase A for 30 minutes to degrade RNA and facilitate the imaging process later. Finally, the chambers were incubated in PBS supplemented with 100µg/ml Prodium Iodide for 10 minutes at room temperature to stain the cells migrated to the bottom face. Between each step the wells were quickly rinsed with PBS to remove solutions from the previous step. For preservation and future imaging the chambers were then placed into 24-well plates containing 1ml PBS per well. This method of fixing and staining migrated pancreatic cells for imaging was described in a recent study (Burdyga et al., 2013).

2.9.1. Imaging and processing Boyden chambers

The chambers were imaged using a 10x dry objective (NA = 0.3) on the Leica AOBS TCS SP2 microscope, with a maximally open pinhole and no digital zoom. Propidium iodide was excited by the 514nm laser line with the emission collected at 570-690nm. The resulting

images were taken with 2 line averaging. Cell profiler software (Carpenter et al., 2006) was used to identify and count the number of migrated cells, stained with propidium iodide, on the bottom surface of the chamber membrane in each condition. The number of migrated cells in each condition was expressed as a % of their respective controls (i.e. conditions in which no test compounds were added). The results were analysed using unpaired, student's t-test; $P \leq 0.05$ was considered statistically significant. The error bars shown in the figures represent the standard error of the mean.

Chapter 3 – Characterisation of physiological cAMP agonists and PDE isoforms in PANC-1 cells

Chapter 3 – Characterisation of PDE isoforms in PANC-1 cells

Overview

cAMP signalling has only been discovered to play a role in PDAC physiology recently. In 2003 a report was published (Farrow et al., 2003) detailing the dominant expression of the PKA RIα subunit in PANC-1 cells; the inhibition of which by both H89 and by RNAi inhibited cell growth and promoted apoptosis. However, in the same study a notable expression of RII subunits was also observed in MiaPaCa-2 and SUIT-2 cells, the other two pancreatic cancer cell lines tested; which were less sensitive to H89 than PANC-1 cells but are still susceptible to its growth inhibiting effects. In another study, the activation of PKA had little effects on proliferation but appeared to provide protection against apoptosis (Boucher et al., 2001). In terms of Epac, MiaPaCa and PANC-1 cell line, as well as in pancreatic cancer tissues, have been reported to overexpress the Epac1 isoform; where both forskolin treatment (to increase global cAMP concentrations) and the preferential activation of Epac1 by 8-pCPT-2'-O-Me-cAMP inhibited cellular growth in a PKA independent manner (Lorenz et al., 2008). These reports imply that Epac1 activation stunts PDAC cell growth; whereas PKA appears to have exactly the opposite effects and protect PDAC cells from apoptosis.

Intriguingly, when cAMP signalling was tested against another important caveat of PDAC physiology- cell migration and invasion, Epac activation appeared to potentiate cell migration, whereas PKA activation potently inhibited cell migration (Burdyga et al., 2013, Zimmerman et al., 2013).

Previous data from our lab has shown that increasing cAMP concentrations by activating adenylyl cyclases using forskolin and inhibiting most PDEs using IBMX additively and

significantly inhibited cell migration and invasion in 5 different PDAC cell lines tested. Collectively, these results point towards the cAMP signalling cascade being important regulators of PDAC physiology; the manipulation of which can provide avenues for developing therapeutic interventions, especially that of metastasis, which is main cause of death in PDAC patients. Although the studies mentioned above have provided valuable insights into the downstream effects of cAMP signalling, the mechanism by which the levels of this second messenger is regulated remains poorly characterised (Zimmerman et al., 2013).

In this chapter we attempt to address this issue by characterising the cAMP signalling toolkit in PDAC cells, using PANC-1 cells as model cell line. To do this, we adopted a pharmacological, live cell imaging approach, in which we used a genetically encoded FRET-based probe to measure changes in cellular cAMP levels as various agents were added. The main focus of this study is two-fold: to find out how cAMP is produced physiologically; and to deduce which family of PDE isoforms is dominant in PANC-1 cells.

3.1. Characterisation of PDE isoforms

3.1.1. Preliminary experiment

Using H134, an Epac-based construct that senses cAMP concentration by measuring the F_{CFP}/F_{YFP} ratio, we measured cAMP concentration in PANC-1 cells whilst manipulating the cAMP machinery. In our preliminary experiments we found that adding IBMX (500µM) to unstimulated cells produced small and inconsistent increases in cAMP (data not shown). Therefore, simply treating PANC-1 cells with isoform-specific PDE inhibitors in baseline conditions is not likely to yield decisive results; prompting another strategy. To this end, as shown in figure 3.1.1, the addition of a sub-maximal concentration of forskolin (500nM)

effectively increased cAMP levels; as an elevated plateau was reached within 5 minutes in PANC-1 cells. Moreover, subsequent addition of IBMX (250µM) while maintaining the presence of forskolin treatment drastically increased cAMP levels as revealed by a further increase of the F_{CFP}/F_{YFP} ratio. These observations suggest that the inconsistent results from IBMX treatment alone is due to low endogenous background AC stimulation in these cells. This is because in the presence of adequate cAMP stimulation, with forskolin in this case, the incomplete inhibition of PDEs was already sufficient to saturate the probe, whereas the signal wasn't as strong when stimulation was absent. Doubling the IBMX concentration from 250µM to 500µM only produced a small increase in the F_{CFP}/F_{YFP} ratio and plateaued; suggesting that 500µM IBMX was enough to maximise the cAMP concentration in PANC-1 cells at 500nM forskolin stimulation. Increasing the concentration of forskolin to 20µM in the presence of IBMX increased the F_{CFP}/F_{YFP} ratio further; suggesting that AC activity was not saturated at 500nM of forskolin.

Therefore, for the protocol to characterise PDE isoforms, it was decided that PANC-1 cells would undergo 15 minutes of background cAMP stimulation by forskolin (500nM) to allow plateau formation and stabilisation before isoform-specific PDE inhibitors were added for 10 minutes without the removal of forskolin. The rationale is that if a particular PDE isoform was active, then inhibiting it would potentiate the forskolin-mediated cAMP response. To this end, 500µM IBMX was added at the end of each experiment as positive control for general PDE activity. During analysis, traces that did not produce stable forskolin-induced plateaus were omitted.

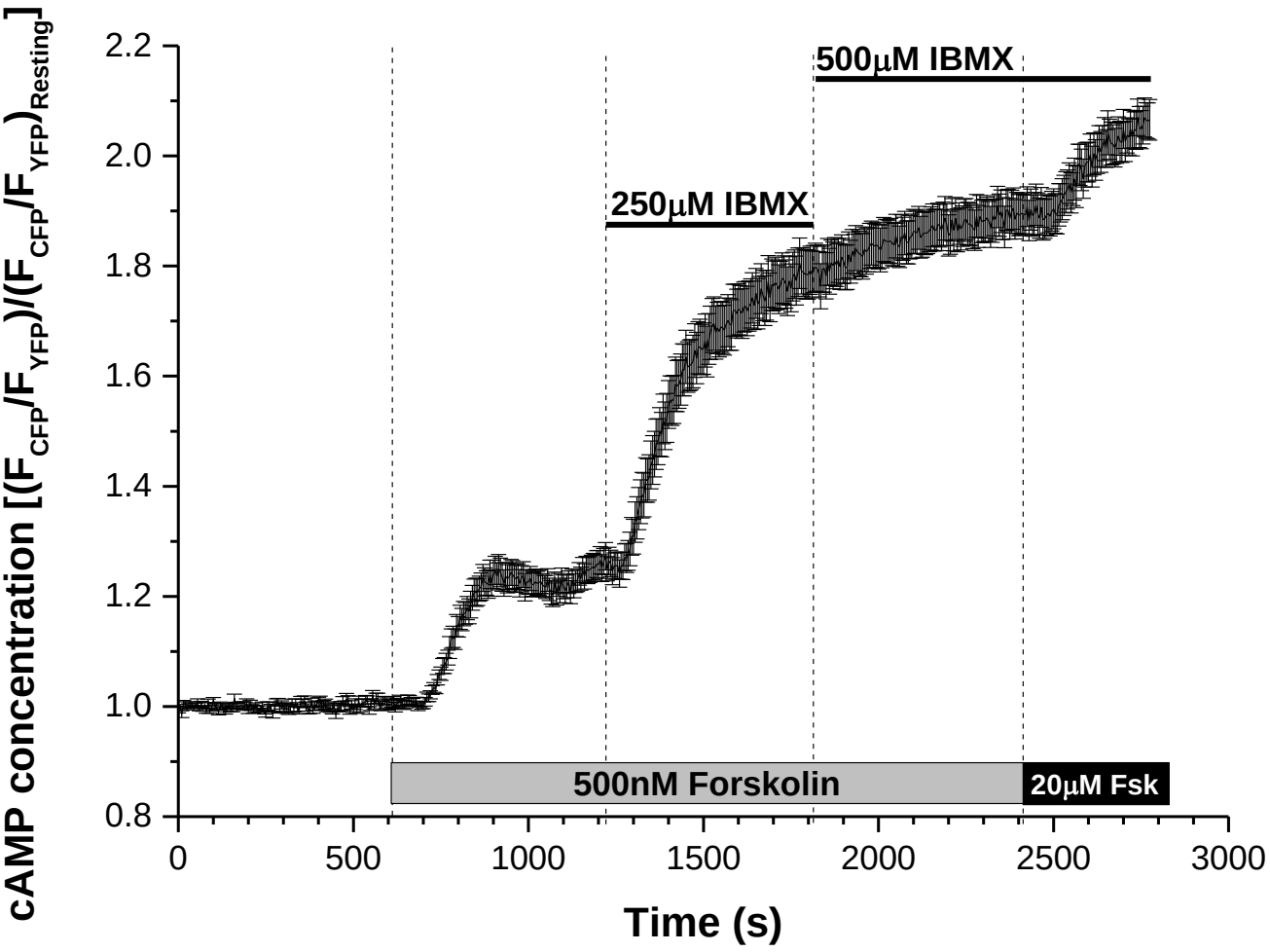

Figure 3.1.1 Effects of forskolin and IBMX on cAMP concentration in PANC-1 cells.

PANC-1 cells transfected with H134 were first subjected to forskolin (500nM) treatment before IBMX (250μM) was added without the removal of forskolin. The concentration of IBMX was doubled (500μM) before the additive increase of forskolin concentration (20μM) at the end of the experiment (n=3 experiments, n=20 cells).

3.1.2. Cilostazol significantly increases cAMP concentration in PANC-1 cells

PDE3 and PDE4 were chosen to be the starting point as it was previously mentioned that both of these isoforms perform the bulk of cAMP destruction in most cells (Bender and Beavo, 2006). Firstly, to reveal PDE activity, we treated PANC-1 cells with the PDE3 inhibitor Cilostazol (CLZ) (Schror, 2002) in the presence of forskolin and recorded the F_{CFP}/F_{YFP} ratio. The addition of 5µM CLZ after the formation of the forkolin-induced cAMP plateau produced additive effects, as reported by the increase in the F_{CFP}/F_{YFP} ratio during CLZ treatment (3.1.2). This observation strongly suggests PDE3 to be active in PANC-1 cells.

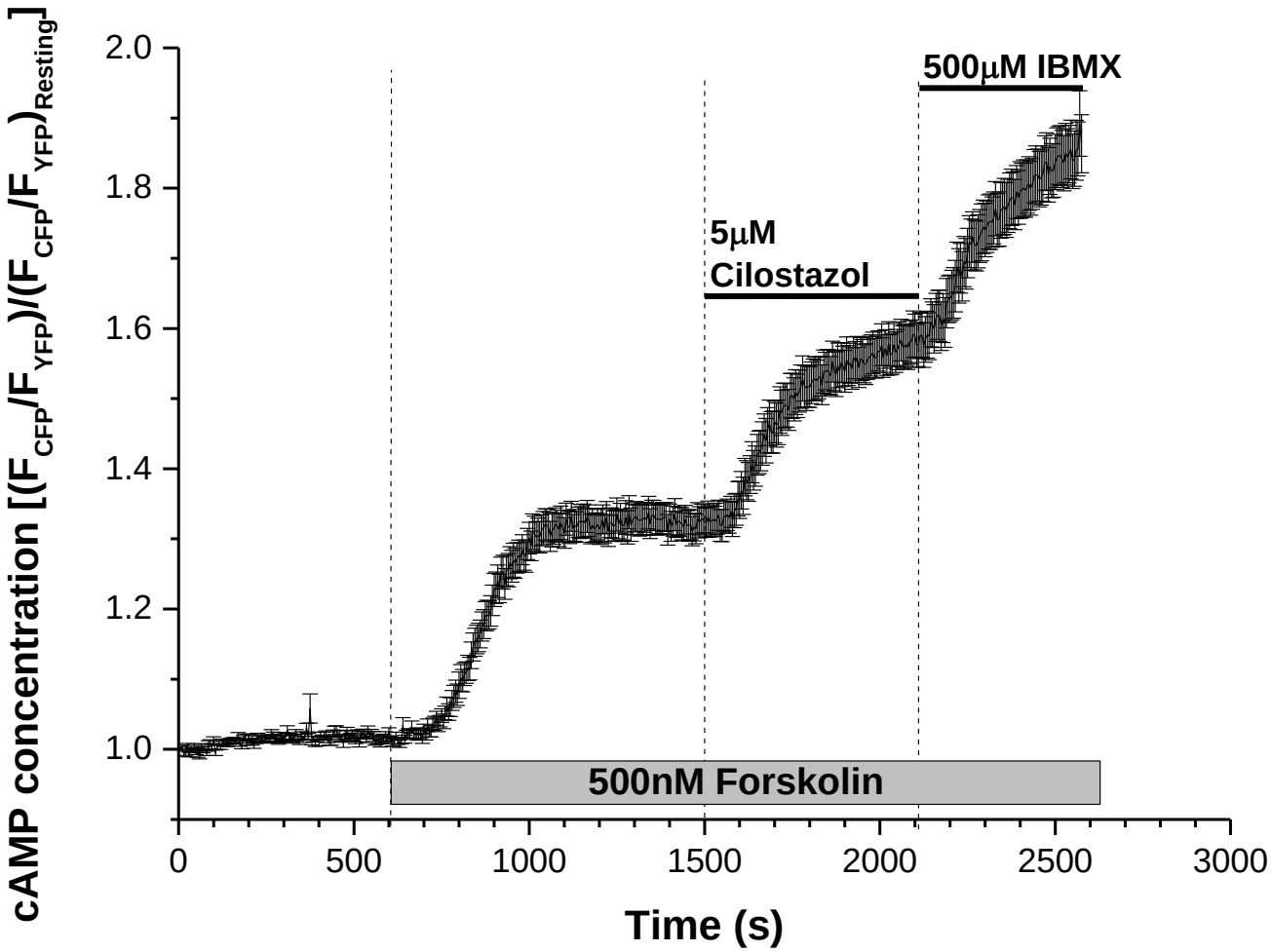

Figure 3.1.2. Cilostazol, an inhibitor of PDE3, significantly increases cAMP concentration in PANC-1 cells.

PANC-1 cells expressing H134 were first treated with forskolin (500nM) for 15 minutes before cilostazol (5μM) was additively applied for 10 minutes. IBMX (500μM) was added at the end of the experiment (n=6 experiments, n=29 cells).

3.1.3. Testing high doses of cilostazol in PANC-1 cells.

Cilostazol has been successfully used for PDE3 inhibition in various systems, with the concentration required depending on the cell type tested. For example, less than 5µM was required in primary human platelets and (Liu et al., 2004), and both concentrations of 1µM and 10µM had been used successfully on human endothelial cells (Kim et al., 2014, Kim et al., 2002, Omi et al., 2004). 10µM was optimal for melanoma cells and chondrocytes (Wei et al., 2014, Wang et al., 2014), whereas higher concentrations of 50µM and 100µM was used for colon cancer cells and human monocytic leukaemia cell lines, respectively (Chuang et al., 2011, Murata et al., 1999).

Therefore, to determine the maximal inhibitory effect of this compound for PDE3, we tested three different concentrations of cilostazol (5µM, 10µM and 50µM) on PANC-1 cells against the background forskolin-induced cAMP response. It seems that 5µM, the smallest concentration tested, appeared to be enough to fully inhibit PDE3 activity in PANC-1 cells and in so doing increasing cAMP production; as higher concentrations of cilostazol (10 and 50µM) did not increase cAMP levels any further, as reported by the $F_{(CFP/YFP)}$ ratio (fig 3.1.3). In conclusion, 5µM cilostazol was sufficient for full PDE3 inhibition in PANC-1 cells.

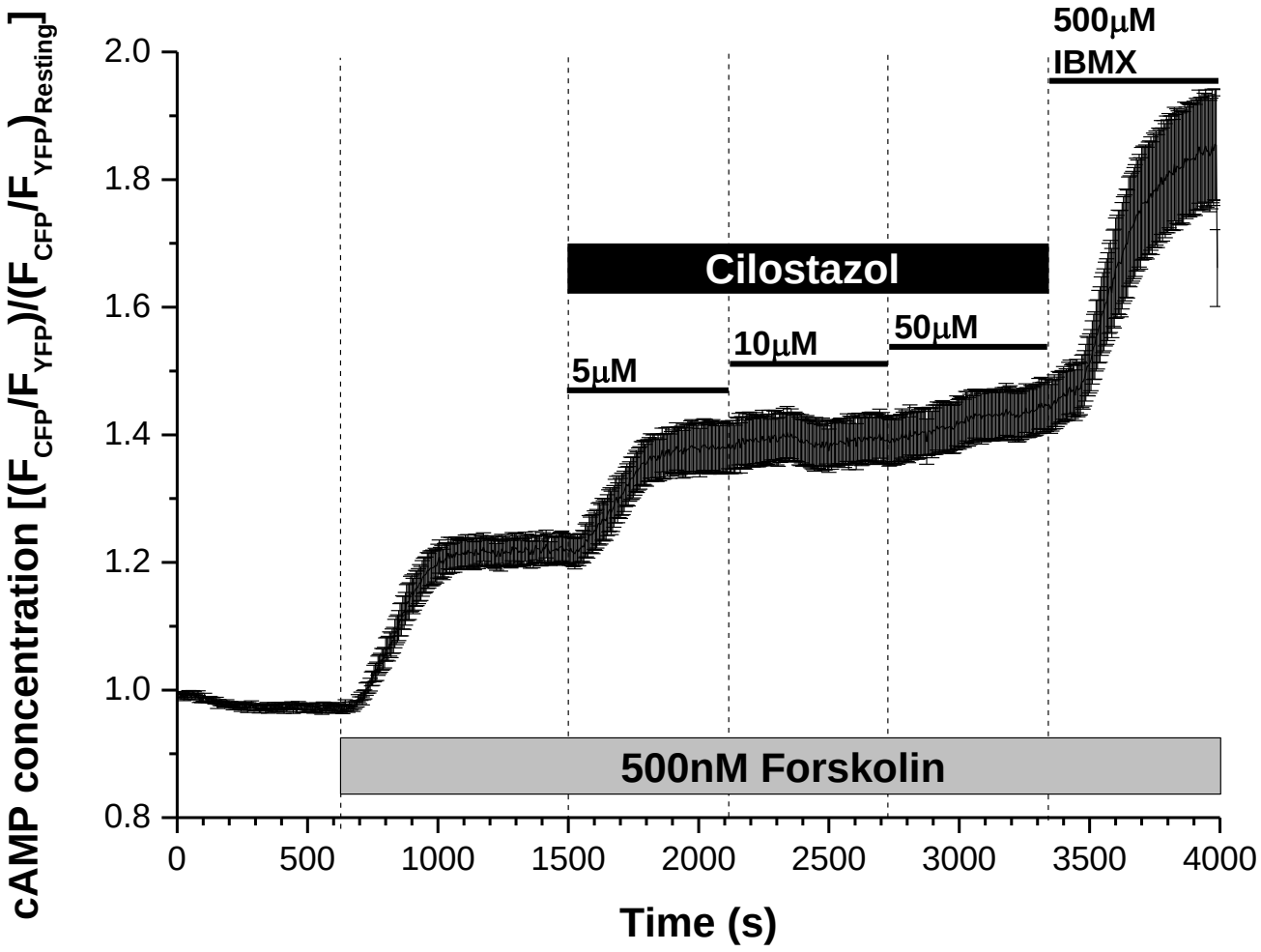

Figure 3.1.3. The effect of increasing concentrations of cilostazol on cAMP levels in PANC-1 cells.

PANC-1 cells expressing H134 were first treated with forskolin (500nM) for 15 minutes before increasing concentrations of cilostazol (5, 10 and then 50μM) were applied additively for 10 minutes. IBMX (500μM) was added at the end of the experiment (n=4 experiments, n=21 cells).

3.1.4. Testing for PDE4 activity in PANC-1 cells

To test for potential PDE4 activity in PANC-1 cells, we used rolipram, a well-known PDE4 inhibitor (Teixeira et al., 1997). After pre-treatment of H134-transfected cells with forskolin, rolipram was added to see if a similar response to cilostazol could be observed. The concentration was set at 10μM, which has been demonstrated to effectively inhibit PDE4 in other human cell types, including some cancers (Moon et al., 2012, Santamaria et al., 1999, Henderson et al., 2014, McEwan et al., 2007, Tsunoda et al., 2012, Marquette et al., 2011). As shown in figure 3.3, PDE4 appeared to be active in PANC-1 cells, as the addition of rolipram after 15 minutes of forskolin pre-treatment caused a resolvable increase in the F_{CFP}/F_{YFP} ratio (figure 3.1.4). These observations suggest that PDE4 is also active in PANC-1 cells, though PDE3 appears to be the more important regulator of cAMP in this cell type.

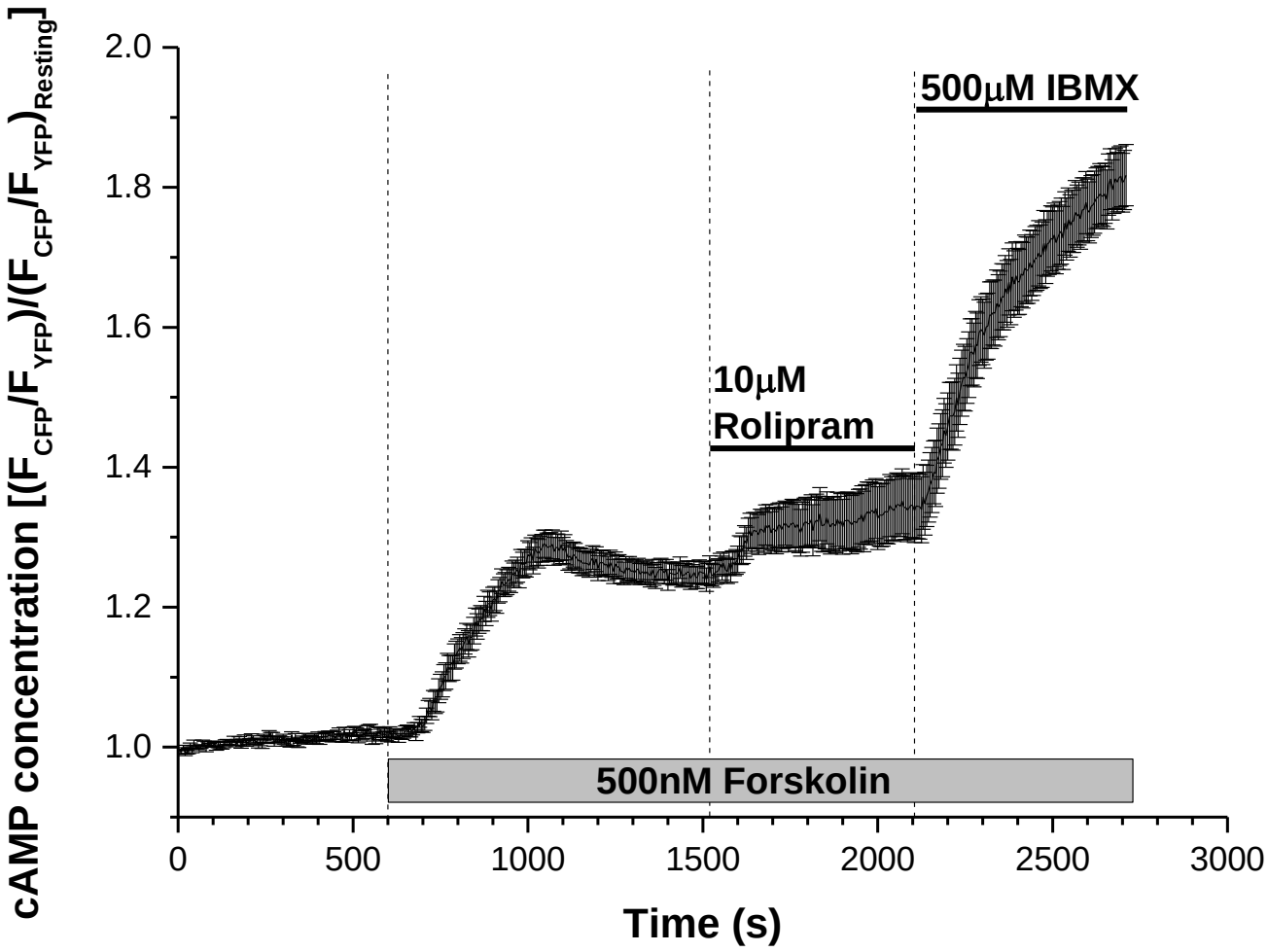

Figure 3.1.4. The effect of rolipram, an inhibitor of PDE4, on cAMP concentration in PANC-1 cells.

PANC-1 cells expressing H134 were first treated with forskolin (500nM) for 15 minutes before they were treated with rolipram (10μM) additively for 10 minutes. IBMX (500μM) was added at the end of the experiment (n=6 experiments, n=33 cells).

3.1.5. Testing for PDE1 activity in PANC-1 cells

8-methoxymethyl-IBMX (8-mm-IBMX), was used at 100µM, a concentration previously reported to inhibit PDE1 activity in pancreatic β-cells and human arterial smooth muscle cells (Tian et al., 2012, Rybalkin et al., 2002). It was used to test for PDE1 activity in PANC-1 cells in the continuous presence of forskolin.

Interestingly, 8-mm-IBMX produced a small but noticeable increase from the forskolin plateau, but the increase returned to pre-treatment levels within 10 minutes (figure 3.1.5). While this does suggests that this Ca^{2+}-sensitive PDE is present and active in PANC-1 cells, but is unlikely to play a major role in the regulation of cAMP levels.

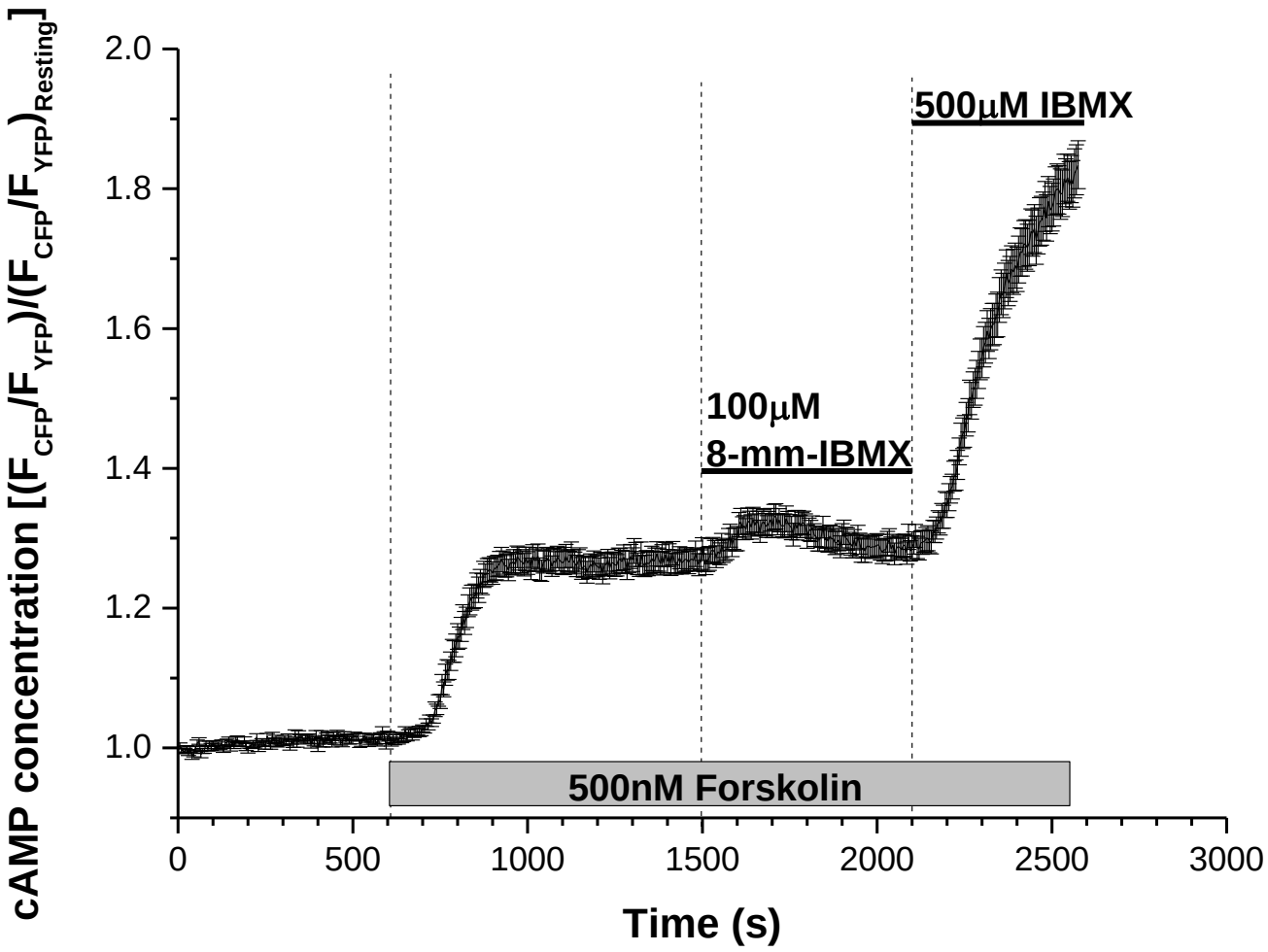

Figure 3.1.5. The effect of 8-mm-IBMX, an inhibitor of PDE1, on cAMP concentration in PANC-1 cells.

PANC-1 cells expressing H134 were first treated with forskolin (500nM) for 15 minutes before 8-methoxymethyl-IBMX (100μM) was applied additively for 10 minutes. IBMX (500μM) was added at the end of the experiment (n=11 experiments, n=42 cells).

3.1.6. Testing for PDE2 activity in PANC-1 cells

To probe for the presence of PDE2 in PANC-1 cells, EHNA, a well-known inhibitor for this isoform (Podzuweit et al., 1995), was used. Although some past studies with EHNA reported that <50μM was sufficient for effective PDE2 inhibition (Saito et al., 2010, Hashemi et al., 2005, Burton et al., 2010, Adderley et al., 2009), in our study we decided to use 100μM, a concentration used to inhibit PDE2 in human melanoma cells (Morita et al., 2013, Hiramoto et al., 2014), in order to maximise the inhibition of this enzyme, if present.

After 15 minutes of forskolin treatment, 100μM EHNA addition did not appeared to have any further effects (figure 3.1.6), suggesting that PDE2 is not active in PANC-1 cells.

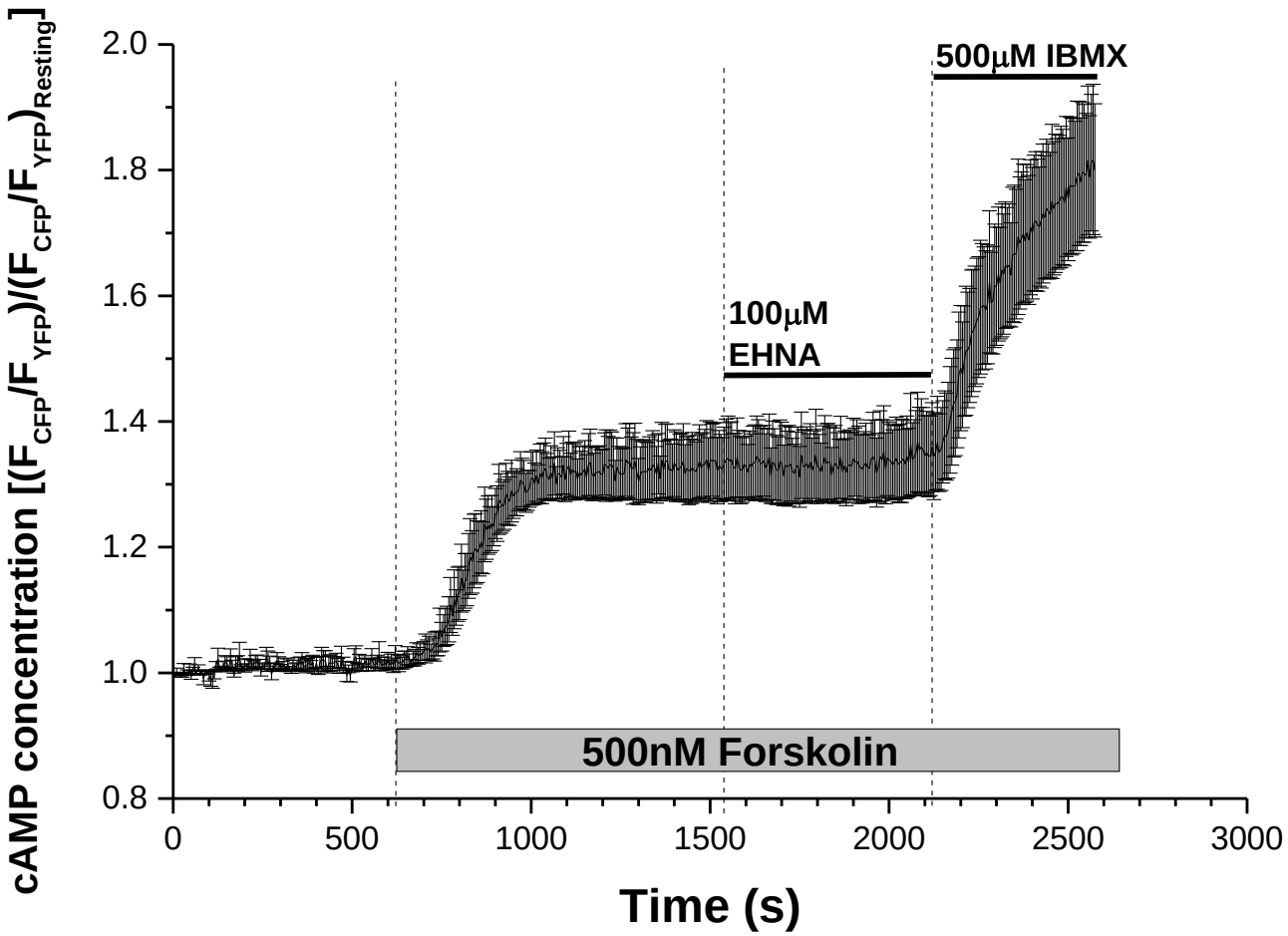

Figure 3.1.6. The effect of EHNA, a PDE2 inhibitor, on cAMP levels in PANC-1 cells.

PANC-1 cells expressing H134 were first treated with forskolin (500nM) for 15 minutes before EHNA (100μM) was applied additively for 10 minutes. IBMX (500μM) was added at the end of the experiment (n=13 experiments, n=47 cells).

3.1.7. Testing for PDE5 activity in PANC-1 cells

To test if preventing cGMP breakdown has any influence on cAMP levels in PANC-1 cells, we treated PANC-1 cells with a highly potent PDE5 inhibitor T-0156 (Mochida et al., 2002), after the induction of forskolin plateau. A concentration of 1µM, previously reported to effectively inhibit PDE5 (Santos et al., 2014, Santos-Silva et al., 2008, Liu et al., 2008), was chosen. As shown in figure 3.1.7, T-0156 in the presence of forskolin induced a slight decrease on the F_{CFP}/F_{YFP} ratio, but the effect was not significant. These results suggest that either endogenous cGMP production is too low to have any effects, or that cGMP accumulation as a result of PDE5 inhibition had no effects on cAMP levels in PANC-1 cells. However, taken together with the results from EHNA experiments shown in figure 3.1.6, the data here suggests that the cGMP-activated PDE2 and the cGMP specific PDE5 are unlikely to have a substantial influence of on cAMP signalling in PANC-1 cells, though the cGMP-induced inhibition of PDE3 remains a possibility.

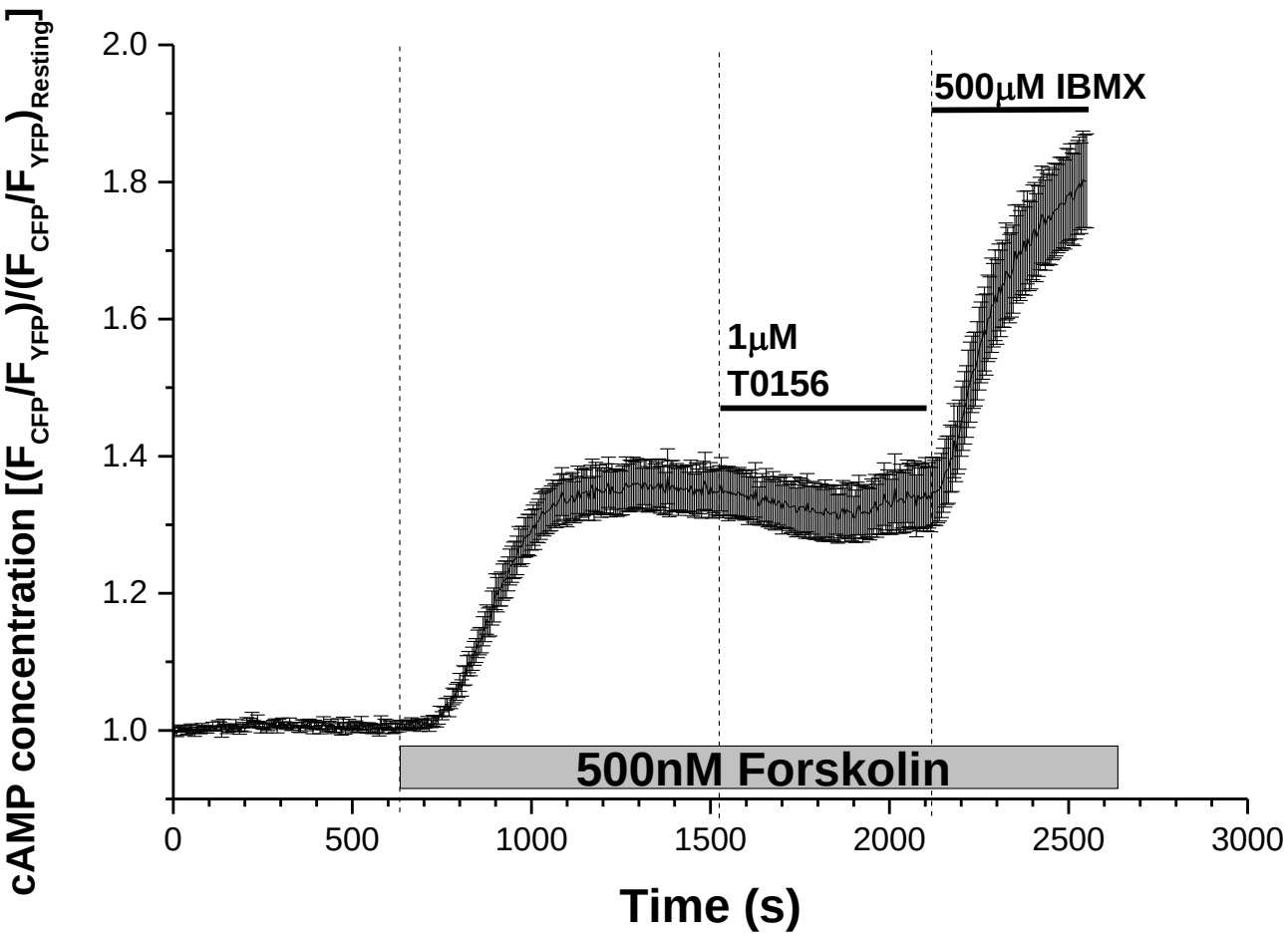

Figure 3.1.7. The effect of PDE5 inhibition on cAMP concentration in PANC-1 cells.

PANC-1 cells expressing H134 were first treated with forskolin (500nM) for 15 minutes before T0156 (1μM) was applied additively for 10 minutes. IBMX (500μM) was added at the end of the experiment (n=6 experiments, n=22 cells).

3.1.8. Testing for PDE7 activity in PANC-1 cells

To test for PDE7 activity in PANC-1 cells, the compound BRL-50481 (BRL), previously reported to inhibit PDE7 selectively with maximum inhibition achieved at 30µM (Smith et al., 2004), was used here. Although previous studies have utilised a higher concentration to inhibit PDE7 activity in other systems (Zhang et al., 2008a, Pekkinen et al., 2008), the concentration chosen for this drug was 10µM for this study as a starting point.

When applied after the induction of a forskolin plateau, 10µM BRL-50481 somehow caused a slight, paradoxical decrease in F_{CFP}/F_{YFP} ratio; which may be due to an off-target effect of this compound (fig 3.1.8). Nonetheless, this was not investigated further as no cell tested displayed any increases in cAMP concentration in response to this compound. This observation suggests that PDE7 activity cannot be revealed by BRL-50481 in PANC-1 cells.

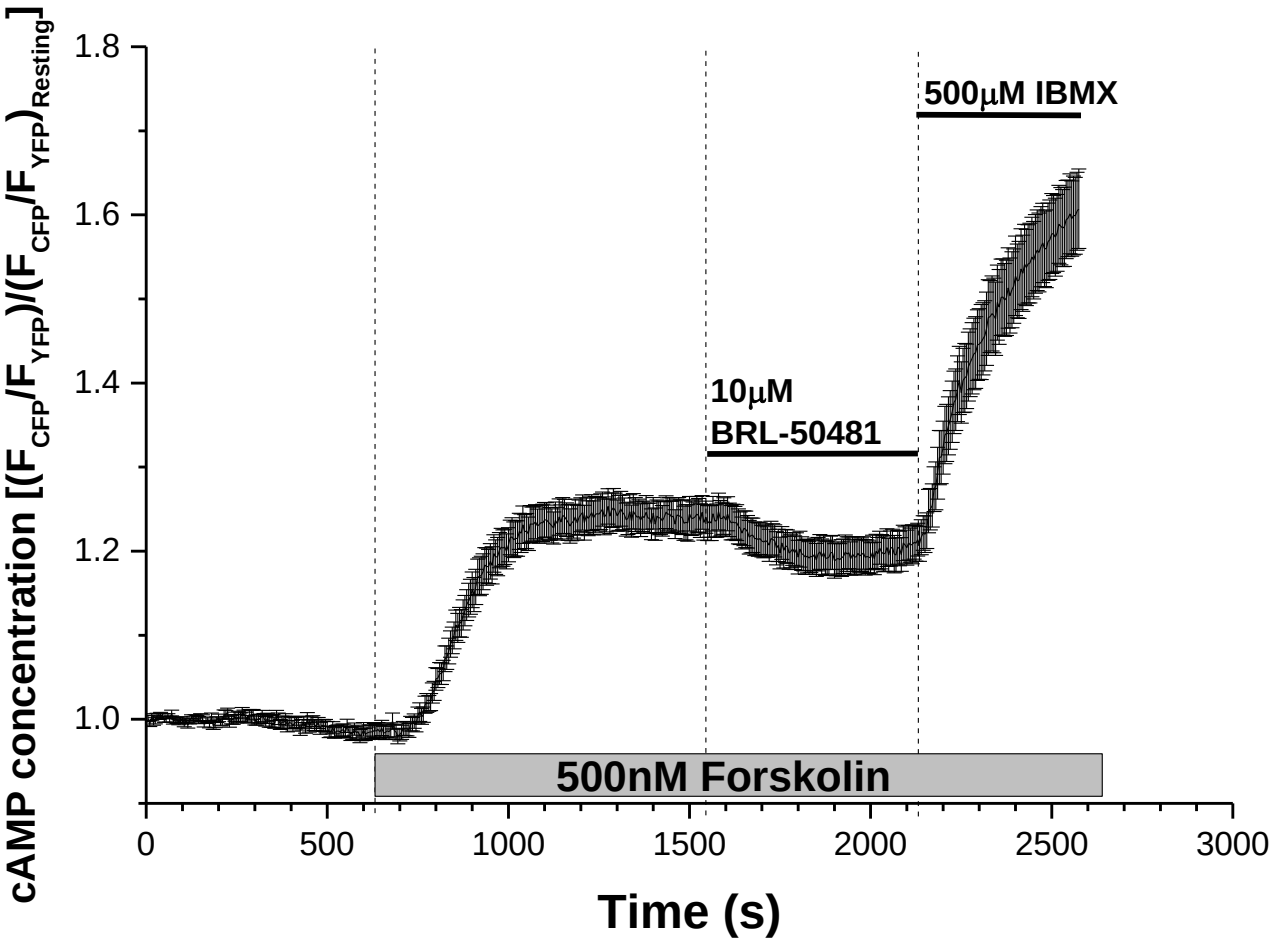

Figure 3.1.8. The effect of BRL-50481, a PDE7 inhibitor, on cAMP levels in PANC-1 cells.

PANC-1 cells expressing H134 were first treated with forskolin (500nM) for 15 minutes before BRL-50481 (10μM) was applied additively for 10 minutes. IBMX (500μM) was added at the end of the experiment (n=10 experiments, n=29 cells).

3.1.9. Testing for PDE11 activity in PANC-1 cells

To test for PDE11 activity in PANC-1 cells we employed the use of the recently discovered inhibitor for this isoform, BC11-38, with an IC_{50} of 0.28μM (Ceyhan et al., 2012). Therefore, as a starting point we decided to use 10μM. After forskolin pre-treatment, BC11-38 did not seem to have any effects on the F_{CFP}/F_{YFP} ratio after the initial increase caused by forskolin treatment (fig 3.1.9); which suggests that PDE11 is not active in PANC-1 cells.

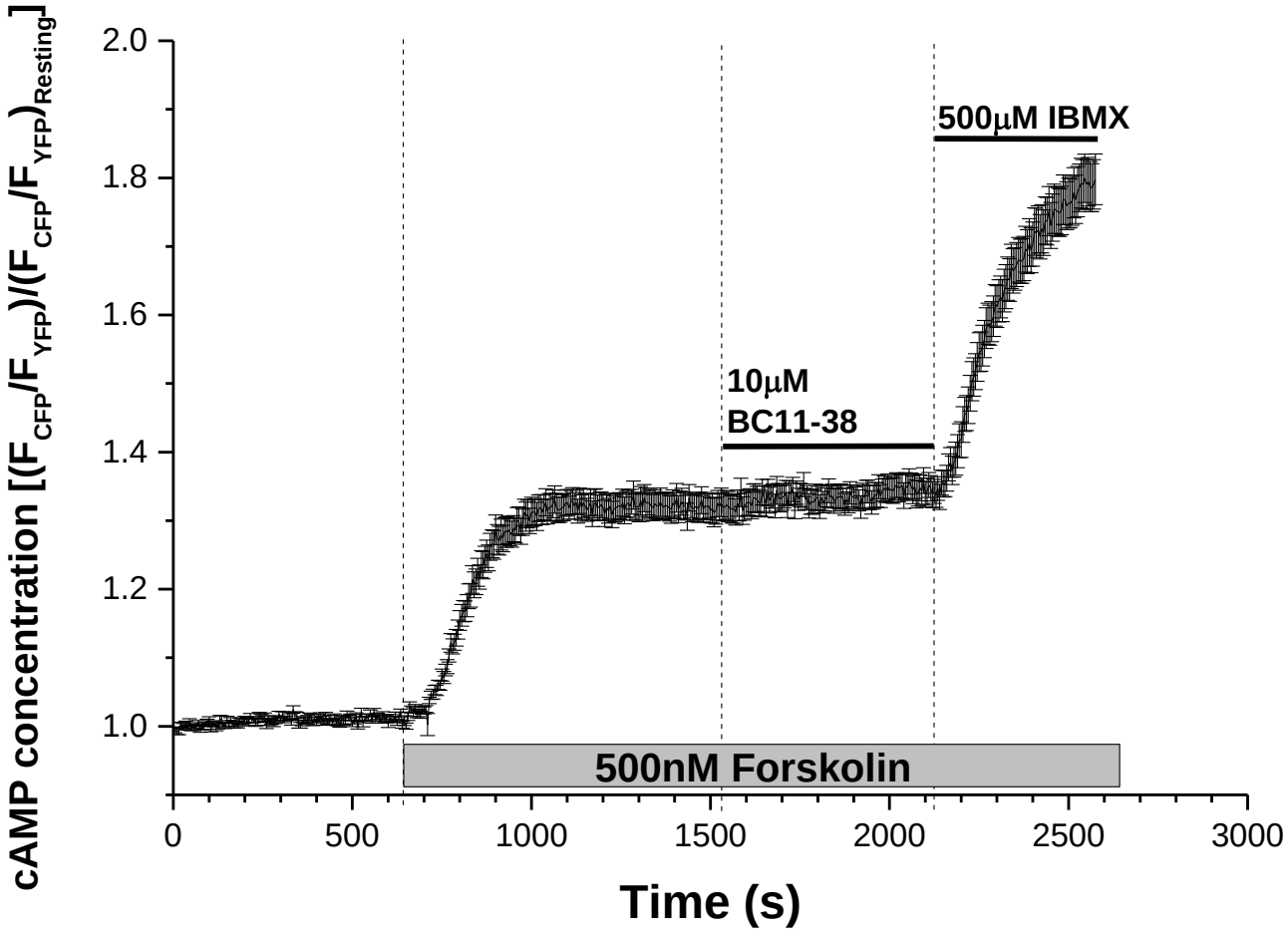

Figure 3.1.9. The effect of BC11-38, an inhibitor of PDE11, on cAMP concentration in PANC-1 cells.

PANC-1 cells expressing H134 were first pre-treated with forskolin (500nM) for 15 minutes before BC11-38 (10μM) was additively applied for 10 minutes. IBMX (500μM) was added at the end of the experiment as the positive control (n=8 experiments, n=16 cells).

3.1.10. A preliminary test for PDE10A activity in PANC-1 cells

Next, the activity of PDE10A was tested, using papaverine, a well-known semi-specific inhibitor for this PDE isoform (Li et al., 2014, Siuciak et al., 2006), at a concentration of 10μM, which was used to successfully inhibit PDE10A (Tian et al., 2011b, Nishi et al., 2008, Hsu et al., 2011). Due to concordant reports across various suppliers of this drug that papaverine also inhibits PDE3 at a nanomolar range, which we now know to be the dominant isoform in PANC-1 cells, cilostazol treatment was carried out 10 minutes before the addition of papaverine to ensure that any cAMP increases observed after papaverine treatment is more likely to be due PDE10A than PDE3. After the increase in the F_{CFP}/F_{YFP} ratio as a result of cilostazol addition, papaverine significantly increased cAMP concentrations further in PANC-1 cells in the presence of cilostazol (figure 3.1.10); suggesting that PDE10A is likely to be active in PANC-1 cells. However, due to the poor selectivity of this compound, other interpretations of these results are possible.

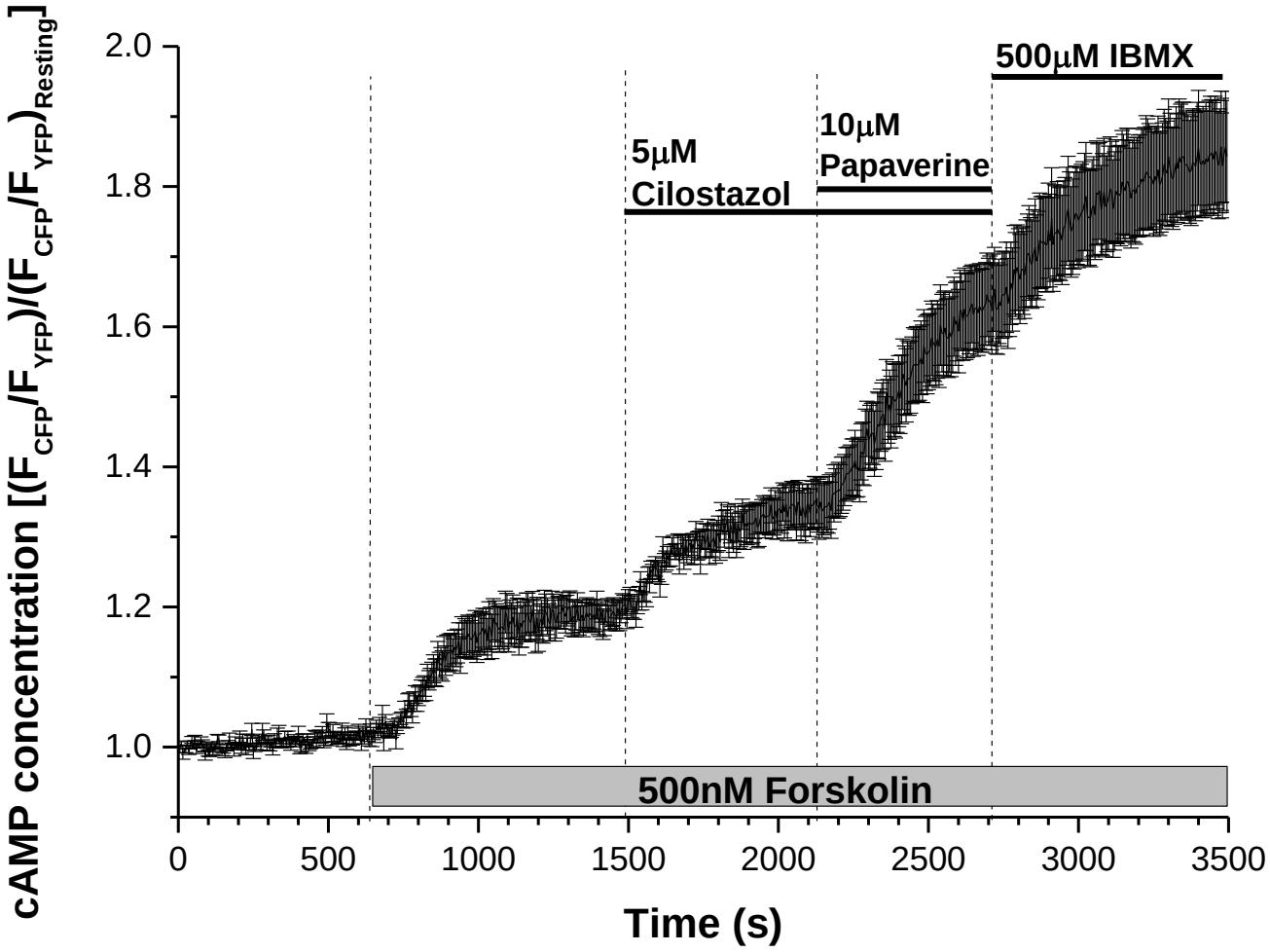

Figure 3.1.10. The effect of papaverine, a semi-specific inhibitor of PDE10A, on cAMP concentration in PANC-1 cells in the presence of cilostazol.

PANC-1 cells expressing H134 were first treated with forskolin (500nM) for 15 minutes before cilostazol (5μM) was applied additively for 10 minutes. Papaverine (10μM) was added in the presence of cilostazol for a further 10 minutes before IBMX (500μM) was added at the end of the experiment (n=2 experiments, n=10 cells).

3.1.11. Testing combined PDE3 and PDE4 inhibition on cAMP signalling in PANC-1 cells

Out of the 7 compounds that were tested alone in this study, cilostazol (CLZ), when applied after the establishment of forskolin plateaus, was the only agent that increased cAMP concentrations in almost all PANC-1 cells tested. Yet, compared with its corresponding positive control (IBMX treatment), only approximately half of the total inhibition at that level of stimulus is down to PDE3. This strongly suggests that although PDE3 is the major isoform in PANC-1 cells, other PDE isoforms were in operation to keep cAMP levels in check. This candidate appears to be PDE4 because while its inhibitor rolipram only increased cAMP concentrations mildly, it was still the second best compound in terms of strength and clarity of response. To test this possibility, a similar experiment to figure 3.1.10 was carried out, in which 5µM CLZ was first added after the induction of the forskolin-induced plateau as a pre-treatment; then the cells were treated with rolipram in the presence of CLZ. As figure 3.1.11 shows, CLZ treatment increased the F_{CFP}/F_{YFP} ratio in the presence of forskolin, and the subsequent addition of rolipram produced an additive increase to the ratio; an effect that brought the relative cAMP concentration close to the maximal response. These results support the hypothesis that PDE3 and PDE4 are both active in PANC-1 cells, and that they carry out the bulk of cAMP destruction in PANC-1 cells.

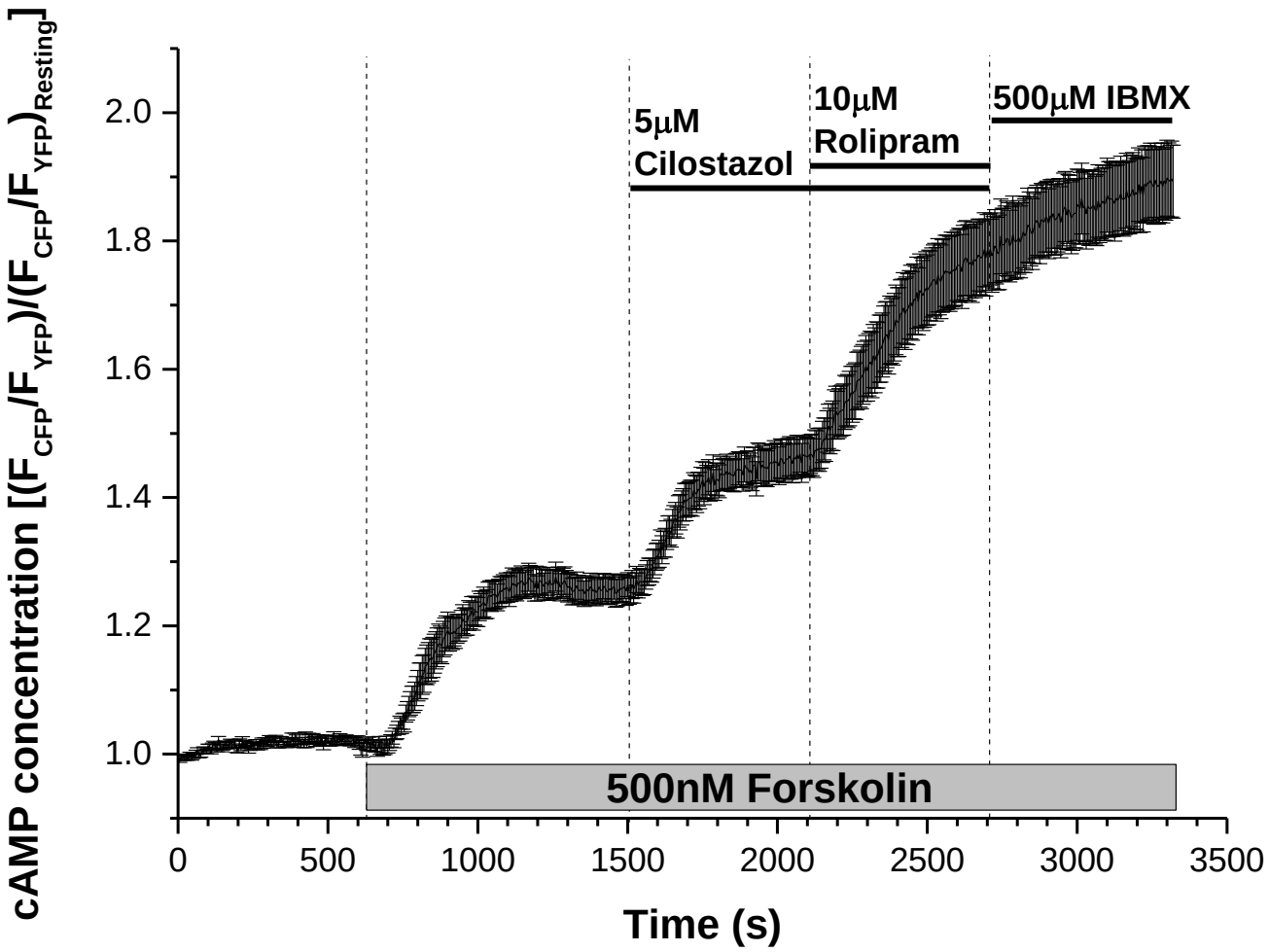

Figure 3.1.11. Effects of rolipram on PANC-1 cells in the presence of Cilostazol.

PANC-1 cells expressing H134 were first treated with forskolin (500nM) for 15 minutes before being treated additively, first with cilostazol (5μM) and then rolipram (10μM), both for 10 minutes. IBMX (500μM) was added at the end of the experiment (n=7 experiments, n=20 cells).

3.2. Characterisation of cAMP agonists in PANC-1 cells

Having established the role of individual PDEs in controlling cAMP responses research direction was then shifted to asking how cAMP signalling can be physiologically activated in PANC-1 cells. Four different well-known Gαs-GPCR agonists, Isoproterenol, Vasoactive Intestinal peptide (VIP), Secretin, and Ilosprost (stable analog of prostacyclin), were tested on H134-transfected cells to measure their cAMP levels.

3.2.1. Effects of β-adrenergic agonists on PANC-1 cAMP levels

Isoproterenol, a well-known β-adrenergic agonist (Roze et al., 1976) in the exocrine pancreas, was first tested for their ability to activate cAMP signalling in H134-transfected PANC-1 cells. As a preliminary measure to first qualitatively observe if this agent has any effects, cells were treated with just 1 concentration, 10nM, of Isoproterenol, for 20 minutes. As shown in figure 3.2.1, 10nM Isoproterenol increased cAMP levels in PANC-1 cells, with the F_{CFP}/F_{YFP} ratio increasing significantly within 5 minutes of treatment before starting to slowly decline after the highest point was reached. This observation confirms the presence of AC-stimulating β-adrenergic receptors in PANC-1 cells.

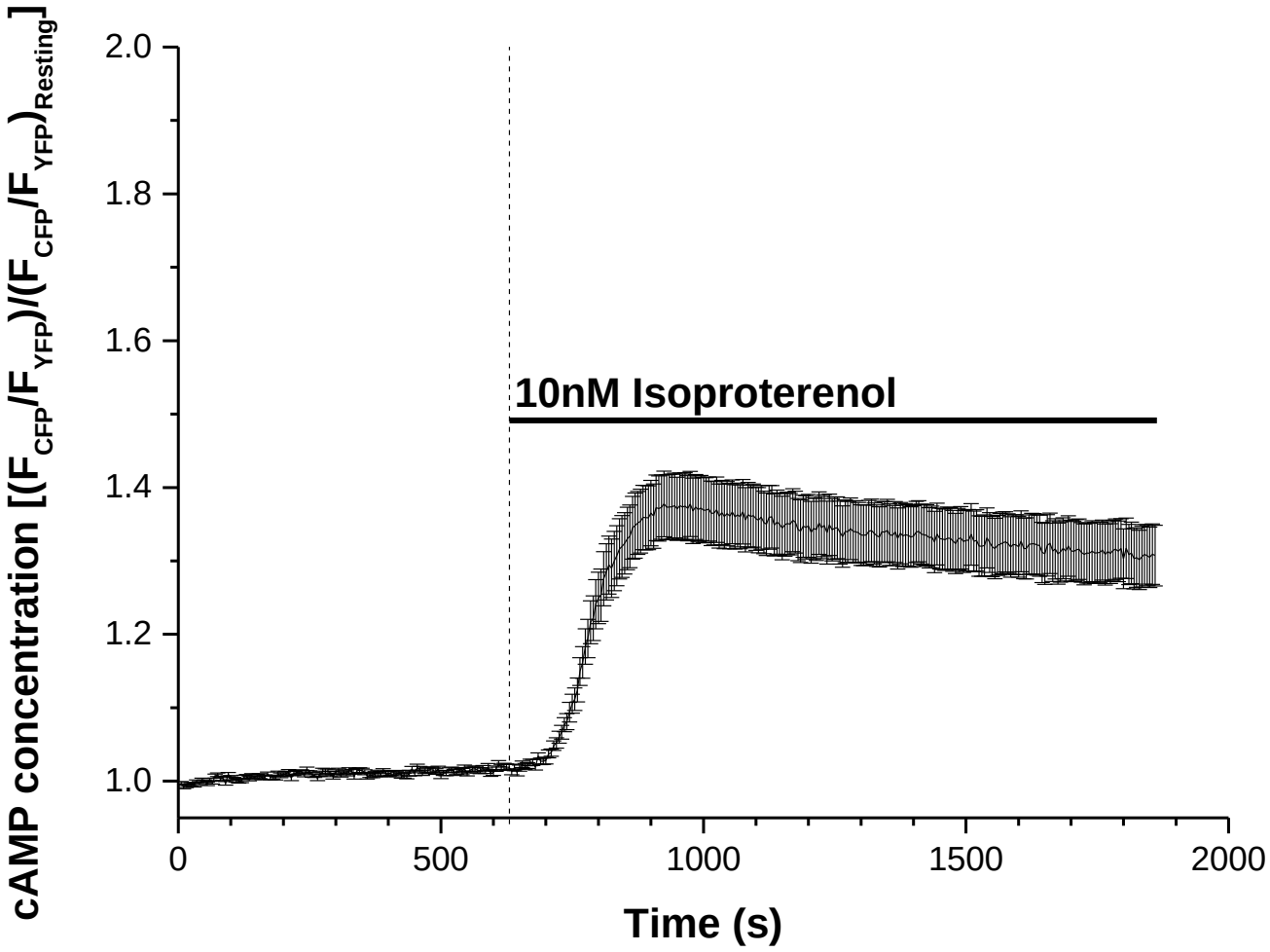

Figure 3.2.1. Isoproterenol increases cAMP levels in PANC-1 cells.

PANC-1 cells expressing H134 were treated with the β-adrenergic agonist isoproterenol (10nM) for 20 minutes (n=10, n=55 cells).

3.2.2. Concentration – dependent response of Isoproterenol in PANC-1 cells

Having found that β-adrenergic receptors are present in PANC-1 cells in figure 3.2.1, we then asked if the isoproterenol response is dependent on the concentration. Therefore, in a similar experiment, H134-transfected PANC-1 cells were treated with increasing concentrations of isoproterenol (1, 10 and then 100nM) as their cAMP levels were measured. Results in figure 3.2.2A have shown that the amount of this Gαs-cAMP stimulation is dependent on the drug concentration; as increasing concentrations of isoproterenol (1nM, 10nM and 100nM) cumulatively increased the F_{CFP}/F_{YFP} ratio.
In a separate set of experiments cells underwent 20 minutes of 1nM isoproterenol treatment before the concentration was increased to 100nM to end the experiment; bypassing the 10nM treatment in 3.2.2A. Figure 3.2.2B appeared to show that 1nM isoproterenol mildly but notably increased the F_{CFP}/F_{YFP} ratio before holding that value at a plateau for 20 minutes, before the subsequent addition of 100nM isoproterenol which drastically increased this ratio further. These observations show that isoproterenol activates cAMP signalling in a dose dependent manner in PANC-1 cells.

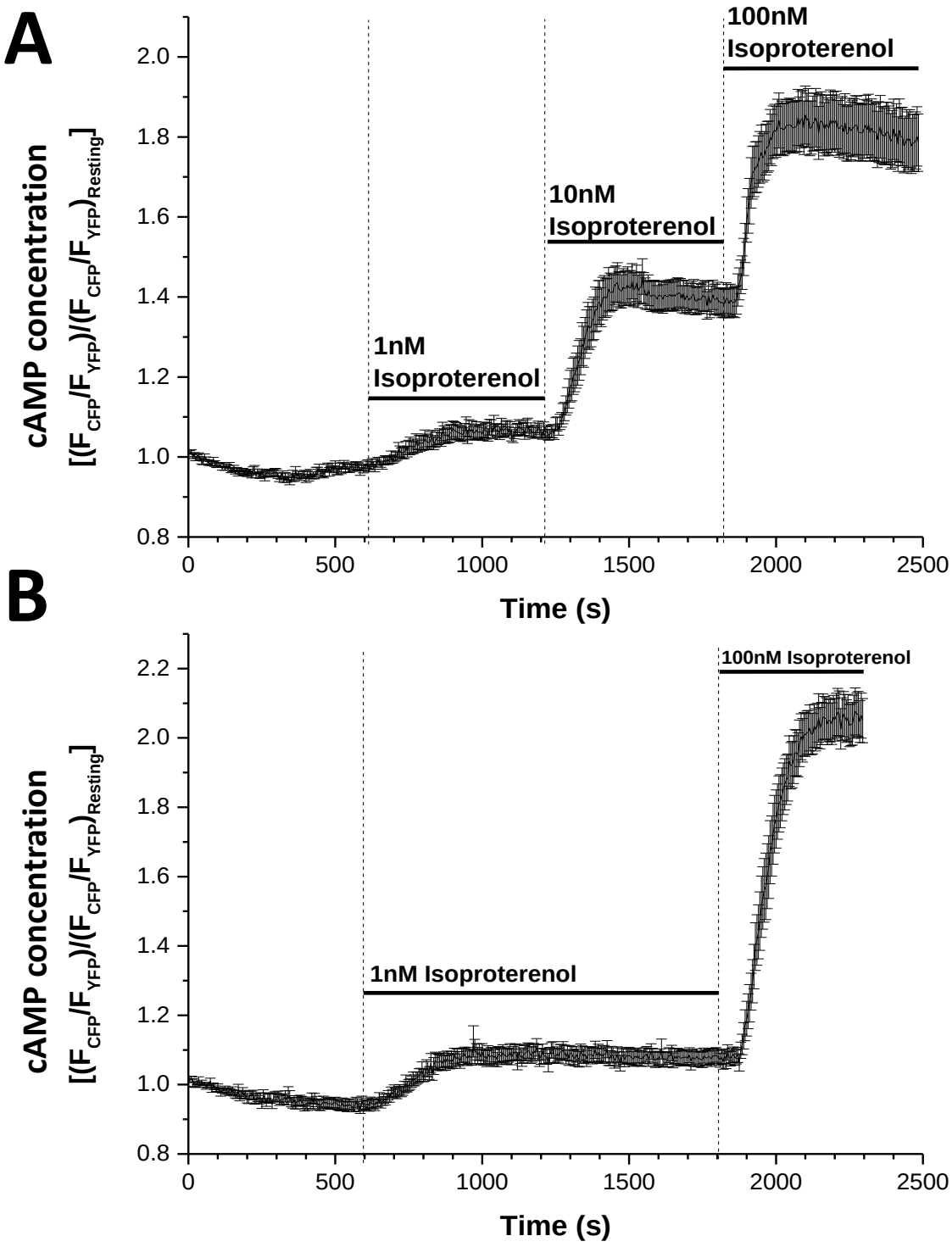
A
cAMP concentration
[(F_CFP/F_YFP)/(F_CFP/F_YFP)_Resting]
1nM Isoproterenol
10nM Isoproterenol
100nM Isoproterenol
Time (s)
B
cAMP concentration
[(F_CFP/F_YFP)/(F_CFP/F_YFP)_Resting]
1nM Isoproterenol
100nM Isoproterenol
Time (s)

Figure 3.2.2. Isoproterenol increases cAMP levels in PANC-1 cells in a dose-dependent manner.

A, PANC-1 cells expressing H134 were treated with increasing concentrations (1nM, 10nM, and 100nM) of the β-adrenergic agonist isoproterenol for 10 minutes each (n=4 experiments, n=27 cells). B, PANC-1 cells expressing H134 were treated with a small concentration of isoproterenol (1nM) for 20 minutes before the isoproterenol treatment concentration was increased 100 fold (n=4 experiments, n=24 cells).

3.2.3. Effects of VIP and Secretin on cAMP signalling in PANC-1 cells

Next, we decided to test the effects of VIP and secretin, two agonists well known to activate cAMP signalling in pancreatic acinar cells (Christophe et al., 1976), from which pancreatic cancers may derive from (Schmid, 2002). H134-transfected PANC-1 cells were treated with increasing concentrations of VIP or secretin (1nM, 10nM, and 100nM) before 100nM isoproterenol was added to show that the same cells can still be externally triggered to produce cAMP. From figure 3.2.3 it seemed that neither VIP (A) nor secretin (B) increased cAMP levels in PANC-1 cells unlike isoproterenol; suggesting that either the activity of VIP and secretin was masked by the high endogenous PDE activity, or that VIP or secretin receptors are not expressed in PANC-1 cells.

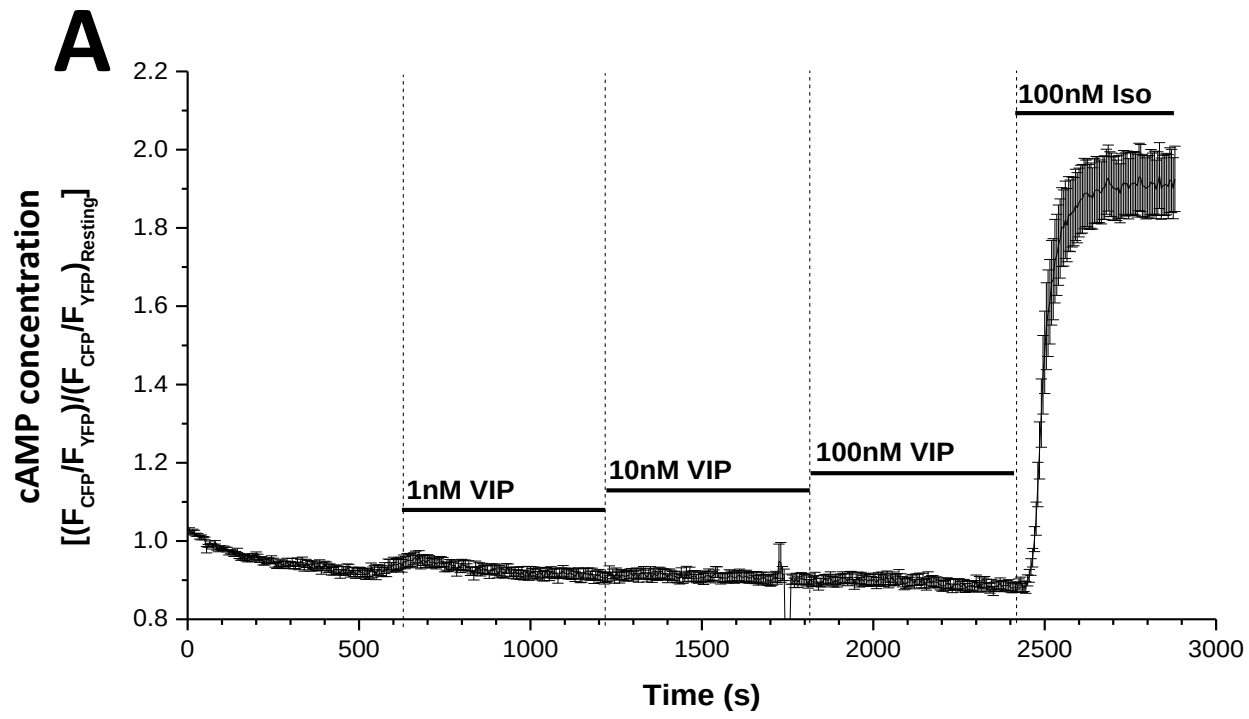
A
cAMP concentration
[(F_CFP/F_YFP)/(F_CFP/F_YFP)_Resting]
2.2
2.0
1.8
1.6
1.4
1.2
1.0
0.8
0
500
1000
1500
2000
2500
3000
Time (s)
1nM VIP
10nM VIP
100nM VIP
100nM Iso

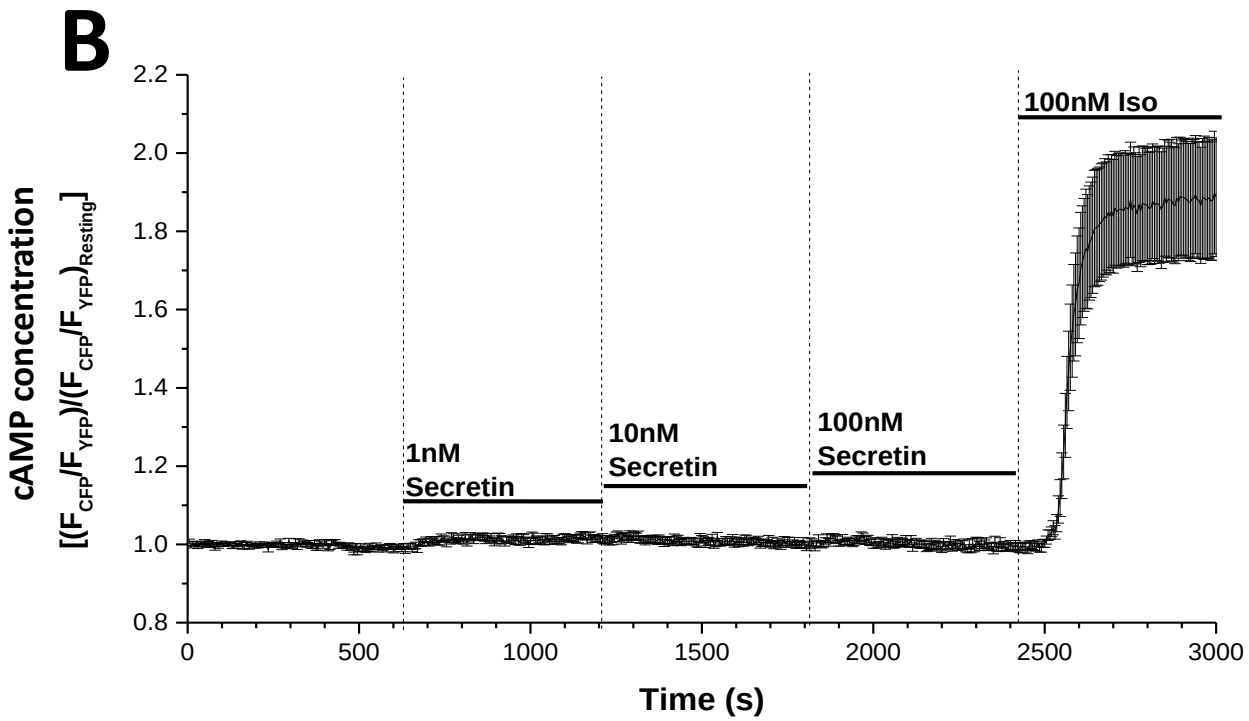
B
cAMP concentration
[(F_CFP/F_YFP)/(F_CFP/F_YFP)_Resting]
2.2
2.0
1.8
1.6
1.4
1.2
1.0
0.8
0
500
1000
1500
2000
2500
3000
Time (s)
1nM
Secretin
10nM
Secretin
100nM
Secretin
100nM Iso

Figure 3.2.3. VIP and secretin do not increase cAMP levels in PANC-1 cells.

PANC-1 cells expressing H134 were treated with increasing concentrations (1nM, 10nM, and 100nM) of VIP for 10 minutes each (n=3 experiments, n=18 cells). B, PANC-1 cells expressing H134 were treated with increasing concentrations (1nM, 10nM, and 100nM) of secretin for 10 minutes each (n=2 experiments, n=10 cells). On both occasions isoproterenol (100nM) was added at the end of each experiment as positive control.

To ask if the lack of cAMP increase as a result of VIP and secretin treatment was due to the high PDE activity in PANC-1 cells, we have also conducted experiments similar to those described in 3.2.3 but utilised IBMX as the positive control. In these experiments we did not observe responses in cAMP concentrations to 100nM of VIP (A) or 100nM secretin (B) treatment as displayed in figure 3.2.4. Considering that Isoproterenol at just 10nM have the capacity to potently increase F_{CFP}/F_{YFP} ratio without the presence of IBMX (figure 3.2.1), this small increase at the end of the experiments is most likely due to IBMX-mediated PDE inhibition rather than VIP or secretin.

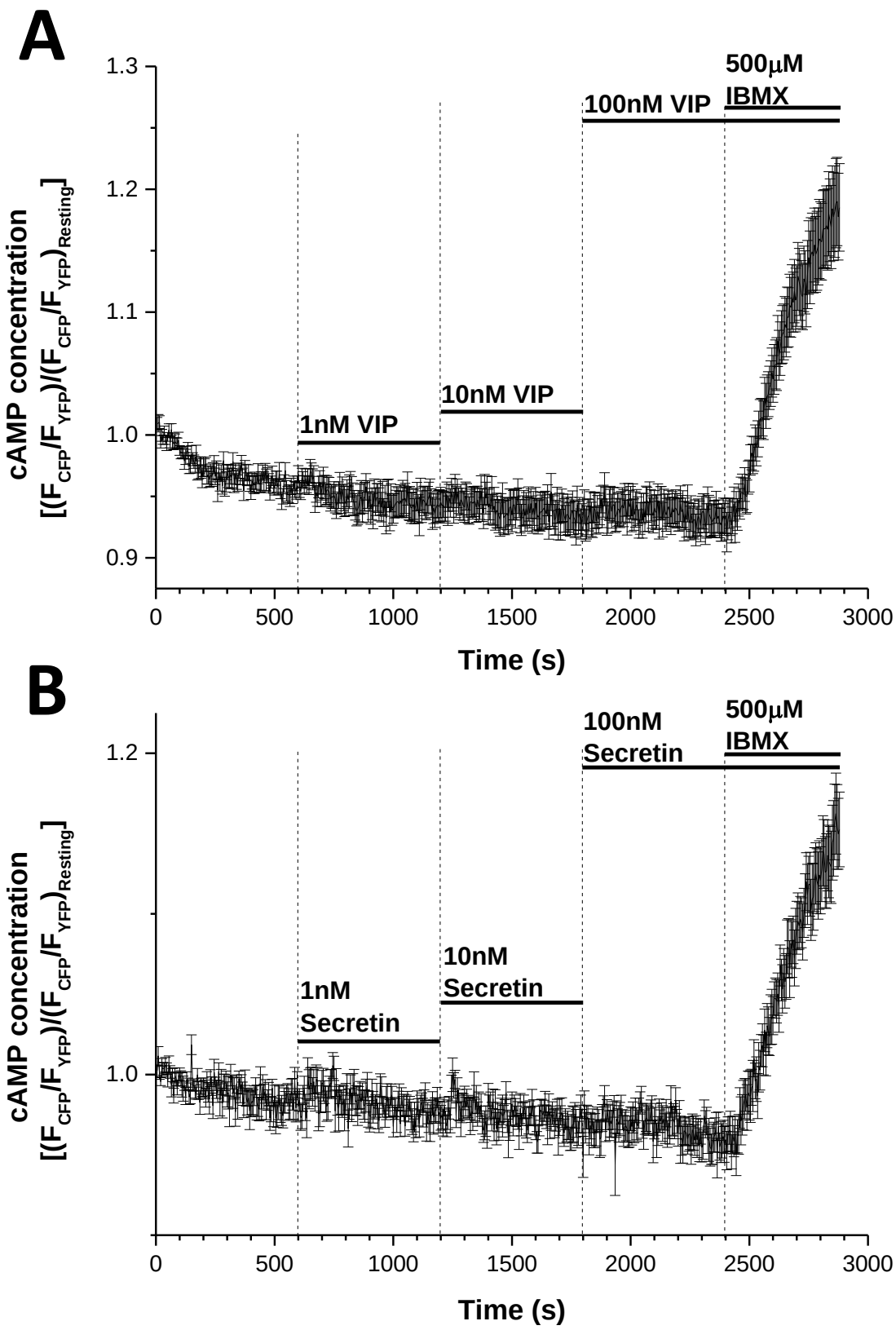
A
cAMP concentration
[(F_CFP/F_YFP)/(F_CFP/F_YFP)_Resting]
1.3
1.2
1.1
1.0
0.9
1nM VIP
10nM VIP
100nM VIP
500μM
IBMX
0
500
1000
1500
2000
2500
3000
Time (s)
B
cAMP concentration
[(F_CFP/F_YFP)/(F_CFP/F_YFP)_Resting]
1.2
1.0
1nM
Secretin
10nM
Secretin
100nM
Secretin
500μM
IBMX
0
500
1000
1500
2000
2500
3000
Time (s)

Figure 3.2.4. VIP and secretin does not increase cAMP levels in PANC-1 cells in the presence of IBMX.

A, PANC-1 cells expressing H134 were treated with increasing concentrations (1nM, 10nM, and 100nM) of VIP (n=4 experiments, n=27 cells). B, PANC-1 cells expressing H134 were treated with increasing concentrations (1nM, 10nM, and 100nM) of secretin (n=3 experiments, n=17 cells). On both occasions 500µM IBMX was added in the presence of the highest concentration of each agonist (100nM VIP or secretin) treatment.

3.2.4. Effects of VIP and secretin on PANC-1 cells after IBMX pre-treatment

In the next attempt to tease out any cAMP increases due to VIP and secretin, IBMX pre-treatment were performed before increasing concentrations of VIP or secretin (10nM and 100nM) were added cumulatively before 100nM isoproterenol was added again as a positive control. However, even in the presence of IBMX, which increased the F_{CFP}/F_{YFP} ratio slightly, neither of the two agonists increased cAMP levels in PANC-1 cells; instead producing a mild decrease in F_{CFP}/F_{YFP} ratios (figure 3.2.5). This finding, combined with those shown in figures 3.2.3 and 3.2.4, support the notion that VIP and secretin receptors are not active in PANC-1 cells.

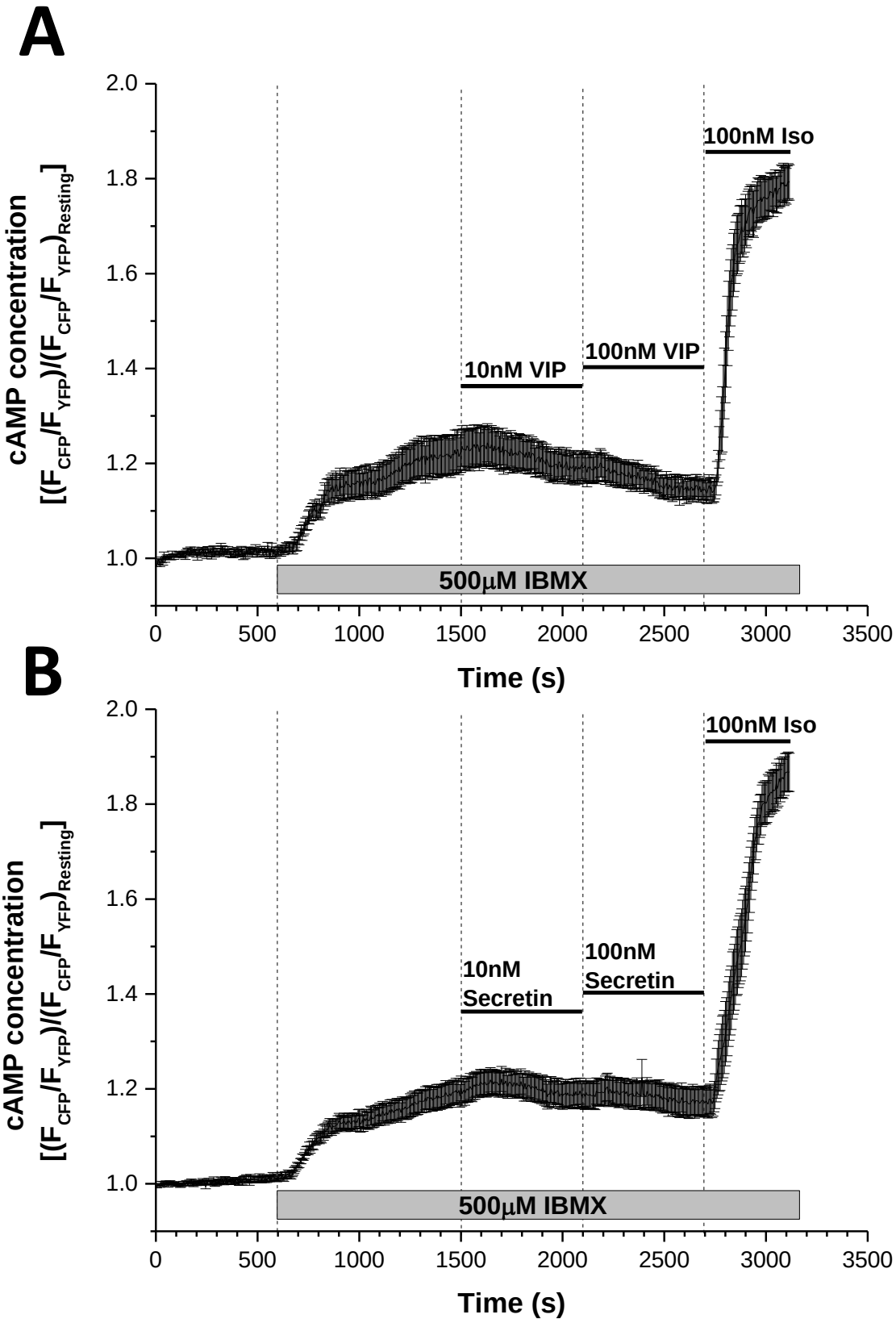
A
cAMP concentration
[(F_CFP/F_YFP)/(F_CFP/F_YFP)_Resting]
2.0
1.8
1.6
1.4
1.2
1.0
100nM Iso
10nM VIP
100nM VIP
500μM IBMX
0
500
1000
1500
2000
2500
3000
3500
Time (s)
B
cAMP concentration
[(F_CFP/F_YFP)/(F_CFP/F_YFP)_Resting]
2.0
1.8
1.6
1.4
1.2
1.0
100nM Iso
10nM
Secretin
100nM
Secretin
500μM IBMX
0
500
1000
1500
2000
2500
3000
3500
Time (s)

Figure 3.2.5. VIP and secretin do not increase cAMP levels in PANC-1 cells in the presence of IBMX.

A, PANC-1 cells expressing H134 were treated with increasing concentrations (10nM, and 100nM) of VIP after 15 minutes of IBMX (500µM) pre-treatment (n=2 experiments, n=12 cells). B, PANC-1 cells expressing H134 were treated with increasing concentrations (10nM, and 100nM) or secretin after 15 minutes of IBMX (500µM) pre-treatment (n=3 experiments, n=19 cells). On both occasions isoproterenol (100nM) was added at the end of experiment.

3.2.5. The effects of Iloprost on cAMP signalling in PANC-1 cells

Next, we sorted to probe the functionality of another Gαs-coupling GPCR, Prostacyclin receptor in PANC-1 cells by using iloprost, a stable analog of prostacyclin. Interestingly, treating H134-transfected PANC-1 cells with 1μM iloprost, the concentration that was widely used in other systems (Hutchison and White, 2014, Tsai et al., 2014b, Whittle et al., 2012, Smyth et al., 2000), mildly activated cAMP signalling (figure 3.2.6A); and the same experiment performed in the presence of IBMX producing similar results (figure 3.2.6B). Although the magnitude of this response is dwarfed by isoproterenol, these results suggest that some PANC-1 cells have functional prostacyclin receptors.

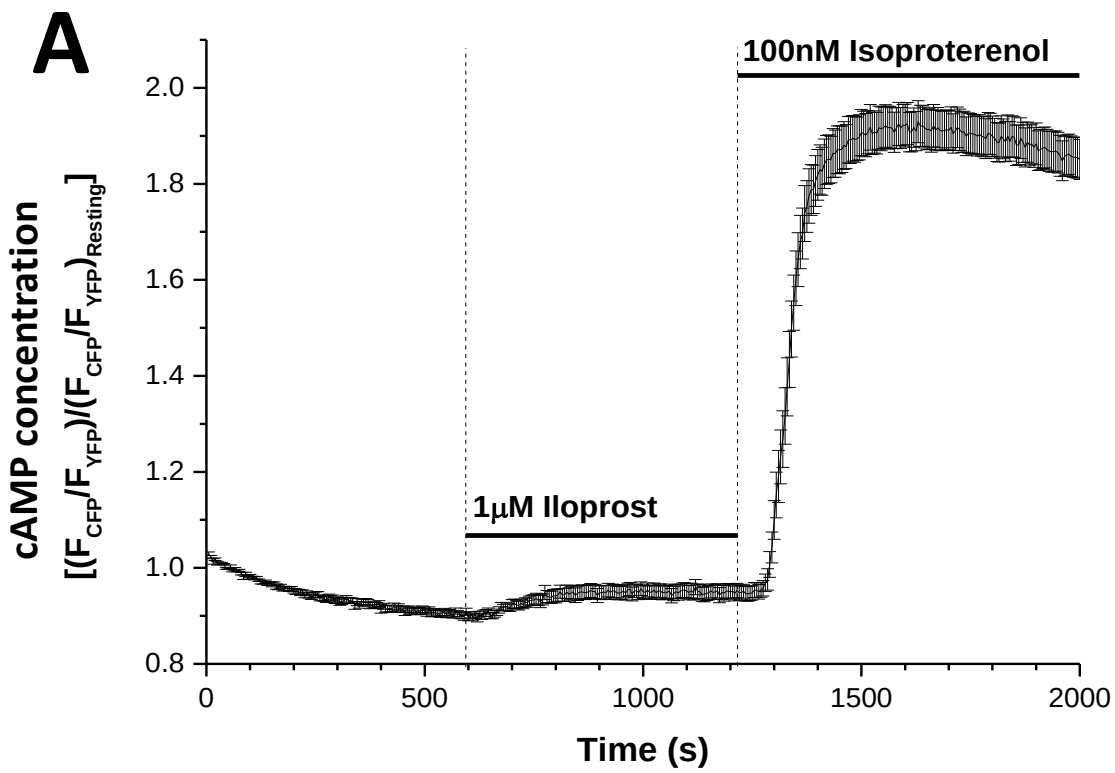
A
100nM Isoproterenol
1μM Iloprost
cAMP concentration
[(F_CFP/F_YFP)/(F_CFP/F_YFP)_Resting]
2.0
1.8
1.6
1.4
1.2
1.0
0.8
0
500
1000
1500
2000
Time (s)

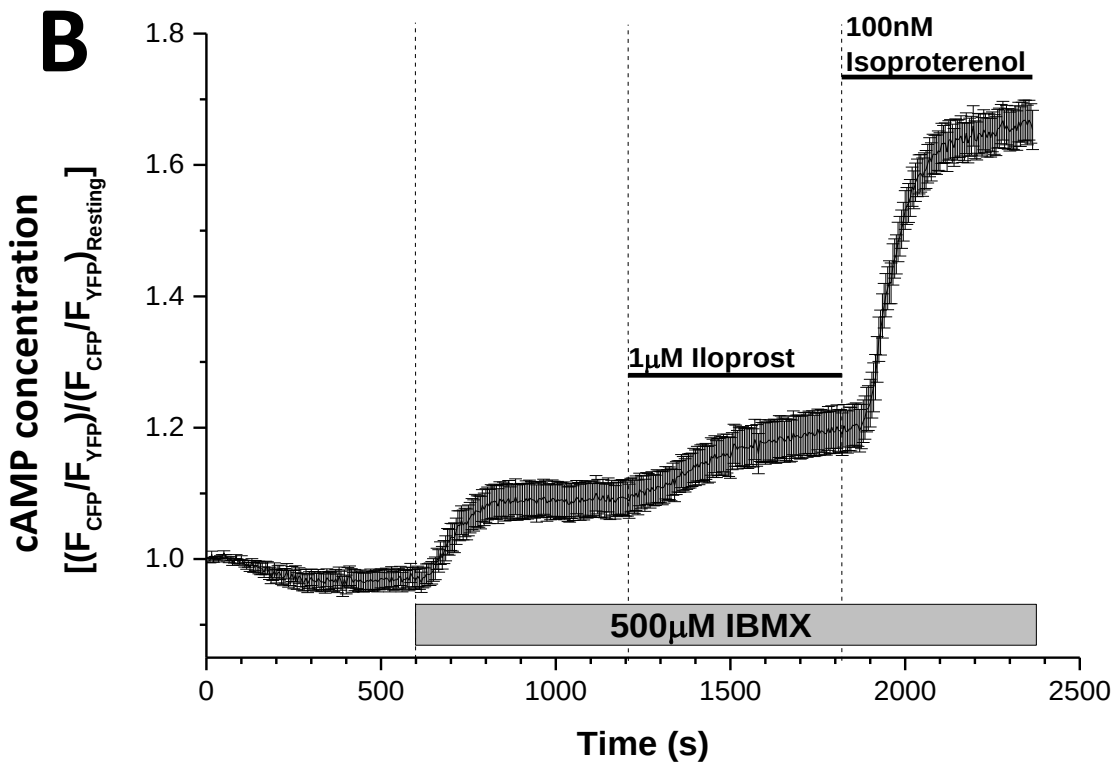
B
100nM
Isoproterenol
1μM Iloprost
500μM IBMX
cAMP concentration
[(F_CFP/F_YFP)/(F_CFP/F_YFP)_Resting]
1.8
1.6
1.4
1.2
1.0
0
500
1000
1500
2000
2500
Time (s)

Figure 3.2.6. Effects of prostacyclin on cAMP levels in PANC-1 cells.

A, PANC-1 cells expressing H134 were treated with a stable analog of prostacyclin, iloprost (1μM), for 10 minutes before isoproterenol (100nM) was added as positive control (n=9 experiments, n=54 cells). B, Same experiment as A, but this time IBMX (500μM) was added 15 minutes prior to iloprost treatment (n=5 experiments, n=33 cells).

3.2.6. Effects of PDE3 inhibition on Isoproterenol-stimulated PANC-1 cells

Forskolin was used for background stimulation in cAMP during PDE characterisation experiments in chapter 3.1. Therefore, we wanted to test the activities of PDE3 and PDE4 when isoproterenol was used instead as a source of cAMP stimulation.

Cilostazol was first tested in a similar protocol to 3.1.2; with the only difference being 500nM forskolin being replaced by 10nM isoproterenol. Figure 3.2.7 shows that 10nM Isoproterenol increased F_{CFP}/F_{YFP} ratio as expected, cilostazol significantly increased this ratio further; (figure 3.2.7), suggesting that PDE3 takes part in the regulation of cAMP concentrations in PANC-1 cells activated by β-adrenergic receptor simulation.

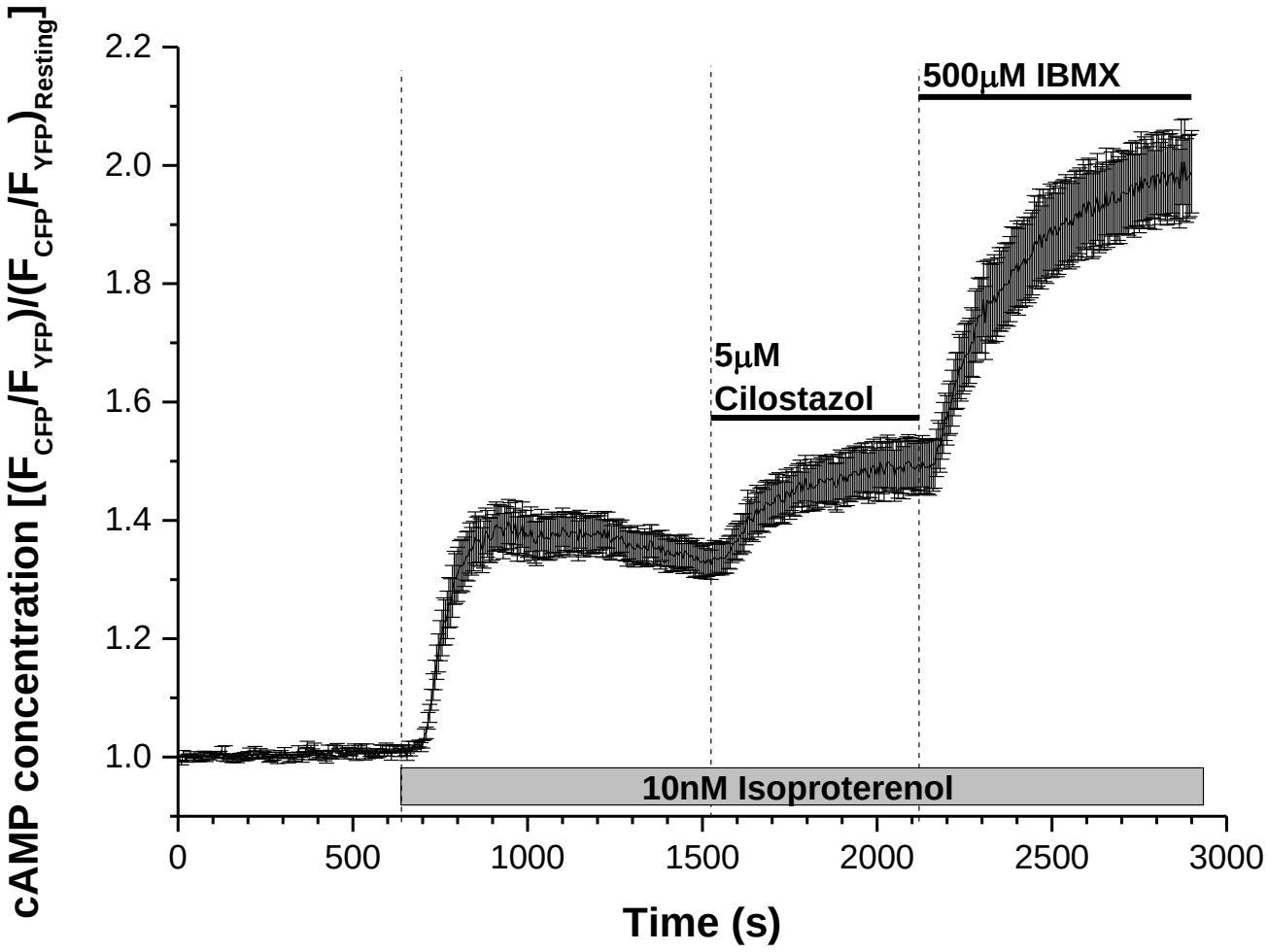

Figure 3.2.7. Cilostazol potentiates isoproterenol-mediated cAMP increases in PANC-1 cells.

PANC-1 cells transfected with H134 were subjected to 15 minutes of isoproterenol (10nM) treatment before being treated additively with cilostazol (5μM) for 10 minutes. IBMX (500μM) was used as positive control for PDE activity (n=3 experiments, n=20 cells).

3.2.7. Effects of PDE4 inhibition on Isoproterenol-stimulated PANC-1 cells

Next, rolipram was added after 10nM isoproterenol pre-treatment to see if PDE4 had any effects in limiting cAMP increases produced by β-adrenergic stimulation. Rolipram addition increased the F_{CFP}/F_{YFP} ratio further from the isoproterenol induced plateau; similar to cilostazol (figure 3.2.8); suggesting that PDE4 also regulates cAMP responses induced by isoproterenol stimulation.

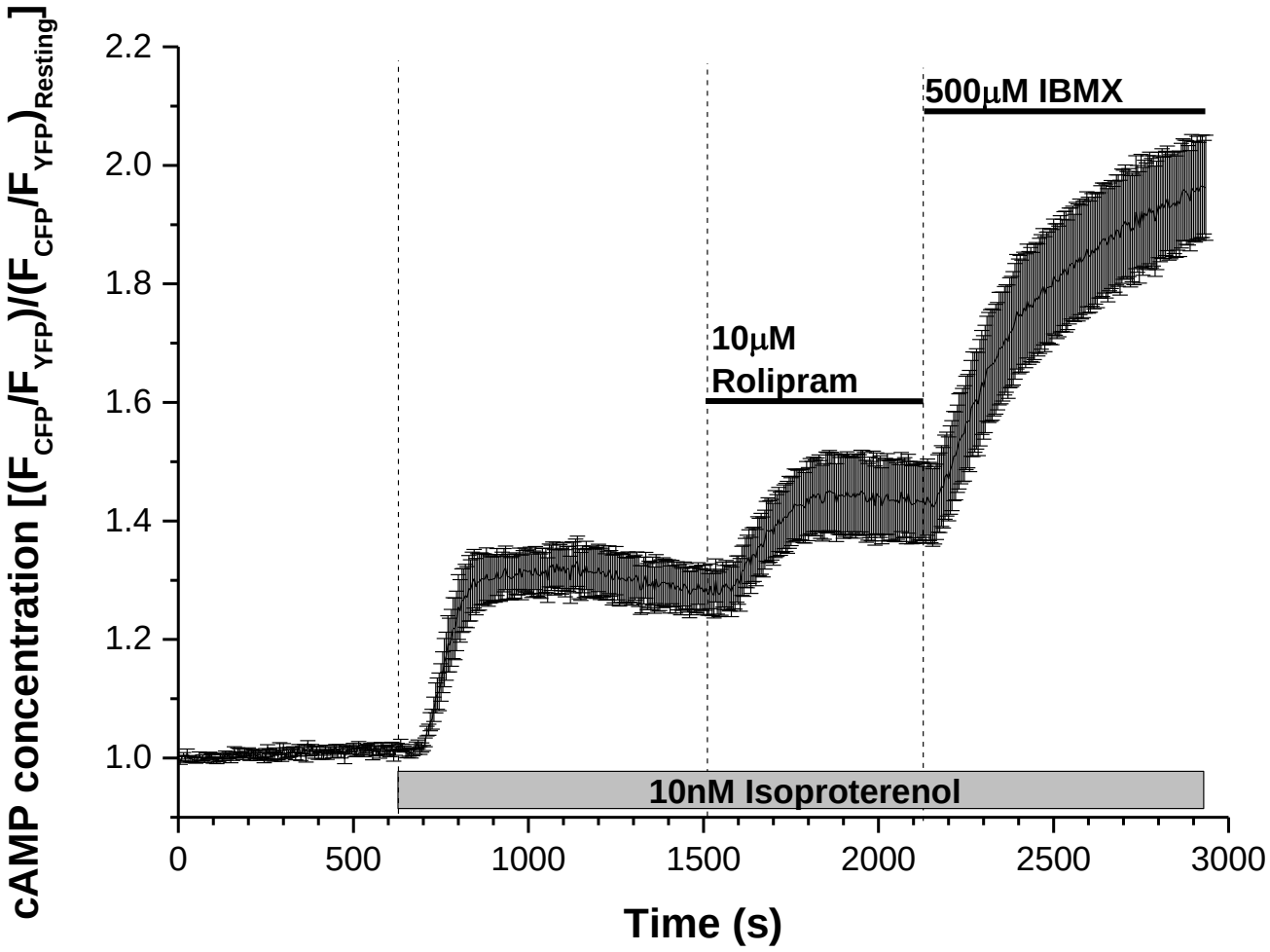

Figure 3.2.8. Rolipram potentiates isoproterenol-mediated cAMP increases in PANC-1 cells.

PANC-1 cells transfected with H134 were subjected to 15 minutes of isoproterenol (10nM) treatment before being treated with roilpram (10μM) for 10 minutes. IBMX (500μM) was used as positive control for PDE activity (n=3 experiments, n=13 cells).

3.2.8. Effect of combined PDE3 and PDE4 inhibition on Isoproterenol-stimulated PANC-1 cells

To test if there is cooperation between PDE3 and PDE4 in limiting cAMP produced by β-adrenergic stimulation like that observed in forskolin-treated cells, we then decided to determine the effect of combined inhibition of both PDE3 and PDE4 on cAMP levels of isoproterenol stimulated PANC-1 cells. Isoproterenol addition induced an increase in F_{CFP}/F_{YFP} ratio before declining very slowly just before cilostazol treatment, which increased the ratio further. The subsequent introduction of rolipram accelerated cAMP production, increasing F_{CFP}/F_{YFP} close to that of the IBMX response (figure 3.2.9). However, this was less than the maximal inhibition produced by IBMX, suggesting that PDE isoforms other than 3 and 4 were active, or that the concentration of rolipram or cilostazol used was not maximal. Nevertheless, this phenomenon was similar to that observed in experiments illustrated by figure 3.1.11; confirming that PDE3 and PDE4 are the main regulators of cAMP signalling in PANC-1 cells.

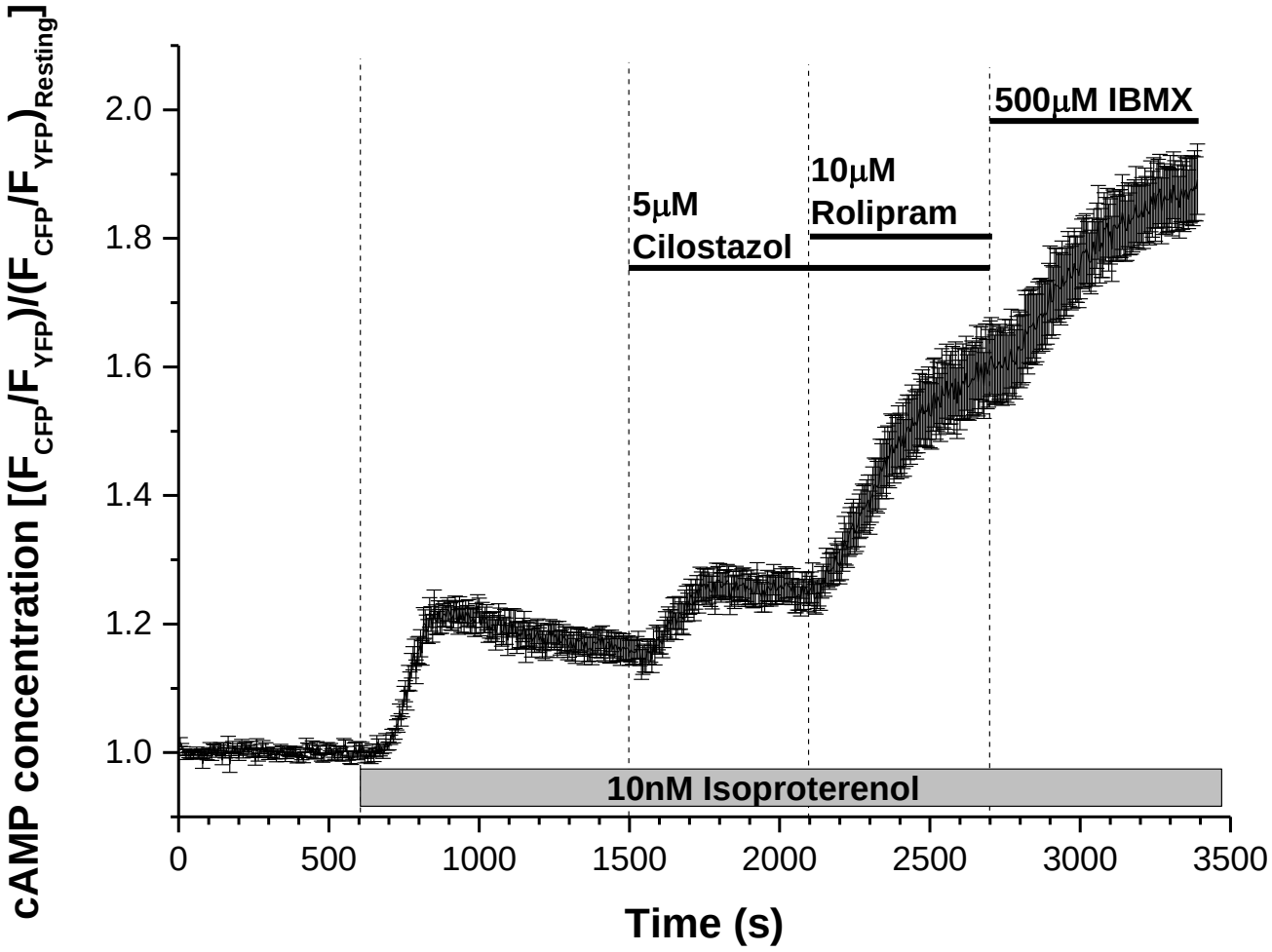

Figure 3.2.9. Cilostazol and rolipram together potentiate Isoproterenol-mediated cAMP increases in PANC-1 cells.

PANC-1 cells transfected with H134 were subjected to 15 minutes of isoproterenol (10nM) treatment before being treated additively, first with cilostazol (5μM) and then rolipram (10μM), both for 10 minutes. IBMX (500μM) was added at the end as positive control for PDE activity (n=3 experiments, n=19 cells).

3.3. cAMP and PANC-1 cell migration

Next, armed with the knowledge that Isoproterenol is the principal physiological cAMP agonist and PDE3 and PDE4 to be the main regulators of cAMP signalling in PANC-1 cells, we then tried to extend the results from our previous study (Burdyga et al., 2013) and asked if these more specific methods of increasing cAMP levels can inhibit cell migration. To this end, we utilised fluorblok transwell assays, which measure PANC-1 cell migration through a porous membrane, to assess this.

3.3.1. Effects of PDE inhibitors and cAMP agonists on PANC-1 cell migration

Fresh from the results described in figures 3.2.7-9, we decided to test the effects cilostazol and rolipram have on random, non-directional PANC-1 cell migration in the presence of isoproterenol. Six different conditions were designated: Control, 10nM isoproterenol alone, 10nM isoproterenol plus 5µM cilostazol, 10nM Isoproterenol plus 10µM rolipram, 10nM Isoproterenol plus 5µM cilostazol plus 10µM rolipram, and finally 10nM isoproterenol plus 500µM IBMX as positive control; with all results normalised to the control conditions. Interestingly, isoproterenol alone did not inhibit cell migration, not even when cilostazol was included with it (fig 3.3.1); instead having a tendency to even increase migration (10% increase for isoproterenol alone, and 20% for isoproterenol plus cilostazol). Strangely, the inclusion of rolipram partly but significantly inhibited migration by 23%, implying that PDE4 may play a bigger role in PANC-1 cell migration than PDE3 in the presence of Isoproterenol. The presence of both cilostazol and rolipram also significantly inhibited migration by 35%, which provided the strongest inhibition aside from IBMX, which was 60%. Combining with the results from figure 3.2.9, this strongly supports the notion that cAMP increase produced

by PDE4 inhibition, and not PDE3, under the influence of β-adrenergic stimulation inhibits PANC-1 cell migration.

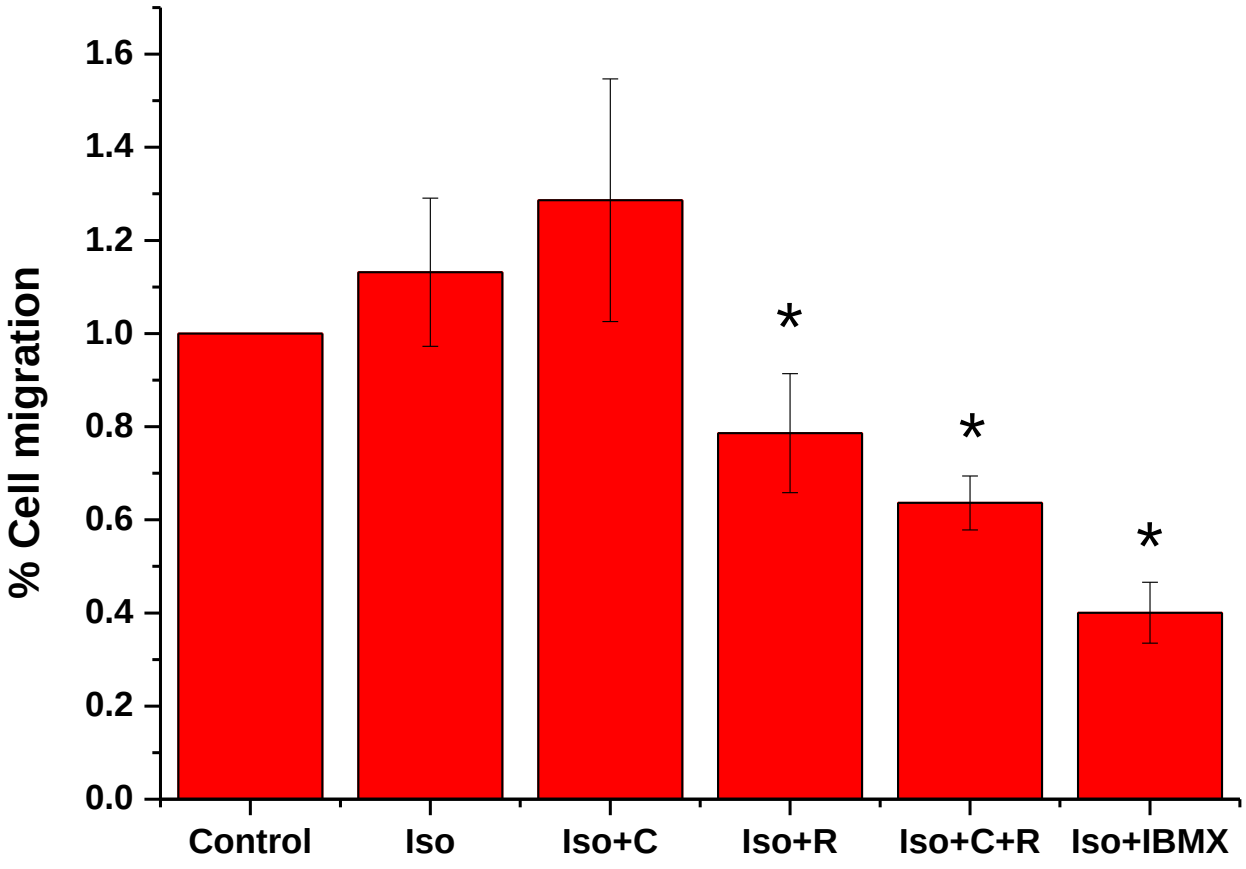

Figure 3.3.1. The effect of isoproterenol and both PDE3 and PDE4 inhibition on random cell migration.

PANC-1 cells were seeded into Boyden Chambers containing equal amounts of FBS (1%) on both the top and bottom wells with 6 different conditions. They were left to migrate through a porous membrane from (fluroblok membrane) for 6 hours and were then fixed and loaded with propidium iodide for imaging. All results were normalised to control. Each Boyden chamber contains duplicates for each condition per experiment, and each experiment was repeated 5 times (n=5 experiments, but n=10 for the number chambers used for each condition). [Key: Iso – Isoproterenol (10nM), C – Cilostazol (5µM), R – Rolipram (10µM), IBMX (500µM)]

3.3.2. Testing the effects of Isoproterenol on PANC-1 cell migration

One observation from figure 3.2.10 was that Isoproterenol had no inhibitory effects on PANC-1 cells. Note that 100nM isoproterenol alone gave a significant increase in F_{CFP}/F_{YFP} ratio, similar to the extent in which PDE3 and PDE4 inhibition together did in the presence of sub-maximal amounts of forskolin and 10nM isoproterenol (fig 3.2.9). Moreover, higher concentrations of isoproterenol (100nM) consistently gave drastic increases in the F_{CFP}/F_{YFP} ratio when used in previous experiments. Therefore, to investigate whether the inhibition of migration brought on by PDE3 and PDE4 inhibition together with 10nM isoproterenol in fig 3.3.1 was due to an increased absolute cAMP concentration, the effects of higher concentrations of isoproterenol on random PANC-1 cell migration was tested. Neither concentration (10nM and 100nM) of isoproterenol alone seemed to have any significant effects on cell migration. It was only when IBMX was included did a significant inhibition take place, again by about 60% (fig 3.3.2). This implies that the cAMP produced via the β-adrenergic receptor route does not inhibit migration of PANC-1 cells.

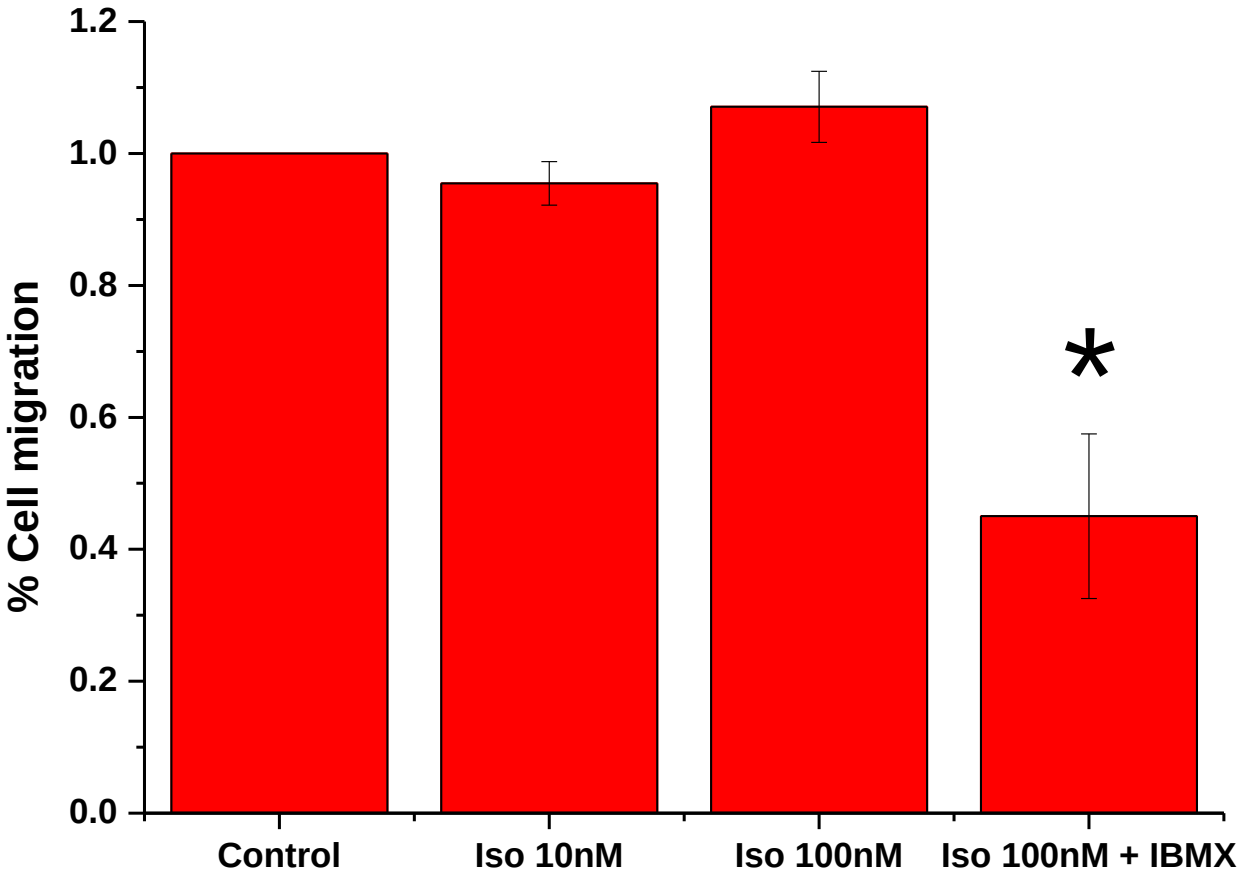

Figure 3.3.2. The effect of isoproterenol on random cell migration.

PANC-1 cells were seeded into Boyden Chambers containing equal amounts of FBS (1%) on both the top and bottom wells with 4 different conditions. They were left to migrate through a porous membrane (fluoroblok membrane) for 6 hours and were then fixed and loaded with propidium iodide. All results were normalised to control. (n=4 repeats, and n=8 in terms of chambers used for each condition tested) [Key: Iso – Isoproterenol, IBMX (500µM)]

3.3.3. Testing the effects of PDE3 and PDE4 inhibition alone on PANC-1 cell migration

After finding that high concentrations of isoproterenol did not have any effects on cell migration, cilostazol and rolipram were tested alone on PANC-1 cells to remove ambiguity caused by the presence of isoproterenol in fig 3.3.1. Six conditions were tested, Control, 5µM cilostazol, 10µM rolipram, 5µM cilostazol plus 10µM rolipram, 500µM IBMX, and 500µM IBMX plus 100nM isoproterenol. IBMX again inhibited migration by about 55% which was consistent with the previous two experiments; and the inclusion of isoproterenol (100nM) in the presence of IBMX also did not have any additional effects, as illustrated by fig 3.3.3. Interestingly, when applied alone, cilostazol seemed to exhibit inhibitory effects on cell migration like rolipram; significantly inhibiting migration by 30% and 20% respectively compared to control (fig 3.3.3). However, when applied together, the same magnitude of inhibition was achieved as for cilostazol alone (30%). These findings suggest that in the absence of cAMP stimulation, PDE3 is the major player in regulating spontaneous PANC-1 cell migration, but PDE4 may also have a role.

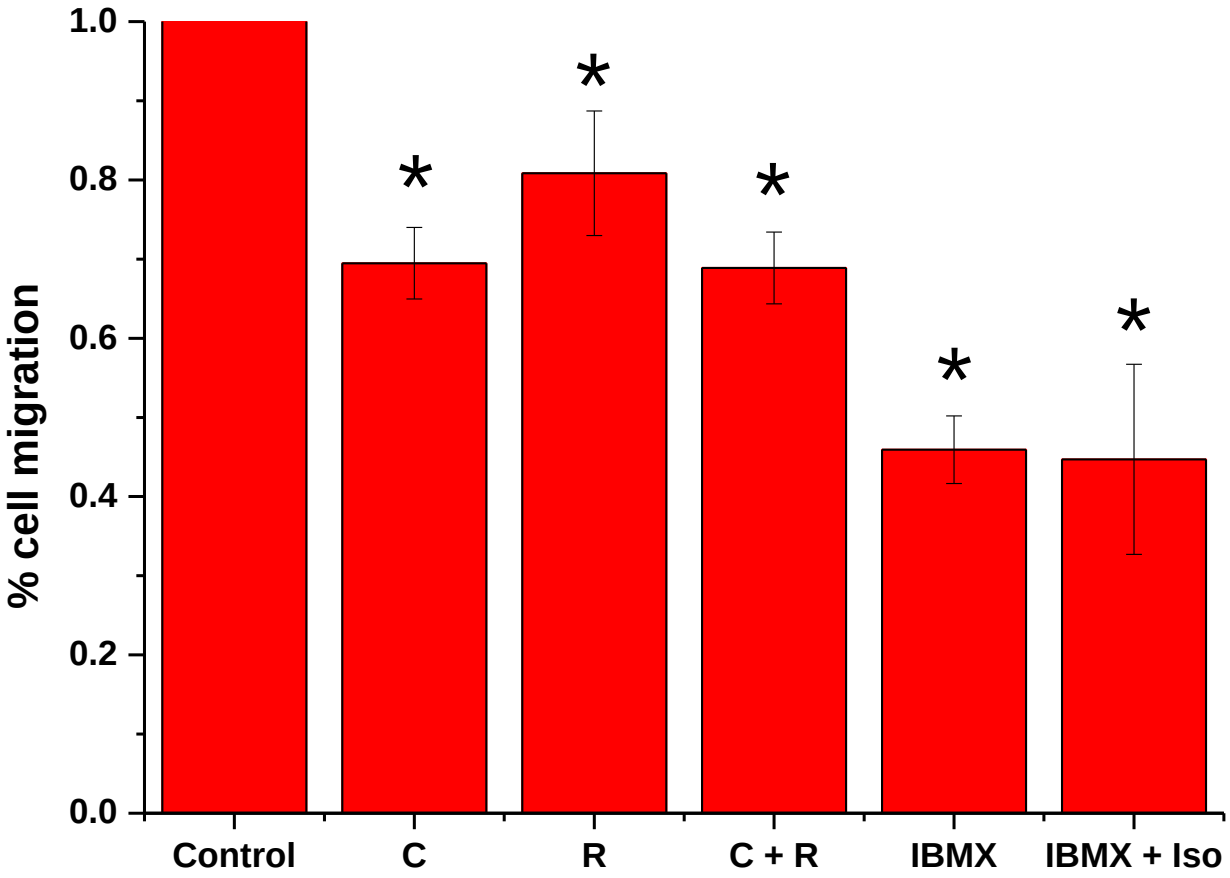

Figure 3.3.3. The effect of PDE3 and PDE4 inhibition and isoproterenol on random cell migration.

PANC-1 cells were seeded into Boyden Chambers containing equal amounts of FBS (1%) on both the top and bottom wells with 6 different conditions. They were left to migrate through a porous membrane for 6 hours and were then fixed and loaded with propidium iodide. All results were normalised to control. (n=4 for the number of repeats, n=8 for the number of chambers used per condition) [Key: C – Cilostazol (5µM), R – Rolipram (10µM), Iso – Isoproterenol (100nM), IBMX (500µM)]

3.3.4. Testing the effects of PDE3 and PDE4 alone on chemotactic PANC-1 cell migration

We repeated the experiments from fig 3.3.3 in a chemotactic setting in which cells seeded in the absence of FBS were migrating towards 5% FBS; all in the same 6 conditions described above. This time cilostazol inhibited cell migration much more dramatically; the 40% inhibition was significant compared to control. Surprisingly, rolipram instead appeared to slightly potentiated cell migration by 20% but not by a statistically significant margin, whereas the combination of cilostazol and rolipram significantly inhibited cell migration by 50%. Interestingly, the presence of 100nM isoproterenol with IBMX this time also significantly inhibited cell migration more than IBMX alone, by 80% (fig 3.3.4). Taken together, these results suggest that in a polarised setting, PDE3 is the dominant player in regulating PANC-1 cell migration mediated by chemoattractants in the form of FBS, and this time β-adrenergic stimulation may also have an additive effect on this process.

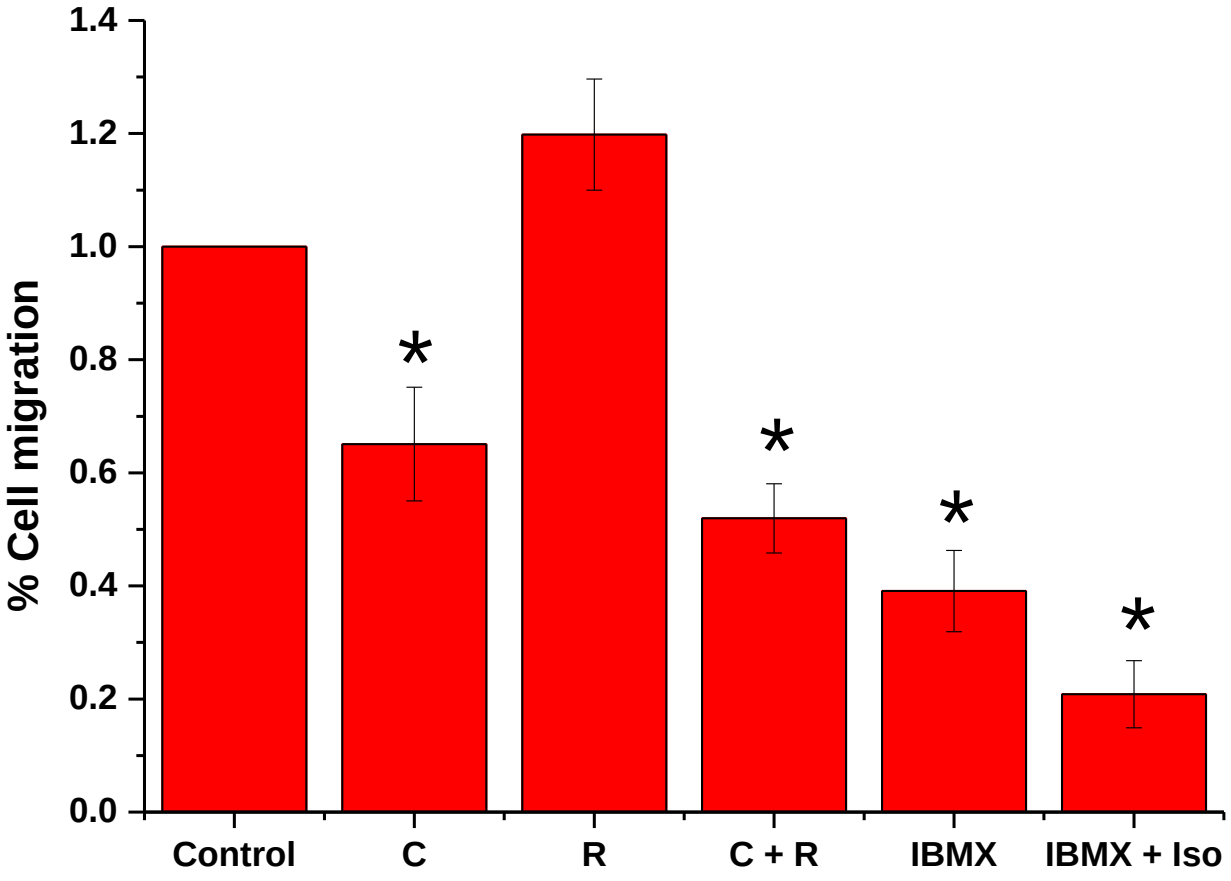

Figure 3.3.4. The effect of PDE3 and PDE4 inhibition and isoproterenol on directional cell migration.

PANC-1 cells were seeded into Boyden Chambers containing 0 FBS in the top wells and FBS (5%) in the bottom wells with 6 different conditions. They were left to migrate through a porous membrane for 6 hours and were then fixed and loaded with propidium iodide. All conditions were normalised to the control. (n=5 experimental repeats, n=10 chambers used per condition) [Key: C – Cilostazol (5µM), R – Rolipram (10µM), Iso – Isoproterenol (100nM), IBMX (500µM)]

3.3.5. Testing the effects of isoproterenol on PKA activity in PANC-1 cells

Given that isoproterenol effectively increased cAMP concentration in PANC-1 cells (fig 3.2.2) much like forskolin, it was perhaps surprising that it had only modest effects on cell migration (although results in fig 3.3.4 did suggest directional migration inhibition in the continuous presence of IBMX). We hence wanted to ask if this was because isoproterenol preferentially activates Epac, previously reported to potentiate PANC-1 cell migration instead of PKA, which inhibits cell migration (Burdyga et al., 2013). To this end, we treated PANC-1 cells transfected with the PKA sensor AKAR4 with increasing concentrations of isoproterenol, in an analogous experiment to that illustrated by fig.3.2.2. As shown in fig. 3.3.5, isoproterenol clearly increased AKAR4 FRET ratio in a dose dependent manner; after 1nM producing only a mild increase in PKA activity, the jump from 1 to 10nM notably increased the ratio. 100nM isoproterenol then caused another significant increase, just short of the maximum. Taken together, it appears that the cAMP increase induced by β-adrenergic receptors on PANC-1 cells can activate PKA, and that the effects of isoproterenol on cell migration was likely to be due to a superposition of Epac and PKA activity.

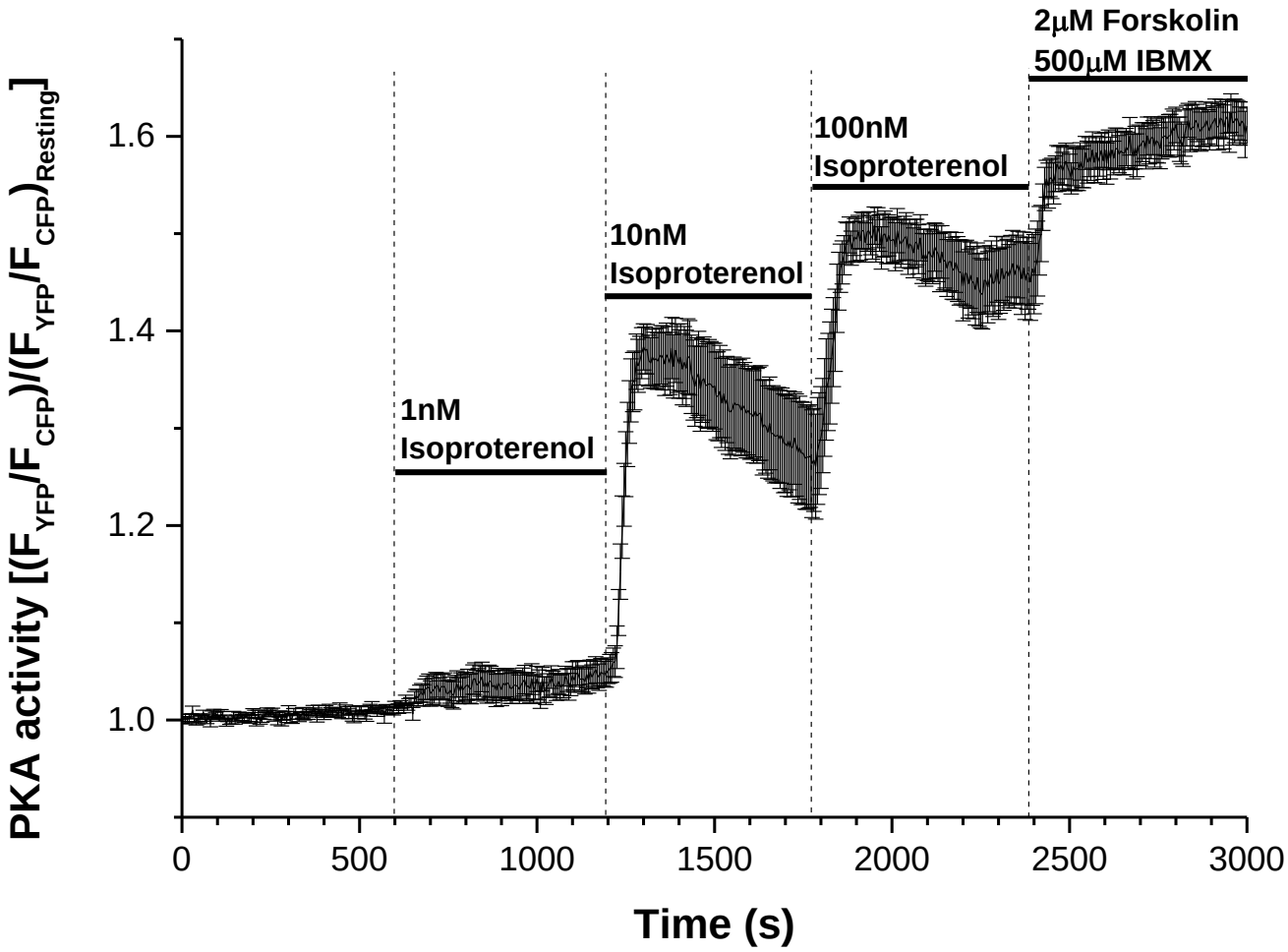

Figure 3.3.5. Effects of increasing concentrations of isoproterenol on PKA activity in PANC-1 cells.

PANC-1 cells transfected with the PKA activity sensor AKAR4 was treated with increasing concentrations of isoproterenol (1, 10 and 100nM), each for 10 minutes, before forskolin (2μM) and IBMX (500μM) were added at the end of the experiment (n=3 experiments, n=10 cells).

Key summary of results in chapter 3

Isoproterenol is the main physiological cAMP agonist in PANC-1 cells, whereas PDE3 and PDE4 are the primary cAMP signalling regulators in PANC-1 cells. However, PDE3 appears to play the bigger inhibitory role on regulating cell migration.

Results from this chapter also suggest the presence of prostacyclin receptors in small amounts, as well as the activity of PDE1 and PDE10. The contribution of these mechanisms to cAMP regulation however was less clear or less substantial, and their effects on cell migration was not investigated.

Chapter 4 – Characterisation of Store operated Ca^{2+} entry in PANC-1 cells

Chapter 4 – Characterisation of Store operated Ca^{2+} entry in PANC-1 cells

Overview

ORAI-STIM punctas form when the ER Ca^{2+} stores are depleted to sustain medium-long term Ca^{2+} signals (Soboloff et al., 2012). The high efficiency and dynamic nature of puncta formation in PANC-1 cells strongly suggests that these cells have a highly competent and responsive Ca^{2+} signalling system (Dingsdale et al., 2013). Therefore, applying a similar pharmacological/live-cell imaging approach used in chapter 3, we aimed to characterise Ca^{2+} signalling in PANC-1 cells. In this chapter particular emphasis will be given to SOCE which was not extensively characterised in this cell type, but is likely to play important physiological and pathophysiological function of these cells.

4.1 Characterisation of Ca^{2+} responses in PANC-1 cells

4.1.1. Neurotensin induces Ca^{2+} responses in PANC-1 cells

The intracellular cytosolic Ca^{2+} dye Fura-2 coupled with live cell imaging was used to investigate Ca^{2+} signalling in PANC-1 cells. Under Ca^{2+} free conditions, neurotensin (NT), a known $G_{\alpha q}$ GPCR agonist of PANC-1 cells (Wang et al., 2011), induced a single spike; indicative of Ca^{2+} release from the ER stores (fig 4.1.1). However, no further Ca^{2+} signals were seen after the initial signal until Ca^{2+} was introduced into the extracellular solution 10 minutes later, when another spike was observed almost immediately after Ca^{2+} application, followed by a plateau. This is indicative of SOCE first being activated which allows Ca^{2+} entry into the cytosol, and the subsequent attainment of equilibrium between SOCE SERCA and PMCA as it removes Ca^{2+} from the cytosol into the ER and outside the cell respectively. Another 10 minutes later, the treatment of thapsigargin (TG), an inhibitor of SERCA, tipped that balance towards SOCE activation as the amplitude of Ca^{2+} signal increased substantially (fig.4.1.1).

Taken together, these results confirm that upon NT application PANC-1 cells release Ca^{2+} from internal stores, which subsequently activate SOCE.

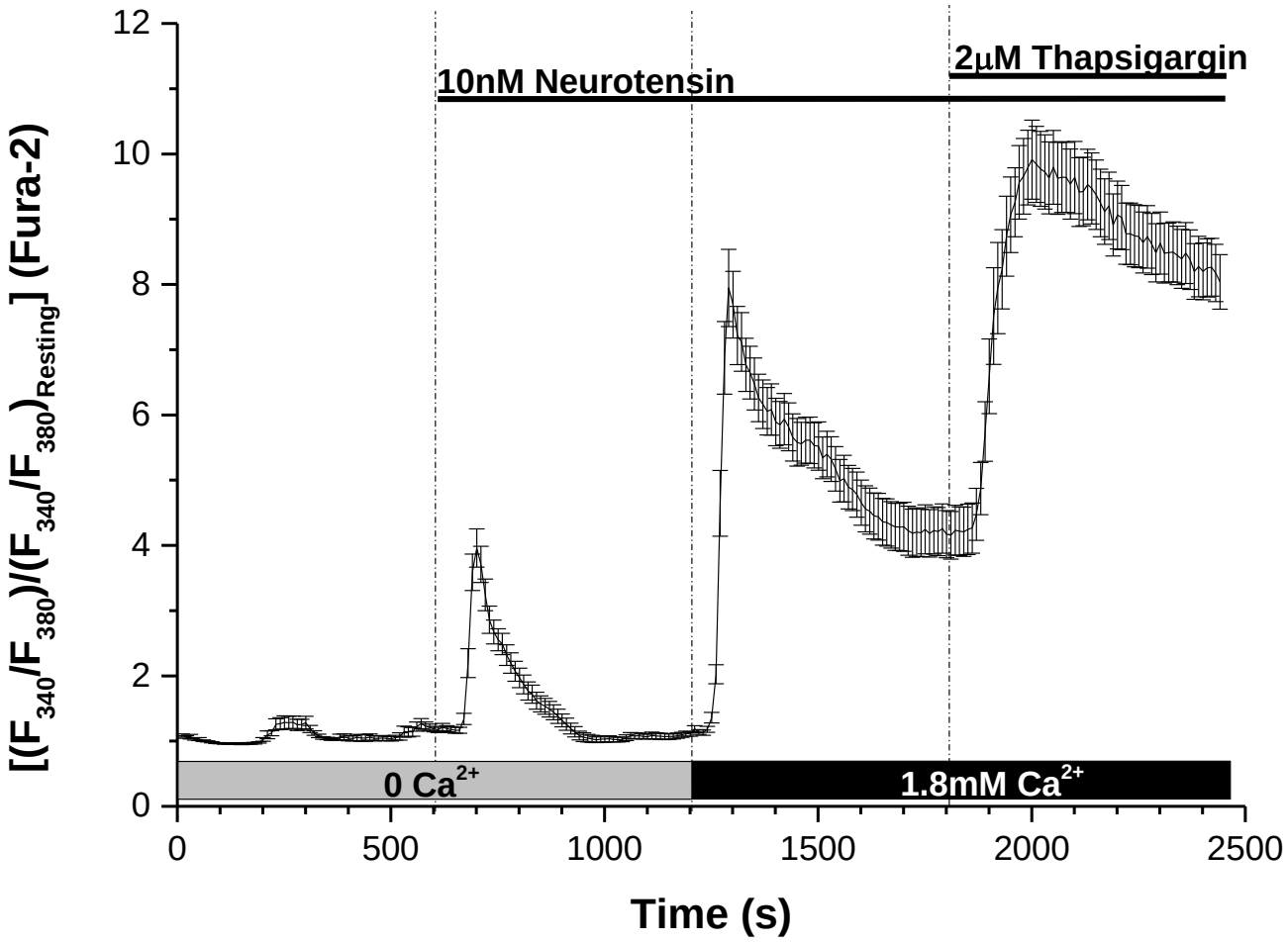

Figure 4.1.1.Ca^{2+} responses to neurotensin and thapsigargin in PANC-1 cells

PANC-1 cells loaded with the Fura-2 dye were first treated with neurotensin (10nM) in a nominally free Ca^{2+}-free solution for 10 minutes before Ca^{2+} (1.8mM) was added to the extracellular solution for another 10 minutes before the application of thapsigargain (2μM) for a further 10 minutes (n=2 experiments, n=46 cells).

4.1.2. Store depletion and SOCE in PANC-1 cells

The fast reaction and high amplitude in response to NT, extracellular Ca^{2+} and TG in fig.4.1.1 suggests that PANC-1 cells have a highly adaptable SOCE process. Therefore, to confirm this phenomenon, a similar experiment to fig 4.1.1 was performed; this time using TG as the agent for depleting intracellular Ca^{2+} stores instead of the physiological agonist NT. Under nominally Ca^{2+} free conditions, the addition of TG also produced a small spike which returned back to the baseline after approximately 10 minutes; and the subsequent addition of Ca^{2+} into the extracellular solution quickly induced a slowly declining plateau (fig 4.1.2). These results indicate that PANC-1 cells have an efficient SOCE system to maintain Ca^{2+} signalling.

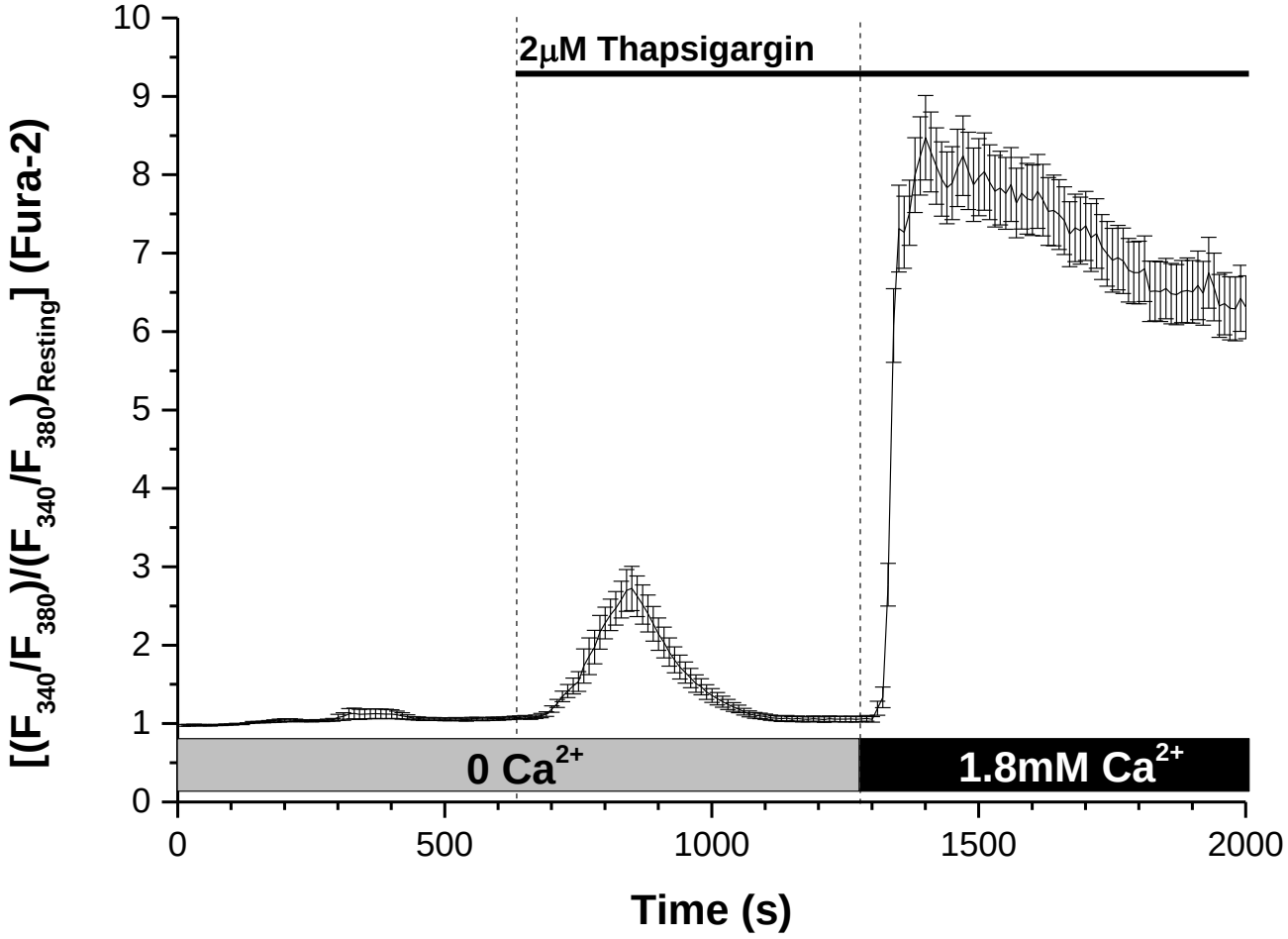

Figure 4.1.2. Store depletion and SOCE in PANC-1 cells.

PANC-1 cells loaded with the Ca^{2+} dye fura-2 were treated with thapigargin (2μM) for 15 minutes to deplete intracellular Ca^{2+} stores before 1.8mM Ca^{2+} was applied to activate store operated Ca^{2+} entry for 15 minutes (n=2 experiments, n=47 cells).

4.2. Pharmacological characterisation of store operated Ca^{2+} entry (SOCE) in PANC-1 cells

Observations from section 4.1 indicated that SOCE is an efficient and dynamic process in PANC-1 cells. In the next part of the study, we then decided to characterise the components of SOCE signalling in PANC-1 cells utilising reported pharmacological inhibitors. A near-comprehensive list of well-known SOCE inhibitors were used in this study: the lanthanide gadolinium (Gd^{3+}) (Dragoni et al., 2014), SKF-96365 (Chen et al., 2013a), Pyr3 (Schleifer et al., 2012), 2-APB (DeHaven et al., 2008), BTP2 (Jairaman and Prakriya, 2013) and the newly discovered ORAI1/3 inhibitor GSK7975A (Derler et al., 2013).

4.2.1. Effects of Gd^{3+} on SOCE in PANC-1 cells

We first tested the ability of Gd^{3+}, which is one of the most effective and well-known inhibitors of SOCE. To prevent Gd^{3+} chelation by FBS, PANC-1 cells were first serum-starved for 3 hours before the start of the experiment for acclimatisation, before being loaded with Fura-2 in the absence of serum. The experiment itself was also carried out in the absence of serum, in which cells were first treated with TG for 10 minutes to pre-deplete the intracellular stores, before extracellular calcium was added to induce SOCE, and form an elevated, slowly declining plateau for 10 minutes (fig 4.2.1). Gd^{3+} was then added to induce inhibition. PANC-1 cell treatment with Gd^{3+} did cause a notable SOCE inhibition in two phases: the first phase comprising of an immediate decrease within 100 seconds of addition, with the second phase being a more 'stabilised decrease', in which $[Ca^{2+}]_{cyt}$ appeared to decrease in a part linear fashion (fig 4.2.1). This suggests that Gd^{3+} is an effective inhibitor of SOCE, although it was still surprising to see that the inhibition was not absolute (i.e. near

100%), as lanthanides are reported to be amongst the best inhibitors of SOCE (Liao et al., 2008).

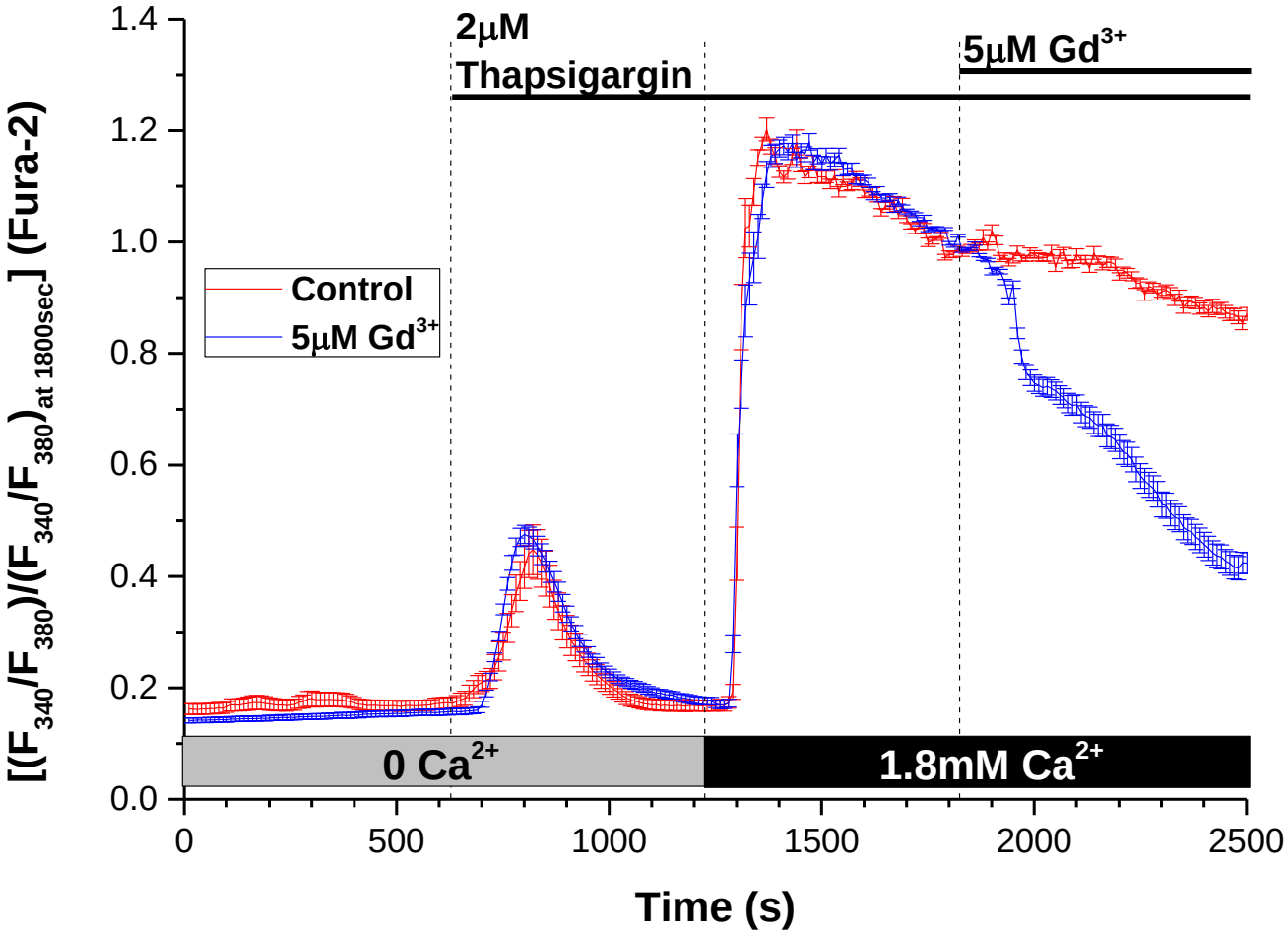

Figure 4.2.1. **Gd^{3+}** ***inhibits SOCE in PANC-1 cells.***

PANC-1 cells loaded with the Fura-2 dye were first treated with thapsigargin (2μM) in Ca^{2+}-free conditions for 10 minutes before Ca^{2+} (1.8mM) was added to the extracellular solution to induce SOCE. 10 minutes later Gadolinium^{3+} (5μM) was added to the extracellular solution. This experiment was carried out entirely in the absence of FBS (n=3 experiments, n=83 cells, all data points here were normalised to the point just before Gd^{3+} was added, at 1800 seconds).

4.2.2. The effect of BTP2 on SOCE in PANC-1 cells

We next tested the effects of BTP2, well-known CRAC channel inhibitor extensively used to inhibit SOCE in non-excitable cells (Ohga et al., 2008, Tsai et al., 2014a, Derler et al., 2013). Fura-2 loaded cells were first treated with TG for 10 minutes to deplete intracellular stores, before 1.8mM Ca^{2+} was added to activate SOCE. 10 minutes after SOCE was activated, cells were treated with 10µM BTP2 and the effects were observed (Yarotskyy and Dirksen, 2012, He et al., 2005). BTP2 effectively inhibited SOCE in PANC-1 cells; the plateau started to decrease about 200 seconds after BTP2 addition, with the decline showing signs of stabilising 10 minutes into the BTP2 treatment (fig 4.2.2). This finding suggests that BTP2-sensitive CRAC channels play a significant part in PANC-1 SOCE, but does not account for all of the Ca^{2+} influx.

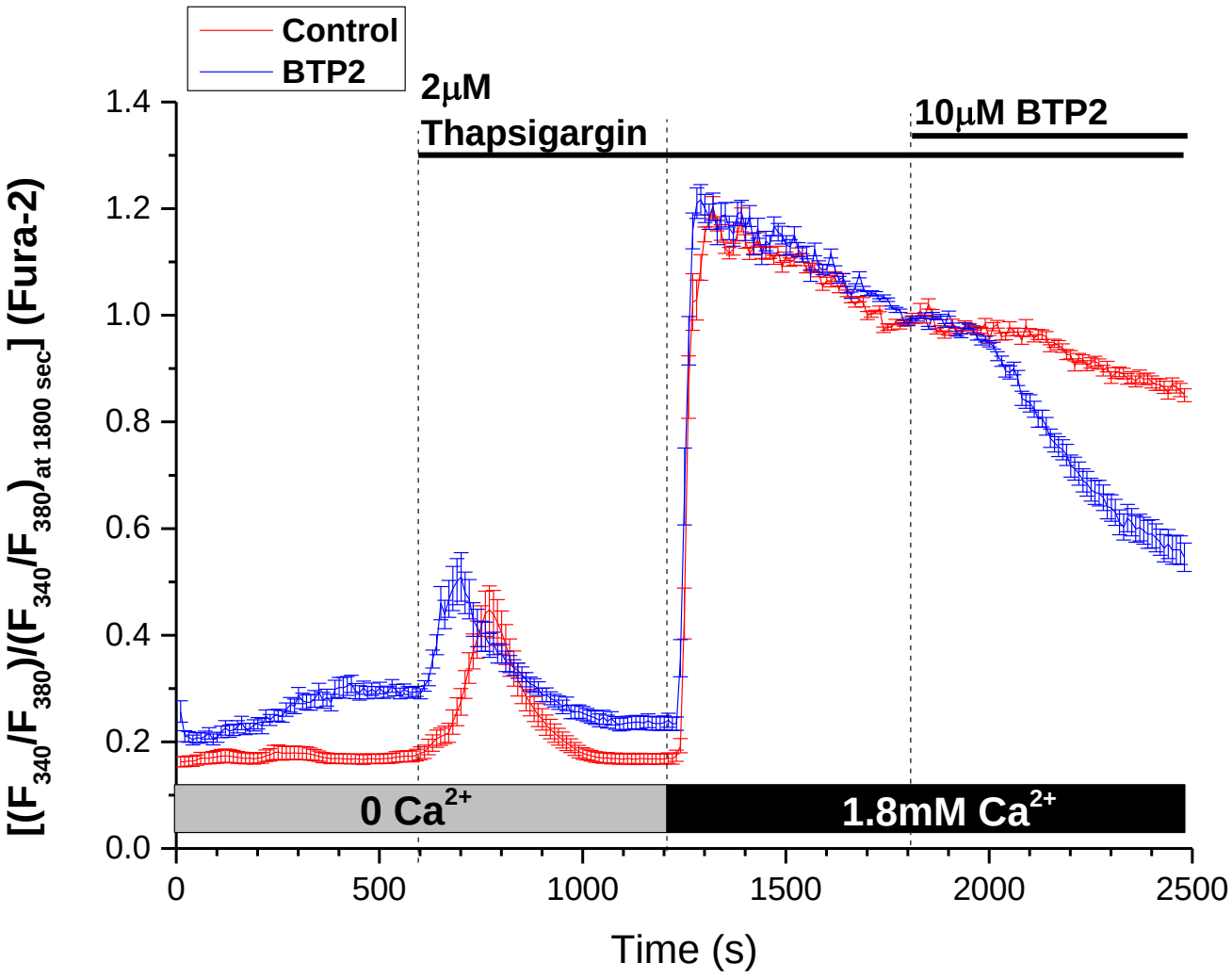

Figure 4.2.2. BTP2 inhibits SOCE in PANC-1 cells.

PANC-1 cells loaded with 5μM Fura-2 dye were first treated with thapsigargin (2μM) for 10 minutes in Ca^{2+}-free conditions before Ca^{2+} (1.8mM) was added to the extracellular solution to trigger SOCE. 10 minutes later BTP2 (10μM) was added to the extracellular solution (n=3 experiments, n=46 cells, all data points here were normalised to the point just before BTP2 was added, at 1800 seconds).

4.2.3. The effect of SKF-96365 in SOCE in PANC-1 cells

As mentioned in the introduction, TRPC channels can also take part in SOCE in a number of cells (Cheng et al., 2013). Therefore, we decided to test this possibility in Fura-2 loaded PANC-1 cells. First, TG was added for 10 minutes to deplete intracellular stores, before 1.8mM Ca^{2+} was added to induce a SOCE plateau much like figs 4.2.1-2. 10 minutes after the plateau was established, treatment with 10µM SKF-96365 (SKF), a well-known TRP channel antagonist (Flemming et al., 2003, Chen et al., 2013a), started and its effects on the SOCE were observed. Interestingly, although there is a hint of a slight inhibition about 5 minutes into SKF treatment, the magnitude of this effect was much smaller than for Gd^{3+} or BTP2 as the SKF trace ran extremely close to the control trace (fig 4.2.3). This observation put doubts in the involvement of TRP channels in SOCE in PANC-1 cells.

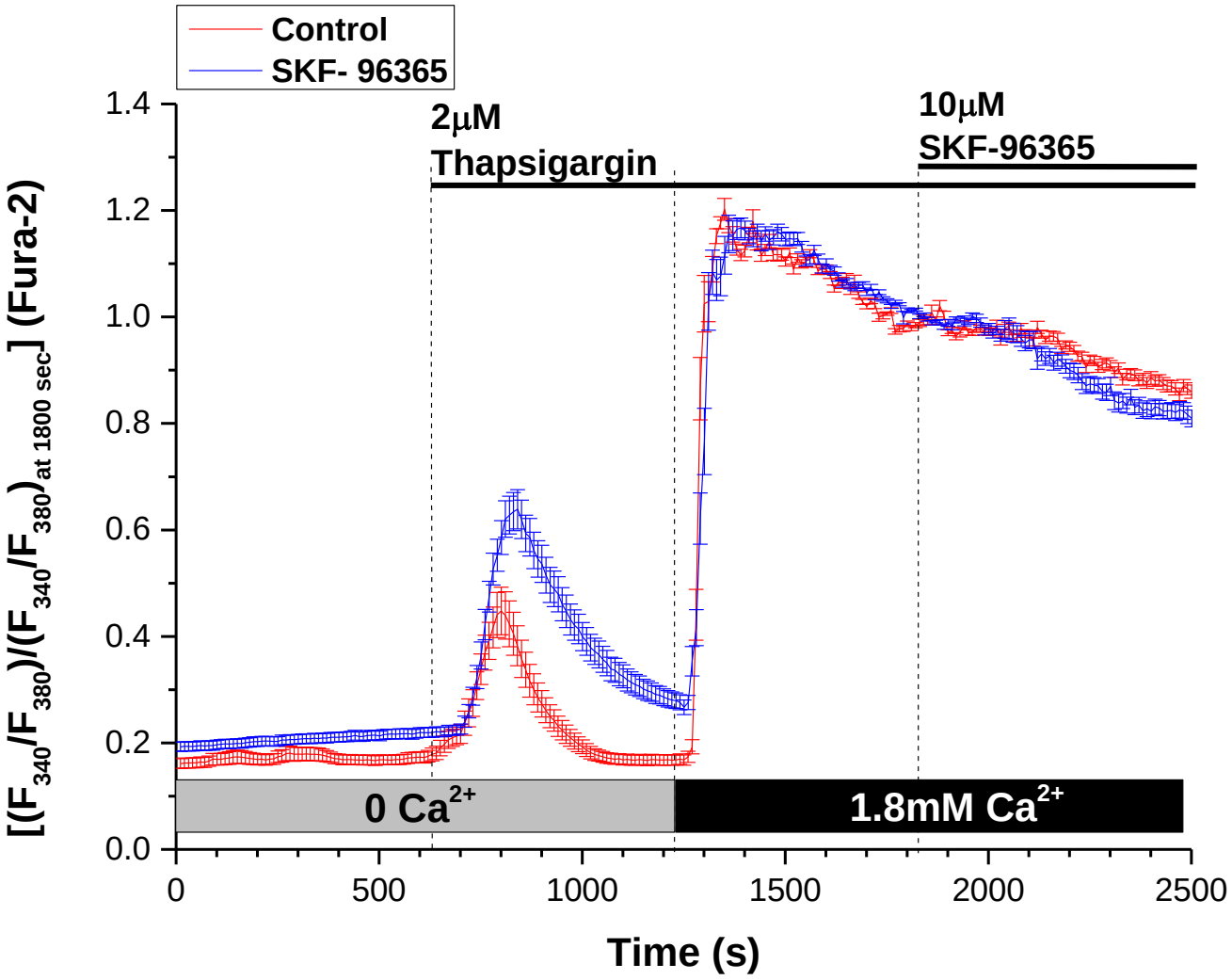

Figure 4.2.3. SKF-96365 has little effects on SOCE in PANC-1 cells.

PANC-1 cells loaded with 5μM Fura-2 dye were first treated with thapsigargin (2μM) in Ca^{2+}-free conditions for 10 minutes before Ca^{2+} (1.8mM) was added to the extracellular solution. 10 minutes following SOCE activation SKF-96365 (10μM) was then added into the extracellular solution (n=3 experiments, n=72 cells, all data points here were normalised to the point just before SKF-96365 was added, at 1800 seconds).

Differences in Ca^{2+}signals as a result of TG-induced store depletion

At this point, it is worth mentioning that the magnitude of signals provided by TG-mediated depletion differs greatly from cell to cell, resulting in significant differences in TG responses in figs 4.2.1-3. Moreover, occasionally some baselines displayed elevated basal $[Ca^{2+}]_{cyt}$ (such as 4.2.2). The reason for this is that in some cells TG induces CICR. However, as this study mainly concerns with SOCE and not store depletion or CICR, we've decided to funnel the study down to SOCE only, and all the subsequent experiments were conducted on TG pre-treated cells. In these experiments, cells were already in contact with TG approximately 10 minutes before the start of the experiment, the total time exposure to TG in Ca^{2+} free extracellular solution was about 20 minutes (10 minutes before the experiment, and 10 minutes during the baseline period in the experiment).

4.2.4. The effect of 2-APB on SOCE in PANC-1 cells

Next, we tested another well-known SOCE inhibitor, 2-APB on SOCE in PANC-1 cells. After 20 minutes of TG pre-treatment, SOCE induction was carried out by the addition of 1.8mM Ca^{2+} for 10 minutes before the addition of high concentrations of 2-APB (50µM), also for 10 minutes. 2-APB appeared to be the most effective SOCE inhibitor in PANC-1 cells to date in our hands; as its application almost completely and immediately obliterated the SOCE response (fig 4.2.4). As 2-APB has so many reported targets including both ORAI and TRP channels as well as IP_3 receptors (Peppiatt et al., 2003, Colton and Zhu, 2007), this does not conclusively put light on exactly what components are involved in SOCE in PANC-1 cells. However, this probably means that PANC-1 cells are unlikely to use ORAI3, which is activated by 2-APB, as a component of the CRAC channels; and does put 2-APB forward as

an effective SOCE inhibitor in PANC-1 cells in future studies, especially as positive control for inhibition.

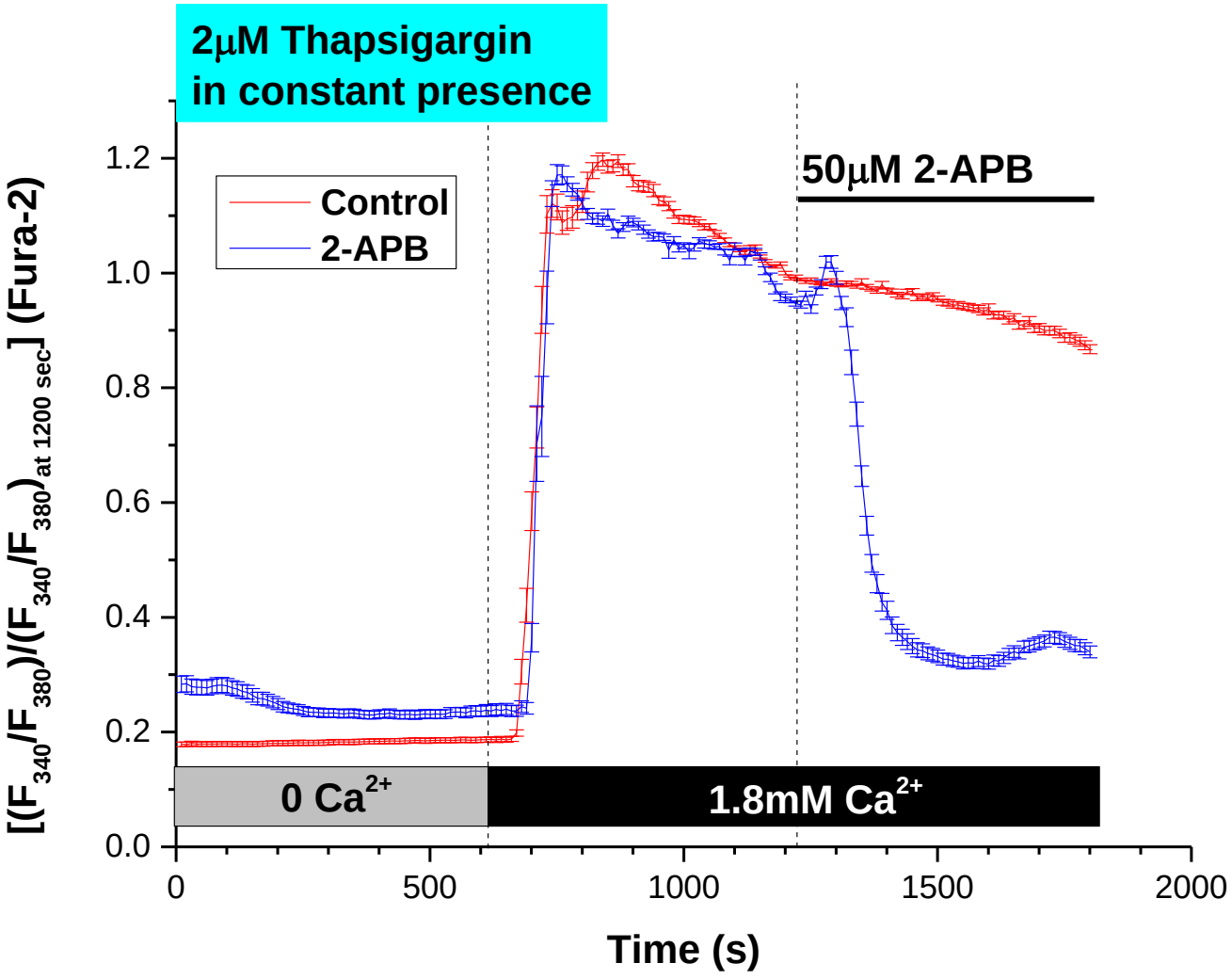

Figure 4.2.4. 2-APB potently inhibits SOCE in PANC-1 cells.

PANC-1 cells loaded with the Fura-2 dye were first pre-treated with thapsigargin (2μM) for approx. 20 minutes in Ca^{2+}-free conditions before Ca^{2+} (1.8mM) was added to the extracellular solution to induce SOCE. 2-APB (50μM) was then added 10 minutes after SOCE activation. Note that thapsigargin (2μM) was present throughout the experiment (n=2 experiments, n=49 cells, all data points here were normalised to the point just before 2-APB was added, at 1200 seconds).

4.2.5. The effect of GSK-7975A on SOCE in PANC-1 cells

We then sorted to test a GSK-7975A, novel compound reported to be selective inhibitors of ORAI1 and ORAI3, on SOCE in PANC-1 cells. In a similar protocol to that described in fig 4.2.4, TG pre-treatment was carried out approximately 10 minutes before the commencement of the experiment. After SOCE was induced by 1.8mM Ca^{2+} addition, various concentrations (10µM and 30µM) of GSK-7975A was tested in separate experiments to determine the dose-dependent effects of this drug on SOCE, as they have not been tested previously in these cells. It seems that the GSK-7975A is also an effective inhibitor of SOCE in PANC-1 cells (Fig 4.2.5); though not as strong as 2-APB (Compare figs 4.2.4 and fig 4.2.5). Quantitatively, both concentrations appeared to have the same end-point effects after 10 minutes, inhibiting the response by about 55-60%; with the higher concentration exerting the effects about 100 seconds quicker than the lower concentration (fig 4.2.5). These results confirm ORAI1 to play a dominant role in SOCE in PANC-1 cells, but other channels may still play a part considering the incomplete inhibition by GSK-7975A.

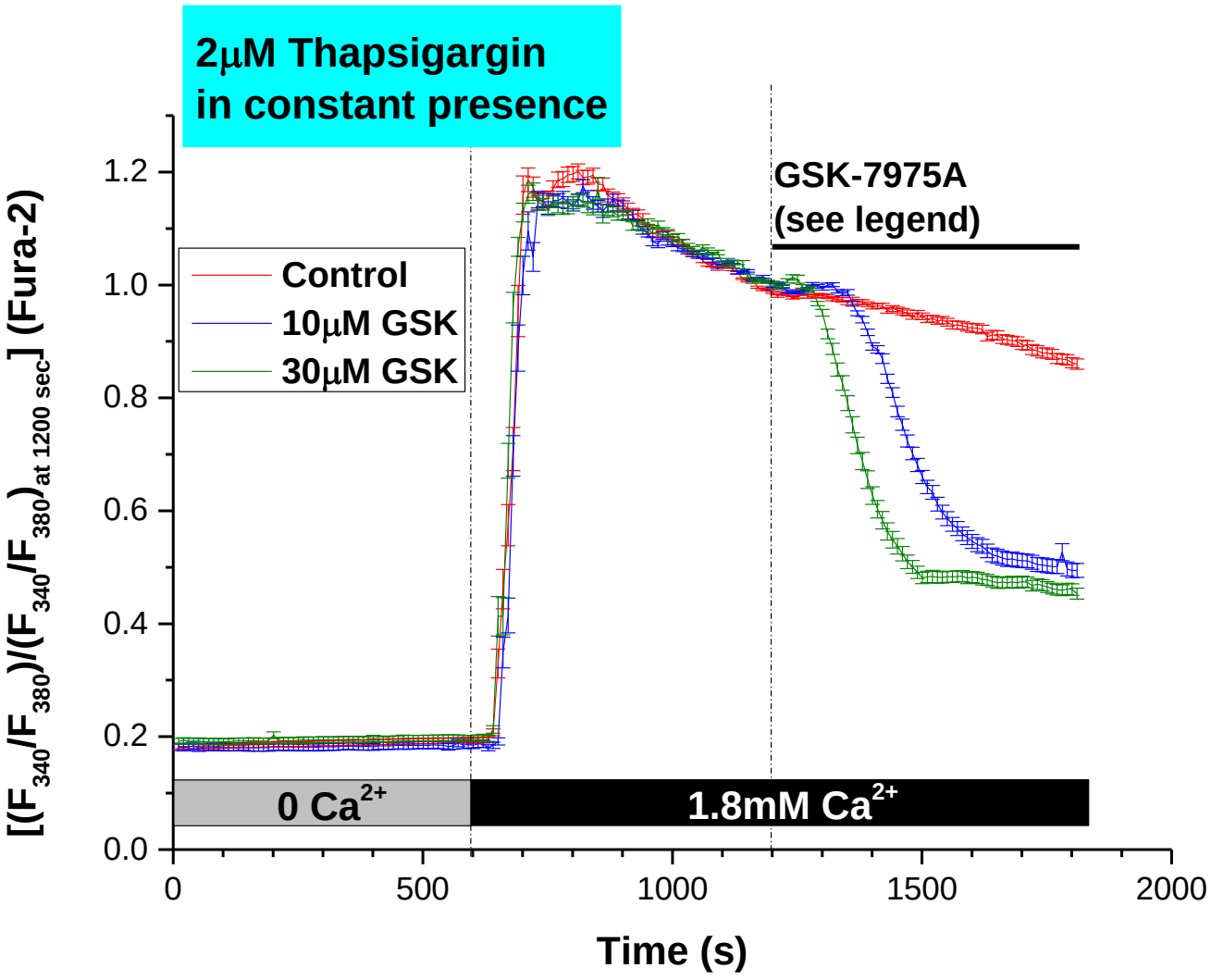

Figure 4.2.5. GSK-7975A inhibits SOCE in PANC-1 cells.

PANC-1 cells loaded with 5μM Fura-2 dye were pre-treated with thapsigargin (2μM) for about 20 minutes in Ca^{2+}-free conditions before Ca^{2+} (1.8mM) was added to the extracellular solution. In separate experiments GSK (10μM or 30μM) was then added after SOCE activation. No GSK was added in the control experiment. Note that thapsigargin (2μM) was continuously present from the start of the experiment (n=5 experiments and n=193 cells for control, n=5 experiments and n=162 cells for 10μM; n= 5 experiments and n=145 cells for 30μM. All data points here were normalised to the point just before GSK-7975A was added, at 1200 seconds).

4.2.6. Effect of nifedipine on SOCE in PANC-1 cells

Pancreatic cancer cells often show a tendency towards invading the nervous system (Buchler et al., 2005). Moreover, in terms of this study, the ease of Ca^{2+} signalling activation in PANC-1 cells led us to test whether this high efficiency is due to the expression of voltage-gated Ca^{2+} channels (VGCCs), which has one of the fastest activation times of all Ca^{2+} channels (more than 1 million fold faster than ORAI1)(Soboloff et al., 2012).

Therefore, we used nifedipine, a well-known antagonist of the VGCC (Mamo et al., 2014, Itzhaki et al., 2011, Kirkman-Brown et al., 2003), to test for their role in SOCE. Here, Fura-2 loaded PANC-1 cells were again pre-treated with TG for 20 minutes to deplete the stores, before the activation of SOCE via 1.8mM Ca^{2+} application to the extracellular HEPES. 10 minutes after SOCE activation, nifedipine treatment ensued. As shown in figure 4.2.6, the application of nifedipine had no effect on $[Ca^{2+}]_{cyt}$. This result strongly suggests against the contribution of VGCCs to SOCE in PANC-1 cells.

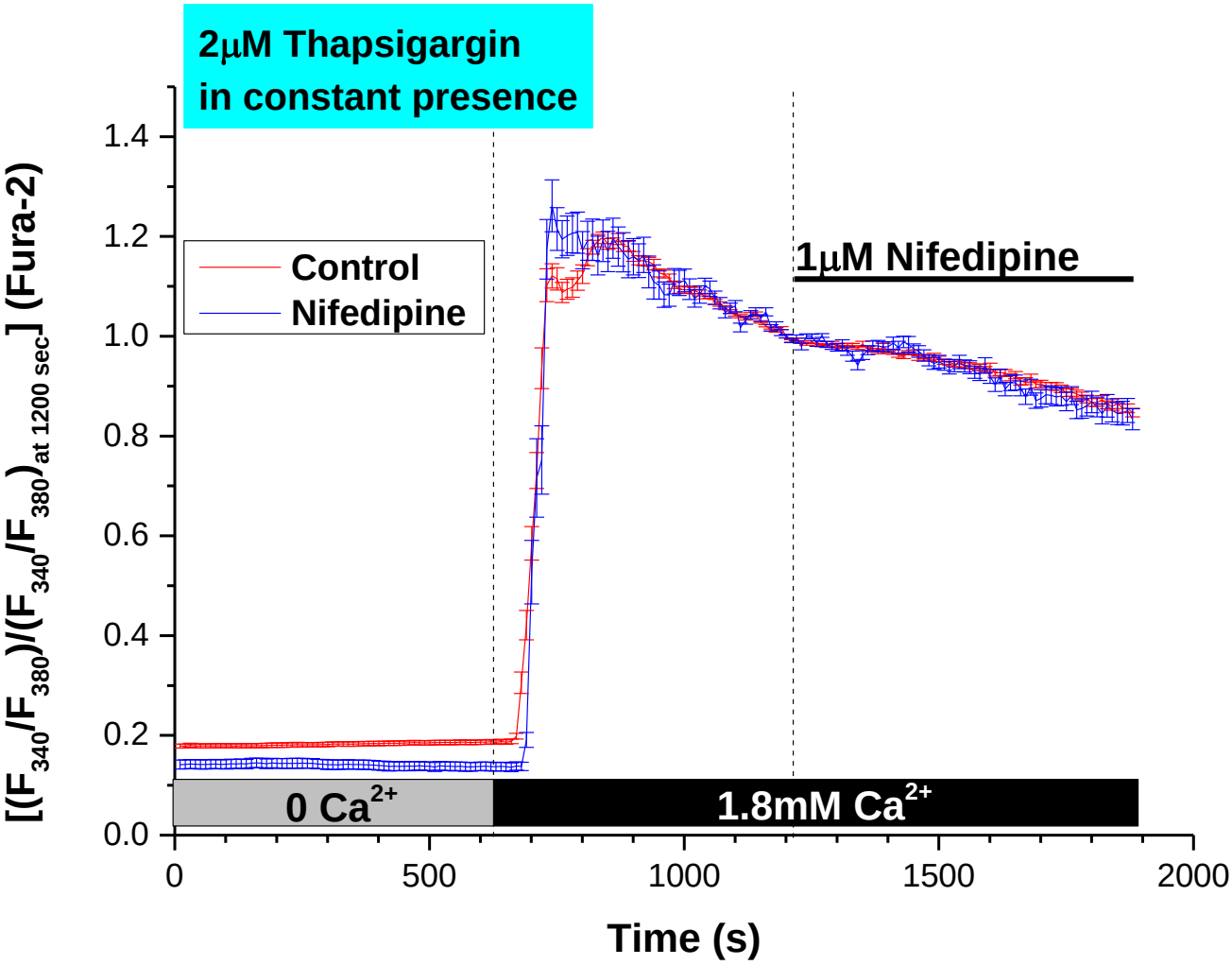

Figure 4.2.6. Nifedipine has no effects on SOCE in PANC-1 cells.

PANC-1 cells loaded with 5μM Fura-2 dye were pre-treated with thapsigargin (2μM) for about 20 minutes in Ca^{2+}-free conditions before Ca^{2+} (1.8mM) was added to the extracellular solution. 10 minutes after SOCE was activated, nifedipine (1μM) was then added to the extracellular solution. Note that thapsigargin (2μM) was continuously present from start of the experiment (n=2 experiments, n=51 cells. all data points here were normalised to the point just before nifedipine was added, at 1200 seconds).

4.2.7. The effects of combined GSK-7975A and 2-APB treatment on SOCE in PANC-1 cells

As the results from fig 4.2.5 showed that there was still approximately 40% of the SOCE response that was not inhibited by GSK-7975A, we then asked whether that remaining component can be diminished by 2-APB, which in experiments illustrated by fig 4.2.4 was shown to be the be best inhibitor of SOCE in PANC-1 cells. In an experiment aiming to test the combination of the two inhibitors, PANC-1 cells loaded with Fura-2 were treated with TG for 10 minutes to deplete the stores before 1.8mM Ca^{2+} was added to induce SOCE; after 10 minutes, the GSK-7975A (30µM) was added for another 10 minutes before ending the experiment with 10 minutes of 2-APB treatment. As shown in figure 4.2.7, GSK-7975A again decreased the plateau by a similar extent as the results illustrated in fig 4.2.5. Subsequent addition of high concentrations of 2-APB almost completely diminished the amplitude of the plateau in the same cells in the continuous presence of GSK-7975A. This implies that the majority of SOCE can be attributed to the ORAI1/3 family, whereas the rest can be down to a component inhibited by 2-APB; and strongly indicates that other types of channels such as ORAI2 or the TRPC family of channels contribute to SOCE in PANC-1 cells.

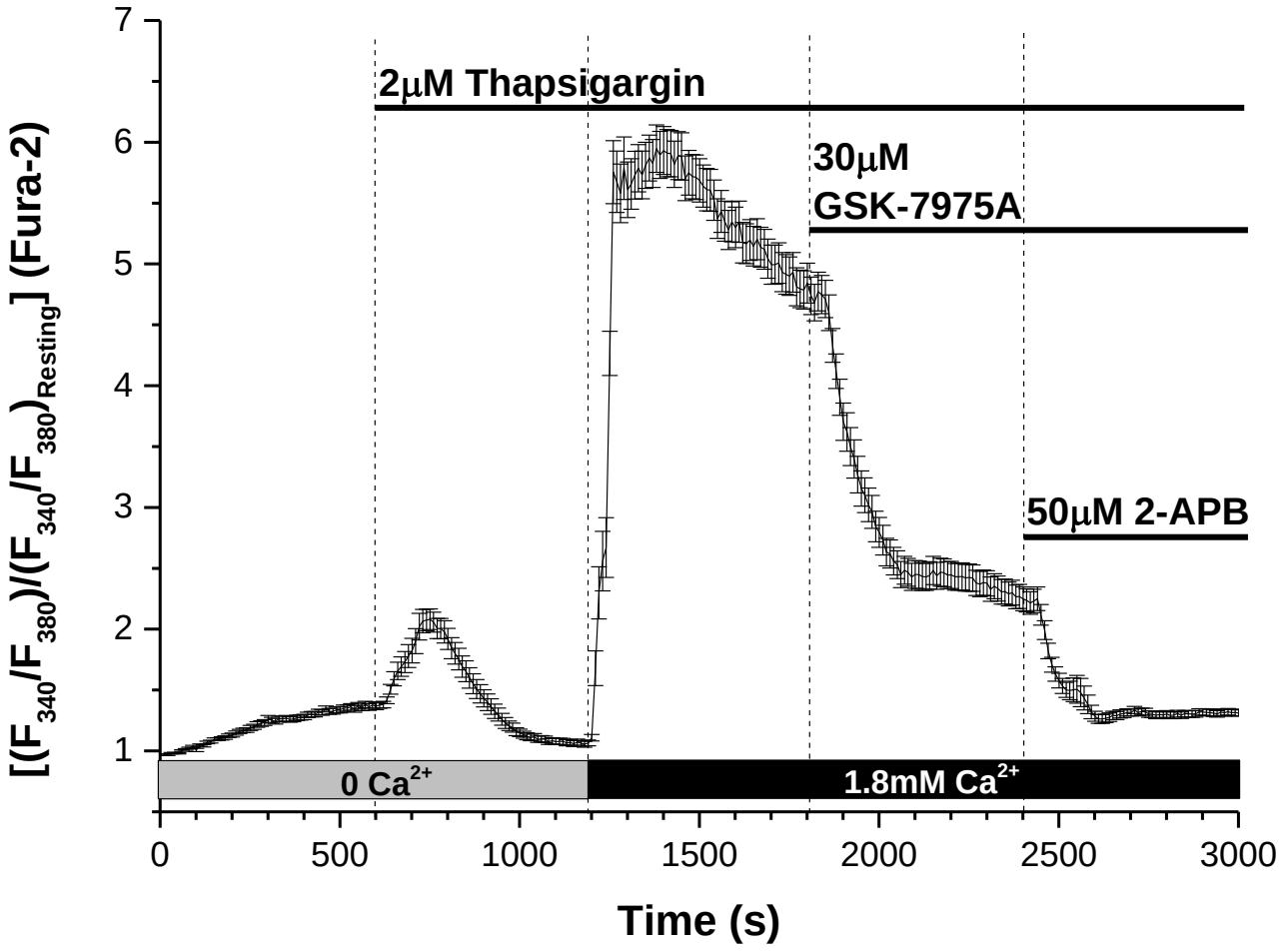

Figure 4.2.7. Combined GSK-7975A and 2-APB treatment potently inhbited SOCE in PANC-1 cells.

PANC-1 cells loaded with the Fura-2 dye were first treated with thapsigargin (2μM) for 10 minutes in Ca^{2+}-free conditions before Ca^{2+} (1.8mM) was added to the extracellular solution to induce SOCE. 10 minutes after SOCE activation GSK (30μM) was added to the extracellular solution and finally 2-APB (50μM) in the continuous presence of GSK (n=3 experiments, n=79 cells).

4.2.8. The effects of combined GSK-7975A and Pyr3 treatment on SOCE in PANC-1 cells

To test the candidacy of TRPC3, one of 2-APB's targets and proposed to be part of the CRAC channel machinery in pancreatic acinar cells (Cheng et al., 2013), we then used Pyr3, previously reported to be an efficient antagonist of this channel, (Zhou and Roper, 2014). Cells were first pre-treated with TG for about 20 minutes before the start of the experiment, then SOCE was activated by the addition of 1.8mM Ca^{2+} to the extracellular solution. 10 minutes later 30µM GSK-7975A was added for another 10 minutes before the addition of Pyr3. GSK-7975A again inhibited the bulk of the SOCE response, which was slightly higher than that recorded in figure 4.2.5 (fig 4.2.8); but Pyr3 application in the presence of GSK-7975A failed to produce further inhibition, unlike 2-APB. This suggests that TRPC3 is not involved in SOCE in PANC-1 cells.

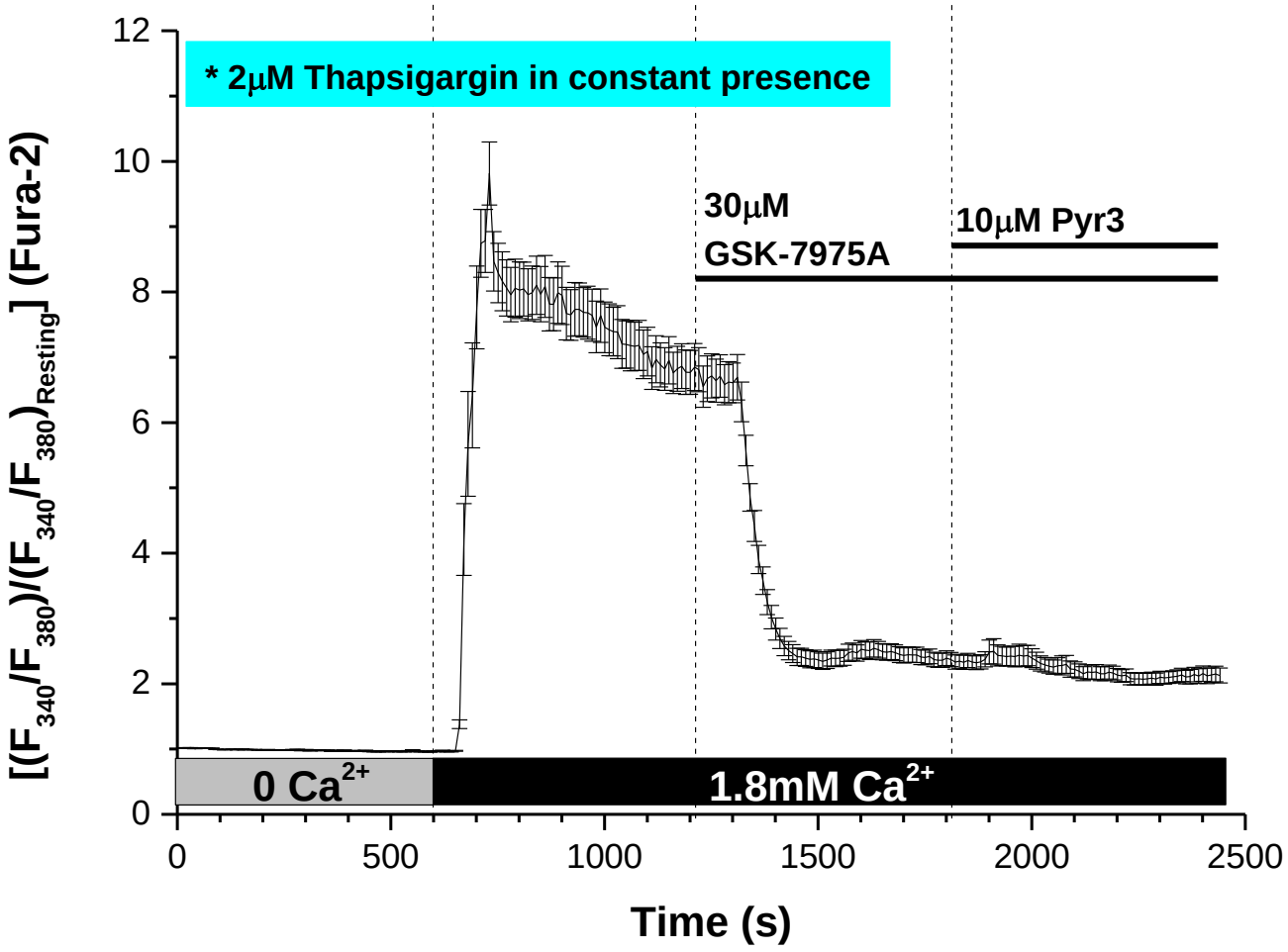

Figure 4.2.8. Pyr3 has no effects on GSK7975A-resistant component of SOCE in PANC-1 cells.

PANC-1 cells loaded with the Fura-2 dye were pre-treated with thapsigargin (2μM) in Ca^{2+}-free conditions for about 20 minutes before Ca^{2+} (1.8mM) was added to the extracellular solution to induce SOCE. GSK-7975A (30μM) was then added for 10 minutes after SOCE activation for 10 minutes before Pyr3 (10μM) treatment commenced in the continuous presence of GSK-7975A. Note that thapsigargin (2μM) was continuously present from the beginning of the experiment (n=2, n=58).

Key results from chapter 4

PANC-1 cells have an efficient Ca^{2+} signalling system, in which Store operated Ca^{2+} entry (SOCE) is particularly effective. ORAI1 channels appear to be the primary contributor to SOCE, but other channels that are sensitive to 2-APB-induced inhibition are likely to complement ORAI1 in this process.

Chapter 5 – The effect of Ca^{2+} signalling on cAMP/PKA signalling in PANC-1 cells

Chapter 5 – The effect of Ca^{2+} signalling on cAMP/PKA signalling in PANC-1 cells

Overview

Some Ca^{2+} signalling processes, especially that of SOCE, can activate cAMP signalling in various cell types; as mentioned in chapter 1.3. Therefore, the aim of this chapter was to apply the results from chapter 4, to ask whether the Ca^{2+} to cAMP cross-talk exists in PANC-1 cells.

In particular, it has been known for a number of years thanks to the work of Cooper's and Hofer's labs that SOCE can directly activate cAMP signalling in a large number of cell types (Willoughby and Cooper, 2007, Lefkimmiatis et al., 2009). Therefore, utilising a similar approach to chapter 3, we decided to measure PKA activity and cAMP levels in PANC-1 cells when Ca^{2+} signalling is manipulated. In this part of the study H134, which was already used in the characterisation of PDEs in chapter 3, measured changes in the relative cAMP concentration; whereas AKAR4 was used to measure downstream PKA activity in PANC-1 cells.

5.1. Effects of Neurotensin treatment on PKA activity in PANC-1 cells

First, to see if the activation of the Ca^{2+} signalling pathway can activate cAMP signalling in PANC-1 cells, in the presence of 1.8mM extracellular Ca^{2+}, we treated AKAR4-transfected cells with NT. As shown in fig 4.3.1A, the addition of 10nM NT transiently increased PKA activity, using the F_{YFP}/F_{CFP} ratio of AKAR4 as readout; giving strong indications that cAMP/PKA signalling can be influenced by G_q-GPCR signalling.

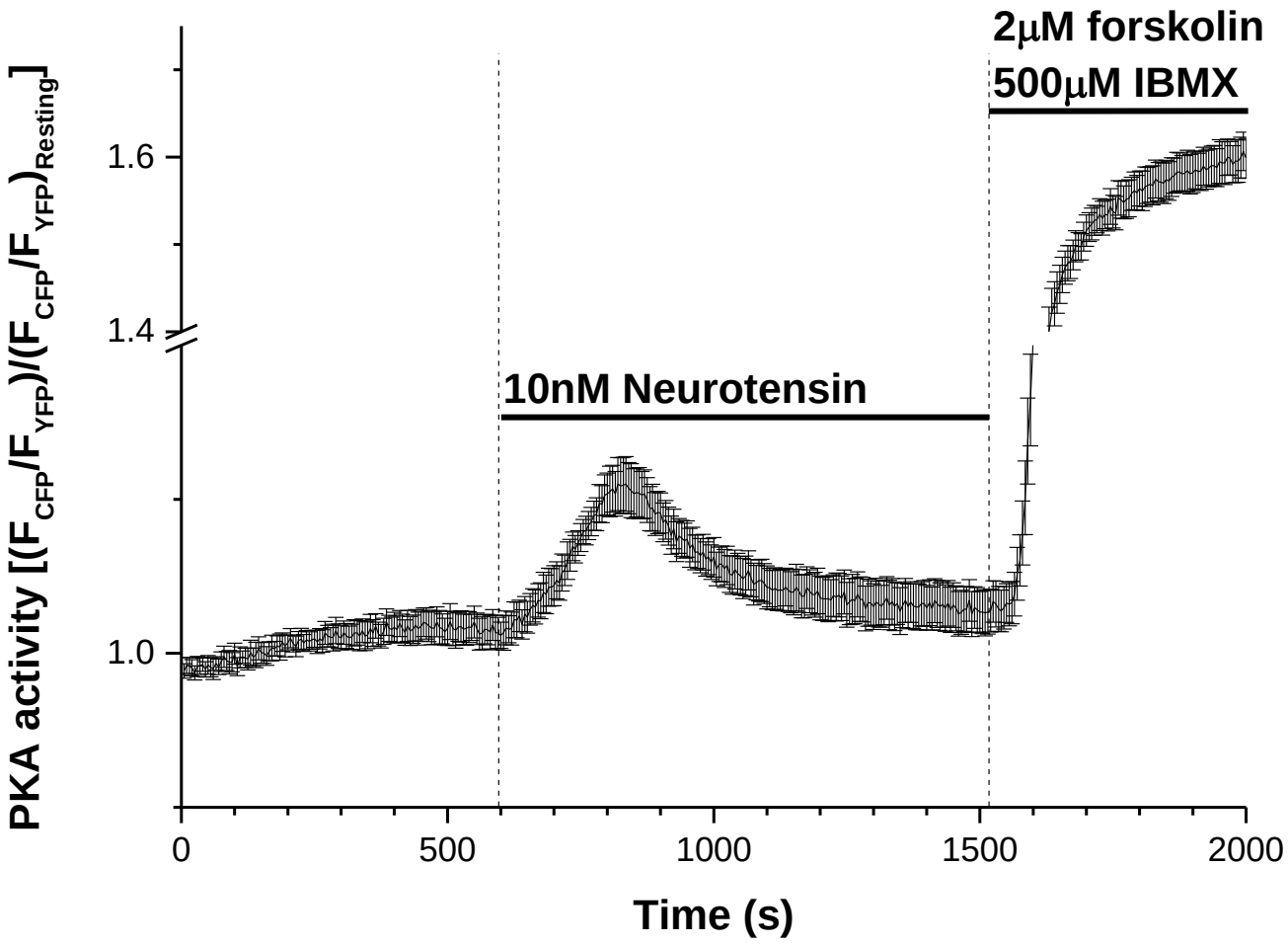

Figure 5.1. Neurotensin transiently increases PKA activity in PANC-1 cells.

A, PANC-1 cells transfected with AKAR4 was treated with neurotensin (10nM) for 10 minutes before forskolin (2μM) and IBMX (500μM) were added as positive control (n=2 experiments, n=10 cells).

5.2. Effects of store depletion and SOCE on cAMP signalling in PANC-1 cells.

Ca^{2+} signalling in non-excitable cells usually involve two core processes– Ca^{2+} release from intracellular stores induced by agonists, and SOCE to replenish stores to sustain signalling. Preliminary experiments described in fig 5.1 illustrated that NT, an effective activator of Ca^{2+} signalling, activates the cAMP signalling pathway. Coupling this with the knowledge that both of these processes can activate cAMP signalling (Lefkimmiatis et al., 2009, Willoughby and Cooper, 2007), we next decided to investigate the specific contributions of SOCE and the release of intracellular stores to cAMP signalling in PANC-1 cells.

5.2.1. Effect of store depletion and SOCE on cAMP levels in PANC-1 cells

PANC-1 cells transfected with H134 underwent 15 minutes of store depletion by TG in nominally Ca^{2+} free HEPES. This was followed by 15 minutes of SOCE induced by the addition of Ca^{2+} to the extracellular solution before 2µM forskolin and 500µM IBMX was used as positive control. Compared to the positive control, both treatments caused very mild effects (5.2.1A); on closer look, store depletion appeared to cause a very small decrease from the baseline whereas subsequent SOCE activation caused a mild transient increase of cAMP levels (5.2.1B).

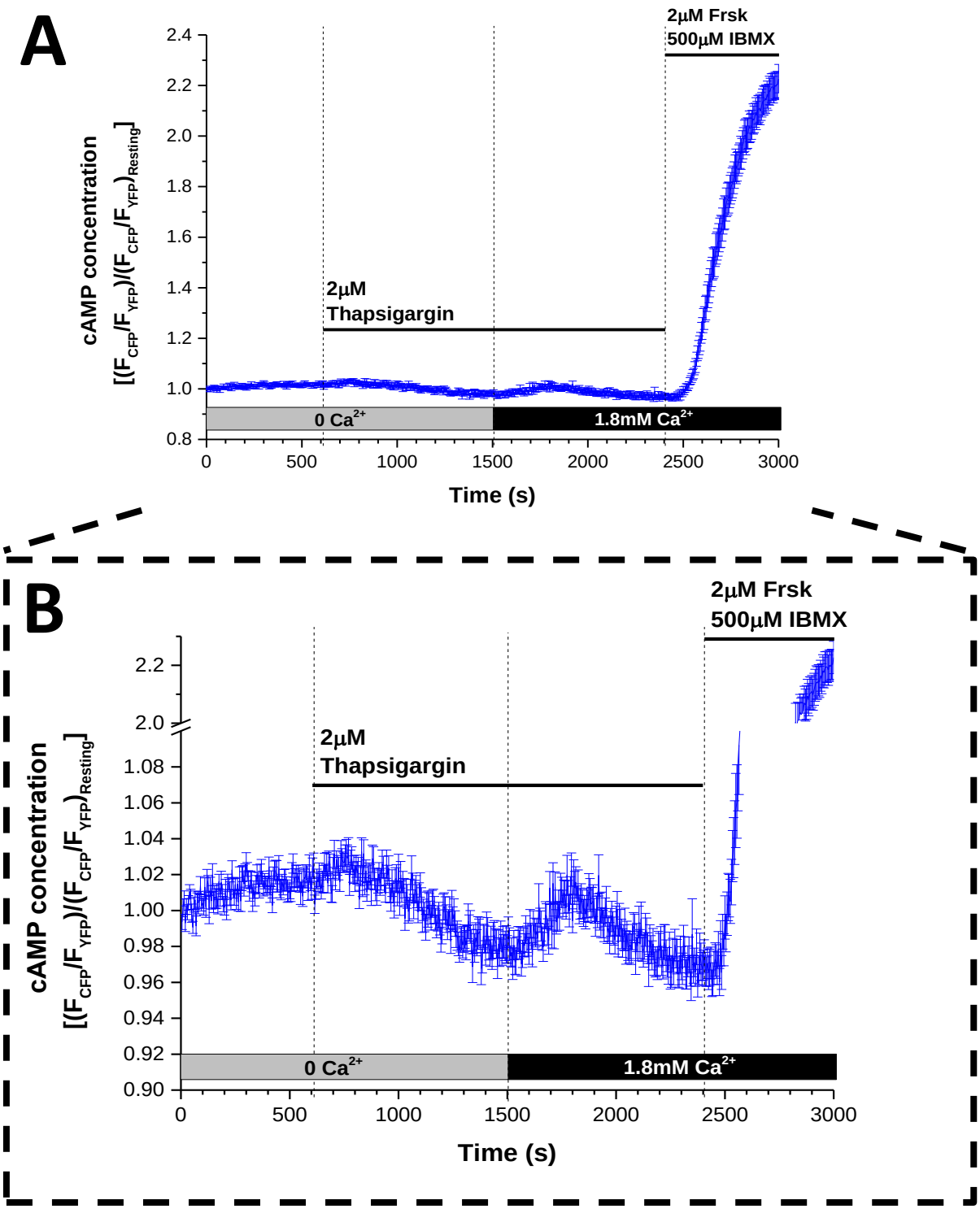

Figure 5.2.1. The effects of store depletion and SOCE on cAMP levels in PANC-1 cells.

A, PANC-1 cells transfected with H134 were treated with thapsigargin (2μM) for 15 minutes before Ca^{2+} (1.8mM) was added to induce SOCE for another 15 minutes. Forskolin (2μM) was used at the end of each experiment as positive control. B, Enlarged figure of A at the lower end of the scale (n=6 experiments, n=47 cells).

5.2.2. Effects of SOCE and store depletion on cAMP levels in PANC-1 cells in the presence of IBMX

Although effects shown in figure 5.2.1 were very small as compared to the positive control, SOCE activation did give a very mild increase in F_{CFP}/F_{YFP} ratio. To test whether the mild effects in response to store depletion and SOCE activation was due to the high PDE activity in PANC-1 cells, the same protocol as in as 5.2.1 was carried out; but this time in the presence of IBMX, which was added 15 minutes before TG application and present thereafter. In these experiments the addition of IBMX caused a slow increase from the baseline, making it difficult to analyse the difference between the baseline and effects caused by TG (figure 5.2.2A). However, on inspection, the addition of TG into Ca^{2+} free solution seemed to slow down the rise of the F_{CFP}/F_{YFP} ratio induced by IBMX. In the presence of IBMX, SOCE activation seemed to cause a small, stable increase in the F_{CFP}/F_{YFP} ratio (figure 5.2.2B). Taken together, these data do point at the existence of a Ca^{2+} to cAMP crosstalk in PANC-1 cells, though the effects are small.

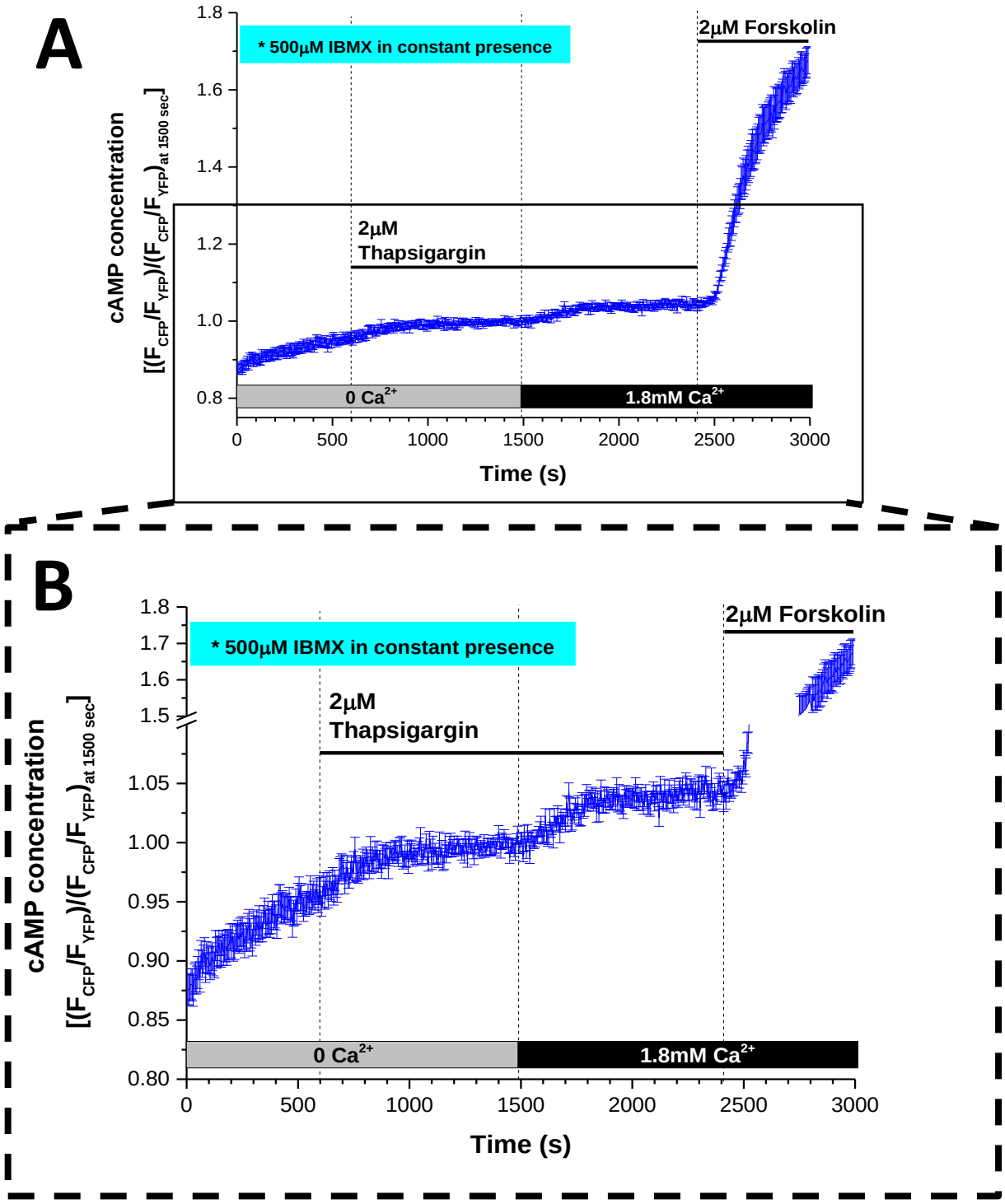
A
* 500μM IBMX in constant presence
2μM Forskolin
2μM
Thapsigargin
0 Ca2+
1.8mM Ca2+
cAMP concentration
[(FCFP/FYFP)/(FCFP/FYFP)at 1500 sec]
Time (s)
B
* 500μM IBMX in constant presence
2μM Forskolin
2μM
Thapsigargin
0 Ca2+
1.8mM Ca2+
cAMP concentration
[(FCFP/FYFP)/(FCFP/FYFP)at 1500 sec]
Time (s)

Figure 5.2.2. The effect of SOCE on cAMP levels in PANC-1 cells in the presence of IBMX.

A, PANC-1 cells transfected with H134 were treated with thapsigargin (2μM) for 15 minutes before Ca^{2+} (1.8mM) was added to induce SOCE. IBMX (500μM) was added 15 minutes before thapsigargin treatment and was present thereafter. Forskolin (2μM) was used at the end of each experiment as positive control. B, Fragment of A on an expanded scale (n= 6 experiments, n=30 cells. All data points here were normalised to the point just before Ca^{2+} was added at 1500 seconds).

5.2.3. The effect of store depletion and SOCE on PKA activity in PANC-1 cells

Next, we opted to examine the impact of store depletion and SOCE have on PKA, one of the main downstream targets of cAMP. By transfecting PANC-1 cells with AKAR4, one can measure relative cellular PKA activity by correlating it to the increase in F_{YFP}/F_{CFP} ratio (opposite to H134). In this study, the protocols used in 5.2.1 and 5.2.2 were repeated, but carried out using PANC-1 cells transfected with AKAR4. Interestingly, SOCE induction caused a notable and significant increase in F_{YFP}/F_{CFP} ratio (figure 5.2.3A). In the presence of IBMX pre-treatment, SOCE also caused an increase in PKA activity (figure 5.2.3B). Interestingly, AKAR4 also seemed to be sensitive enough to detect a mild increase in the F_{YFP}/F_{CFP} ratio as a result of TG treatment, the effect of which appearing to be slightly higher and more stable when IBMX was present (comparing the same component in figures 5.2.3A and 5.2.3B). In conclusion, these data suggest that the mild cAMP increase in response to SOCE detected by H134 (fig 5.2.1-2) may be translated to more significant increases in PKA activity downstream (fig 5.2.3); as a secondary observation, it appeared that store-depletion can also increase PKA activity.

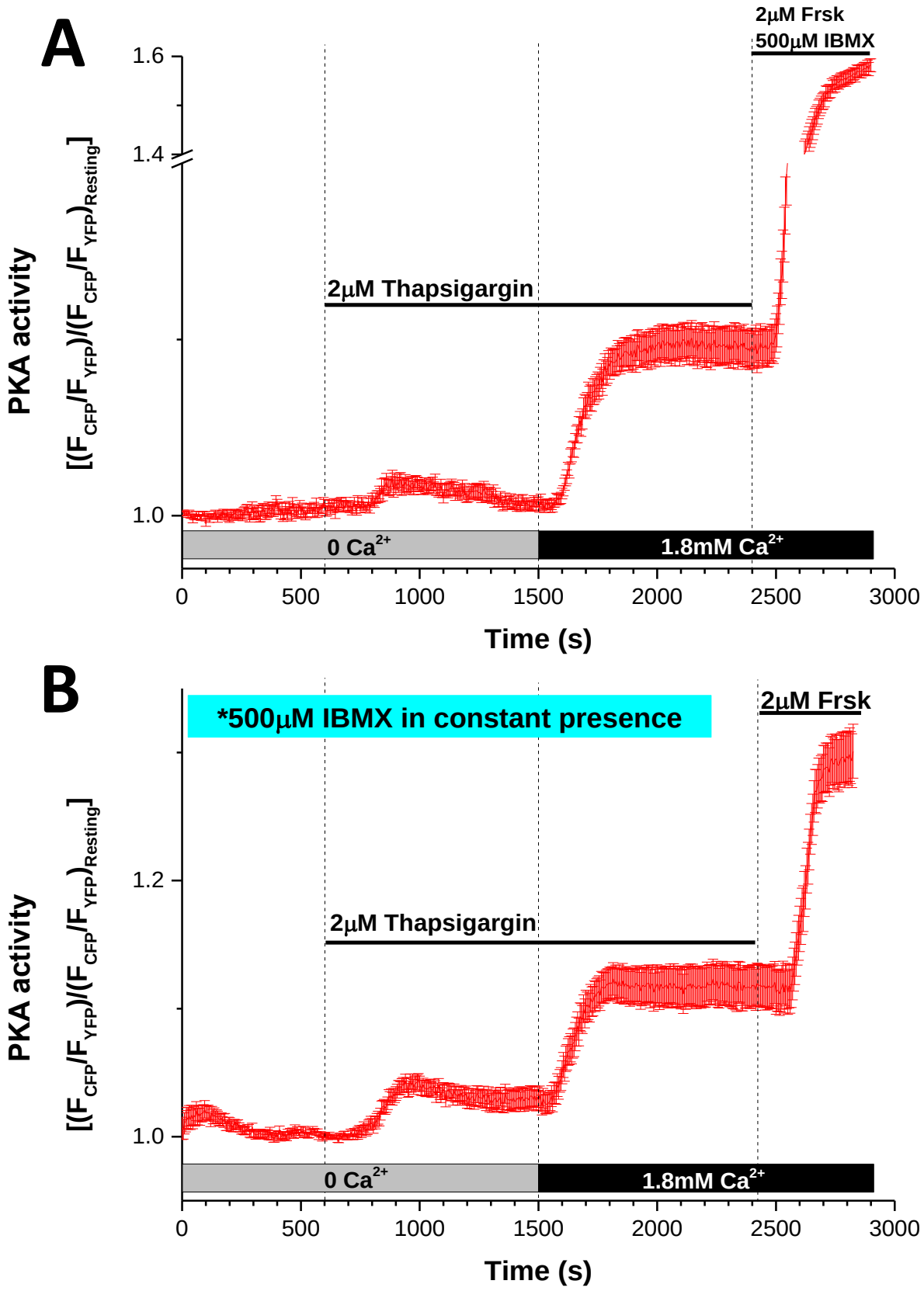
A
2μM Frsk
500μM IBMX
2μM Thapsigargin
0 Ca2+
1.8mM Ca2+
PKA activity
[(FCFP/FYFP)/(FCFP/FYFP)Resting]
Time (s)
B
*500μM IBMX in constant presence
2μM Frsk
2μM Thapsigargin
0 Ca2+
1.8mM Ca2+
PKA activity
[(FCFP/FYFP)/(FCFP/FYFP)Resting]
Time (s)

Figure 5.2.3. SOCE increases PKA activity in PANC-1 cells.

A, PANC-1 cells transfected with AKAR4 were treated with thapsigargin (2μM) for 15 minutes before Ca^{2+} (1.8mM) was added to induce SOCE for 15 minutes. Forskolin (2μM) and IBMX (500μM) was added at the end of each experiment as positive control (n=6 experiments, n=41 cells). B, The same experiment as in A, but IBMX (500μM) was added 15 minutes before thapsigargin treatment and was present thereafter. Forskolin (2μM) was used at the end of each experiment as positive control (n=5 experiments, n=34 cells).

5.2.4. The effect of IBMX on store depletion or SOCE

In this part of the project we decided to test if PDE inhibition modifies Ca^{2+} responses in PANC-1 cells as Ca^{2+} measurements were carried out in Fura-2 loaded PANC-1 cells. In nominally Ca^{2+} free conditions, the cells were first treated with IBMX for 15 minutes, before the application of TG for 15 minutes and finally the addition of 1.8mM Ca^{2+} into the extracellular solution. Figure 5.2.4 shows that both store depletion and SOCE still took place unhindered; confirming that PDE inhibition does not suppress either of the two Ca^{2+} signalling processes.

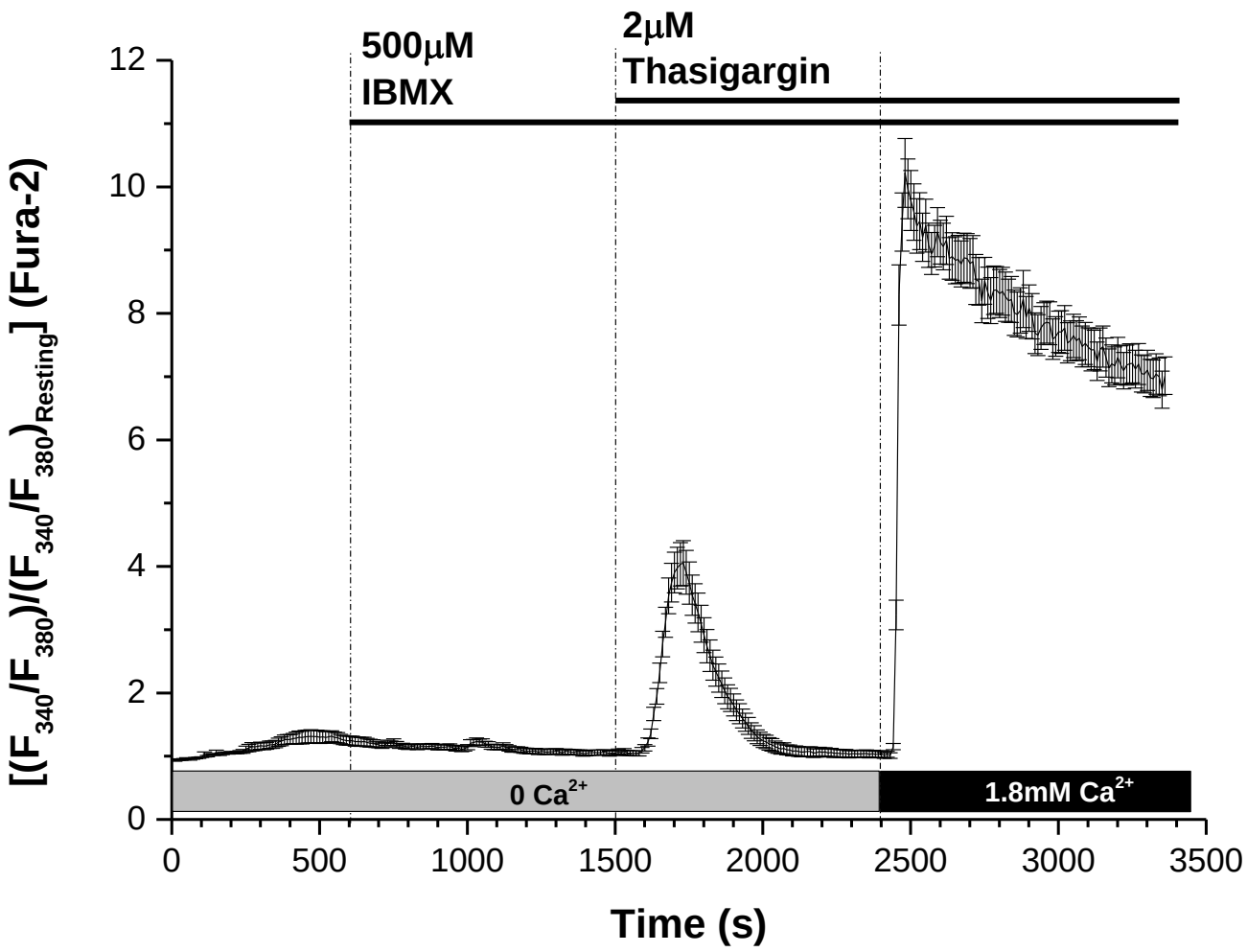

Figure 5.2.4. Store operated Ca^{2+} entry (SOCE) in PANC-1 cells recorded in the presence of IBMX.

PANC-1 cells loaded with Fura-2 were first pre-treated with IBMX (500μM) for 15 minutes before thapsigargin (2μM) was added to induce store depletion for 15 minutes. Ca^{2+} (1.8mM) was added at the end for 15 minutes to induce SOCE (n=2 experiments, n=65 cells).

5.3. Testing the dependency of SOCE-mediated PKA activity on Ca^{2+} in PANC-1 cells

After discovering that SOCE can activate PKA activity in PANC-1 cells, we then carried out a series of experiments in an attempt to characterise this phenomenon. For this study we applied the methodology described in chapter 5.2.3 to answer this question. Here, we decided to focus upon increases in PKA activity as a result of SOCE even though small increases were also observed as a result of store depletion.

5.3.1. SOCE-induced increase in PKA activity in PANC-1 cells is suppressed by removal of extracellular Ca^{2+}

Removing extracellular Ca^{2+} is one effective way of inhibiting SOCE. Therefore, in this experiment we decided to test if this procedure will suppress SOCE-activated PKA responses in PANC-1 cells. To do this, PANC-1 cells transfected with AKAR4 was first simultaneously treated with 500µM IBMX and 2µM TG for 15 minutes in nominally Ca^{2+} free conditions, 1.8mM Ca^{2+} was then introduced into the extracellular solution to initiate SOCE. Figure 5.3.1 shows that SOCE did indeed induce an increase in the F_{YFP}/F_{CFP} ratio, but afterwards the removal of Ca^{2+} from the extracellular solution resulted in a significant decline in the PKA response; implying that this SOCE-mediated PKA increase is influenced by Ca^{2+} entry into the cell.

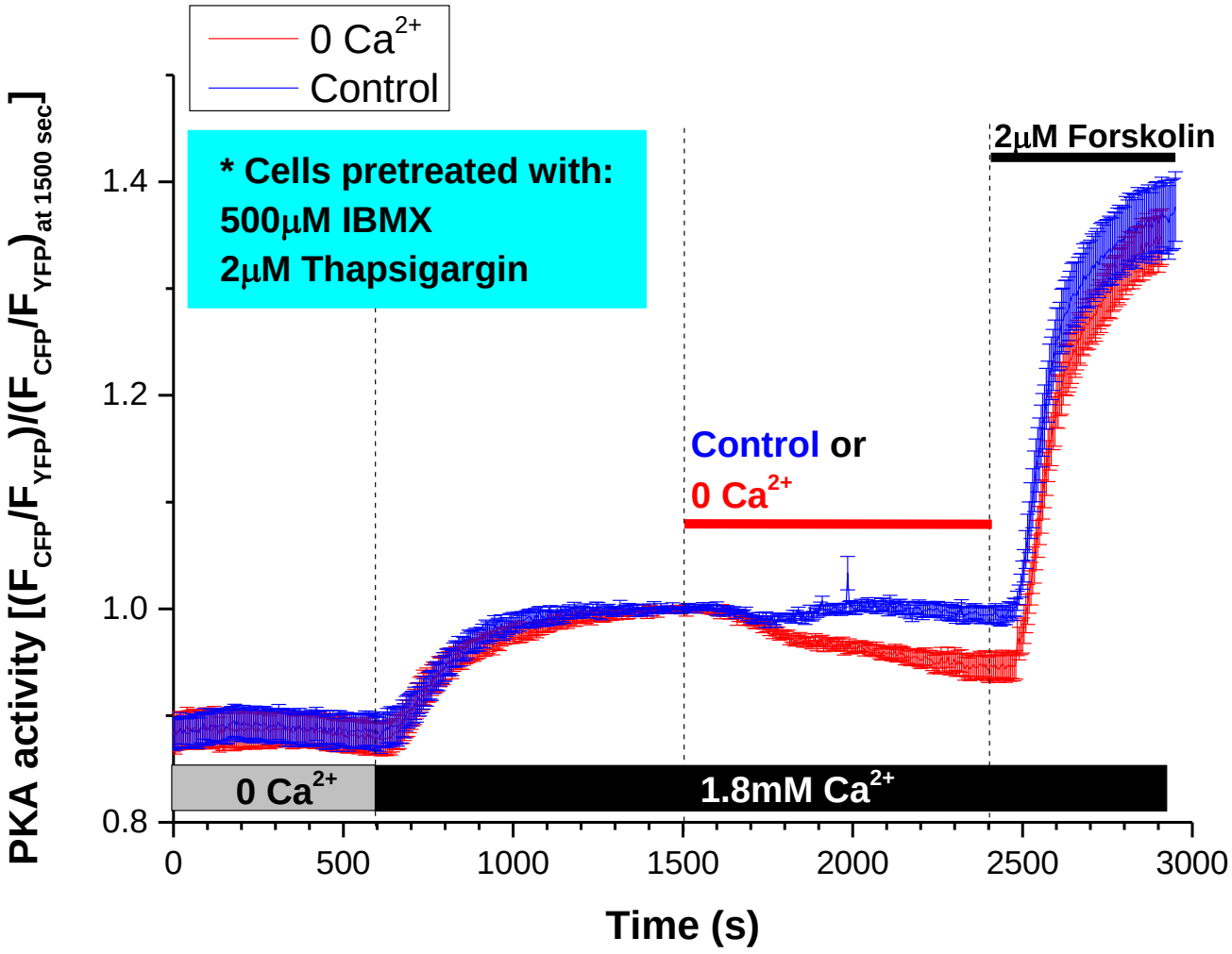

Figure 5.3.1. PKA activity in PANC-1 cells is dependent on Ca^{2+} entry via SOCE.

PANC-1 cells transfected with AKAR4 were treated with thapsigargin (2μM) and IBMX (500μM) simultaneously for 15 minutes before Ca^{2+} (1.8mM) was added for a further 15 minutes to induce SOCE. Extracellular Ca^{2+} was then removed by the re-introduction of Ca^{2+}-free solution for 15 minutes; whereas in the control, Ca^{2+} was not removed. Forskolin (2μM) was applied at the end of each experiment as positive control (n=5 experiments, and n=25 cells for 0 Ca^{2+}; n=3 experiments and n=20 cells for control. All data points here were normalised to the point just before Ca^{2+} was removed at 1500 seconds).

5.3.2. Testing the dependency of SOCE-mediated PKA activity on ORAI channels in PANC-1 cells

One of the major conclusions from section 4.2 was that ORAI1 is the main contributor to SOCE in PANC-1 cells. Therefore, we next went one step upstream of Ca^{2+} entry and asked whether this SOCE-mediated PKA activation is dependent on ORAI activity. In these experiments, we measured PKA activity utilising the protocol similar to that illustrated in figure 5.3.1. Fifteen minutes after SOCE was activated in AKAR4 transfected cells pre-treated with both IBMX and TG, 30µM GSK-7975A, a selective inhibitor of ORAI channels, was added to inhibit SOCE (see in fig 4.2.6 for the effect of GSK-7975A on SOCE). Compared to control, GSK-7975A application significantly inhibited SOCE-dependent PKA activity (fig 5.3.2); reducing the increase almost to pre-SOCE levels. Altogether, results described in 5.3.1 and 5.3.2 strongly suggest that SOCE-dependent PKA activity is ORAI and Ca^{2+} entry dependent.

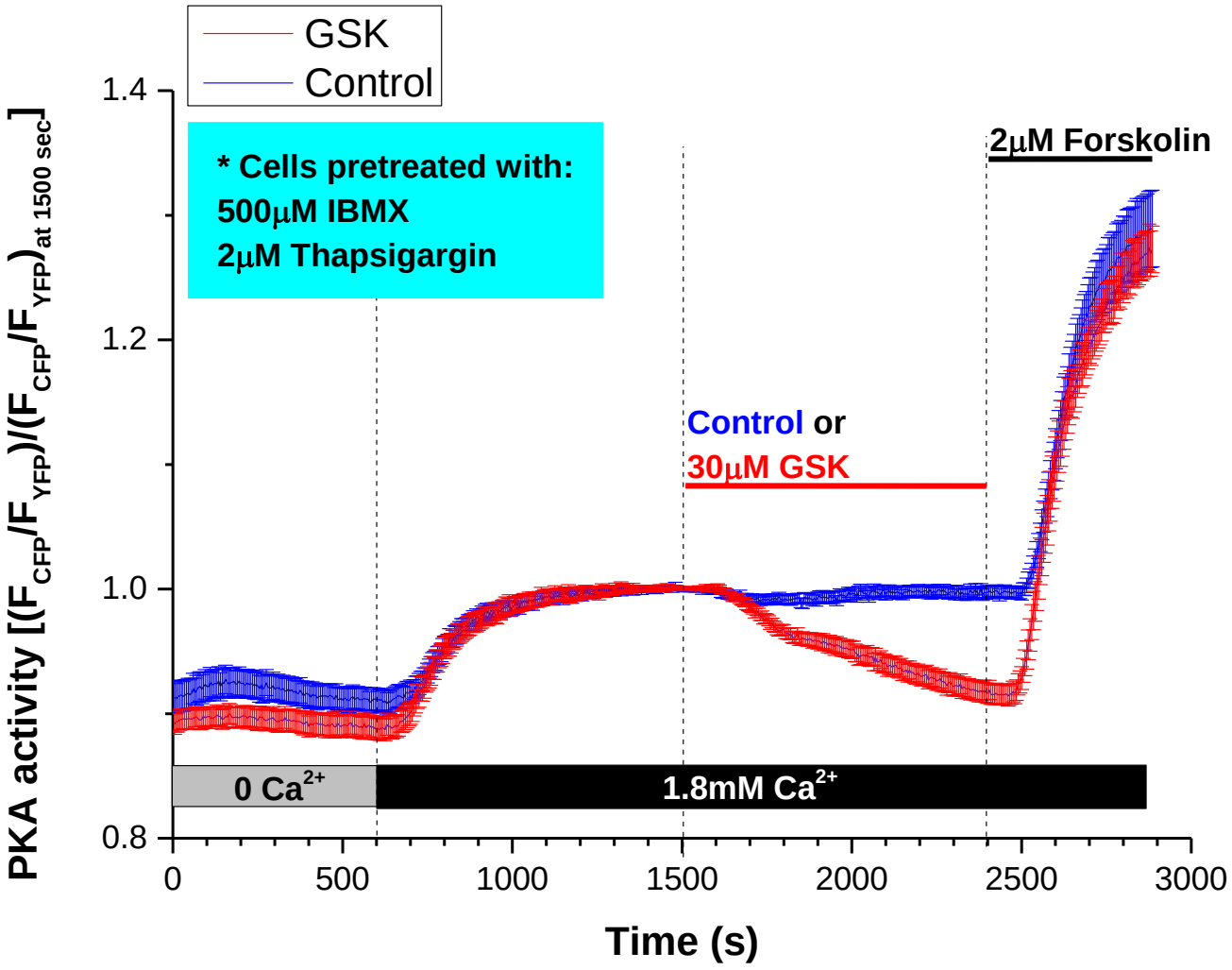

Figure 5.3.2. The Ca^{2+}-induced increase in PKA activity in PANC-1 cells is ORAI dependent.

PANC-1 cells transfected with AKAR4 were treated with thapsigargin (2μM) and IBMX (500μM) simultaneously for 15 minutes before 1.8mM Ca^{2+} was added to induce SOCE. 15 minutes after SOCE induction GSK-7975A (30μM) was added whereas in the control no drug was added. Forskolin (2μM) was applied at the end of each experiment as positive control (n=6 experiments and n=39 cells for GSK-7975A; n=5 experiments and n=25 cells for control. All data points here were normalised to the point just before GSK-7975A was added, at 1500 seconds).

5.3.3. Testing the dependency of SOCE-induced AKAR4 responses on H89 in PANC-1 cells

Experiments in this section aimed to verify that SOCE-induced AKAR4 responses can indeed be attributed to PKA. In these experiments PANC-1 cells transfected with AKAR4 were pre-treated with IBMX and TG for 15 minutes before SOCE was activated via external Ca^{2+} application. Following SOCE activation, which increases the AKAR4 FRET response, 10µM H89, a PKA inhibitor that had been used successfully in our hands previously (Burdyga et al., 2013), was added before forskolin was used as positive control. Notably, H89 application; completely obliterated the increase in F_{YFP}/F_{CFP} ratio back to pre-SOCE activation levels as compared to the control (fig 5.3.3). Furthermore, even after wash off, some degree of inhibition still remained as the positive control in H89-treated cells was also reduced as compared to control. This observation strongly supports the notion that SOCE-induced increase to the F_{YFP}/F_{CFP} ratio as reported by the AKAR4 probe is PKA dependent.

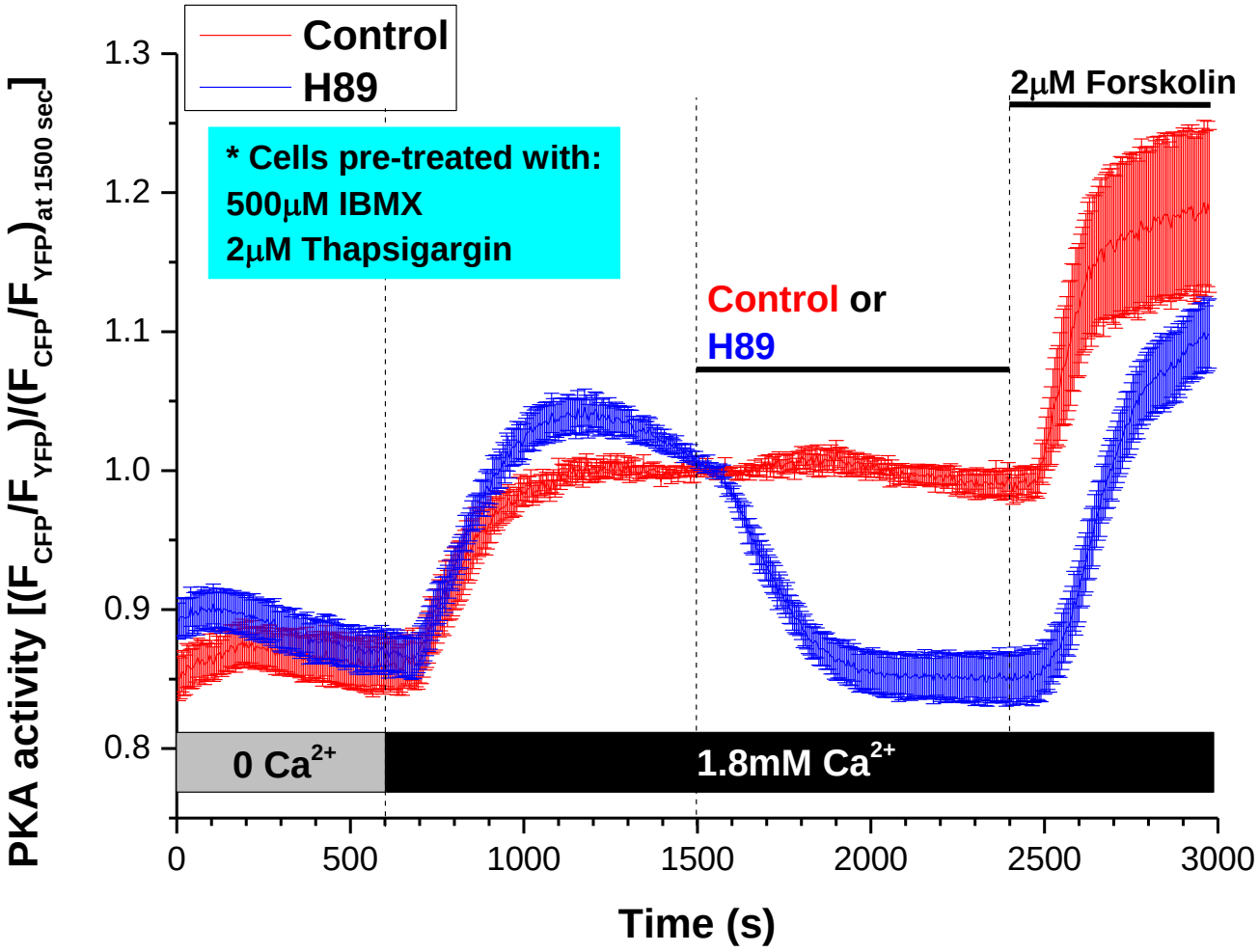

Figure 5.3.3. The Ca^{2+}-induced increase in the AKAR4 F_{YFP}/F_{CFP} ratio in PANC-1 cells is H89 dependent.

PANC-1 cells transfected with AKAR4 were treated with thapsigargin (2μM) and IBMX (500μM) together for 15 minutes before Ca^{2+} (1.8mM) was added for a further 15 minutes to induce SOCE. Cells were then treated with the PKA inhibitor H89 (10μM); whereas in the control no drug was added. Forskolin (2μM) was applied at the end of each experiment as positive control (n=4 experiments and n=13 cells for H89; n=4 experiments and n=12 cells for control. All data points here were normalised to the point just before H89 was added, at 1500 seconds).

5.4. Correlation of ER-PM junctions and areas of high PKA activity in PANC-1 cells

This and other studies revealed cAMP/PKA-dependent regulation of PANC-1 cell migration. We therefore decided to characterise the distribution of PKA activity in PANC-1 cells with particular emphases on PKA activity in the proximity of the leading edge, where the essential component of the migratory machinery are localised. To characterise the distribution of PKA activity we utilised commercially available antibodies against phosphorylated PKA substrates (Marcinkiewicz et al., 2006). Considering the observed SOCE-dependent activation of PKA responses (see fig 5.2.3) we also decided to investigate the localisation of ER-PM junctions, which serve as platforms for SOCE (Lewis, 2011).

In our laboratory we possess the necessary tools for the visualisation of ER-PM junctions which serves as platforms for SOCE - the PM-FRB-mRFP + ER-FKBP-CFP rapamycin-induced dimerization system (Varnai et al., 2007) and high resolution confocal microscopy. In this part of the study we also used commercially available antibodies against PKA substrate to visualise the distribution of PKA activity.

5.4.1. Mapping the localisation of endogenous ER-PM junctions in PANC-1 cells

It has been known for some time that SOCE is activated in ER-PM junctions in most non-excitable cells. More specifically, in PANC-1 cells these ER-PM junctions tend to be situated in the cell periphery adjacent to the leading edges, according to previous published data in our laboratory (Dingsdale et al., 2013). Therefore, to confirm this finding in this particular study we utilised the hetereodimerisation system involving two proteins modelled from an mTOR backbone – PM-FRB-mRFP and ER-FKBP-CFP. When rapamycin is added, if these two

constructs are within 10-14nm of each other, they will be cross-linked, inducing the colocalisation of mRFP and CFP fluorescence (Varnai et al., 2007). This technique is used to visualise ER-PM junctions already pre-formed under basal conditions, and random contacts where the ER and PM are in close proximity by chance. PANC-1 cells transfected with these two constructs were treated with 100nM rapamycin for 3 minutes before being fixed and imaged.

PM-ER punctas, as made visible by this method, seem to localise in the cell periphery; and appeared to congregate in the area behind the leading edge (fig 5.1). Although it is too early to extrapolate at this stage, this observation suggests that the machinery contained in ER-PM junctions regulate cell migration from just behind the leading edge, possibly in the transition zone or the lamella behind the lamellipodia.

ER-CFP

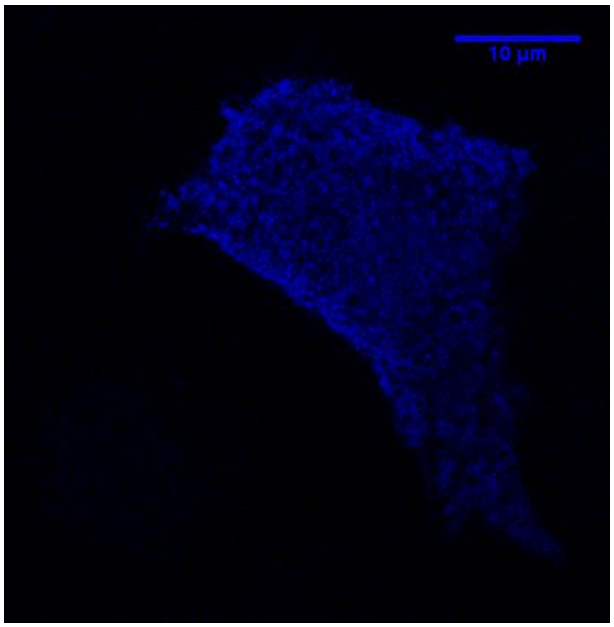

PM-mRFP

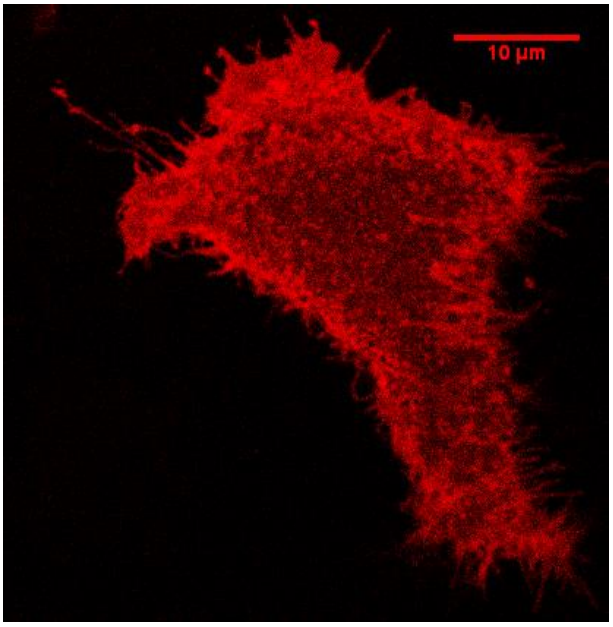

PM-mRFP + ER-CFP

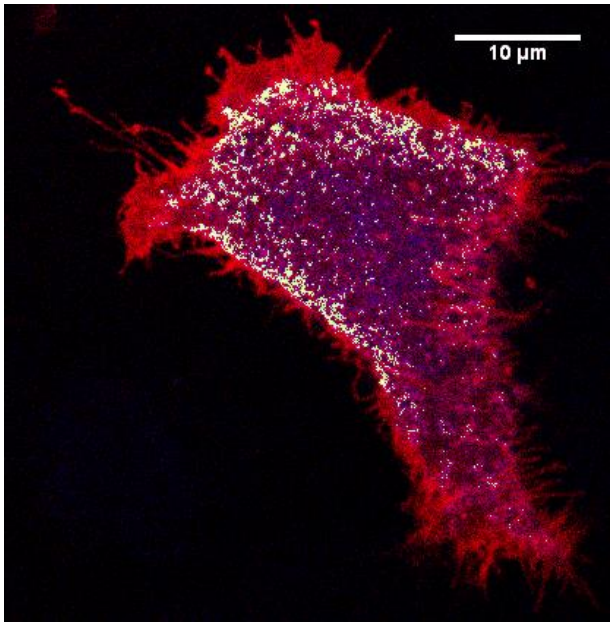

mRFP+CFP
co-localisation map

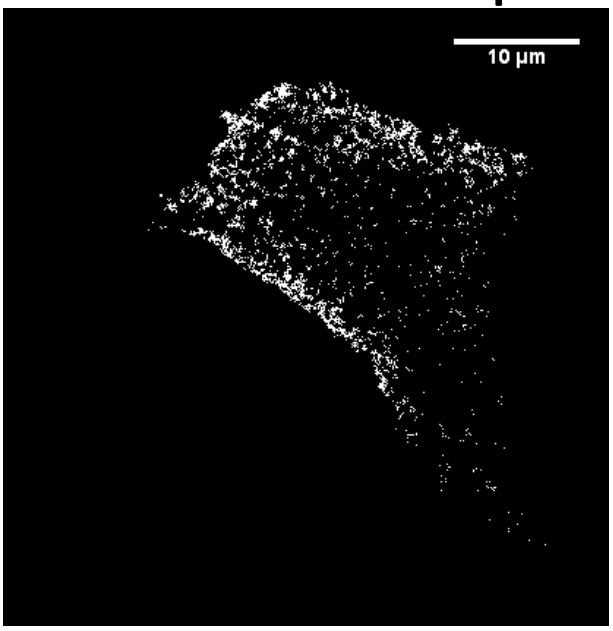

Figure 5.4.1. Mapping the localisation of endogenous ER-PM junctions in PANC-1 cells.

PANC-1 cells co-transfected with the PM-FRB-mRFP (red panel) and ER-FKBP-CFP (blue panel) constructs were first incubated in Na^+-HEPES-based solution supplemented with 1.8mM Ca^{2+} and 1% FBS for approximately 30 minutes at 37^oC and 5% CO_2 before being treated with Rapamycin (100nM). The cells were then fixed using 4% PFA and imaged with a confocal microscope. CFP and mRFP fluorescence emissions were recorded simultaneously. The bottom confocal optical slice of the cell (i.e. slice closest to the coverslip) was taken for processing. The resulting images were then analysed using the colocaliseRGB plugin on the ImageJ software, which performed a pixel analysis on the images; and then produce a map to show where in the cell CFP and mRFP fluorescence overlapped by the greatest amount, which is assumed to be the locations of the ER-PM junctions (displayed by white spots). PM-mRFP + ER-CFP panels show where the ER-PM junctions are located with respect to the plasma membrane as reported by PM-mRFP staining. This cell is representative of 3 independent experiments.

5.4.2. Mapping out the location of PKA activity in PANC-1 cells

In an effort to elucidate the distribution of PKA activity in PANC-1 cells, we then decided to use the immunofluorescence approach using the antibody specific for phosphorylated PKA substrate. Unstimulated PANC-1 cells maintained in 1% FBS and 1.8mM Ca^{2+} for 30 minutes were fixed and stained for phospho-PKA substrate using Alexa 488 as the secondary antibody. Interestingly, there seems to be heavy staining for PKA substrates in the leading edges of migrating cells and in the nucleus (fig 5.4.2). There was also staining in the cytosol, with a generally dispersed intensity gradually decreasing towards the cell periphery before almost disappearing in the region just behind the leading edge. These observations strongly suggest high PKA activity in the nucleus and the leading edge.

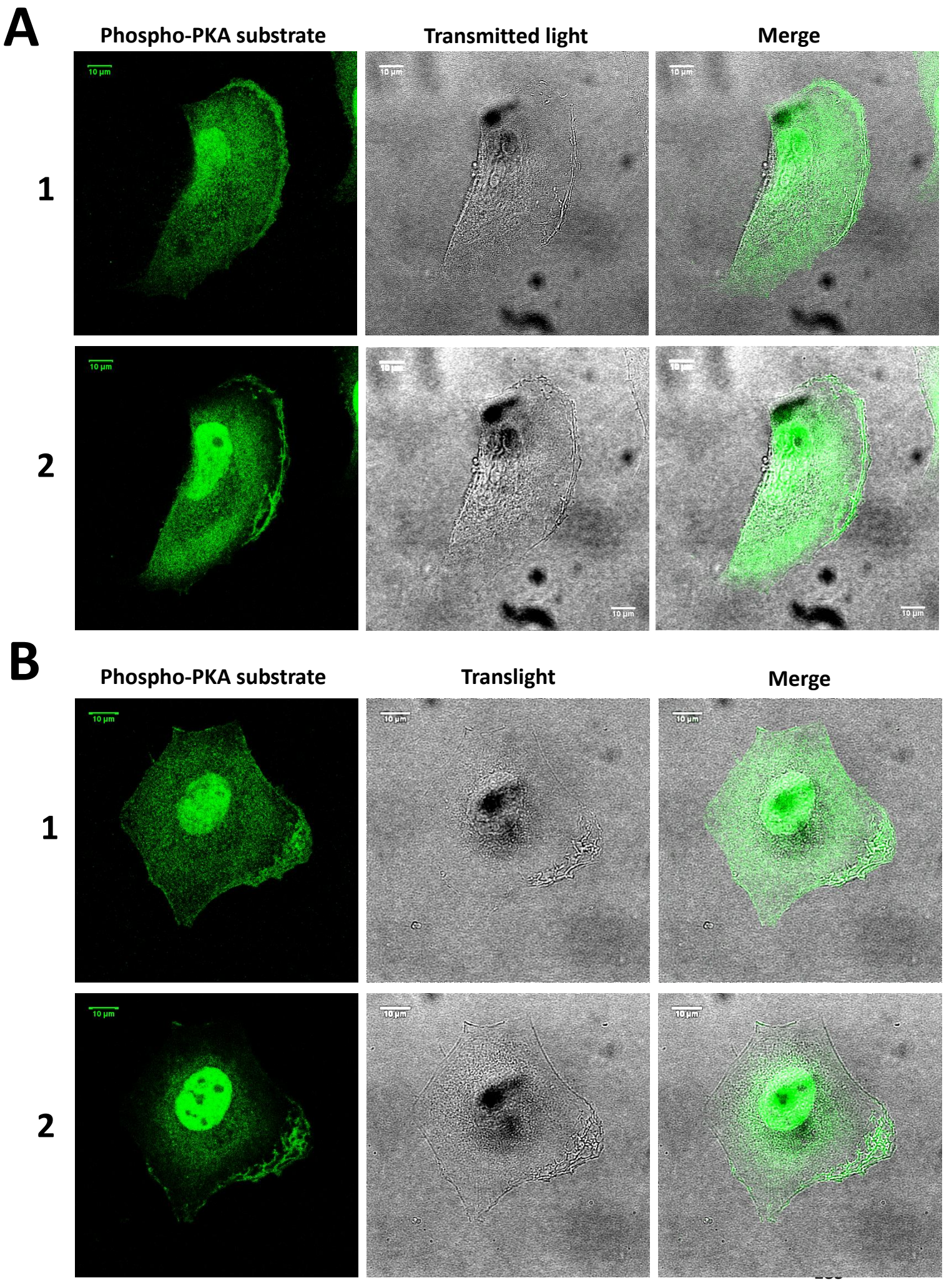
A
Phospho-PKA substrate
Transmitted light
Merge
1
2
B
Phospho-PKA substrate
Translight
Merge
1
2
10 µm

Figure 5.4.2. PKA substrates accumulate in the nucleus and leading edges of migrating PANC-1 cells.

Unstimulated PANC-1 cells maintained in Na^+-HEPES based solution plus 1% FBS and 1.8mM Ca^{2+} for 30 minutes were immuno-stained for phospho-PKA substrates and were then imaged via confocal microscopy, with Alexa488 conjugated to the secondary antibody for readout. Two different confocal slices of two different cells are shown: A1 and B1, confocal section closest to the coverslip; A2 and B2, sections positioned a few μm above the coverslip to reveal the ruffles. These two cells are representative of at least 5 independent experiments.

5.4.3. Mapping the location of PKA substrates and actin in PANC-1 cells

Such a significant presence of phosphorylated PKA substrates in the leading edges of PANC-1 cells implies that PKA is likely to have a role in the regulation of cell migration, and would co-localise with polymerised actin. In an attempt to verify this statement the same PKA staining experiments as described in 5.4.2 was done here, but in PANC-1 cells transfected with Lifeact-RFP. Figure 5.4.3 shows that in 4 different migrating PANC-1 cells imaged, the leading edge actin displayed notable colocalisation with phospho-PKA substrates. These observations confirm the spatial proximity of PKA substrates and polymerised actin in the leading edge. Such spatial proximity could be important for cAMP/PKA-dependent regulation of migration described in this cell type (Burdyga et al., 2013, Zimmerman et al., 2013).

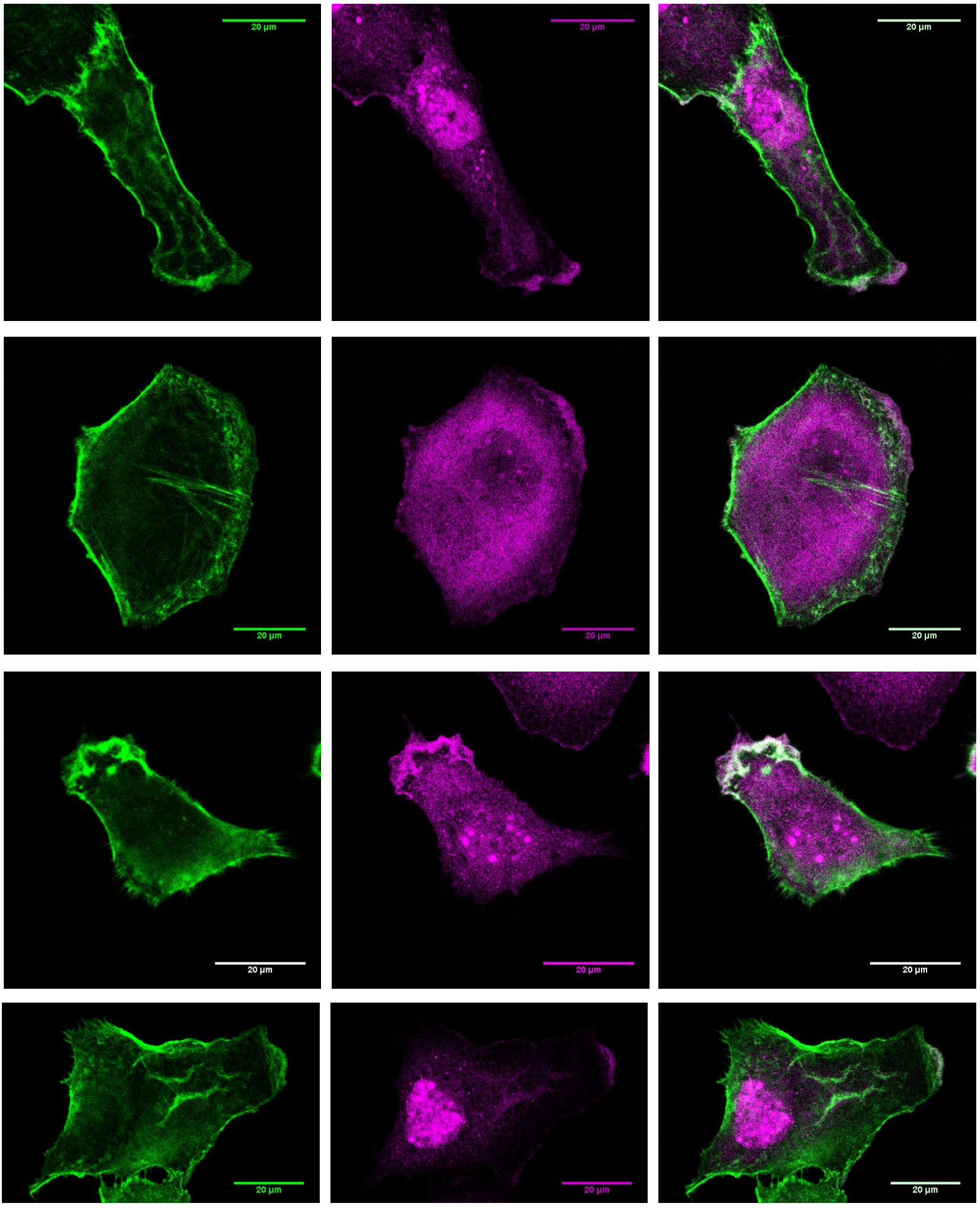
Lifeact-RFP
Phospho-PKA substrate
Merge
20 µm

Figure 5.4.3. Phospho-PKA substrate partially co-localise with leading edge actin ruffles in PANC-1 cells.

PANC-1 cells transfected with Lifeact-RFP maintained in Na^+-HEPES based solution plus 1% FBS and 1.8mM Ca^{2+} for 30 minutes were immunostained with phospho-PKA substrate antibody (using alexa488 as the secondary antibody) before being imaged using a confocal microscope. All images were recorded from the ventral parts of the cell closest to the coverslip and processed using the ImageJ software. Lifeact-RFP is in green, phospho-PKA substrates are in magenta; and the areas of co-localisation are in white. Scale bars in all panels represent 20μm. These 4 cells are representative of 2 independent experiments.

Key summary from chapter 5

Store operated Ca^{2+} entry can effectively increase PKA activity in PANC-1 cells, in a process that is sensitive to the inhibition of ORAI1.

ER-PM junctions, which are platforms for SOCE, are concentrated behind the leading edge. On the other hand, high densities of phosphorylated PKA substrates were observed in the leading edge, where phospho-PKA substrates co-localise with actin. High density of phospho-PKA substrates was also observed in the nucleus.

Chapter 6 – Discussion

Chapter 6 – Discussion

The main aim of chapter 3 was to see if more specific ways of increasing cAMP levels in pancreatic cancer cells than forskolin and IBMX can be found after finding that increasing global cellular cAMP concentration significantly inhibited migration and invasion in pancreatic cancer cell lines. The results from the first part of the study suggests that under basal conditions, the cAMP signalling pathway is unlikely to be endogenously active in PANC-1 cells because in the sole presence of PDE inhibition by IBMX, increases in cAMP levels was slow and low in magnitude; whereas in the presence of stimulation like forskolin and isoproterenol IBMX rapidly saturated the probe within minutes. This implicates that like other cancers, PDAC has high endogenous PDE activity to keep basal cytosolic cAMP levels as low as possible (Savai et al., 2010).

6.1. PDE3 and PDE4 are the main regulators of cAMP in PANC-1 cells

One notable observation from chapter 3.1 was that PDE3 seemed to be the main cAMP regulator in PANC-1 cells, whereas PDE4 also appeared to be active, albeit at a lower magnitude. However, rolipram dramatically increased cAMP levels in nearly every cell tested when PDE3 was inhibited previously. This observed hierarchical nature of PDE3 and PDE4 activity in PANC-1 cells suggests that PDE3 may act as the 'sentinel' of cAMP signalling, serving as the first point of regulation to prevent the overstimulation of the pathway in the cytosol. As a result, PDE3 (i.e. A and/or B isoforms) and PDE4 could play non-redundant roles in this cell type by the virtue of different cellular locations; where PDE3 is located near ACs where cAMP is made, and PDE4 is located deeper in the cell. Indeed, PM-specific PDE3 activity was seen previously in pheochromocytoma cells, where it regulates EGF and NGF-

mediated nuclear ERK activity (Herbst et al., 2011). Also, the apparent PDE3-PDE4 synergy observed in this study is not uncommon, as it was also observed in the pancreatic β-cell line MIN6 cells (Tian et al., 2012), brown adipose tissue (Kraynik et al., 2013), vascular smooth muscle cells (VSMC); and in airway smooth muscle, where the application of both PDE3 and PDE4 inhibitors together had a more potent relaxant effect than when either was added alone (Shakur et al., 2001).

In terms of cancer, PDE3 expression and activity has been reported in only a few studies. Notable examples include human squamous cell carcinomas (Shimizu et al., 2002) and neoplastic submandibular gland intercalated duct (Murata et al., 2001), where cilostamide has growth inhibitory effects; and melanomas, where the treatment of the cell line B16-F10 with cilostazol promoted melanin production in a PKA/CREB dependent manner (Wei et al., 2014). PDE3 is also found to be expressed in three different hepatoma cell lines, where their exact functions remains elusive (Murata et al., 1996); moreover, PDE3B expression has been found in trace levels in human chronic lymphocytic leukaemia (C-LL) cells when PDE4 was inhibited as a compensatory mechanism (Moon et al., 2002).

In non-cancerous tissues, PDE3A is expressed in the heart, vascular smooth muscle, oocytes and platelets; whereas PDE3B is found predominantly in adipose tissues, hepatocytes and pancreatic islets (Shakur et al., 2001). The activation of PDE3 is predominantly via phosphorylation by PKA and protein kinase B (PKB, also known as Akt kinase), which is counteracted by the phosphatase PP2A (Shakur et al., 2001, Bender and Beavo, 2006). Interestingly, when PDE3 was first discovered in adipocytes, the insulin signalling pathway was one of the first discovered mechanisms that activate this isozyme (Shakur et al., 2001). In this case, the activation of the insulin receptor results in the activation of PI3K, leading to

the activation of PKB, which then in turn phosphorylates PDE3, activating the enzyme to destroy cAMP (Shakur et al., 2001). In cells that take part in metabolism, this PKB-PDE3 pathway serves to counteract and modulate catecholamine-induced lipolysis (Shakur et al., 2001). In the context of this study, insulin and insulin-like growth factor (IGF) receptors have been found expressed on a various PDAC cell lines (Fisher et al., 1996), including PANC-1 cells, where it appeared to potentiate cell proliferation as well as GPCR-mediated Ca^{2+} signalling in a PI3K dependent manner (Young and Rozengurt, 2010). Given the proximity of PDAC (exocrine pancreas) to the endocrine pancreas, it is not unreasonable to hypothesise that PDAC may be in a microenvironment where local insulin levels is high (Nakagawa et al., 1993, Bertelli et al., 2001); and chronic insulin stimulation can hold PDE3 at a constitutively active state to keep cAMP levels down. Supporting this interpretation, destruction of β-cells, which produces insulin, inhibited pancreatic tumour development, whereas agents that help β-cells to proliferate also promoted carcinogenesis in a BOP-induced PDAC model in hamsters (Hennig et al., 2004). Keeping this in mind, it would be useful to use antagonists of insulin receptors (Schaffer et al., 2008) and inhibitors of PKB/Akt to test this hypothesis.

In contrast to PDE3, the link between PDE4 and cancer is better established. PDE4A and PDE4D is highly expressed and active in a variety of lung cancer cell lines in response to hypoxia (Pullamsetti et al., 2013) and TGFβ activation (Kolosionek et al., 2009); where the downstream activation of NF-κB, Nrf2, p38, ERK and increases of ROS levels have all been reported as a result of PDE4-mediated cAMP suppression (Yeo et al., 2014, He et al., 2014, Wagner et al., 2002, Kolosionek et al., 2009). In brain tumours, PDE4A (especially the super-short PDE4A1 isoform) is reported to play a significant role in facilitating tumour and xenograft growth downstream of Ca^{2+} and phospholipase D (PLD) signalling by sculpting the

intracellular cAMP gradient (Sengupta et al., 2011, Warrington et al., 2010, Goldhoff et al., 2008, Gallagher et al., 2004, Chen et al., 2002, Schmidt et al., 2010). Colorectal cancer cells overexpress PDE4B (PDE4B2) as a result of oncogenic KRAS signalling, which suppressed apoptosis, possibly via the PI3K-Akt pathway, and potentiated the disassembly of epithelial tight junctions (Tsunoda et al., 2014, Tsunoda et al., 2012, McEwan et al., 2007). This PDE4B-Akt relationship is also reported to be excessively active in B-cell lymphomas to mediate glucocorticoid resistance (Kim et al., 2011, Smith et al., 2005). In prostate cancer, PDE4D appears to play a central role in proliferation and tumourigenesis (Rahrmann et al., 2009), where the PDE4D7 isoform appears to regulate cAMP levels in the sub-plasmalemmal compartments of androgen sensitive prostate cancer cells (Henderson et al., 2014). Moreover, PDE4 activity has been reported in melanoma cells downstream of ERK signalling to confer glucocorticoid resistance (Marquette et al., 2011, Kowalczyk et al., 2009, Narita et al., 2007). Elsewhere, the presence of PDE4 in other cancers is also observed in B-cell lineage chronic lymphocytic leukaemia cells (B-CLL) (Dong et al., 2010, Meyers et al., 2009, Meyers et al., 2007, Tiwari et al., 2005, Moon and Lerner, 2003), osteosarcoma cells (Ahlstrom et al., 2005, Narita et al., 2003), retinoblastoma cells (White et al., 2004) and pheochromocytoma cells (Chang et al., 1997). Interestingly, in nearly all of the cases mentioned above, the inhibition of PDE4 by rolipram or removal by RNAi resulted in growth inhibition, cell cycle arrest, decreased tumour size and increased apoptosis; implicating PDE4 to be a potentially important target for the development of cancer treatment.

In the context of this study, it remains unclear how PDE4 is regulated in PANC-1 cells; therefore it would be interesting to measure cAMP levels in the presence of PKA and ERK (both reported activators of PDE4) activators and inhibitors. This is to test whether a cAMP-

PKA feedback exists in this cell type and, to see if ERK, which is a downstream component of oncogenic Kras, activates PDE4. Moreover, due to half of the KRAS expressed in PANC-1 cells being constitutively active (Deer et al., 2010), it would also be useful to measure ERK activity in PANC-1 cells using cellular probes for ERK activity developed recently (Harvey et al., 2008) to test if basal ERK activity is indeed elevated in PANC-1 cells.

This study also points towards the activity of PDE1 and PDE10A in PANC-1 cells. 8-mm-IBMX was chosen on the basis that it inhibited PDE1 in pancreatic β- cells (Tian et al., 2012). However, one must be cautious when confirming this because 8-mm-IBMX does not inhibit PDE1 fully at lower concentrations but displays inhibition of PDE4 at high concentrations (Dunkern and Hatzelmann, 2007). Therefore, the small, transient increase of cAMP reported here could be due to an off-target inhibition of PDE4 or a genuine effect on PDE1. Secondly, regarding the inhibition of PDE10A, papaverine is a semi-specific inhibitor for this isoform, as it has has been used to study PDE10A in various organs including the lung and the striatal neurones, where this isozyme is predominantly expressed (Xie et al., 2006, Tian et al., 2011b, Siuciak et al., 2006). In this study, papaverine dramatically increased cAMP levels in PANC-1 cells when PDE3 was also inhibited. This can be interpreted as a genuine inhibition on PDE10A, or it can be due to an off-target inhibition of other PDEs. This is because papaverine has also been described as a non-specific PDE inhibitor, as it also displayed IC_{50} at low micromolar ranges for PDE3 and PDE4 (Siuciak et al., 2006). Indeed, the increase in cAMP levels caused by 10μM papaverine appeared quite similar to that produced by rolipram; implying that PDE4 activity was also inhibited by papaverine treatment. On the other hand, PDE10A has also been recently reported to be expressed in human colon tumour cell lines, where 10μM papaverine treatment as well as PDE10 knockdown inhibited

cell growth by 60% but in a cGMP dependent manner (Li et al., 2014). Therefore, a comprehensive biochemical analysis of PDE1C and PDE10A is required to investigate the presence of PDE1 and PDE10 in PANC-1 cells.

The last set of results from chapter 3.1 was that the potent PDE5 inhibitor T0156 did not have any effects on cAMP levels induced by forskolin. The direct conclusion from this experiment was that T0156 did not have any effects on cAMP-hydrolysing PDEs in PANC-1 cells. In terms of cGMP signalling, however, this experiment was carried out in conditions where the stimulation of intracellular cGMP pathway has not been validated; so the inhibition of cGMP breakdown here may mean a slow accumulation of cGMP much like the cAMP in the presence of IBMX alone, where cGMP levels in the cell after 10 minutes of PDE5 inhibition could be too low to affect cAMP levels in the cell. Indeed, PDE5A1 and PKG1 activity has been reported in multiple PDAC cell lines including PANC-1 cells, the blockade of which resulted in reduced migration and proliferation and induced cytotoxicity (Karakhanova et al., 2014). Moreover, nitric oxide, (NO), a well-known activator of cGMP/PKG signalling, has recently been observed to potentiate migration and invasion in carbon ion irradiated PANC-1 cells; with the PI3K-Akt and RhoA signalling pathways being the possible downstream effectors (Fujita et al., 2014). Therefore, as well as biochemical analyses, it would be useful to repeat this experiment in the presence of guanylyl cyclase activators and PDE5 inhibitors to probe the potential cAMP-cGMP cross-talk further in PANC-1 cells. Indeed, much like cAMP, genetically encoded FRET-based cGMP/PKG sensors have also been recently created (Niino et al., 2010, Sprenger and Nikolaev, 2013) which, given the relative success rate of PANC-1 cell transfection and cAMP measurement, would also be useful in answering these questions.

Therefore, the next part of this study would be to go deeper into the mechanism, starting with asking which of the 2 isoforms of PDE3 and which of the 4 isoforms of PDE4 are present in PANC-1 cells, either via RT-PCR or western blotting; before deducing the localisation of PDE3 and PDE4 in relation to each other by immunofluorescence. Note that PDE8, which is a cAMP-specific isoform that is insensitive to IBMX-mediated inhibition, was not tested pharmacologically as the inhibitor, PF-04957325 (Shimizu-Albergine et al., 2012), is not yet commercially available. However, with the reported synergy between PDE8 and PDE4 in mind (Demirbas et al., 2013) it would be interesting to biochemically probe for its presence in PANC-1 cells.

6.2. β-adrenergic agonists are the principal physiological cAMP agonist in PANC-1 cells

The results of chapter 3 also suggests that β-adrenergic receptors (β-ARs) maybe the dominant Gαs-coupling GPCR to mediate cAMP signalling, as isoproterenol increased cAMP levels in PANC-1 cells in a dose-dependent manner. β-ARs are physiologically receptors for catecholamines adrenaline and noradrenaline, which are neurotransmitters produced during stress responses. There are generally two types of β-ARs, β1 and β2, to which noradrenaline is the physiological agonist of β1-AR and adrenaline is the agonist of β2-AR (Schuller and Al-Wadei, 2010); whereas isoproterenol, the agent used in this study, can activate both types. The finding that isoproterenol readily increased cAMP concentrations in PANC-1 cells is not too surprising, as pancreatic cancer cells have been reported to express both types (β1 and β2) of ARs in a number of studies, with β2 being the dominant isoform (Lin et al., 2012). Indeed, β-ARs have been prominently reported to affect the physiology of

a wide range of cancers, where they can modulate proliferation/growth, cell migration/invasion and apoptosis (Tang et al., 2013). The purpose of this study was to confirm that the β-ARs expressed on PANC-1 cells can increase cellular cAMP levels when activated, which was achieved with isoproterenol. The next step of this study would be to use β1 and β2-selective agonists to specifically investigate if the two β-AR subtypes have differential effects on cAMP signalling in this cell type. This is in light of reports in the past that β1 and β2 expressed on the same cell can mediate different downstream effects (Communal et al., 1999, Richter et al., 2008). Immediately downstream, we have also found that both PDE4 and PDE3 regulates cAMP produced by β-ARs; with the same observations made of the cAMP levels being the highest when PDE4 and PDE3 inhibitors were present together than either was present alone. Therefore, it would also be interesting to couple β1/ β2-selective agonists with isoform-specific PDE inhibitors in cAMP measurements to probe if the two receptors are coupled with distinct macromolecular complexes containing different PDE isoforms. Furthermore, although we have yet to test this possibility at this stage, it would be intriguing to use pertussis toxin to test if the Gαi subunit opposes the isoproterenol-mediated cAMP activation and, if either of the β-AR subtypes can couple to this AC-inhibitory subunit when activated.

Data from chapter 3 also showed that VIP and secretin, prominent cAMP agonists in the pancreas and other organs of the digestive system, did not appear to increase cAMP levels in PANC-1 cells as compared to isoproterenol at increasing concentrations (1, 10 and 100nM); even when PDE activity was inhibited. In the normal exocrine pancreas VIP, secreted by vagal parasympathetic nerve terminals, binds to VIP-1 and VIP-2 receptors (also known as $VPAC_1$ and $VPAC_2$ respectively) to modulate the secretion of digestive enzymes in

acinar cells and fluid/electrolyte secretion in ductal cells (Sabbatini et al., 2013, Lee et al., 2012). Our current observations supports previous reports that PANC-1 cells only weakly express the VIP-1 receptor but do not couple ligand binding to cAMP production (Jiang et al., 1997, Igarashi et al., 2002, al-Nakkash et al., 1996, Ding et al., 2002). However, looking at the literature, it seemed that PANC-1 and MiaPaCa-2 cell lines represent the minority in terms of VIP signalling; as it was found that intact human PDAC tumours express both VIP-1 and VIP-2 receptors and, apart from MiaPaCa-2 and PANC-1 cells, most other PDAC cell lines actually express VIP-1 (but not VIP-2) receptors (Jiang et al., 1997, Ding et al., 2002). Moreover, activation of VIP-1 receptor in PDAC cells that express them by nanomolar concentrations of VIP increased intracellular cAMP levels in a dose-dependent manner. When tested in one of the PDAC cell lines (Capan-2) that endogenously express VIP-1 receptors and in a non-cancerous cell line (Chinese hamster ovary, CHO cells) ectopically expressing VIP-1 receptors, VIP actually promoted cell proliferation (Jiang et al., 1997, Ding et al., 2002); supporting similar studies carried out nearly 30 years ago (Ruellan et al., 1986, Estival et al., 1983). Therefore, it would be inappropriate at this stage to extrapolate the conclusions of this part of the study to all PDAC cell types; but it would be interesting to study the mechanism in which VIP-mediated cAMP production mediates cell growth/migration in responsive cells such as Capan-2 cells.

In the healthy normal pancreas, secretin, produced by intestinal S cells, is the principal inducer of bicarbonate and fluid secretion in the pancreatic duct; via its group B family of Gαs-coupling GPCRs (Lee et al., 2012). Secretin receptors are expressed extensively in ductal epithelial cells and acinar cells (Chey and Chang, 2003, Korner et al., 2005). However, during neoplastic transformation the expression of secretin receptors seem to significantly

decrease and become more heterogenous (Korner et al., 2005). Moreover, although multiple pancreatic cancer cell lines were found to express secretin receptors; their ability to stimulate cAMP production was impaired in response to secretin, requiring very high concentrations of this ligand for activation (Ding et al., 2002). In that particular study, PANC-1 cells, alongside MiaPaCa-2 cells, did not respond to secretin at all, even at micromolar concentrations (Ding et al., 2002). This was proposed to be due to their expression of a dominant-negative, soluble form of the secretin receptor, which is a splice variant form in which the third and fourth exon (expressing the N-terminal tail) was spliced out (Ding et al., 2002, Hayes et al., 2007). Not only do they not respond to secretin, the splice variants disrupted the normal functions of wild-type secretin receptors. Therefore, in this study it was not a surprise to see that PANC-1 cells failed to respond to secretin. Interestingly, ectopic expression of functional secretin receptors in Chinese hamster ovary (CHO) cells actually resulted in growth inhibition, suggesting that the intracellular pathway generated by secretin-generated cAMP signalling is growth-inhibitory (Ding et al., 2002). Therefore, unlike VIP, results from our current study that PANC-1 cells have defective secretin signalling correlated relatively well with other PDAC cell types.

As an extension of this study, apart from VIP and secretin, it would also be useful to test other agents reported to modulate cAMP in the pancreas and PDAC cells like somatostatin (Li et al., 2004), Pituitary adendylyl-cyclase activating peptide (PACAP) (Hollande et al., 1995), peptide YY and neuropeptide Y (Liu et al., 1995, Vona-Davis and McFadden, 2007, Schwetz et al., 2013), GABA (Takehara et al., 2007, Al-Wadei et al., 2012), acetylcholine (Ackerman et al., 1989) and cholecystokinin/gastrin (Smith et al., 1996, Thommesen et al., 2001, Cayrol et al., 2006).

PDAC cells and samples have been reported to overexpress cyclooxygenase-2 (COX-2), which partly mediate the aggressive phenotype of this cancer (Hennig et al., 2002, Hennig et al., 2005, Ding et al., 2001, Tucker et al., 1999). COX-2 is an enzyme that catalyses the production of the prostaglandin family of signalling molecules from arachidonic acid (Hausmann et al., 2014). Among this family, the two best described prostaglandins are prostaglandin E_2 (PGE_2) and prostacyclin (also called prostaglandin I_2); which mediate signalling by activating an equally diverse family of GPCRs (DP, EP1-4, FP, IP, and TP), the specificity of which depending on the cell type as reviewed previously (Hata and Breyer, 2004, Coleman et al., 1994). In pancreatic cancer, PGE_2 appeared to be the dominant downstream effector of the overexpressed COX-2 (Hasan et al., 2008); with increased expression of metalloproteinases and enhanced migration/invasion as one of its major documented effects (Ito et al., 2004, Eibl et al., 2003). Prostacyclin, on the other hand, has not been studied in PDAC. In other organs, prostacyclin mainly targets the vascular endothelium and erythrocytes to mediate anti-platelet and vasodilatory effects (Vane and Botting, 1995) via the IP receptor. As the IP receptor is a Gαs-coupling GPCR which stimulates cAMP signalling when activated, we decided to test the ability of prostacyclin to increase cAMP in PANC-1 cells.

To do this, iloprost, a stable analog of prostacyclin, was used in this study. Our preliminary results showed that iloprost treatment resulted in a modest increase of cAMP levels, both when applied alone or in the presence of IBMX. However, the cAMP responses observed here was still less consistent and lower in amplitude as compared to that produced by isoproterenol. There could be two reasons for this - either trace amounts of IP receptors are expressed on PANC-1 cells, or the off-target activation of EP1 receptors (which couple to the

Gαq subunit to activate the PLC pathway) by iloprost may have influenced cAMP concentrations as a secondary effect (Abramovitz et al., 2000). The first hypothesis can be tested easily by using RT-PCR or western blotting for IP receptor presence, as well as to see if prostacyclin is made in PANC-1 cells like PGE_2. Indeed, PANC-1 cells have an established PGE_2 autocrine signalling loop, meaning that they can make and secrete their own PGE_2 as well as respond to PGE_2 at the cell surface (Ito et al., 2004). Therefore, it would be interesting to see if a parallel signalling loop exists for prostacyclin in the regulation of cAMP levels in PANC-1 cells. The second hypothesis can be tested by asking if EP1 receptor is expressed in PANC-1 cells, as well as by measuring cellular Ca^{2+} levels in response to iloprost. The results from these proposed experiments would still not confirm the hypothesis, but can at least invalidate it or confirm the existence of an EP1-Ca^{2+} pathway in PANC-1 cells; which would be interesting as a Ca^{2+} →cAMP crosstalk exists in this cell type (chapter 5). Given that 5 out of 8 prostanoid receptors are linked to the activation of AC while the other 3 are linked to either Ca^{2+} mobilisation or the inhibition of ACs (Breyer et al., 2001, Negishi et al., 1995); and PGE_2 potentiates PANC-1 cell migration/invasion while an increase in cAMP signalling had the opposite effects, it would be interesting to next see if PGE_2 can directly regulate prostacyclin and/or cAMP signalling in PANC-1 and indeed PDAC cells and tumours. Furthermore, one can investigate if other agonists of the prostaglandin family such as thromboxane, prostaglandin D2 and F2α can mediate cAMP signalling.

6.3. Isoproterenol has little effects on PANC-1 cell migration

After finding that β-ARs are capable of physiological cAMP activation, whereas PDE3 and PDE4 are the dominant cAMP destroyers in PANC-1 cells, the second aim of chapter 3 was to

apply these findings to test if manipulating each of these cAMP signalling components can influence PANC-1 cell migration further downstream; as reported by Boyden chamber assays.

Despite its ability to increase cAMP levels in PANC-1 cells, isoproterenol did not inhibit PANC-1 cell migration even at very high concentrations (100nM) whereas forskolin (Burdyga et al., 2013) and IBMX alone did. In comparison, despite having next to no effects on random migration, high concentrations of isoproterenol (100nM) inhibited directional migration in the presence of IBMX compared to just IBMX alone; suggesting that β-AR signalling may have a role to play in chemotactic PANC-1 cell migration. Given that β-AR signalling is generally associated with a potentiation, and not inhibition, of cell migration and invasion of a wide range of cancer cells (Tang et al., 2013), this observation from our study is not entirely surprising. There could be a few reasons why cAMP increases from β-AR signalling failed to inhibit cell migration; but it was unlikely to be due to the preferential activation of Epac, which potentiates PANC-1 cell migration (Burdyga et al., 2013), instead of PKA because isoproterenol can also ably activate PKA in a dose dependent manner. It is likely here that both arms of the pathway are active in response to isoproterenol; such that the downstream effects of PKA and Epac are mutually cancelled out upstream of cell migration. However, it is also possible that the activation of β-adrenergic receptors could mediate off-target effects via the Gβγ subunit (Kim et al., 2012, Kang et al., 2014), or by coupling to different Gα subsunits such as Gαi, to either directly counteract cAMP signalling, or activate a cAMP-independent pathway to stimulate migration (Kirui et al., 2010). As mentioned earlier, isoproterenol can activate both β1 and β2 receptors and can therefore potentially trigger both Gαs and Gαi signalling simultaneously. On this regard, noradrenaline

has already been tested with regards to the migration and invasion of pancreatic cancer cells, but yielded ambiguous results in which 2 studies reported increases whereas 1 study reported inhibition (Huang et al., 2012, Guo et al., 2009, Stock et al., 2013). On the other hand, in another study blockage of β-AR signalling by antagonists has also been reported to suppress pancreatic cancer cell migration and invasion, with β2 playing a larger role in this process than β1 by upregulating COX-2, MMP family and VEGF (Zhang et al., 2010). Therefore, with evidence that the two β-AR subtypes can produce different signalling outcomes, next it would be more appropriate to assess the role of β1 specific agonists such as denopamine and β2 specific agonists such as clenbuterol on PANC-1 cell migration (Baker, 2010), as well as the application of pertussis toxin to test the effects of Gαi (mentioned earlier). This study can also be coupled with immunofluorescence in colocalisation studies to deduce where the β-ARs are in relation to different Gα-subunits in migrating cells. It is interesting to note here that β-AR signalling has been reported to transactivate EGF receptors (EGFR) in immortalised pancreatic ductal cells (Askari et al., 2005), and EGFR has been shown to mediate PDAC cell migration (Stock et al., 2014). Therefore, this transactivation mechanism provides another avenue in which cAMP-dependent inhibition of cell migration could be neutralised. Alternatively, as the migration experiment was carried out in 6-hours, the second reason could be that chronic receptor stimulation caused the internalisation of the receptors into a compartment of the cell where the receptor cannot influence cell migration. This hypothesis can be tested via immunofluorescence of β-adrenergic receptor distribution in migrating PANC-1 cells before and after isoproterenol stimulation; as well as a measurement of cAMP concentrations of PANC-1 cells that had undergone 6 hours of constant isoproterenol treatment to see if the cells can still respond to β-AR activation.

6.4. PDE3 is the principal regulator of the cAMP signalling arm that modulates PANC-1 cell migration

Aside from β-AR signalling, results from chapter 3 also implied that both PDE4 and PDE3 activity regulates PANC-1 cell migration; as cilostazol and rolipram application effectively inhibited cell migration. Under basal conditions, both PDE3 and PDE4 share the workload in regulating cAMP pools that influence spontaneous cell migration; though PDE3 is more likely to carry a higher importance in this physiological process. Intriguingly, in the presence of isoproterenol, PDE4 seemed to have a larger role to play than PDE3 in PANC-1 cell migration, as rolipram inhibited cell migration but cilostazol had no effects; though PDE3 cannot be ruled out in this case because cilostazol and rolipram produced additive inhibitory effects on cell migration. As we've found earlier both PDE3 and PDE4 can regulate cAMP levels derived from β-AR, these results suggest that the pool of cAMP generated by β-AR signalling that can regulate cell migration is likely to be influenced mainly by PDE4 activity, where the synergy between PDE3 and PDE4 observed in the corresponding cAMP measurements also appeared to translate into the regulation of cell migration downstream; in an effect similar to that reported previously on vascular smooth muscle cells (Palmer et al., 1998). Of course, until the specificities of the β-Adrenergic pathway are better understood in PANC-1 cells, it is not productive at this stage to extrapolate any further. This can however be probed further by immunostaining for PDE3, 4 and the different subtypes of β-ARs in migrating PANC-1 cells to look at their locations with respect to each other.

When migrating up the chemoattractant (5% FBS in this case) gradient, the results profile was similar to that observed for random migration, but with a larger magnitude of effects. The synergy between PDE3 and PDE4 on cAMP levels also did not apply to directional

migration, with PDE3 carrying the bulk of regulation of this process; interestingly, PDE4 inhibition did not reduce directional PANC-1 cell migration compared to control this time, instead showing a slight tendency to increase directional migration. These results implicate PDE3 as being more important than PDE4 in modulating directional chemotactic PANC-1 cell migration.

Collectively, these observations strongly suggest that the cAMP pathway that modulates PANC-1 cell migration is regulated principally by PDE3; though other PDE isoforms may also play a role in this process. This supports the results from a previous study that cilostamide (at 100μM) inhibited random migration, invasion and TGFβ-induced migration (Zimmerman et al., 2013) of PANC-1 cells. On the other hand, the finding that PDE4 may regulate migration in the presence of β-AR stimulation supports the idea that in terms of this physiological process, cAMP signalling in PANC-1 cells is compartmentalised, where PDE3 may have more influence on cAMP levels produced non-specifically (e.g. forskolin) or by the basal activity of the ACs; whereas PDE4 may regulate cAMP derived from more specific modes of GPCR signalling, such as that of β-ARs, though overlaps likely occur due to cilostazol also potentiating cAMP levels from isoproterenol treatment. Indeed, experiments in which we observed most prominent suppression of migration by PDE3 inhibition was in the absence of added cAMP agonists; moreover, cilostazol and rolipram produced additive effects on cAMP levels in PANC-1 cells, but this synergy did not translate into cell migration downstream unless isoproterenol was present. Therefore, one could test the effects of cliostazol and rolipram in the presence of sub-maximal concentrations of forskolin instead of isoproterenol on cell migration to examine this hypothesis. Furthermore, parallel studies would also need to be made once the comprehensive characterisation of effective cAMP

agonists is complete, as it appears that PANC-1 cell migration depends as much on the mode of cAMP production as on the PDEs that sculpt the signal. Lastly, the repeated observations that IBMX produced higher levels of migration inhibition than combined PDE3/4 inhibition in both 'basal' conditions and in the presence of isoproterenol suggests that either other PDE isoforms may be present in the regulation of PANC-1 cell migration, or that the concentrations of cilostazol and rolipram used was not high enough to produce full PDE inhibition.

Thus far, apart from the Zimmerman study (Zimmerman et al., 2013), reports that PDE3 inhibition directly suppressed cell migration in other cancers has only been reported once before, in colon cancer cells (Murata et al., 1999). The only other cell type in which PDE3 has also been observed to regulate cell migration is human vascular endothelial cells, (Netherton and Maurice, 2005, Palmer et al., 1998) with the formation of a signalosome consisting of PDE3, Epac1 and PI3Kγ presenting one possible mechanism with which to orquestrate cell adhesion, spreading and locomotion (Wilson et al., 2011). In comparison, PDE4 is better represented in terms of cancer cell migration. For example, in breast cancer cell lines, PDE4 inhibition has been documented to suppress integrin-induced formation of lamellopodia and downstream chemotactic migration and invasion (O'Connor et al., 1998), but strangely PKA inhibition also inhibited this process (O'Connor and Mercurio, 2001). In addition, in the same cells PDE4 inhibition decreased constitutive Ca^{2+} entry, another process important for the migration of this cell type, by activating PKA (Clarysse et al., 2014). In melanoma cells PDE4 is also a prominent regulator of cAMP/PKA signalling, the inhibition of which also inhibited cell migration (Watanabe et al., 2012).

Now with the knowledge that PDE3 has the greatest influence on cAMP-mediated regulation of PANC-1 cell migration, this study could also be coupled with the examination of the localisation of PDE3, Epac and the PKA catalytic subunits in migrating PANC-1 cells in an attempt to visualise any potential signalosomes.

6.5. PANC-1 cells have highly effective Ca^{2+} signalling systems

After taking the first steps into characterising cAMP signalling in PANC-1 cells, the main objective of chapter 5 was to establish if a cross-talk exists between Ca^{2+} and cAMP signalling, namely whether Ca^{2+} can influence cAMP levels in this cell type. However, before that main study could take place, we had to ask what the main components of the Ca^{2+} signalling machinery are in the cell. The answers of this question would refine the tools (i.e. identify specific inhibitors) with which to study the influences of Ca^{2+} signalling on cAMP, which was the main focus of chapter 4.

Despite the variations, Ca^{2+} signalling in non-excitable cells generally follow the same reaction scheme – agonist stimulation → 2^{nd} messenger production → Ca^{2+} release from intracellular stores → SOCE to refill the stores. Therefore, for our first experiment we tested this scheme by measuring cytosolic Ca^{2+} levels using neurotensin (NT) as the agonist. In nominally Ca^{2+} free conditions, NT induced a Ca^{2+} signal within seconds, underlining the high efficiency of Ca^{2+} signalling in this cell type. It is very likely that this is due to compartmentalised signalling of this ion, typified by the proximity of IP_3 receptors to PM signalling complexes to minimise diffusion distance. As it was shown recently that ER-PM junctions are prominent in PANC-1 cells and that they turnover efficiently (Dingsdale et al., 2013), it is not unreasonable to propose that the relay of cell signalling from PM surface

receptors to the ER takes place near such junctions. Therefore, it would be useful in the future to also examine the localisation of NTR and IP_3Rs in PANC-1 cells to test this.

In the same experiment, following the depletion of intracellular stores, the addition of extracellular Ca^{2+} induced a substantial signal almost immediately; confirming the rapid responsiveness and effectiveness of SOCE. The subsequent stabilisation of the Ca^{2+} signal roughly to the magnitude of the NT spike implies that SOCE was sustaining the NT signal that was counteracted by another mechanism. Of course, as NTR is also a GPCR, one cannot rule out the possibility that NTR was internalised within minutes of stimulation here (Savdie et al., 2006). Thapsigargin (TG) treatment in the presence of NT almost doubled the magnitude of Ca^{2+} signal, again within seconds, strongly suggesting that SERCA was the one of the main opposing mechanism in suppressing the Ca^{2+} signal. The effects of PMCA or NCX on the SOCE signal in this particular case was not tested in this thesis, so we cannot rule out the activity of these two pumps on the PM having an influence on Ca^{2+} homeostasis. It would be worth testing the role of SERCA, PMCA and NCX in PANC-1 cells to ask which exchanger/pump is the most important for the maintenance of low resting cytosolic Ca^{2+} levels in this cell type.

Having confirmed the efficiency of Ca^{2+} signalling in PANC-1 cells, we decided to deplete intracellular stores passively by TG-induced SERCA inhibition under nominally Ca^{2+} free conditions, and then introduce extracellular Ca^{2+} to activate SOCE in the absence of NT. The inhibition of SERCA induced a robust signal; however, the signature of the signal, which is typified by a slight 100s delay after TG addition, followed by a rapid singular spike, suggests the existence of Ca^{2+} induced Ca^{2+} release (CICR) from the ER, which is a phenomenon in which the presence of Ca^{2+} in the vicinity activates ryanodine receptors (RyRs) on the ER,

which mediates a number of processes, with both cardiac and smooth muscle contraction being the best studied (Van Petegem, 2012). RyR expression has been found in breast cancer cells (Saldana et al., 2009), where a recent study correlated RyR expression levels positively with breast cancer cell growth and tumour grade (Abdul et al., 2008). In nasopharyngeal carcinoma cells, the Ca^{2+} channel TRPM7 was proposed to induce RyR-mediated CICR to promote cell migration (Chen et al., 2010). Secondly, this also suggests that the ER membrane in PANC-1 cells is leaky to Ca^{2+} i.e. this ion can spontaneously traverse the ER membrane, which may explain why these cells often display spontaneous Ca^{2+} activity in the presence of only 1% serum and extracellular Ca^{2+}. Lastly, much like cAMP, NT is only one of potentially many Ca^{2+} agonists in PANC-1 cells, and the ability of this cell to generate spontaneous Ca^{2+} signals in serum make the characterisation of agonists difficult. Therefore, next it would be interesting to first characterise the expression and localisation of the Ca^{2+} signalling toolkit in PANC-1 cells immediately downstream of GPCR or RTK-activated Ca^{2+} signalling, namely from PLCγ/PLCβ onwards to IP3Rs, SERCA, PMCA and possibly RyRs, in the modulation of PANC-1 cell physiology.

The signal observed after the activation of SOCE in the presence of TG was much more stable and quantitatively larger as compared to NT, confirming the prominence of SERCA in the regulation of Ca^{2+} signalling in PANC-1 cells. This supports the past observations that the inhibition of this ER Ca^{2+} pump by either cyclopiazonic acid or TG induced the formation of STIM-ORAI puncta within seconds of addition (Dingsdale et al., 2013). Additionally, given that the Ca^{2+} buffering role of mitochondria is indispensable to the normal function of mouse pancreatic acinar cells (Voronina et al., 2014), one of the potential ancestors of PDAC, it would be intriguing to see what roles mitochondria play in the PANC-1 cell SOCE

process; especially that induced by NT as compared to SERCA inhibitors because mitochondrial Ca^{2+} buffering has been reported to be vital for SOCE in HUVEC cells and IP_3-dependent (but not TG-dependent) SOCE activation in HeLa cells (Deak et al., 2014, Naghdi et al., 2010).

6.6. ORAI1 is the dominant SOCE channel in PANC-1 cells

After describing the efficiency of Ca^{2+} signalling in PANC-1 cells the focus was shifted onto characterising the machinery involved in SOCE, a process pivotal for the long term stability of Ca^{2+} signalling in non-excitable cells; specifically on the PM channels involved in SOCE. The purpose of this study was to find the best possible inhibitor of SOCE for the Ca^{2+}-cAMP cross-talk study. This investigation utilised the experimental scheme in which TG was used instead of NT due to the former being more effective at activating SOCE. The resulting data from this part of the study shows that ORAI1 appears to be the main constituent in the SOCE machinery, as its corresponding inhibitor GSK-7975A efficiently inhibited SOCE by well over 50%. However, the observation that this magnitude of inhibition is not 90% or more suggests that it is more than likely that Ca^{2+} channels other than ORAI1 also contribute to SOCE in this cell type. However, ORAI3 is not likely to be one of the candidates because GSK-7975A is also an inhibitor of ORAI3, and also because of the observation that this GSK-7975A-resistant component of SOCE can also be inhibited by 2-APB; a well-known activator of ORAI3 (Schindl et al., 2008). This leaves ORAI2 in this family that remains to be tested. In an attempt to see what other channels mediate SOCE we also tested the possible role of VGCC in PANC-1 cells, The VGCC inhibitor nifedipine failed to elicit any changes in SOCE, indicating that VGCC are unlikely to be involved in this process. The ability of 2-APB to obliterate SOCE in PANC-1 cells prompted us to test the roles of the TRPC family of channels

in this process, as 2-APB has also been shown to inhibit TRPC channels (Jiang et al., 2013). TRPC3 is unlikely to take part in SOCE in PANC-1 cells, as its channel blocker Pyr3 did not affect the GSK-7975A-resistant component of SOCE. Furthermore, the addition of SKF-96365 alone, considered as a wide-range inhibitor of multiple TRPC channels (Song et al., 2014), did not have any influences on the SOCE plateau either, suggesting that this family of Ca^{2+} channels are unlikely to take part in SOCE in PANC-1 cells. It is important to point out here though that in the past we have consistently observed that SKF-96365 significantly inhibited PANC-1 cell migration; meaning that TRPC channels may yet have a role in PANC-1 cells. More importantly, contribution of TRPC channels to SOCE is often ORAI-dependent (Cheng et al., 2013). As we did not test the role of SKF-96365 on the GSK-7975A-resistant component of SOCE in this study, the active role of this family of channels on SOCE in PANC-1 cells cannot be ruled out. This is especially the case for TRPC1, which has the strongest claim to be a SOCE channel in the TRPC family (Cheng et al., 2013).

Apart from the properties of other channels on the PM, the prospect of intracellular Ca^{2+} buffering during SOCE by organelles other than the ER, such as the mitochondria, also cannot be ruled out. Indeed, mitochondria can import Ca^{2+} via a uniporter MCU when the cytosolic Ca^{2+} concentration is high and extrude the ion via a specialised NCX (NCLX) in a mechanism that is not fully understood; essentially making this organelle a Ca^{2+} buffer (Voronina et al., 2014). As mitochondria can specifically take in Ca^{2+} derived from SOCE (Deak et al., 2014), it is not unreasonable to hypothesise that during the maximal plateau phase of SOCE mitochondria imports Ca^{2+} into its matrix in PANC-1 cells; such that when ORAI1 was blocked or when extracellular Ca^{2+} was removed, the Ca^{2+} stockpiled in the

mitochondria during SOCE could be released from the matrix and equilibrated with the cytosol.

Overall, our results here indicate that ORAI1 is the principal SOCE channel of PANC-1 cells, supporting previous studies (Kondratska et al., 2014); though the expression of ORAI2 and TRPC1 needs to be tested. If these channels are expressed, one can look at the localisation of these channels in relation to ORAI1. It would also be advantageous to measure mitochondrial Ca^{2+} levels during SOCE activation and inhibition using specifically targeted genetically encoded Ca^{2+} sensors or mitochondria-localised fluorescent probes (Bonora et al., 2013), all in the continuous presence of GSK.

6.7. SOCE activates PKA activity in PANC-1 cells

After characterising the best tools for manipulating the Ca^{2+} signalling cascade in PANC-1 cells, we decided to probe the existence of a Ca^{2+}→ cAMP crosstalk in PANC-1 cells (see chapter 5). First, the treatment of PANC-1 cells with NT both in the presence of extracellular Ca^{2+} and serum induced a small but notable increase in PKA activity, the effect of which appearing to be transient. This NT response provided the first indication that activation of the Ca^{2+} signalling cascade also activates cAMP signalling. As this increase in PKA activity is likely to be a compound effect of all 4 steps of Ca^{2+} activation (agonist stimulation, IP_3 production, Ca^{2+} release/depletion from stores, SOCE activation); we focused on the effects of the last two steps, because their stimulating effects on cAMP signalling have been reported in other cell types (Lefkimmiatis et al., 2009, Cooper and Tabbasum, 2014). Interestingly, TG-induced SOCE ably increased PKA activity, the effect of which appearing to be sustainable even in the absence of PDE inhibition. This effect appears to be dependent

on the properties of ORAI1 channels and the Ca^{2+} entry, because the application of GSK-7975A or the removal of extracellular Ca^{2+}, also successfully suppressed SOCE-induced PKA activity. On the other hand, the activation of the same Ca^{2+} signalling processes only modestly increased cAMP concentration; even in the presence of IBMX to inhibit PDE activity.

The first hypothesis that can be derived from this observation is that SOCE only activated a small subset of AC isoforms, and the resultant cAMP that was produced was only enough to register a small increase on the H134 probe; however, this same modest increase in cAMP was already sufficient to activate PKA downstream to an extent that the AKAR4 probe can detect this. Supporting this, SOCE-activated PKA activity represented only a fraction of the maximal response, suggesting that not all AC isoforms were activated by this process. Moreover, this observation also suggests that SOCE preferentially activate PKA rather than Epac; this is because the H134 construct is modelled upon Epac and, despite the engineered Q270E mutation to drop its dissociation constant for cAMP, still only reported mild increases in F_{CFP}/F_{YFP} ratio in the presence of IBMX. This phenomenon has actually been reported before in the rat pancreatic acini, when cholecystokinin (CCK), a Ca^{2+} agonist in the normal pancreas, significantly increased PKA activity despite only mild increases being observed for the corresponding measurements of cAMP concentration (Marino et al., 1993). At this stage, given that the general signalling properties of all AC isoforms are known, an expression analysis of the different AC isoforms in PANC-1 cells would answer many remaining questions; the most important of which is whether AC1 and/or AC8 expression in these cells is the reason for this SOCE-activated PKA activity. Of course, one also cannot rule out the possibility that Ca^{2+}-inhibited isoforms AC5 and/or AC6 are also present in PANC-1

cells, as a recent study showed that AC6 is expressed in the mouse pancreatic acini, the activity of which was enhanced by Ca^{2+} chelation; whereas AC1 or AC8 are absent (Sabbatini et al., 2013). The combined occurrence of AC5/6 inhibition and AC1/8 activation could be one of the reasons why NT only induced a weak PKA response as compared to SOCE after pharmacological store depletion.

This study measured the cAMP/PKA pathway at a whole cell level. Therefore, another reason why the measured of cAMP levels turned out to be small in response to SOCE could be due to the compartmentalised nature of this signalling pathway, where instead of a global increase, the cAMP increase could have occurred in a defined area of the cell where cAMP levels are tightly controlled, such that it is out of the scope of sensitivity for the H134 probe. In a previous study, a cAMP probe Epac-camps was fused onto AC8 to successfully measure cAMP levels in the vicinity of the enzyme in pancreatic β-cells (Everett and Cooper, 2013). Therefore, to test that hypothesis it would be useful to utilise specifically localised probes to measure cAMP/PKA signalling closer to the cell membrane where cAMP is first produced. Indeed, AC1 and AC8 signal predominantly in lipid rafts, where its sensitivity to SOCE is due its close proximity to ORAI1 channels; whereas AC2, which is not directly sensitive to Ca^{2+}, are evenly distributed throughout the membrane (Willoughby et al., 2012a, Willoughby et al., 2010b). This possibility could be tested via the use of AKAR4-Kras and Lyn-AKAR4, variants of the AKAR4 probes that are targeted to the lipid-raft and non-raft sections of the membrane respectively (Depry et al., 2011), these probes can be used to compare compartmentalised PKA activity at the membrane in response to SOCE. Additionally, cyclodextrin, which disrupts the lipid raft by extracting cholesterol from the PM, can be applied here to see if it can alter this form of PKA signalling (Zidovetzki and

Levitan, 2007). Due to the dependency of AC1 and AC8 activation on calmodulin, it would also be a good control to test calmodulin inhibitors on this SOCE-mediated PKA activity.

If AC1 and AC8 are not expressed in PANC-1 cells, then the activation of PKA as a result of SOCE could also be due to cAMP independent effects. In particular, a novel cAMP-independent PKA activation mechanism was reported recently in mouse acinar cells, where smad3/smad4 can directly interact with the regulatory subunit of PKA downstream of TGFβ signalling to activate CREB (Yang et al., 2008). In another study sphingosine has been shown to activate PKA type II independent of cAMP without the dissociation of C subsunits from the R subunits in COS cells (Ma et al., 2005). Given that sphingolipids can act as a second messengers in other cancers (human leukaemia and colonic carcinoma cell lines) (Sweeney et al., 1996), and that PDAC cells have an adept TGFβ/Smad3 signalling system themselves (Nicolas and Hill, 2003), these hypotheses cannot be ruled out. Secondly, this increase in F_{YFP}/F_{CFP} ratio by SOCE activation could also be a result of protein phosphatase (PP) inhibition. AKAR4 is a PKA substrate; therefore it is also a reporter for the phosphorylation status of PKA substrates. The reversibility of AKAR4 phosphorylation as a result of forskolin and IBMX removal (Burdyga et al., 2013) suggests that this negative feedback mechanism by PPs for this probe is just as effective in PANC-1 cells, but not well known. Therefore, prior to establishing if there is a link between SOCE and the inhibition of PPs, it would first be useful to characterise PKA opposing phosphatases in PANC-1 cells by using known inhibitors. On the other hand, it is also possible that this phenomenon is entirely independent of cAMP/PKA signalling; and is instead due to calmodulin-dependent protein kinase-2 (CaMKII) activity. This is because both PKA and CamKII have almost identical consensus substrate sequences (RRXS/T for PKA, RXXS/T for CamKII) (Ubersax and Ferrell, 2007), culminating in

the ability of CaMKII to phosphorylate substrates that were originally known to be targets of only PKA, such as CREB (Souza et al., 2012). In addition, in a recent study, SOCE has been found to directly activate the CaMKII/Raf/ERK signalling pathway in melanoma cells to potentiate migration and proliferation (Umemura et al., 2014). Linking this to our study, although the PKA inhibitor H89 potently inhibited SOCE-induced PKA activity in PANC-1 cells, H89 is also known to inhibit other kinases including CaMKII to a lesser extent. Therefore, as an additional control for PKA activity one should use CaMKII inhibitors like KN-62 to see if AKAR4 can also be phosphorylated by this kinase.

6.8. PKA substrates accumulate in the leading edge and in the nucleus

The purpose of the second part of chapter 5 was to investigate whether the SOCE→ PKA→ regulation of cell migration system exists in PANC-1 cells under basal conditions (1% serum, extracellular Ca^{2+} present). The localisation of PKA substrates was studied as readout for PKA activity using immunofluorescence. Results from this study clearly showed that the nucleus and the extreme leading edges are the locations where PKA activity appears to be the highest. In the nucleus, the prime candidate for the high phospho-PKA substrate fluorescence is p-CREB, which has been previously found to be basally active in PDAC cells (Zhang et al., 2010); and responsible for the activation of the transcription of the miRNA miR-373, and downregulates tumour suppressor proteins TP53INP1 and LATS2 to promote PDAC cell growth (Zhang et al., 2013).

In another finding, the colocalisation of phospho-PKA substrate with actin in the leading edge suggests that PKA regulates PANC-1 cell migration via the modulation of actin in the lamellipodia. To accurately confirm that this distribution of phosphorylated PKA substrates

is indeed due to the preferential activation of PKA activity in the leading edge it would be useful to correlate this to the localisation of endogenous type I and type II PKA regulatory and catalytic subunits, as well as the localisation of CaMKII to see if this kinase also contributed to the observed co-localisation. Alternatively, to confirm that phosphorylated PKA substrates are actually in close proximity with actin one can also use antibodies against actin to reveal the endogenous distribution of actin. Indeed, this characteristic of PKA activation in migrating cells is actually quite common , as PKA has an already large and still growing list of substrates involved in cell migration (Howe, 2011). For example, in migrating breast cancer and colon carcinoma cells, PKA activity is the highest in the leading edge, mediated by AKAP-Lbc anchoring (Paulucci-Holthauzen et al., 2009); furthermore, AKAP anchoring of PKA R subunits is also important to ensure that the leading edge has the highest PKA activity in migrating epithelial ovarian cancer cells, which is vital for cell migration and extracellular matrix invasion (McKenzie et al., 2011). This phenomenon also extends to non-cancerous cells like Chinese hamster ovary (CHO) cells, where PKA activity downstream of integrin signalling is important for the maintenance of cell polarity via a PIP_3-dependent mechanism (Lim et al., 2008). Given that global increase of PKA activity in PANC-1 cells suppresses migration (Burdyga et al., 2013), this compartmentalised effect of PKA activity in the leading edge in wild-type conditions is very likely a result of PKA anchoring, possibly via AKAPs. On this subject, knowledge regarding the AKAPs in PDACs is severely lacking; therefore it would be beneficial to characterise the type of AKAPs expressed in PANC-1 cells and then define the signature of the signalosome formed by the AKAPs. In particular, AKAP13 (or AKAP-Lbc) would be intriguing due to its ability to act as a RhoGEF as well as an adaptor protein for PKA. As an adaptor it has been shown to increase the proficiency of the Raf-MEK-ERK1/2 signalling pathway by cooperating with another

scaffolding protein KSR-1 (kinase suppressor of RAS-1) to bring Raf in proximity to MEK and ERK1/2 while also recruiting PKA to the macromolecular complex; where PKA phosphorylate KSR-1 and ERK1/2 to enhance the signalling (Smith et al., 2010). Given that this pathway is downstream of both KRAS and EGF, prominent signalling pathways in PANC-1 cells (Collisson et al., 2012, Binker et al., 2009), this mechanism of producing signalling efficiency could mediate the pathophysiology of PDACs. Another fascinating prospect are previous findings that α4 integrin can itself act as an AKAP to trap PKA signalling at the leading edge of the cell to facilitate cell migration in CHO cells (Lim et al., 2007). Although PANC-1 cells mainly express α5 integrin (Yao et al., 2011, Niu et al., 2010), it remains a possibility that this cell type may utilise integrin to compartmentalise PKA signalling to regulate cell migration. In terms of its RhoGEF activity, AKAP-lbc has been reported to activate RhoA downstream of combined integrin and LPA-stimulated signalling; which is required for downstream Rac1 activation, lamellae formation and cell motility in breast cancer cells (O'Connor et al., 2012). This GEF property may be significant if expressed in PANC-1 cells because PKA-mediated inhibition of cell migration appears to be partly via the suppression of RhoA and RhoC activity (Zimmerman et al., 2013), and PKA anchored by AKAP-lbc may provide an avenue in which RhoA and RhoC activity can be regulated. In addition to AKAPs, it would also be important to check the localisation of active RhoA and RhoC in migrating PANC-1 cells to see if they are part of the phospho-PKA substrate population in the lamellipodia detected here.

6.9 ER-PM junctions reside in areas of low phospho-PKA concentration immediately bedhind the leading edge

In most of the migrating cells imaged, the region immediately behind the PKA substrate-rich lamellipodia is relatively free of PKA substrates, suggesting that in the lamella, PKA activity is

the lowest in PANC-1 cells. Interestingly, this 'PKA free' area appears to be the compartment in which endogenous ER-PM junctions congregate in polarised cells, supporting previous descriptions that STIM-ORAI punctas in PANC-1 cells are just behind the actin-rich leading edge (Dingsdale et al., 2013). This suggests that components of ER-PM junctions may have negating effects on PKA signalling in the immediate vicinity. There, the negation of PKA activity by SOCE could be either by the activation of PDEs or PPs in a Ca^{2+}-dependent manner, possibly via PDE1 (breaks down cAMP) or calcineurin (CaN, removes the phosphate group put there by PKA). Indeed, results from chapter 3 indicate that the activity of PDE1, which is activated by Ca^{2+} signalling (Goraya and Cooper, 2005), remains inconclusive in PANC-1 cells. It should also be noted that calcineurin (also known as PP2B) has been well documented to oppose PKA phosphorylation (Santana et al., 2002). These observations underline the need to biochemically characterise PPs and PDE isoforms and their localisation in PANC-1 cells. Alternatively, in light of the finding that SOCE actually increased global PKA activity in PANC-1 cells, ER-PM junctions also tended to form a 'band' of some sort in the lamella, in close proximity to the lamellipodia, suggesting that SOCE taking place in those junctions can feed forward into the leading edge to activate PKA.

Like cAMP, Ca^{2+} signalling is also an effective regulator of cell migration in its own right (Tsai and Meyer, 2012, Monteith et al., 2012). For example, STIM1-activated SOCE plays a vital role for cervical cancer cell migration, where STIM1 served to increase the number of actomyosin complexes to enhance the force of contractility in migrating cervical cancer cells (Chen et al., 2013b); as well as facilitating focal adhesion turnover via the protease calpain and kinase Pyk2, both Ca^{2+}-regulated enzymes (Yang et al., 2009, Chen et al., 2011). STIM1 is also indispensable for the migration of breast cancer cells, where SOCE is required for

metastasis (Yang et al., 2009). In addition, TRPC1, another SOCE channel candidate, is required in the lamellipodia of glioma cells to maintain cell polarity during EGF-stimulated chemotactic migration (Fabian et al., 2008, Bomben et al., 2011). Downstream, an elegant study performed on migrating HUVEC cells provided valuable insight into the mechanism in which components and messengers of the Ca^{2+} signalling toolkit are manoeuvred around the cell to regulate migration (Tsai and Meyer, 2012). There, the authors observed that RTK, PMCA and STIM punctas are preferentially accumulated at the leading edge, establishing a DAG gradient in which the 'front' of the cell contains the highest DAG concentration; while the cytosolic Ca^{2+} gradient was inversed, with the back of the cell containing the highest Ca^{2+} concentration. Intriguingly, in PANC-1 cells, the basal activity of PLCγ, a physiological activator of Ca^{2+} signalling, has been found to be elevated in the presence of serum (Stock et al., 2013), which, coupled with the highly efficient SOCE system in this cell type, may contribute to the ability of this cell line to spontaneously form membrane ruffles and migrate without any other interventions.

Although a Ca^{2+}-cAMP crosstalk has been known for some time, studies on the consequences downstream of SOCE activated cAMP signalling is still at an infancy. So far we have only found one study, in which Ca^{2+} activated cAMP/PKA signalling is important for the spontaneous activation of action potentials in cardiac pacemaker cells (Yaniv et al., 2011); that reported a physiological effect as a result of this mode of signalling. Therefore, the proximity of STIM1 punctas and endogenous ER-PM junctions to phosphorylated PKA substrates in migrating PANC-1 cells, coupled with the ability of SOCE to activate PKA as observed in the live cell experiments, implies that this mode of signalling occurs at the leading edge to regulate cell migration, which is promising. However, to reinforce this

statement the localisation of the AC isoforms expressed in PANC-1 cells would need to be checked in conjunction with ORAI1 (and possibly other SOCE-mediating channels) after the activation of SOCE. Additionally, the expression of AKAP79, reported on numerous occasions to bridge Ca^{2+} and cAMP signalling together near the cell membrane (Willoughby et al., 2012b, Willoughby et al., 2010a, Shen and Cooper, 2013, Hinke et al., 2012), can be tested to see if this AKAP has a hand in facilitating this interaction in PANC-1 cells. Secondly, as this study did not concern STIM2, which is considered to play a housekeeping role in maintaining basal ER Ca^{2+} levels in cells under physiological conditions (Soboloff et al., 2012), it would also be useful to couple measurements of STIM2 distribution with the ER-PM linker protocol to see how they correlate in PANC-1 cells under basal, non-stimulated conditions. Further down the line, as the physiological consequence of SOCE activated PKA responses in PANC-1 cells is still unknown, and PKA phosphorylates and subsequently inhibit RhoA and RhoC activity in PANC-1 cells, it would be interesting to address what, if any, effects SOCE activation can have on these two Rho GTPases. Lastly, it would be particularly intriguing to study this when PANC-1 cells are grown on a lawn of matrigel in order to see if these relationships between Ca^{2+} and cAMP signalling observed in study here can be applied by the cells to regulate invasion and 3-dimensional migration/invasion.

6.10. Concluding remarks

This study coupled live-cell imaging approach with pharmacology, taking advantage of novel, genetically-encoded FRET based sensors to characterise the components of the cAMP signalling pathway in PANC-1 cells. There are over 20 different PDAC cell lines (Thu et al., 2014), each with different origins, genotypes and adhesive, invasive and tumorigenic phenotypes, as comprehensively reviewed previously (Deer et al., 2010). PANC-1 cells were

originally derived from a primary tumour at the head of the pancreas that metastasised locally to the duodenal wall and the peripancreatic lymph node. It carries a heterozygous activating mutation in the KRAS gene, homozygous deletions to the p16 gene and mutations in the TP53 gene (Lieber et al., 1975). PANC-1 cells have the advantage over other cell lines for being easily transfectable with plasmids and loaded with dye for real-time, physiological experiments; whereas its weakness is its poor tumorigenicity; even when injected into immune-compromised mice, making translational in vivo studies using this cell line difficult (Momose et al., 2010). In the prior studies we have tested BxPC-3, Capan-2, SUIT-2 and MiaPaCa-2 cells in Boyden Chamber studies, all of which displayed significant inhibition of migration in response to increases in cAMP levels; which supports the notion that the inhibitory effects of cAMP on cell migration is genuine in PDAC (Burdyga et al., 2013).

Our study identified PDE3 and PDE4 to be the main terminators of cAMP signalling in PANC-1 cells, whereas isoproterenol is the main cAMP agonist. However, in terms of cell migration isoproterenol is not a good potential target for blocking metastasis, as it had very little effects on cell migration. Moreover, it appeared that combined PDE3/4 inhibition was the best target as for inhibiting migration; putting forward PDE3/4 inhibitors as a potential candidate for reducing metastasis formation. In the second part of the study it was Ca^{2+} signalling, especially SOCE, appeared to be able to activate cAMP signalling in PANC-1 cells, which effectively translated into PKA activity. Immunofluorescence data showed that phosphorylated PKA substrates are accumulated at the lamellipodia of migrating cells, where they colocalised with actin. ER-PM junctions under basal conditions are situated immediately behind the actin-rich areas in the leading edge. This implies that SOCE-mediated PKA activity could have a role in PANC-1 cell migration, which warrants further

investigation. To further develop this study it would be advantageous to carry out biochemical characterisation of the cAMP cascade components, specifically the isoforms of AC, and the splice variants of PDE3 and PDE4 that are expressed in PANC-1 cells. Furthermore, with the observations that different components of the cAMP pathway expressed in the same cell can have differential effects on cellular growth and cell migration in PDAC cells, it would be very important to determine how the machinery of this signalling cascade is spatially coordinated. Lastly, there is extensive genetic and epigenetic heterogeneity present in PDAC tumors (Arensman et al., 2014, Thu et al., 2014). Therefore, to relate the results reported here from 'PANC-1 cells' to 'PDAC', some experiments reported in the thesis would need to be carried out on other PDAC cell lines, and then the specified interventions applied onto in vivo models such as the 'KPC' mice, which spontaneously develop aggressive PDAC (Guerra and Barbacid, 2013) to evaluate the role of cAMP signalling casual in more pathology-relevant conditions.

I hope that this study will be a useful stepping stone for further research that will elucidate the mechanism regulating migration, invasion and the formation of metastases of PDAC cells. The knowledge will hopefully accelerate development of treatment against PDAC.

REFERENCES

ABDUL, M., RAMLAL, S. & HOOSEIN, N. 2008. Ryanodine receptor expression correlates with tumor grade in breast cancer. *Pathol Oncol Res,* 14**,** 157-60.

ABRAMOVITZ, M., ADAM, M., BOIE, Y., CARRIERE, M., DENIS, D., GODBOUT, C., LAMONTAGNE, S., ROCHETTE, C., SAWYER, N., TREMBLAY, N. M., BELLEY, M., GALLANT, M., DUFRESNE, C., GAREAU, Y., RUEL, R., JUTEAU, H., LABELLE, M., OUIMET, N. & METTERS, K. M. 2000. The utilization of recombinant prostanoid receptors to determine the affinities and selectivities of prostaglandins and related analogs. *Biochim Biophys Acta,* 1483**,** 285-93.

ACKERMAN, M. S., ROESKE, W. R., HECK, R. J. & KORC, M. 1989. Identification and characterization of muscarinic receptors in cultured human pancreatic carcinoma cells. *Pancreas,* 4**,** 363-70.

ADDERLEY, S. P., DUFAUX, E. A., SRIDHARAN, M., BOWLES, E. A., HANSON, M. S., STEPHENSON, A. H., ELLSWORTH, M. L. & SPRAGUE, R. S. 2009. Iloprost- and isoproterenol-induced increases in cAMP are regulated by different phosphodiesterases in erythrocytes of both rabbits and humans. *Am J Physiol Heart Circ Physiol,* 296**,** H1617-24.

AHLSTROM, M., PEKKINEN, M., HUTTUNEN, M. & LAMBERG-ALLARDT, C. 2005. Dexamethasone down-regulates cAMP-phosphodiesterase in human osteosarcoma cells. *Biochem Pharmacol,* 69**,** 267-75.

AL-NAKKASH, L., SIMMONS, N. L., LINGARD, J. M. & ARGENT, B. E. 1996. Adenylate cyclase activity in human pancreatic adenocarcinoma cell lines. *Int J Pancreatol,* 19**,** 39-47.

AL-WADEI, H. A., AL-WADEI, M. H., ULLAH, M. F. & SCHULLER, H. M. 2012. Celecoxib and GABA cooperatively prevent the progression of pancreatic cancer in vitro and in xenograft models of stress-free and stress-exposed mice. *PLoS One,* 7**,** e43376.

ALBIGES-RIZO, C., DESTAING, O., FOURCADE, B., PLANUS, E. & BLOCK, M. R. 2009. Actin machinery and mechanosensitivity in invadopodia, podosomes and focal adhesions. *J Cell Sci,* 122**,** 3037-49.

AMIEUX, P. S., CUMMINGS, D. E., MOTAMED, K., BRANDON, E. P., WAILES, L. A., LE, K., IDZERDA, R. L. & MCKNIGHT, G. S. 1997. Compensatory regulation of RIalpha protein levels in protein kinase A mutant mice. *J Biol Chem,* 272**,** 3993-8.

AMIEUX, P. S. & MCKNIGHT, G. S. 2002. The essential role of RI alpha in the maintenance of regulated PKA activity. *Ann N Y Acad Sci,* 968**,** 75-95.

ANG, K. L. & ANTONI, F. A. 2002. Reciprocal regulation of calcium dependent and calcium independent cyclic AMP hydrolysis by protein phosphorylation. *J Neurochem,* 81**,** 422-33.

ANTUNES, G., SEBASTIAO, A. M. & SIMOES DE SOUZA, F. M. 2014. Mechanisms of regulation of olfactory transduction and adaptation in the olfactory cilium. *PLoS One,* 9**,** e105531.

ARENSMAN, M. D., KOVOCHICH, A. N., KULIKAUSKAS, R. M., LAY, A. R., YANG, P. T., LI, X., DONAHUE, T., MAJOR, M. B., MOON, R. T., CHIEN, A. J. & DAWSON, D. W. 2014. WNT7B mediates autocrine Wnt/beta-catenin signaling and anchorage-independent growth in pancreatic adenocarcinoma. *Oncogene,* 33**,** 899-908.

ARTHUR, W. T., QUILLIAM, L. A. & COOPER, J. A. 2004. Rap1 promotes cell spreading by localizing Rac guanine nucleotide exchange factors. *J Cell Biol,* 167**,** 111-22.

ASKARI, M. D., TSAO, M. S. & SCHULLER, H. M. 2005. The tobacco-specific carcinogen, 4-(methylnitrosamino)-1-(3-pyridyl)-1-butanone stimulates proliferation of immortalized human pancreatic duct epithelia through beta-adrenergic transactivation of EGF receptors. *J Cancer Res Clin Oncol,* 131**,** 639-48.

AUSTIN, R. C. 2009. The unfolded protein response in health and disease. *Antioxid Redox Signal,* 11**,** 2279-87.

AVRAAMIDES, C. J., GARMY-SUSINI, B. & VARNER, J. A. 2008. Integrins in angiogenesis and lymphangiogenesis. *Nat Rev Cancer,* 8**,** 604-17.

BAILLIE, G. S., MACKENZIE, S. J., MCPHEE, I. & HOUSLAY, M. D. 2000. Sub-family selective actions in the ability of Erk2 MAP kinase to phosphorylate and regulate the activity of PDE4 cyclic AMP-specific phosphodiesterases. *Br J Pharmacol,* 131**,** 811-9.

BAKER, J. G. 2010. The selectivity of beta-adrenoceptor agonists at human beta1-, beta2- and beta3-adrenoceptors. *Br J Pharmacol,* 160**,** 1048-61.

BEARD, M. B., OLSEN, A. E., JONES, R. E., ERDOGAN, S., HOUSLAY, M. D. & BOLGER, G. B. 2000. UCR1 and UCR2 domains unique to the cAMP-specific phosphodiesterase family form a discrete module via electrostatic interactions. *J Biol Chem,* 275**,** 10349-58.

BENARROCH, E. E. 2013. HCN channels: function and clinical implications. *Neurology,* 80**,** 304-10.

BENDER, A. T. & BEAVO, J. A. 2006. Cyclic nucleotide phosphodiesterases: molecular regulation to clinical use. *Pharmacol Rev,* 58**,** 488-520.

BERRIDGE, M. J., BOOTMAN, M. D. & RODERICK, H. L. 2003. Calcium signalling: dynamics, homeostasis and remodelling. *Nat Rev Mol Cell Biol,* 4**,** 517-29.

BERTELLI, E., REGOLI, M., ORAZIOLI, D. & BENDAYAN, M. 2001. Association between islets of Langerhans and pancreatic ductal system in adult rat. Where endocrine and exocrine meet together? *Diabetologia,* 44**,** 575-84.

BIEL, M., WAHL-SCHOTT, C., MICHALAKIS, S. & ZONG, X. 2009. Hyperpolarization-activated cation channels: from genes to function. *Physiol Rev,* 89**,** 847-85.

BINKER, M. G., BINKER-COSEN, A. A., RICHARDS, D., OLIVER, B. & COSEN-BINKER, L. I. 2009. EGF promotes invasion by PANC-1 cells through Rac1/ROS-dependent secretion and activation of MMP-2. *Biochem Biophys Res Commun,* 379**,** 445-50.

BOMBEN, V. C., TURNER, K. L., BARCLAY, T. T. & SONTHEIMER, H. 2011. Transient receptor potential canonical channels are essential for chemotactic migration of human malignant gliomas. *J Cell Physiol,* 226**,** 1879-88.

BONORA, M., GIORGI, C., BONONI, A., MARCHI, S., PATERGNANI, S., RIMESSI, A., RIZZUTO, R. & PINTON, P. 2013. Subcellular calcium measurements in mammalian cells using jellyfish photoprotein aequorin-based probes. *Nat Protoc,* 8**,** 2105-18.

BOS, J. L. 2006. Epac proteins: multi-purpose cAMP targets. *Trends Biochem Sci,* 31**,** 680-6.

BOS, J. L., REHMANN, H. & WITTINGHOFER, A. 2007. GEFs and GAPs: critical elements in the control of small G proteins. *Cell,* 129**,** 865-77.

BOUCHER, M. J., DUCHESNE, C., LAINE, J., MORISSET, J. & RIVARD, N. 2001. cAMP protection of pancreatic cancer cells against apoptosis induced by ERK inhibition. *Biochem Biophys Res Commun,* 285**,** 207-16.

BRABEK, J., CONSTANCIO, S. S., SHIN, N. Y., POZZI, A., WEAVER, A. M. & HANKS, S. K. 2004. CAS promotes invasiveness of Src-transformed cells. *Oncogene,* 23**,** 7406-15.

BRADLEY, J., FRINGS, S., YAU, K. W. & REED, R. 2001. Nomenclature for ion channel subunits. *Science,* 294**,** 2095-6.

BRANCH, K. M., HOSHINO, D. & WEAVER, A. M. 2012. Adhesion rings surround invadopodia and promote maturation. *Biol Open,* 1**,** 711-22.

BRAUN, M., RAMRACHEYA, R., BENGTSSON, M., ZHANG, Q., KARANAUSKAITE, J., PARTRIDGE, C., JOHNSON, P. R. & RORSMAN, P. 2008. Voltage-gated ion channels in human pancreatic beta-cells: electrophysiological characterization and role in insulin secretion. *Diabetes,* 57**,** 1618-28.

BRAVO-CORDERO, J. J., MAGALHAES, M. A., EDDY, R. J., HODGSON, L. & CONDEELIS, J. 2013. Functions of cofilin in cell locomotion and invasion. *Nat Rev Mol Cell Biol,* 14**,** 405-15.

BREER, H., BOEKHOFF, I. & TAREILUS, E. 1990. Rapid kinetics of second messenger formation in olfactory transduction. *Nature,* 345**,** 65-8.

BREYER, R. M., BAGDASSARIAN, C. K., MYERS, S. A. & BREYER, M. D. 2001. Prostanoid receptors: subtypes and signaling. *Annu Rev Pharmacol Toxicol,* 41**,** 661-90.

BRIDGEWATER, R. E., NORMAN, J. C. & CASWELL, P. T. 2012. Integrin trafficking at a glance. *J Cell Sci,* 125**,** 3695-701.

BRZESKA, H., SZCZEPANOWSKA, J., MATSUMURA, F. & KORN, E. D. 2004. Rac-induced increase of phosphorylation of myosin regulatory light chain in HeLa cells. *Cell Motil Cytoskeleton,* 58**,** 186-99.

BUCHLER, P., GAZDHAR, A., SCHUBERT, M., GIESE, N., REBER, H. A., HINES, O. J., GIESE, T., CEYHAN, G. O., MULLER, M., BUCHLER, M. W. & FRIESS, H. 2005. The Notch signaling pathway is related to neurovascular progression of pancreatic cancer. *Ann Surg,* 242**,** 791-800, discussion 800-1.

BURDYGA, A., CONANT, A., HAYNES, L., ZHANG, J., JALINK, K., SUTTON, R., NEOPTOLEMOS, J., COSTELLO, E. & TEPIKIN, A. 2013. cAMP inhibits migration, ruffling and paxillin accumulation in focal adhesions of pancreatic ductal adenocarcinoma cells: effects of PKA and EPAC. *Biochim Biophys Acta,* 1833**,** 2664-72.

BURTON, P., ADAMS, D. R., ABRAHAM, A., ALLCOCK, R. W., JIANG, Z., MCCAHILL, A., GILMOUR, J., MCABNEY, J., KAUPISCH, A., KANE, N. M., BAILLIE, G. S., BAKER, A. H., MILLIGAN, G., HOUSLAY, M. D. & MOUNTFORD, J. C. 2010. Erythro-9-(2-hydroxy-3-nonyl)adenine (EHNA) blocks differentiation and maintains the expression of pluripotency markers in human embryonic stem cells. *Biochem J,* 432**,** 575-84.

CABRERA-VERA, T. M., VANHAUWE, J., THOMAS, T. O., MEDKOVA, M., PREININGER, A., MAZZONI, M. R. & HAMM, H. E. 2003. Insights into G protein structure, function, and regulation. *Endocr Rev,* 24**,** 765-81.

CADD, G. & MCKNIGHT, G. S. 1989. Distinct patterns of cAMP-dependent protein kinase gene expression in mouse brain. *Neuron,* 3**,** 71-9.

CAHALAN, M. D. 2009. STIMulating store-operated Ca(2+) entry. *Nat Cell Biol,* 11**,** 669-77.

CALLOWAY, N., HOLOWKA, D. & BAIRD, B. 2010. A basic sequence in STIM1 promotes Ca2+ influx by interacting with the C-terminal acidic coiled coil of Orai1. *Biochemistry,* 49**,** 1067-71.

CARPENTER, A. E., JONES, T. R., LAMPRECHT, M. R., CLARKE, C., KANG, I. H., FRIMAN, O., GUERTIN, D. A., CHANG, J. H., LINDQUIST, R. A., MOFFAT, J., GOLLAND, P. & SABATINI, D. M. 2006. CellProfiler: image analysis software for identifying and quantifying cell phenotypes. *Genome Biol,* 7**,** R100.

CAYROL, C., CLERC, P., BERTRAND, C., GIGOUX, V., PORTOLAN, G., FOURMY, D., DUFRESNE, M. & SEVA, C. 2006. Cholecystokinin-2 receptor modulates cell adhesion through beta 1-integrin in human pancreatic cancer cells. *Oncogene,* 25**,** 4421-8.

CEYHAN, O., BIRSOY, K. & HOFFMAN, C. S. 2012. Identification of biologically active PDE11-selective inhibitors using a yeast-based high-throughput screen. *Chem Biol,* 19**,** 155-63.

CHANG, Y. H., CONTI, M., LEE, Y. C., LAI, H. L., CHING, Y. H. & CHERN, Y. 1997. Activation of phosphodiesterase IV during desensitization of the A2A adenosine receptor-mediated cyclic AMP response in rat pheochromocytoma (PC12) cells. *J Neurochem,* 69**,** 1300-9.

CHEN, B., BRINKMANN, K., CHEN, Z., PAK, C. W., LIAO, Y., SHI, S., HENRY, L., GRISHIN, N. V., BOGDAN, S. & ROSEN, M. K. 2014a. The WAVE regulatory complex links diverse receptors to the actin cytoskeleton. *Cell,* 156**,** 195-207.

CHEN, C., TAO, T., WEN, C., HE, W. Q., QIAO, Y. N., GAO, Y. Q., CHEN, X., WANG, P., CHEN, C. P., ZHAO, W., CHEN, H. Q., YE, A. P., PENG, Y. J. & ZHU, M. S. 2014b. Myosin Light Chain Kinase (MLCK) Regulates Cell Migration in a Myosin Regulatory Light Chain Phosphorylation-Independent Mechanism. *J Biol Chem*.

CHEN, J. P., LUAN, Y., YOU, C. X., CHEN, X. H., LUO, R. C. & LI, R. 2010. TRPM7 regulates the migration of human nasopharyngeal carcinoma cell by mediating Ca(2+) influx. *Cell Calcium,* 47**,** 425-32.

CHEN, L. F. & GREENE, W. C. 2004. Shaping the nuclear action of NF-kappaB. *Nat Rev Mol Cell Biol,* 5**,** 392-401.

CHEN, T., ZHU, J., ZHANG, C., HUO, K., FEI, Z. & JIANG, X. F. 2013a. Protective effects of SKF-96365, a non-specific inhibitor of SOCE, against MPP+-induced cytotoxicity in PC12 cells: potential role of Homer1. *PLoS One,* 8**,** e55601.

CHEN, T. C., WADSTEN, P., SU, S., RAWLINSON, N., HOFMAN, F. M., HILL, C. K. & SCHONTHAL, A. H. 2002. The type IV phosphodiesterase inhibitor rolipram induces expression of the cell cycle inhibitors p21(Cip1) and p27(Kip1), resulting in growth inhibition, increased differentiation, and subsequent apoptosis of malignant A-172 glioma cells. *Cancer Biol Ther,* 1**,** 268-76.

CHEN, Y. F., CHIU, W. T., CHEN, Y. T., LIN, P. Y., HUANG, H. J., CHOU, C. Y., CHANG, H. C., TANG, M. J. & SHEN, M. R. 2011. Calcium store sensor stromal-interaction molecule 1-dependent signaling plays an important role in cervical cancer growth, migration, and angiogenesis. *Proc Natl Acad Sci U S A,* 108**,** 15225-30.

CHEN, Y. T., CHEN, Y. F., CHIU, W. T., WANG, Y. K., CHANG, H. C. & SHEN, M. R. 2013b. The ER Ca(2)(+) sensor STIM1 regulates actomyosin contractility of migratory cells. *J Cell Sci,* 126**,** 1260-7.

CHENG, K. T., LIU, X., ONG, H. L., SWAIM, W. & AMBUDKAR, I. S. 2011. Local Ca(2)+ entry via Orai1 regulates plasma membrane recruitment of TRPC1 and controls cytosolic Ca(2)+ signals required for specific cell functions. *PLoS Biol,* 9**,** e1001025.

CHENG, K. T., ONG, H. L., LIU, X. & AMBUDKAR, I. S. 2013. Contribution and regulation of TRPC channels in store-operated Ca2+ entry. *Curr Top Membr,* 71**,** 149-79.

CHEY, W. Y. & CHANG, T. M. 2003. Secretin, 100 years later. *J Gastroenterol,* 38**,** 1025-35.

CHO-CHUNG, Y. S. 1990. Role of cyclic AMP receptor proteins in growth, differentiation, and suppression of malignancy: new approaches to therapy. *Cancer Res,* 50**,** 7093-100.

CHRISTOPHE, J. P., CONLON, T. P. & GARDNER, J. D. 1976. Interaction of porcine vasoactive intestinal peptide with dispersed pancreatic acinar cells from the guinea pig. Binding of radioiodinated peptide. *J Biol Chem,* 251**,** 4629-34.

CHU, G. C., KIMMELMAN, A. C., HEZEL, A. F. & DEPINHO, R. A. 2007. Stromal biology of pancreatic cancer. *J Cell Biochem,* 101**,** 887-907.

CHUANG, S. Y., YANG, S. H., CHEN, T. Y. & PANG, J. H. 2011. Cilostazol inhibits matrix invasion and modulates the gene expressions of MMP-9 and TIMP-1 in PMA-differentiated THP-1 cells. *Eur J Pharmacol,* 670**,** 419-26.

CLAPHAM, D. E. 2007. Calcium signaling. *Cell,* 131**,** 1047-58.

CLARYSSE, L., GUEGUINOU, M., POTIER-CARTEREAU, M., VANDECASTEELE, G., BOUGNOUX, P., CHEVALIER, S., CHANTOME, A. & VANDIER, C. 2014. cAMP-PKA inhibition of SK3 channel reduced both Ca(2+) entry and cancer cell migration by regulation of SK3-Orai1 complex. *Pflugers Arch,* 466**,** 1921-32.

COLE, C., BARBER, J. D. & BARTON, G. J. 2008. The Jpred 3 secondary structure prediction server. *Nucleic Acids Res,* 36**,** W197-201.

COLEMAN, R. A., SMITH, W. L. & NARUMIYA, S. 1994. International Union of Pharmacology classification of prostanoid receptors: properties, distribution, and structure of the receptors and their subtypes. *Pharmacol Rev,* 46**,** 205-29.

COLLEDGE, M. & SCOTT, J. D. 1999. AKAPs: from structure to function. *Trends Cell Biol,* 9**,** 216-21.

COLLISSON, E. A., TREJO, C. L., SILVA, J. M., GU, S., KORKOLA, J. E., HEISER, L. M., CHARLES, R. P., RABINOVICH, B. A., HANN, B., DANKORT, D., SPELLMAN, P. T., PHILLIPS, W. A., GRAY, J. W. & MCMAHON, M. 2012. A central role for RAF-->MEK-->ERK signaling in the genesis of pancreatic ductal adenocarcinoma. *Cancer Discov,* 2**,** 685-93.

COLTON, C. K. & ZHU, M. X. 2007. 2-Aminoethoxydiphenyl borate as a common activator of TRPV1, TRPV2, and TRPV3 channels. *Handb Exp Pharmacol***,** 173-87.

COMMUNAL, C., SINGH, K., SAWYER, D. B. & COLUCCI, W. S. 1999. Opposing effects of beta(1)- and beta(2)-adrenergic receptors on cardiac myocyte apoptosis : role of a pertussis toxin-sensitive G protein. *Circulation,* 100**,** 2210-2.

CONSONNI, S. V., GLOERICH, M., SPANJAARD, E. & BOS, J. L. 2012. cAMP regulates DEP domain-mediated binding of the guanine nucleotide exchange factor Epac1 to phosphatidic acid at the plasma membrane. *Proc Natl Acad Sci U S A,* 109**,** 3814-9.

CONTI, M., ANDERSEN, C. B., RICHARD, F., MEHATS, C., CHUN, S. Y., HORNER, K., JIN, C. & TSAFRIRI, A. 2002. Role of cyclic nucleotide signaling in oocyte maturation. *Mol Cell Endocrinol,* 187**,** 153-9.

CONTI, M. & BEAVO, J. 2007. Biochemistry and physiology of cyclic nucleotide phosphodiesterases: essential components in cyclic nucleotide signaling. *Annu Rev Biochem,* 76**,** 481-511.

COOPER, D. M. & TABBASUM, V. G. 2014. Adenylate cyclase-centred microdomains. *Biochem J,* 462**,** 199-213.

CORBIN, J. D., TURKO, I. V., BEASLEY, A. & FRANCIS, S. H. 2000. Phosphorylation of phosphodiesterase-5 by cyclic nucleotide-dependent protein kinase alters its catalytic and allosteric cGMP-binding activities. *Eur J Biochem,* 267**,** 2760-7.

COTE, J. F. & VUORI, K. 2007. GEF what? Dock180 and related proteins help Rac to polarize cells in new ways. *Trends Cell Biol,* 17**,** 383-93.

COVINGTON, E. D., WU, M. M. & LEWIS, R. S. 2010. Essential role for the CRAC activation domain in store-dependent oligomerization of STIM1. *Mol Biol Cell,* 21**,** 1897-907.

COWGILL, S. M. & MUSCARELLA, P. 2003. The genetics of pancreatic cancer. *Am J Surg,* 186**,** 279-86.

CRAVEN, K. B. & ZAGOTTA, W. N. 2006. CNG and HCN channels: two peas, one pod. *Annu Rev Physiol,* 68**,** 375-401.

CYGNAR, K. D. & ZHAO, H. 2009. Phosphodiesterase 1C is dispensable for rapid response termination of olfactory sensory neurons. *Nat Neurosci,* 12**,** 454-62.

DANG, I., GORELIK, R., SOUSA-BLIN, C., DERIVERY, E., GUERIN, C., LINKNER, J., NEMETHOVA, M., DUMORTIER, J. G., GIGER, F. A., CHIPYSHEVA, T. A., ERMILOVA, V. D., VACHER, S., CAMPANACCI, V., HERRADA, I., PLANSON, A. G., FETICS, S., HENRIOT, V., DAVID, V., OGUIEVETSKAIA, K., LAKISIC, G., PIERRE, F., STEFFEN, A., BOYREAU, A., PEYRIERAS, N., ROTTNER, K., ZINN-JUSTIN, S., CHERFILS, J., BIECHE, I., ALEXANDROVA, A. Y., DAVID, N. B., SMALL, J. V., FAIX, J., BLANCHOIN, L. & GAUTREAU, A. 2013. Inhibitory signalling to the Arp2/3 complex steers cell migration. *Nature,* 503**,** 281-4.

DAO, K. K., TEIGEN, K., KOPPERUD, R., HODNELAND, E., SCHWEDE, F., CHRISTENSEN, A. E., MARTINEZ, A. & DOSKELAND, S. O. 2006. Epac1 and cAMP-dependent protein kinase holoenzyme have similar cAMP affinity, but their cAMP domains have distinct structural features and cyclic nucleotide recognition. *J Biol Chem,* 281**,** 21500-11.

DAS, R., MAZHAB-JAFARI, M. T., CHOWDHURY, S., SILDAS, S., SELVARATNAM, R. & MELACINI, G. 2008. Entropy-driven cAMP-dependent allosteric control of inhibitory interactions in exchange proteins directly activated by cAMP. *J Biol Chem,* 283**,** 19691-703.

DE ROOIJ, J., REHMANN, H., VAN TRIEST, M., COOL, R. H., WITTINGHOFER, A. & BOS, J. L. 2000. Mechanism of regulation of the Epac family of cAMP-dependent RapGEFs. *J Biol Chem,* 275**,** 20829-36.

DEAK, A. T., BLASS, S., KHAN, M. J., GROSCHNER, L. N., WALDECK-WEIERMAIR, M., HALLSTROM, S., GRAIER, W. F. & MALLI, R. 2014. IP3-mediated STIM1 oligomerization requires intact mitochondrial Ca2+ uptake. *J Cell Sci,* 127**,** 2944-55.

DEER, E. L., GONZALEZ-HERNANDEZ, J., COURSEN, J. D., SHEA, J. E., NGATIA, J., SCAIFE, C. L., FIRPO, M. A. & MULVIHILL, S. J. 2010. Phenotype and genotype of pancreatic cancer cell lines. *Pancreas,* 39**,** 425-35.

DEGERMAN, E., AHMAD, F., CHUNG, Y. W., GUIRGUIS, E., OMAR, B., STENSON, L. & MANGANIELLO, V. 2011. From PDE3B to the regulation of energy homeostasis. *Curr Opin Pharmacol,* 11**,** 676-82.

DEHAVEN, W. I., SMYTH, J. T., BOYLES, R. R., BIRD, G. S. & PUTNEY, J. W., JR. 2008. Complex actions of 2-aminoethyldiphenyl borate on store-operated calcium entry. *J Biol Chem,* 283**,** 19265-73.

DEHAVEN, W. I., SMYTH, J. T., BOYLES, R. R. & PUTNEY, J. W., JR. 2007. Calcium inhibition and calcium potentiation of Orai1, Orai2, and Orai3 calcium release-activated calcium channels. *J Biol Chem,* 282**,** 17548-56.

DELCORE, R., RODRIGUEZ, F. J., FORSTER, J., HERMRECK, A. S. & THOMAS, J. H. 1996. Significance of lymph node metastases in patients with pancreatic cancer undergoing curative resection. *Am J Surg,* 172**,** 463-8; discussion 468-9.

DEMIRBAS, D., WYMAN, A. R., SHIMIZU-ALBERGINE, M., CAKICI, O., BEAVO, J. A. & HOFFMAN, C. S. 2013. A yeast-based chemical screen identifies a PDE inhibitor that elevates steroidogenesis in mouse Leydig cells via PDE8 and PDE4 inhibition. *PLoS One,* 8**,** e71279.

DENINNO, M. P., ANDREWS, M., BELL, A. S., CHEN, Y., ELLER-ZARBO, C., ESHELBY, N., ETIENNE, J. B., MOORE, D. E., PALMER, M. J., VISSER, M. S., YU, L. J., ZAVADOSKI, W. J. & MICHAEL GIBBS, E. 2009. The discovery of potent, selective, and orally bioavailable PDE9 inhibitors as potential hypoglycemic agents. *Bioorg Med Chem Lett,* 19**,** 2537-41.

DEPRY, C., ALLEN, M. D. & ZHANG, J. 2011. Visualization of PKA activity in plasma membrane microdomains. *Mol Biosyst,* 7**,** 52-8.

DERLER, I., FAHRNER, M., MUIK, M., LACKNER, B., SCHINDL, R., GROSCHNER, K. & ROMANIN, C. 2009. A Ca2(+)release-activated Ca2(+) (CRAC) modulatory domain (CMD) within STIM1 mediates fast Ca2(+)-dependent inactivation of ORAI1 channels. *J Biol Chem,* 284**,** 24933-8.

DERLER, I., SCHINDL, R., FRITSCH, R., HEFTBERGER, P., RIEDL, M. C., BEGG, M., HOUSE, D. & ROMANIN, C. 2013. The action of selective CRAC channel blockers is affected by the Orai pore geometry. *Cell Calcium,* 53**,** 139-51.

DI BENEDETTO, G., PENDIN, D., GREOTTI, E., PIZZO, P. & POZZAN, T. 2014. Ca2+ and cAMP cross-talk in mitochondria. *J Physiol,* 592**,** 305-12.

DI BENEDETTO, G., ZOCCARATO, A., LISSANDRON, V., TERRIN, A., LI, X., HOUSLAY, M. D., BAILLIE, G. S. & ZACCOLO, M. 2008. Protein kinase A type I and type II define distinct intracellular signaling compartments. *Circ Res,* 103**,** 836-44.

DING, W. Q., CHENG, Z. J., MCELHINEY, J., KUNTZ, S. M. & MILLER, L. J. 2002. Silencing of secretin receptor function by dimerization with a misspliced variant secretin receptor in ductal pancreatic adenocarcinoma. *Cancer Res,* 62**,** 5223-9.

DING, X. Z., TONG, W. G. & ADRIAN, T. E. 2001. Cyclooxygenases and lipoxygenases as potential targets for treatment of pancreatic cancer. *Pancreatology,* 1**,** 291-9.

DINGSDALE, H., OKEKE, E., AWAIS, M., HAYNES, L., CRIDDLE, D. N., SUTTON, R. & TEPIKIN, A. V. 2013. Saltatory formation, sliding and dissolution of ER-PM junctions in migrating cancer cells. *Biochem J,* 451**,** 25-32.

DITTMER, P. J., DELL'ACQUA, M. L. & SATHER, W. A. 2014. Ca2+/calcineurin-dependent inactivation of neuronal L-type Ca2+ channels requires priming by AKAP-anchored protein kinase A. *Cell Rep,* 7**,** 1410-6.

DODGE-KAFKA, K. L., SOUGHAYER, J., PARE, G. C., CARLISLE MICHEL, J. J., LANGEBERG, L. K., KAPILOFF, M. S. & SCOTT, J. D. 2005. The protein kinase A anchoring protein mAKAP coordinates two integrated cAMP effector pathways. *Nature,* 437**,** 574-8.

DONG, H., ZITT, C., AURIGA, C., HATZELMANN, A. & EPSTEIN, P. M. 2010. Inhibition of PDE3, PDE4 and PDE7 potentiates glucocorticoid-induced apoptosis and overcomes glucocorticoid resistance in CEM T leukemic cells. *Biochem Pharmacol,* 79**,** 321-9.

DOSTMANN, W. R. & TAYLOR, S. S. 1991. Identifying the molecular switches that determine whether (Rp)-cAMPS functions as an antagonist or an agonist in the activation of cAMP-dependent protein kinase I. *Biochemistry,* 30**,** 8710-6.

DRAGONI, S., LAFORENZA, U., BONETTI, E., REFORGIATO, M., POLETTO, V., LODOLA, F., BOTTINO, C., GUIDO, D., RAPPA, A., PAREEK, S., TOMASELLO, M., GUARRERA, M. R., CINELLI, M. P., ARONICA, A., GUERRA, G., BAROSI, G., TANZI, F., ROSTI, V. & MOCCIA, F. 2014. Enhanced expression of Stim, Orai, and TRPC transcripts and proteins in endothelial progenitor cells isolated from patients with primary myelofibrosis. *PLoS One,* 9**,** e91099.

DUCHEN, M. R. 2000. Mitochondria and calcium: from cell signalling to cell death. *J Physiol,* 529 Pt 1**,** 57-68.

DUNKERN, T. R. & HATZELMANN, A. 2007. Characterization of inhibitors of phosphodiesterase 1C on a human cellular system. *FEBS J,* 274**,** 4812-24.
DYACHOK, O., ISAKOV, Y., SAGETORP, J. & TENGHOLM, A. 2006. Oscillations of cyclic AMP in hormone-stimulated insulin-secreting beta-cells. *Nature,* 439**,** 349-52.
EDWARDS, M., ZWOLAK, A., SCHAFER, D. A., SEPT, D., DOMINGUEZ, R. & COOPER, J. A. 2014. Capping protein regulators fine-tune actin assembly dynamics. *Nat Rev Mol Cell Biol,* 15**,** 677-89.
EIBL, G., BRUEMMER, D., OKADA, Y., DUFFY, J. P., LAW, R. E., REBER, H. A. & HINES, O. J. 2003. PGE(2) is generated by specific COX-2 activity and increases VEGF production in COX-2-expressing human pancreatic cancer cells. *Biochem Biophys Res Commun,* 306**,** 887-97.
ELIASSON, L., MA, X., RENSTROM, E., BARG, S., BERGGREN, P. O., GALVANOVSKIS, J., GROMADA, J., JING, X., LUNDQUIST, I., SALEHI, A., SEWING, S. & RORSMAN, P. 2003. SUR1 regulates PKA-independent cAMP-induced granule priming in mouse pancreatic B-cells. *J Gen Physiol,* 121**,** 181-97.
ESPOSITO, G., JAISWAL, B. S., XIE, F., KRAJNC-FRANKEN, M. A., ROBBEN, T. J., STRIK, A. M., KUIL, C., PHILIPSEN, R. L., VAN DUIN, M., CONTI, M. & GOSSEN, J. A. 2004. Mice deficient for soluble adenylyl cyclase are infertile because of a severe sperm-motility defect. *Proc Natl Acad Sci U S A,* 101**,** 2993-8.
ESTIVAL, A., MOUNIELOU, P., TROCHERIS, V., SCEMAMA, J. L., CLEMENTE, F., HOLLANDE, E. & RIBET, A. 1983. Presence of VIP receptors in a human pancreatic adenocarcinoma cell line. Modulation of the cAMP response during cell proliferation. *Biochem Biophys Res Commun,* 111**,** 958-63.
EVERETT, K. L. & COOPER, D. M. 2013. An improved targeted cAMP sensor to study the regulation of adenylyl cyclase 8 by Ca2+ entry through voltage-gated channels. *PLoS One,* 8**,** e75942.
FABIAN, A., FORTMANN, T., DIETERICH, P., RIETHMULLER, C., SCHON, P., MALLY, S., NILIUS, B. & SCHWAB, A. 2008. TRPC1 channels regulate directionality of migrating cells. *Pflugers Arch,* 457**,** 475-84.
FAHRNER, M., DERLER, I., JARDIN, I. & ROMANIN, C. 2013. The STIM1/Orai signaling machinery. *Channels (Austin),* 7**,** 330-43.
FAHRNER, M., MUIK, M., DERLER, I., SCHINDL, R., FRITSCH, R., FRISCHAUF, I. & ROMANIN, C. 2009. Mechanistic view on domains mediating STIM1-Orai coupling. *Immunol Rev,* 231**,** 99-112.
FAN, H. C., FERNANDEZ-HERNANDO, C. & LAI, J. H. 2014. Protein kinase C isoforms in atherosclerosis: pro- or anti-inflammatory? *Biochem Pharmacol,* 88**,** 139-49.
FARROW, B., RYCHAHOU, P., MURILLO, C., O'CONNOR K, L., IWAMURA, T. & EVERS, B. M. 2003. Inhibition of pancreatic cancer cell growth and induction of apoptosis with novel therapies directed against protein kinase A. *Surgery,* 134**,** 197-205.
FESKE, S., SKOLNIK, E. Y. & PRAKRIYA, M. 2012. Ion channels and transporters in lymphocyte function and immunity. *Nat Rev Immunol,* 12**,** 532-47.
FISCHER, Q. S., BEAVER, C. J., YANG, Y., RAO, Y., JAKOBSDOTTIR, K. B., STORM, D. R., MCKNIGHT, G. S. & DAW, N. W. 2004. Requirement for the RIIbeta isoform of PKA, but not calcium-stimulated adenylyl cyclase, in visual cortical plasticity. *J Neurosci,* 24**,** 9049-58.
FISCHMEISTER, R., CASTRO, L., ABI-GERGES, A., ROCHAIS, F. & VANDECASTEELE, G. 2005. Species- and tissue-dependent effects of NO and cyclic GMP on cardiac ion channels. *Comp Biochem Physiol A Mol Integr Physiol,* 142**,** 136-43.
FISHER, D. A., SMITH, J. F., PILLAR, J. S., ST DENIS, S. H. & CHENG, J. B. 1998a. Isolation and characterization of PDE8A, a novel human cAMP-specific phosphodiesterase. *Biochem Biophys Res Commun,* 246**,** 570-7.
FISHER, D. A., SMITH, J. F., PILLAR, J. S., ST DENIS, S. H. & CHENG, J. B. 1998b. Isolation and characterization of PDE9A, a novel human cGMP-specific phosphodiesterase. *J Biol Chem,* 273**,** 15559-64.

FISHER, W. E., BOROS, L. G. & SCHIRMER, W. J. 1996. Insulin promotes pancreatic cancer: evidence for endocrine influence on exocrine pancreatic tumors. *J Surg Res,* 63**,** 310-3.
FLEMMING, R., XU, S. Z. & BEECH, D. J. 2003. Pharmacological profile of store-operated channels in cerebral arteriolar smooth muscle cells. *Br J Pharmacol,* 139**,** 955-65.
FLYNN, G. E., JOHNSON, J. P., JR. & ZAGOTTA, W. N. 2001. Cyclic nucleotide-gated channels: shedding light on the opening of a channel pore. *Nat Rev Neurosci,* 2**,** 643-51.
FRANCIS, S. H., BLOUNT, M. A. & CORBIN, J. D. 2011. Mammalian cyclic nucleotide phosphodiesterases: molecular mechanisms and physiological functions. *Physiol Rev,* 91**,** 651-90.
FRANTZ, C., STEWART, K. M. & WEAVER, V. M. 2010. The extracellular matrix at a glance. *J Cell Sci,* 123**,** 4195-200.
FRISCHAUF, I., SCHINDL, R., DERLER, I., BERGSMANN, J., FAHRNER, M. & ROMANIN, C. 2008. The STIM/Orai coupling machinery. *Channels (Austin),* 2**,** 261-8.
FU, D., WAKABAYASHI, Y., LIPPINCOTT-SCHWARTZ, J. & ARIAS, I. M. 2011. Bile acid stimulates hepatocyte polarization through a cAMP-Epac-MEK-LKB1-AMPK pathway. *Proc Natl Acad Sci U S A,* 108**,** 1403-8.
FUJITA, M., IMADOME, K., ENDO, S., SHOJI, Y., YAMADA, S. & IMAI, T. 2014. Nitric oxide increases the invasion of pancreatic cancer cells via activation of the PI3K-AKT and RhoA pathways after carbon ion irradiation. *FEBS Lett,* 588**,** 3240-50.
GALLAGHER, H. C., BACON, C. L., ODUMERU, O. A., GALLAGHER, K. F., FITZPATRICK, T. & REGAN, C. M. 2004. Valproate activates phosphodiesterase-mediated cAMP degradation: relevance to C6 glioma G1 phase progression. *Neurotoxicol Teratol,* 26**,** 73-81.
GALPERIN, M. Y., NIKOLSKAYA, A. N. & KOONIN, E. V. 2001. Novel domains of the prokaryotic two-component signal transduction systems. *FEMS Microbiol Lett,* 203**,** 11-21.
GAMANUMA, M., YUASA, K., SASAKI, T., SAKURAI, N., KOTERA, J. & OMORI, K. 2003. Comparison of enzymatic characterization and gene organization of cyclic nucleotide phosphodiesterase 8 family in humans. *Cell Signal,* 15**,** 565-74.
GAMM, D. M., BAUDE, E. J. & UHLER, M. D. 1996. The major catalytic subunit isoforms of cAMP-dependent protein kinase have distinct biochemical properties in vitro and in vivo. *J Biol Chem,* 271**,** 15736-42.
GILLES-GONZALEZ, M. A. & GONZALEZ, G. 2004. Signal transduction by heme-containing PAS-domain proteins. *J Appl Physiol (1985),* 96**,** 774-83.
GLADING, A., HAN, J., STOCKTON, R. A. & GINSBERG, M. H. 2007. KRIT-1/CCM1 is a Rap1 effector that regulates endothelial cell cell junctions. *J Cell Biol,* 179**,** 247-54.
GLOERICH, M. & BOS, J. L. 2010. Epac: defining a new mechanism for cAMP action. *Annu Rev Pharmacol Toxicol,* 50**,** 355-75.
GOLD, M. G., GONEN, T. & SCOTT, J. D. 2013. Local cAMP signaling in disease at a glance. *J Cell Sci,* 126**,** 4537-43.
GOLDHOFF, P., WARRINGTON, N. M., LIMBRICK, D. D., JR., HOPE, A., WOERNER, B. M., JACKSON, E., PERRY, A., PIWNICA-WORMS, D. & RUBIN, J. B. 2008. Targeted inhibition of cyclic AMP phosphodiesterase-4 promotes brain tumor regression. *Clin Cancer Res,* 14**,** 7717-25.
GOLDSTEIN, A. L., HANNAPPEL, E. & KLEINMAN, H. K. 2005. Thymosin beta4: actin-sequestering protein moonlights to repair injured tissues. *Trends Mol Med,* 11**,** 421-9.
GORAYA, T. A. & COOPER, D. M. 2005. Ca2+-calmodulin-dependent phosphodiesterase (PDE1): current perspectives. *Cell Signal,* 17**,** 789-97.
GORAYA, T. A., MASADA, N., CIRUELA, A., WILLOUGHBY, D., CLYNES, M. A. & COOPER, D. M. 2008. Kinetic properties of Ca2+/calmodulin-dependent phosphodiesterase isoforms dictate intracellular cAMP dynamics in response to elevation of cytosolic Ca2+. *Cell Signal,* 20**,** 359-74.

GRANDOCH, M., ROSCIONI, S. S. & SCHMIDT, M. 2010. The role of Epac proteins, novel cAMP mediators, in the regulation of immune, lung and neuronal function. *Br J Pharmacol,* 159**,** 265-84.

GRINER, E. M. & KAZANIETZ, M. G. 2007. Protein kinase C and other diacylglycerol effectors in cancer. *Nat Rev Cancer,* 7**,** 281-94.

GRONHOLM, M., VOSSEBEIN, L., CARLSON, C. R., KUJA-PANULA, J., TEESALU, T., ALFTHAN, K., VAHERI, A., RAUVALA, H., HERBERG, F. W., TASKEN, K. & CARPEN, O. 2003. Merlin links to the cAMP neuronal signaling pathway by anchoring the RIbeta subunit of protein kinase A. *J Biol Chem,* 278**,** 41167-72.

GU, J. L., MULLER, S., MANCINO, V., OFFERMANNS, S. & SIMON, M. I. 2002. Interaction of G alpha(12) with G alpha(13) and G alpha(q) signaling pathways. *Proc Natl Acad Sci U S A,* 99**,** 9352-7.

GUERRA, C. & BARBACID, M. 2013. Genetically engineered mouse models of pancreatic adenocarcinoma. *Mol Oncol,* 7**,** 232-47.

GUIRGUIS, E., HOCKMAN, S., CHUNG, Y. W., AHMAD, F., GAVRILOVA, O., RAGHAVACHARI, N., YANG, Y., NIU, G., CHEN, X., YU, Z. X., LIU, S., DEGERMAN, E. & MANGANIELLO, V. 2013. A role for phosphodiesterase 3B in acquisition of brown fat characteristics by white adipose tissue in male mice. *Endocrinology,* 154**,** 3152-67.

GUO, K., MA, Q., WANG, L., HU, H., LI, J., ZHANG, D. & ZHANG, M. 2009. Norepinephrine-induced invasion by pancreatic cancer cells is inhibited by propranolol. *Oncol Rep,* 22**,** 825-30.

GUPTA, M. & YARWOOD, S. J. 2005. MAP1A light chain 2 interacts with exchange protein activated by cyclic AMP 1 (EPAC1) to enhance Rap1 GTPase activity and cell adhesion. *J Biol Chem,* 280**,** 8109-16.

HALLS, M. L. & COOPER, D. M. 2011. Regulation by Ca2+-signaling pathways of adenylyl cyclases. *Cold Spring Harb Perspect Biol,* 3**,** a004143.

HAMM, H. E. 1998. The many faces of G protein signaling. *J Biol Chem,* 273**,** 669-72.

HANSEN, G., JIN, S., UMETSU, D. T. & CONTI, M. 2000. Absence of muscarinic cholinergic airway responses in mice deficient in the cyclic nucleotide phosphodiesterase PDE4D. *Proc Natl Acad Sci U S A,* 97**,** 6751-6.

HARVEY, C. D., EHRHARDT, A. G., CELLURALE, C., ZHONG, H., YASUDA, R., DAVIS, R. J. & SVOBODA, K. 2008. A genetically encoded fluorescent sensor of ERK activity. *Proc Natl Acad Sci U S A,* 105**,** 19264-9.

HASAN, S., SATAKE, M., DAWSON, D. W., FUNAHASHI, H., ANGST, E., GO, V. L., REBER, H. A., HINES, O. J. & EIBL, G. 2008. Expression analysis of the prostaglandin E2 production pathway in human pancreatic cancers. *Pancreas,* 37**,** 121-7.

HASHEMI, M., KARAMI-TEHRANI, F., GHAVAMI, S., MADDIKA, S. & LOS, M. 2005. Adenosine and deoxyadenosine induces apoptosis in oestrogen receptor-positive and -negative human breast cancer cells via the intrinsic pathway. *Cell Prolif,* 38**,** 269-85.

HASHIGUCHI, H., NAKAZAKI, M., KORIYAMA, N., FUKUDOME, M., ASO, K. & TEI, C. 2006. Cyclic AMP/cAMP-GEF pathway amplifies insulin exocytosis induced by Ca2+ and ATP in rat islet beta-cells. *Diabetes Metab Res Rev,* 22**,** 64-71.

HASHIMOTO, Y., SHARMA, R. K. & SODERLING, T. R. 1989. Regulation of Ca2+/calmodulin-dependent cyclic nucleotide phosphodiesterase by the autophosphorylated form of Ca2+/calmodulin-dependent protein kinase II. *J Biol Chem,* 264**,** 10884-7.

HATA, A. N. & BREYER, R. M. 2004. Pharmacology and signaling of prostaglandin receptors: multiple roles in inflammation and immune modulation. *Pharmacol Ther,* 103**,** 147-66.

HAUSMANN, S., KONG, B., MICHALSKI, C., ERKAN, M. & FRIESS, H. 2014. The role of inflammation in pancreatic cancer. *Adv Exp Med Biol,* 816**,** 129-51.

HAYES, G. M., CARRIGAN, P. E., DONG, M., REUBI, J. C. & MILLER, L. J. 2007. A novel secretin receptor splice variant potentially useful for early diagnosis of pancreatic carcinoma. *Gastroenterology,* 133**,** 853-61.

HE, L. P., HEWAVITHARANA, T., SOBOLOFF, J., SPASSOVA, M. A. & GILL, D. L. 2005. A functional link between store-operated and TRPC channels revealed by the 3,5-bis(trifluoromethyl)pyrazole derivative, BTP2. *J Biol Chem,* 280**,** 10997-1006.

HE, N., KIM, N., SONG, M., PARK, C., KIM, S., PARK, E. Y., YIM, H. Y., KIM, K., PARK, J. H., KIM, K. I., ZHANG, F., MILLS, G. B. & YOON, S. 2014. Integrated Analysis of Transcriptomes of Cancer Cell Lines and Patient Samples Reveals STK11/LKB1-Driven Regulation of cAMP Phosphodiesterase-4D. *Mol Cancer Ther,* 13**,** 2463-73.

HEIST, E. K. & SCHULMAN, H. 1998. The role of Ca2+/calmodulin-dependent protein kinases within the nucleus. *Cell Calcium,* 23**,** 103-14.

HENDERSON, D. J., BYRNE, A., DULLA, K., JENSTER, G., HOFFMANN, R., BAILLIE, G. S. & HOUSLAY, M. D. 2014. The cAMP phosphodiesterase-4D7 (PDE4D7) is downregulated in androgen-independent prostate cancer cells and mediates proliferation by compartmentalising cAMP at the plasma membrane of VCaP prostate cancer cells. *Br J Cancer,* 110**,** 1278-87.

HENNIG, R., DING, X. Z. & ADRIAN, T. E. 2004. On the role of the islets of Langerhans in pancreatic cancer. *Histol Histopathol,* 19**,** 999-1011.

HENNIG, R., DING, X. Z., TONG, W. G., SCHNEIDER, M. B., STANDOP, J., FRIESS, H., BUCHLER, M. W., POUR, P. M. & ADRIAN, T. E. 2002. 5-Lipoxygenase and leukotriene B(4) receptor are expressed in human pancreatic cancers but not in pancreatic ducts in normal tissue. *Am J Pathol,* 161**,** 421-8.

HENNIG, R., GRIPPO, P., DING, X. Z., RAO, S. M., BUCHLER, M. W., FRIESS, H., TALAMONTI, M. S., BELL, R. H. & ADRIAN, T. E. 2005. 5-Lipoxygenase, a marker for early pancreatic intraepithelial neoplastic lesions. *Cancer Res,* 65**,** 6011-6.

HERBST, K. J., ALLEN, M. D. & ZHANG, J. 2011. Spatiotemporally regulated protein kinase A activity is a critical regulator of growth factor-stimulated extracellular signal-regulated kinase signaling in PC12 cells. *Mol Cell Biol,* 31**,** 4063-75.

HERMANS, E. 2003. Biochemical and pharmacological control of the multiplicity of coupling at G-protein-coupled receptors. *Pharmacol Ther,* 99**,** 25-44.

HINKE, S. A., NAVEDO, M. F., ULMAN, A., WHITING, J. L., NYGREN, P. J., TIAN, G., JIMENEZ-CALIANI, A. J., LANGEBERG, L. K., CIRULLI, V., TENGHOLM, A., DELL'ACQUA, M. L., SANTANA, L. F. & SCOTT, J. D. 2012. Anchored phosphatases modulate glucose homeostasis. *EMBO J,* 31**,** 3991-4004.

HIRAMOTO, K., MURATA, T., SHIMIZU, K., MORITA, H., INUI, M., MANGANIELLO, V. C., TAGAWA, T. & ARAI, N. 2014. Role of phosphodiesterase 2 in growth and invasion of human malignant melanoma cells. *Cell Signal,* 26**,** 1807-17.

HOFMANN, F., BIEL, M. & KAUPP, U. B. 2005. International Union of Pharmacology. LI. Nomenclature and structure-function relationships of cyclic nucleotide-regulated channels. *Pharmacol Rev,* 57**,** 455-62.

HOLLANDE, E., FANJUL, M., CLARET, S., FORGUE-LAFITTE, M. E. & BARA, J. 1995. Effects of VIP on the regulation of mucin secretion in cultured human pancreatic cancer cells (Capan-1). *In Vitro Cell Dev Biol Anim,* 31**,** 227-33.

HONG, J. H., LI, Q., KIM, M. S., SHIN, D. M., FESKE, S., BIRNBAUMER, L., CHENG, K. T., AMBUDKAR, I. S. & MUALLEM, S. 2011. Polarized but differential localization and recruitment of STIM1, Orai1 and TRPC channels in secretory cells. *Traffic,* 12**,** 232-45.

HOOVER, P. J. & LEWIS, R. S. 2011. Stoichiometric requirements for trapping and gating of Ca2+ release-activated Ca2+ (CRAC) channels by stromal interaction molecule 1 (STIM1). *Proc Natl Acad Sci U S A,* 108**,** 13299-304.

HOSHI, N., LANGEBERG, L. K., GOULD, C. M., NEWTON, A. C. & SCOTT, J. D. 2010. Interaction with AKAP79 modifies the cellular pharmacology of PKC. *Mol Cell,* 37**,** 541-50.

HOSHINO, D., BRANCH, K. M. & WEAVER, A. M. 2013. Signaling inputs to invadopodia and podosomes. *J Cell Sci,* 126**,** 2979-89.

HOSHINO, T., SAKISAKA, T., BABA, T., YAMADA, T., KIMURA, T. & TAKAI, Y. 2005. Regulation of E-cadherin endocytosis by nectin through afadin, Rap1, and p120ctn. *J Biol Chem,* 280**,** 24095-103.

HOTH, M. & PENNER, R. 1992. Depletion of intracellular calcium stores activates a calcium current in mast cells. *Nature,* 355**,** 353-6.

HOTH, M. & PENNER, R. 1993. Calcium release-activated calcium current in rat mast cells. *J Physiol,* 465**,** 359-86.

HOU, X., PEDI, L., DIVER, M. M. & LONG, S. B. 2012. Crystal structure of the calcium release-activated calcium channel Orai. *Science,* 338**,** 1308-13.

HOUSLAY, M. D. & ADAMS, D. R. 2003. PDE4 cAMP phosphodiesterases: modular enzymes that orchestrate signalling cross-talk, desensitization and compartmentalization. *Biochem J,* 370**,** 1-18.

HOWE, A. K. 2004. Regulation of actin-based cell migration by cAMP/PKA. *Biochim Biophys Acta,* 1692**,** 159-74.

HOWE, A. K. 2011. Cross-talk between calcium and protein kinase A in the regulation of cell migration. *Curr Opin Cell Biol,* 23**,** 554-61.

HRUBAN, R. H., ADSAY, N. V., ALBORES-SAAVEDRA, J., COMPTON, C., GARRETT, E. S., GOODMAN, S. N., KERN, S. E., KLIMSTRA, D. S., KLOPPEL, G., LONGNECKER, D. S., LUTTGES, J. & OFFERHAUS, G. J. 2001. Pancreatic intraepithelial neoplasia: a new nomenclature and classification system for pancreatic duct lesions. *Am J Surg Pathol,* 25**,** 579-86.

HSU, Y. T., LIAO, G., BI, X., OKA, T., TAMURA, S. & BAUDRY, M. 2011. The PDE10A inhibitor, papaverine, differentially activates ERK in male and female rat striatal slices. *Neuropharmacology,* 61**,** 1275-81.

HUANG, L. J., DURICK, K., WEINER, J. A., CHUN, J. & TAYLOR, S. S. 1997. Identification of a novel protein kinase A anchoring protein that binds both type I and type II regulatory subunits. *J Biol Chem,* 272**,** 8057-64.

HUANG, X. Y., WANG, H. C., YUAN, Z., HUANG, J. & ZHENG, Q. 2012. Norepinephrine stimulates pancreatic cancer cell proliferation, migration and invasion via beta-adrenergic receptor-dependent activation of P38/MAPK pathway. *Hepatogastroenterology,* 59**,** 889-93.

HUSTON, E., LYNCH, M. J., MOHAMED, A., COLLINS, D. M., HILL, E. V., MACLEOD, R., KRAUSE, E., BAILLIE, G. S. & HOUSLAY, M. D. 2008. EPAC and PKA allow cAMP dual control over DNA-PK nuclear translocation. *Proc Natl Acad Sci U S A,* 105**,** 12791-6.

HUTCHISON, M. R. & WHITE, P. C. 2014. Prostacyclin regulates bone growth via the Epac/Rap1 pathway. *Endocrinology***,** en20141348.

HUTTENLOCHER, A. & HORWITZ, A. R. 2011. Integrins in cell migration. *Cold Spring Harb Perspect Biol,* 3**,** a005074.

IDEVALL-HAGREN, O., BARG, S., GYLFE, E. & TENGHOLM, A. 2010. cAMP mediators of pulsatile insulin secretion from glucose-stimulated single beta-cells. *J Biol Chem,* 285**,** 23007-18.

IGARASHI, H., ITO, T., HOU, W., MANTEY, S. A., PRADHAN, T. K., ULRICH, C. D., 2ND, HOCART, S. J., COY, D. H. & JENSEN, R. T. 2002. Elucidation of vasoactive intestinal peptide pharmacophore for VPAC(1) receptors in human, rat, and guinea pig. *J Pharmacol Exp Ther,* 301**,** 37-50.

IRANNEJAD, R. & VON ZASTROW, M. 2014. GPCR signaling along the endocytic pathway. *Curr Opin Cell Biol,* 27**,** 109-16.

ITO, H., DUXBURY, M., BENOIT, E., CLANCY, T. E., ZINNER, M. J., ASHLEY, S. W. & WHANG, E. E. 2004. Prostaglandin E2 enhances pancreatic cancer invasiveness through an Ets-1-dependent induction of matrix metalloproteinase-2. *Cancer Res,* 64**,** 7439-46.

ITZHAKI, I., RAPOPORT, S., HUBER, I., MIZRAHI, I., ZWI-DANTSIS, L., ARBEL, G., SCHILLER, J. & GEPSTEIN, L. 2011. Calcium handling in human induced pluripotent stem cell derived cardiomyocytes. *PLoS One,* 6**,** e18037.

JAHNSEN, T., HEDIN, L., LOHMANN, S. M., WALTER, U. & RICHARDS, J. S. 1986. The neural type II regulatory subunit of cAMP-dependent protein kinase is present and regulated by hormones in the rat ovary. *J Biol Chem,* 261**,** 6637-9.

JAIRAMAN, A. & PRAKRIYA, M. 2013. Molecular pharmacology of store-operated CRAC channels. *Channels (Austin),* 7**,** 402-14.

JARNAESS, E. & TASKEN, K. 2007. Spatiotemporal control of cAMP signalling processes by anchored signalling complexes. *Biochem Soc Trans,* 35**,** 931-7.

JEONG, H. W., LI, Z., BROWN, M. D. & SACKS, D. B. 2007. IQGAP1 binds Rap1 and modulates its activity. *J Biol Chem,* 282**,** 20752-62.

JEONG, S. W. & IKEDA, S. R. 1998. G protein alpha subunit G alpha z couples neurotransmitter receptors to ion channels in sympathetic neurons. *Neuron,* 21**,** 1201-12.

JIANG, H. N., ZENG, B., ZHANG, Y., DASKOULIDOU, N., FAN, H., QU, J. M. & XU, S. Z. 2013. Involvement of TRPC channels in lung cancer cell differentiation and the correlation analysis in human non-small cell lung cancer. *PLoS One,* 8**,** e67637.

JIANG, S., KOPRAS, E., MCMICHAEL, M., BELL, R. H., JR. & ULRICH, C. D., 2ND 1997. Vasoactive intestinal peptide (VIP) stimulates in vitro growth of VIP-1 receptor-bearing human pancreatic adenocarcinoma-derived cells. *Cancer Res,* 57**,** 1475-80.

JIN, S. L. & CONTI, M. 2002. Induction of the cyclic nucleotide phosphodiesterase PDE4B is essential for LPS-activated TNF-alpha responses. *Proc Natl Acad Sci U S A,* 99**,** 7628-33.

KANG, B. H., SHIM, Y. J., TAE, Y. K., SONG, J. A., CHOI, B. K., PARK, I. S. & MIN, B. H. 2014. Clusterin stimulates the chemotactic migration of macrophages through a pertussis toxin sensitive G-protein-coupled receptor and Gbetagamma-dependent pathways. *Biochem Biophys Res Commun,* 445**,** 645-50.

KAR, P., BAKOWSKI, D., DI CAPITE, J., NELSON, C. & PAREKH, A. B. 2012. Different agonists recruit different stromal interaction molecule proteins to support cytoplasmic Ca2+ oscillations and gene expression. *Proc Natl Acad Sci U S A,* 109**,** 6969-74.

KARAKHANOVA, S., GOLOVASTOVA, M., PHILIPPOV, P. P., WERNER, J. & BAZHIN, A. V. 2014. Interlude of cGMP and cGMP/protein kinase G type 1 in pancreatic adenocarcinoma cells. *Pancreas,* 43**,** 784-94.

KASE, D. & IMOTO, K. 2012. The Role of HCN Channels on Membrane Excitability in the Nervous System. *J Signal Transduct,* 2012**,** 619747.

KASS, G. E. & ORRENIUS, S. 1999. Calcium signaling and cytotoxicity. *Environ Health Perspect,* 107 Suppl 1**,** 25-35.

KATAGIRI, K., IMAMURA, M. & KINASHI, T. 2006. Spatiotemporal regulation of the kinase Mst1 by binding protein RAPL is critical for lymphocyte polarity and adhesion. *Nat Immunol,* 7**,** 919-28.

KAUPP, U. B. & SEIFERT, R. 2002. Cyclic nucleotide-gated ion channels. *Physiol Rev,* 82**,** 769-824.

KAWASAKI, H., SPRINGETT, G. M., MOCHIZUKI, N., TOKI, S., NAKAYA, M., MATSUDA, M., HOUSMAN, D. E. & GRAYBIEL, A. M. 1998. A family of cAMP-binding proteins that directly activate Rap1. *Science,* 282**,** 2275-9.

KELLY, M. P., LOGUE, S. F., BRENNAN, J., DAY, J. P., LAKKARAJU, S., JIANG, L., ZHONG, X., TAM, M., SUKOFF RIZZO, S. J., PLATT, B. J., DWYER, J. M., NEAL, S., PULITO, V. L., AGOSTINO, M. J., GRAUER, S. M., NAVARRA, R. L., KELLEY, C., COMERY, T. A., MURRILLS, R. J., HOUSLAY, M. D. & BRANDON, N. J. 2010. Phosphodiesterase 11A in brain is enriched in ventral hippocampus and deletion causes psychiatric disease-related phenotypes. *Proc Natl Acad Sci U S A,* 107**,** 8457-62.

KERAVIS, T. & LUGNIER, C. 2012. Cyclic nucleotide phosphodiesterase (PDE) isozymes as targets of the intracellular signalling network: benefits of PDE inhibitors in various diseases and perspectives for future therapeutic developments. *Br J Pharmacol,* 165**,** 1288-305.

KERN, S. E., SHI, C. & HRUBAN, R. H. 2011. The complexity of pancreatic ductal cancers and multidimensional strategies for therapeutic targeting. *J Pathol,* 223**,** 295-306.

KHAN, S. M., SLENO, R., GORA, S., ZYLBERGOLD, P., LAVERDURE, J. P., LABBE, J. C., MILLER, G. J. & HEBERT, T. E. 2013. The expanding roles of Gbetagamma subunits in G protein-coupled receptor signaling and drug action. *Pharmacol Rev,* 65**,** 545-77.

KILTS, J. D., GERHARDT, M. A., RICHARDSON, M. D., SREERAM, G., MACKENSEN, G. B., GROCOTT, H. P., WHITE, W. D., DAVIS, R. D., NEWMAN, M. F., REVES, J. G., SCHWINN, D. A. & KWATRA, M. M. 2000. Beta(2)-adrenergic and several other G protein-coupled receptors in human atrial membranes activate both G(s) and G(i). *Circ Res,* 87**,** 705-9.

KIM, E. K., YUN, S. J., HA, J. M., KIM, Y. W., JIN, I. H., WOO, D. H., LEE, H. S., HA, H. K. & BAE, S. S. 2012. Synergistic induction of cancer cell migration regulated by Gbetagamma and phosphatidylinositol 3-kinase. *Exp Mol Med,* 44**,** 483-91.

KIM, H. Y., PARK, S. Y., LEE, S. W., LEE, H. R., LEE, W. S., RHIM, B. Y., HONG, K. W. & KIM, C. D. 2014. Inhibition of HMGB1-induced angiogenesis by cilostazol via SIRT1 activation in synovial fibroblasts from rheumatoid arthritis. *PLoS One,* 9**,** e104743.

KIM, K. Y., SHIN, H. K., CHOI, J. M. & HONG, K. W. 2002. Inhibition of lipopolysaccharide-induced apoptosis by cilostazol in human umbilical vein endothelial cells. *J Pharmacol Exp Ther,* 300**,** 709-15.

KIM, M. S., ZENG, W., YUAN, J. P., SHIN, D. M., WORLEY, P. F. & MUALLEM, S. 2009. Native Store-operated Ca2+ Influx Requires the Channel Function of Orai1 and TRPC1. *J Biol Chem,* 284**,** 9733-41.

KIM, S. W., RAI, D. & AGUIAR, R. C. 2011. Gene set enrichment analysis unveils the mechanism for the phosphodiesterase 4B control of glucocorticoid response in B-cell lymphoma. *Clin Cancer Res,* 17**,** 6723-32.

KIMURA, K., ITO, M., AMANO, M., CHIHARA, K., FUKATA, Y., NAKAFUKU, M., YAMAMORI, B., FENG, J., NAKANO, T., OKAWA, K., IWAMATSU, A. & KAIBUCHI, K. 1996. Regulation of myosin phosphatase by Rho and Rho-associated kinase (Rho-kinase). *Science,* 273**,** 245-8.

KINCAID, R. L., STITH-COLEMAN, I. E. & VAUGHAN, M. 1985. Proteolytic activation of calmodulin-dependent cyclic nucleotide phosphodiesterase. *J Biol Chem,* 260**,** 9009-15.

KIRKMAN-BROWN, J. C., BARRATT, C. L. & PUBLICOVER, S. J. 2003. Nifedipine reveals the existence of two discrete components of the progesterone-induced [Ca2+]i transient in human spermatozoa. *Dev Biol,* 259**,** 71-82.

KIRUI, J. K., XIE, Y., WOLFF, D. W., JIANG, H., ABEL, P. W. & TU, Y. 2010. Gbetagamma signaling promotes breast cancer cell migration and invasion. *J Pharmacol Exp Ther,* 333**,** 393-403.

KLARENBEEK, J. B., GOEDHART, J., HINK, M. A., GADELLA, T. W. & JALINK, K. 2011. A mTurquoise-based cAMP sensor for both FLIM and ratiometric read-out has improved dynamic range. *PLoS One,* 6**,** e19170.

KLEENE, S. J. 2008. The electrochemical basis of odor transduction in vertebrate olfactory cilia. *Chem Senses,* 33**,** 839-59.

KOBILKA, B. K. 2007. G protein coupled receptor structure and activation. *Biochim Biophys Acta,* 1768**,** 794-807.

KOLOSIONEK, E., SAVAI, R., GHOFRANI, H. A., WEISSMANN, N., GUENTHER, A., GRIMMINGER, F., SEEGER, W., BANAT, G. A., SCHERMULY, R. T. & PULLAMSETTI, S. S. 2009. Expression and activity of phosphodiesterase isoforms during epithelial mesenchymal transition: the role of phosphodiesterase 4. *Mol Biol Cell,* 20**,** 4751-65.

KONDRATSKA, K., KONDRATSKYI, A., YASSINE, M., LEMONNIER, L., LEPAGE, G., MORABITO, A., SKRYMA, R. & PREVARSKAYA, N. 2014. Orai1 and STIM1 mediate SOCE and contribute to apoptotic resistance of pancreatic adenocarcinoma. *Biochim Biophys Acta,* 1843**,** 2263-9.

KOPP, J. L., VON FIGURA, G., MAYES, E., LIU, F. F., DUBOIS, C. L., MORRIS, J. P. T., PAN, F. C., AKIYAMA, H., WRIGHT, C. V., JENSEN, K., HEBROK, M. & SANDER, M. 2012. Identification of Sox9-dependent acinar-to-ductal reprogramming as the principal mechanism for initiation of pancreatic ductal adenocarcinoma. *Cancer Cell,* 22**,** 737-50.

KORNER, M., HAYES, G. M., REHMANN, R., ZIMMERMANN, A., FRIESS, H., MILLER, L. J. & REUBI, J. C. 2005. Secretin receptors in normal and diseased human pancreas: marked reduction of receptor binding in ductal neoplasia. *Am J Pathol,* 167**,** 959-68.

KOWALCZYK, P., KINJO, T., KOWALCZYK, M., WALASZEK, Z., HANAUSEK, M. & SLAGA, T. J. 2009. Effect of phosphodiesterase antagonists on glucocorticoid mediated growth inhibition in murine skin cell lines. *Eur J Pharmacol,* 610**,** 29-36.

KRAUSE, M. & GAUTREAU, A. 2014. Steering cell migration: lamellipodium dynamics and the regulation of directional persistence. *Nat Rev Mol Cell Biol,* 15**,** 577-90.

KRAYNIK, S. M., MIYAOKA, R. S. & BEAVO, J. A. 2013. PDE3 and PDE4 isozyme-selective inhibitors are both required for synergistic activation of brown adipose tissue. *Mol Pharmacol,* 83**,** 1155-65.

KRUGER, S., HAAS, M., ORMANNS, S., BACHMANN, S., SIVEKE, J. T., KIRCHNER, T., HEINEMANN, V. & BOECK, S. 2014. Translational research in pancreatic ductal adenocarcinoma: Current evidence and future concepts. *World J Gastroenterol,* 20**,** 10769-10777.

LAFERLA, F. M. 2002. Calcium dyshomeostasis and intracellular signalling in Alzheimer's disease. *Nat Rev Neurosci,* 3**,** 862-72.

LAFUENTE, E. M., VAN PUIJENBROEK, A. A., KRAUSE, M., CARMAN, C. V., FREEMAN, G. J., BEREZOVSKAYA, A., CONSTANTINE, E., SPRINGER, T. A., GERTLER, F. B. & BOUSSIOTIS, V. A. 2004. RIAM, an Ena/VASP and Profilin ligand, interacts with Rap1-GTP and mediates Rap1-induced adhesion. *Dev Cell,* 7**,** 585-95.

LANDA, L. R., JR., HARBECK, M., KAIHARA, K., CHEPURNY, O., KITIPHONGSPATTANA, K., GRAF, O., NIKOLAEV, V. O., LOHSE, M. J., HOLZ, G. G. & ROE, M. W. 2005. Interplay of Ca2+ and cAMP signaling in the insulin-secreting MIN6 beta-cell line. *J Biol Chem,* 280**,** 31294-302.

LAW, A. L., VEHLOW, A., KOTINI, M., DODGSON, L., SOONG, D., THEVENEAU, E., BODO, C., TAYLOR, E., NAVARRO, C., PERERA, U., MICHAEL, M., DUNN, G. A., BENNETT, D., MAYOR, R. & KRAUSE, M. 2013. Lamellipodin and the Scar/WAVE complex cooperate to promote cell migration in vivo. *J Cell Biol,* 203**,** 673-89.

LEE, D. C., CARMICHAEL, D. F., KREBS, E. G. & MCKNIGHT, G. S. 1983. Isolation of a cDNA clone for the type I regulatory subunit of bovine cAMP-dependent protein kinase. *Proc Natl Acad Sci U S A,* 80**,** 3608-12.

LEE, K. P., CHOI, S., HONG, J. H., AHUJA, M., GRAHAM, S., MA, R., SO, I., SHIN, D. M., MUALLEM, S. & YUAN, J. P. 2014. Molecular determinants mediating gating of Transient Receptor Potential Canonical (TRPC) channels by stromal interaction molecule 1 (STIM1). *J Biol Chem,* 289**,** 6372-82.

LEE, M. G., OHANA, E., PARK, H. W., YANG, D. & MUALLEM, S. 2012. Molecular mechanism of pancreatic and salivary gland fluid and HCO3 secretion. *Physiol Rev,* 92**,** 39-74.

LEE, R., WOLDA, S., MOON, E., ESSELSTYN, J., HERTEL, C. & LERNER, A. 2002. PDE7A is expressed in human B-lymphocytes and is up-regulated by elevation of intracellular cAMP. *Cell Signal,* 14**,** 277-84.

LEFKIMMIATIS, K., LERONNI, D. & HOFER, A. M. 2013. The inner and outer compartments of mitochondria are sites of distinct cAMP/PKA signaling dynamics. *J Cell Biol,* 202**,** 453-62.

LEFKIMMIATIS, K., SRIKANTHAN, M., MAIELLARO, I., MOYER, M. P., CURCI, S. & HOFER, A. M. 2009. Store-operated cyclic AMP signalling mediated by STIM1. *Nat Cell Biol,* 11**,** 433-42.

LEFKIMMIATIS, K. & ZACCOLO, M. 2014. cAMP signaling in subcellular compartments. *Pharmacol Ther,* 143**,** 295-304.

LEWIS, R. S. 2011. Store-operated calcium channels: new perspectives on mechanism and function. *Cold Spring Harb Perspect Biol,* 3.

LI, M., LI, W., KIM, H. J., YAO, Q., CHEN, C. & FISHER, W. E. 2004. Characterization of somatostatin receptor expression in human pancreatic cancer using real-time RT-PCR. *J Surg Res,* 119**,** 130-7.

LI, N., LEE, K., XI, Y., ZHU, B., GARY, B. D., RAMIREZ-ALCANTARA, V., GURPINAR, E., CANZONERI, J. C., FAJARDO, A., SIGLER, S., PIAZZA, J. T., CHEN, X., ANDREWS, J., THOMAS, M., LU, W., LI, Y., LAAN, D. J., MOYER, M. P., RUSSO, S., EBERHARDT, B. T., YET, L., KEETON, A. B., GRIZZLE, W. E. & PIAZZA, G. A. 2014. Phosphodiesterase 10A: a novel target for selective inhibition of colon tumor cell growth and beta-catenin-dependent TCF transcriptional activity. *Oncogene*.

LI, S., TSALKOVA, T., WHITE, M. A., MEI, F. C., LIU, T., WANG, D., WOODS, V. L., JR. & CHENG, X. 2011. Mechanism of intracellular cAMP sensor Epac2 activation: cAMP-induced conformational changes identified by amide hydrogen/deuterium exchange mass spectrometry (DXMS). *J Biol Chem,* 286**,** 17889-97.

LIAO, Y., ERXLEBEN, C., ABRAMOWITZ, J., FLOCKERZI, V., ZHU, M. X., ARMSTRONG, D. L. & BIRNBAUMER, L. 2008. Functional interactions among Orai1, TRPCs, and STIM1 suggest a STIM-regulated heteromeric Orai/TRPC model for SOCE/Icrac channels. *Proc Natl Acad Sci U S A,* 105**,** 2895-900.

LIEBER, M., MAZZETTA, J., NELSON-REES, W., KAPLAN, M. & TODARO, G. 1975. Establishment of a continuous tumor-cell line (panc-1) from a human carcinoma of the exocrine pancreas. *Int J Cancer,* 15**,** 741-7.

LIM, C. J., HAN, J., YOUSEFI, N., MA, Y., AMIEUX, P. S., MCKNIGHT, G. S., TAYLOR, S. S. & GINSBERG, M. H. 2007. Alpha4 integrins are type I cAMP-dependent protein kinase-anchoring proteins. *Nat Cell Biol,* 9**,** 415-21.

LIM, C. J., KAIN, K. H., TKACHENKO, E., GOLDFINGER, L. E., GUTIERREZ, E., ALLEN, M. D., GROISMAN, A., ZHANG, J. & GINSBERG, M. H. 2008. Integrin-mediated protein kinase A activation at the leading edge of migrating cells. *Mol Biol Cell,* 19**,** 4930-41.

LIN, X., LUO, K., LV, Z. & HUANG, J. 2012. Beta-adrenoceptor action on pancreatic cancer cell proliferation and tumor growth in mice. *Hepatogastroenterology,* 59**,** 584-8.

LIS, A., PEINELT, C., BECK, A., PARVEZ, S., MONTEILH-ZOLLER, M., FLEIG, A. & PENNER, R. 2007. CRACM1, CRACM2, and CRACM3 are store-operated Ca2+ channels with distinct functional properties. *Curr Biol,* 17**,** 794-800.

LITJENS, T., HARLAND, M. L., ROBERTS, M. L., BARRITT, G. J. & RYCHKOV, G. Y. 2004. Fast Ca(2+)-dependent inactivation of the store-operated Ca2+ current (ISOC) in liver cells: a role for calmodulin. *J Physiol,* 558**,** 85-97.

LIU, C., TAKAHASHI, M., LI, Y., DILLON, T. J., KAECH, S. & STORK, P. J. 2010. The interaction of Epac1 and Ran promotes Rap1 activation at the nuclear envelope. *Mol Cell Biol,* 30**,** 3956-69.

LIU, C. D., BALASUBRAMANIAM, A., SAXTON, R. E., PAIVA, M. & MCFADDEN, D. W. 1995. Human pancreatic cancer growth is inhibited by peptide YY and BIM-43004-1. *J Surg Res,* 58**,** 707-12.

LIU, C. Q., LEUNG, F. P., LEE, V. W., LAU, C. W., YAO, X., LU, L. & HUANG, Y. 2008. Prevention of nitroglycerin tolerance in vitro by T0156, a selective phosphodiesterase type 5 inhibitor. *Eur J Pharmacol,* 590**,** 250-4.

LIU, J., YUE, P., ARTYM, V. V., MUELLER, S. C. & GUO, W. 2009. The role of the exocyst in matrix metalloproteinase secretion and actin dynamics during tumor cell invadopodia formation. *Mol Biol Cell,* 20**,** 3763-71.

LIU, Y., CONE, J., LE, S. N., FONG, M., TAO, L., SHOAF, S. E., BRICMONT, P., CZERWIEC, F. S., KAMBAYASHI, J., YOSHITAKE, M. & SUN, B. 2004. Cilostazol and dipyridamole synergistically inhibit human platelet aggregation. *J Cardiovasc Pharmacol,* 44**,** 266-73.

LIZARRAGA, F., POINCLOUX, R., ROMAO, M., MONTAGNAC, G., LE DEZ, G., BONNE, I., RIGAILL, G., RAPOSO, G. & CHAVRIER, P. 2009. Diaphanous-related formins are required for invadopodia formation and invasion of breast tumor cells. *Cancer Res,* 69**,** 2792-800.

LONDON, E., NESTEROVA, M., SINAII, N., SZAREK, E., CHANTURIYA, T., MASTROYANNIS, S. A., GAVRILOVA, O. & STRATAKIS, C. A. 2014. Differentially Regulated Protein Kinase A (PKA) Activity in Adipose Tissue and Liver Is Associated With Resistance to Diet-Induced Obesity and Glucose Intolerance in Mice That Lack PKA Regulatory Subunit Type IIalpha. *Endocrinology,* 155**,** 3397-408.

LONG, S. B., CAMPBELL, E. B. & MACKINNON, R. 2005. Crystal structure of a mammalian voltage-dependent Shaker family K+ channel. *Science,* 309**,** 897-903.
LORENZ, R., ALEKSIC, T., WAGNER, M., ADLER, G. & WEBER, C. K. 2008. The cAMP/Epac1/Rap1 pathway in pancreatic carcinoma. *Pancreas,* 37**,** 102-3.
LUDWIG, A., BUDDE, T., STIEBER, J., MOOSMANG, S., WAHL, C., HOLTHOFF, K., LANGEBARTELS, A., WOTJAK, C., MUNSCH, T., ZONG, X., FEIL, S., FEIL, R., LANCEL, M., CHIEN, K. R., KONNERTH, A., PAPE, H. C., BIEL, M. & HOFMANN, F. 2003. Absence epilepsy and sinus dysrhythmia in mice lacking the pacemaker channel HCN2. *EMBO J,* 22**,** 216-24.
LUU, W., SHARPE, L. J., GELISSEN, I. C. & BROWN, A. J. 2013. The role of signalling in cellular cholesterol homeostasis. *IUBMB Life,* 65**,** 675-84.
LUXENBURG, C., GEBLINGER, D., KLEIN, E., ANDERSON, K., HANEIN, D., GEIGER, B. & ADDADI, L. 2007. The architecture of the adhesive apparatus of cultured osteoclasts: from podosome formation to sealing zone assembly. *PLoS One,* 2**,** e179.
MA, Y., PITSON, S., HERCUS, T., MURPHY, J., LOPEZ, A. & WOODCOCK, J. 2005. Sphingosine activates protein kinase A type II by a novel cAMP-independent mechanism. *J Biol Chem,* 280**,** 26011-7.
MAIELLARO, I., LEFKIMMIATIS, K., MOYER, M. P., CURCI, S. & HOFER, A. M. 2012. Termination and activation of store-operated cyclic AMP production. *J Cell Mol Med,* 16**,** 2715-25.
MAITRA, A., FUKUSHIMA, N., TAKAORI, K. & HRUBAN, R. H. 2005. Precursors to invasive pancreatic cancer. *Adv Anat Pathol,* 12**,** 81-91.
MAITRA, A. & HRUBAN, R. H. 2008. Pancreatic cancer. *Annu Rev Pathol,* 3**,** 157-88.
MAMO, Y. A., ANGUS, J. A., ZIOGAS, J., SOEDING, P. F. & WRIGHT, C. E. 2014. The role of voltage-operated and non-voltage-operated calcium channels in endothelin-induced vasoconstriction of rat cerebral arteries. *Eur J Pharmacol,* 742C**,** 65-73.
MARCINKIEWICZ, A., GAUTHIER, D., GARCIA, A. & BRASAEMLE, D. L. 2006. The phosphorylation of serine 492 of perilipin a directs lipid droplet fragmentation and dispersion. *J Biol Chem,* 281**,** 11901-9.
MARINO, C. R., LEACH, S. D., SCHAEFER, J. F., MILLER, L. J. & GORELICK, F. S. 1993. Characterization of cAMP-dependent protein kinase activation by CCK in rat pancreas. *FEBS Lett,* 316**,** 48-52.
MARQUETTE, A., ANDRE, J., BAGOT, M., BENSUSSAN, A. & DUMAZ, N. 2011. ERK and PDE4 cooperate to induce RAF isoform switching in melanoma. *Nat Struct Mol Biol,* 18**,** 584-91.
MARTIN, N. P., WHALEN, E. J., ZAMAH, M. A., PIERCE, K. L. & LEFKOWITZ, R. J. 2004. PKA-mediated phosphorylation of the beta1-adrenergic receptor promotes Gs/Gi switching. *Cell Signal,* 16**,** 1397-403.
MASADA, N., CIRUELA, A., MACDOUGALL, D. A. & COOPER, D. M. 2009. Distinct mechanisms of regulation by Ca2+/calmodulin of type 1 and 8 adenylyl cyclases support their different physiological roles. *J Biol Chem,* 284**,** 4451-63.
MASCIARELLI, S., HORNER, K., LIU, C., PARK, S. H., HINCKLEY, M., HOCKMAN, S., NEDACHI, T., JIN, C., CONTI, M. & MANGANIELLO, V. 2004. Cyclic nucleotide phosphodiesterase 3A-deficient mice as a model of female infertility. *J Clin Invest,* 114**,** 196-205.
MAURICE, D. H., KE, H., AHMAD, F., WANG, Y., CHUNG, J. & MANGANIELLO, V. C. 2014. Advances in targeting cyclic nucleotide phosphodiesterases. *Nat Rev Drug Discov,* 13**,** 290-314.
MAURICE, D. H., PALMER, D., TILLEY, D. G., DUNKERLEY, H. A., NETHERTON, S. J., RAYMOND, D. R., ELBATARNY, H. S. & JIMMO, S. L. 2003. Cyclic nucleotide phosphodiesterase activity, expression, and targeting in cells of the cardiovascular system. *Mol Pharmacol,* 64**,** 533-46.
MCALLISTER-LUCAS, L. M., HAIK, T. L., COLBRAN, J. L., SONNENBURG, W. K., SEGER, D., TURKO, I. V., BEAVO, J. A., FRANCIS, S. H. & CORBIN, J. D. 1995. An essential aspartic acid at each of two allosteric cGMP-binding sites of a cGMP-specific phosphodiesterase. *J Biol Chem,* 270**,** 30671-9.
MCEWAN, D. G., BRUNTON, V. G., BAILLIE, G. S., LESLIE, N. R., HOUSLAY, M. D. & FRAME, M. C. 2007. Chemoresistant KM12C colon cancer cells are addicted to low cyclic AMP levels in a

phosphodiesterase 4-regulated compartment via effects on phosphoinositide 3-kinase. *Cancer Res,* 67**,** 5248-57.
MCKENZIE, A. J., CAMPBELL, S. L. & HOWE, A. K. 2011. Protein kinase A activity and anchoring are required for ovarian cancer cell migration and invasion. *PLoS One,* 6**,** e26552.
MCNALLY, B. A., SOMASUNDARAM, A., YAMASHITA, M. & PRAKRIYA, M. 2012. Gated regulation of CRAC channel ion selectivity by STIM1. *Nature,* 482**,** 241-5.
METRICH, M., LAURENT, A. C., BRECKLER, M., DUQUESNES, N., HMITOU, I., COURILLAU, D., BLONDEAU, J. P., CROZATIER, B., LEZOUALC'H, F. & MOREL, E. 2010. Epac activation induces histone deacetylase nuclear export via a Ras-dependent signalling pathway. *Cell Signal,* 22**,** 1459-68.
MEYERS, J. A., SU, D. W. & LERNER, A. 2009. Chronic lymphocytic leukemia and B and T cells differ in their response to cyclic nucleotide phosphodiesterase inhibitors. *J Immunol,* 182**,** 5400-11.
MEYERS, J. A., TAVERNA, J., CHAVES, J., MAKKINJE, A. & LERNER, A. 2007. Phosphodiesterase 4 inhibitors augment levels of glucocorticoid receptor in B cell chronic lymphocytic leukemia but not in normal circulating hematopoietic cells. *Clin Cancer Res,* 13**,** 4920-7.
MOCHIDA, H., TAKAGI, M., INOUE, H., NOTO, T., YANO, K., FUJISHIGE, K., SASAKI, T., YUASA, K., KOTERA, J., OMORI, K. & KIKKAWA, K. 2002. Enzymological and pharmacological profile of T-0156, a potent and selective phosphodiesterase type 5 inhibitor. *Eur J Pharmacol,* 456**,** 91-8.
MOCHLY-ROSEN, D., DAS, K. & GRIMES, K. V. 2012. Protein kinase C, an elusive therapeutic target? *Nat Rev Drug Discov,* 11**,** 937-57.
MOMOSE, I., OHBA, S., TATSUDA, D., KAWADA, M., MASUDA, T., TSUJIUCHI, G., YAMORI, T., ESUMI, H. & IKEDA, D. 2010. Mitochondrial inhibitors show preferential cytotoxicity to human pancreatic cancer PANC-1 cells under glucose-deprived conditions. *Biochem Biophys Res Commun,* 392**,** 460-6.
MONGILLO, M. & ZACCOLO, M. 2006. A complex phosphodiesterase system controls beta-adrenoceptor signalling in cardiomyocytes. *Biochem Soc Trans,* 34**,** 510-1.
MONTEITH, G. R., DAVIS, F. M. & ROBERTS-THOMSON, S. J. 2012. Calcium channels and pumps in cancer: changes and consequences. *J Biol Chem,* 287**,** 31666-73.
MOON, E., LEE, R., NEAR, R., WEINTRAUB, L., WOLDA, S. & LERNER, A. 2002. Inhibition of PDE3B augments PDE4 inhibitor-induced apoptosis in a subset of patients with chronic lymphocytic leukemia. *Clin Cancer Res,* 8**,** 589-95.
MOON, E. Y., LEE, G. H., LEE, M. S., KIM, H. M. & LEE, J. W. 2012. Phosphodiesterase inhibitors control A172 human glioblastoma cell death through cAMP-mediated activation of protein kinase A and Epac1/Rap1 pathways. *Life Sci,* 90**,** 373-80.
MOON, E. Y. & LERNER, A. 2003. PDE4 inhibitors activate a mitochondrial apoptotic pathway in chronic lymphocytic leukemia cells that is regulated by protein phosphatase 2A. *Blood,* 101**,** 4122-30.
MOORE, P. S., BEGHELLI, S., ZAMBONI, G. & SCARPA, A. 2003. Genetic abnormalities in pancreatic cancer. *Mol Cancer,* 2**,** 7.
MORITA, H., MURATA, T., SHIMIZU, K., OKUMURA, K., INUI, M. & TAGAWA, T. 2013. Characterization of phosphodiesterase 2A in human malignant melanoma PMP cells. *Oncol Rep,* 29**,** 1275-84.
MOTIANI, R. K., STOLWIJK, J. A., NEWTON, R. L., ZHANG, X. & TREBAK, M. 2013a. Emerging roles of Orai3 in pathophysiology. *Channels (Austin),* 7**,** 392-401.
MOTIANI, R. K., ZHANG, X., HARMON, K. E., KELLER, R. S., MATROUGUI, K., BENNETT, J. A. & TREBAK, M. 2013b. Orai3 is an estrogen receptor alpha-regulated Ca(2)(+) channel that promotes tumorigenesis. *FASEB J,* 27**,** 63-75.
MOU, T. C., MASADA, N., COOPER, D. M. & SPRANG, S. R. 2009. Structural basis for inhibition of mammalian adenylyl cyclase by calcium. *Biochemistry,* 48**,** 3387-97.
MOUSSAWI, K. & KALIVAS, P. W. 2010. Group II metabotropic glutamate receptors (mGlu2/3) in drug addiction. *Eur J Pharmacol,* 639**,** 115-22.

MUIK, M., FAHRNER, M., DERLER, I., SCHINDL, R., BERGSMANN, J., FRISCHAUF, I., GROSCHNER, K. & ROMANIN, C. 2009. A Cytosolic Homomerization and a Modulatory Domain within STIM1 C Terminus Determine Coupling to ORAI1 Channels. *J Biol Chem,* 284**,** 8421-6.

MUIK, M., FAHRNER, M., SCHINDL, R., STATHOPULOS, P., FRISCHAUF, I., DERLER, I., PLENK, P., LACKNER, B., GROSCHNER, K., IKURA, M. & ROMANIN, C. 2011. STIM1 couples to ORAI1 via an intramolecular transition into an extended conformation. *EMBO J,* 30**,** 1678-89.

MURATA, K., KAMEYAMA, M., FUKUI, F., OHIGASHI, H., HIRATSUKA, M., SASAKI, Y., KABUTO, T., MUKAI, M., MAMMOTO, T., AKEDO, H., ISHIKAWA, O. & IMAOKA, S. 1999. Phosphodiesterase type III inhibitor, cilostazol, inhibits colon cancer cell motility. *Clin Exp Metastasis,* 17**,** 525-30.

MURATA, T., SUGATANI, T., SHIMIZU, K., MANGANIELLO, V. C. & TAGAWA, T. 2001. Phosphodiesterase 3 as a potential target for therapy of malignant tumors in the submandibular gland. *Anticancer Drugs,* 12**,** 79-83.

MURATA, T., TAIRA, M. & MANGANIELLO, V. C. 1996. Differential expression of cGMP-inhibited cyclic nucleotide phosphodiesterases in human hepatoma cell lines. *FEBS Lett,* 390**,** 29-33.

MURPHY, J. A., CRIDDLE, D. N., SHERWOOD, M., CHVANOV, M., MUKHERJEE, R., MCLAUGHLIN, E., BOOTH, D., GERASIMENKO, J. V., RARATY, M. G., GHANEH, P., NEOPTOLEMOS, J. P., GERASIMENKO, O. V., TEPIKIN, A. V., GREEN, G. M., REEVE, J. R., JR., PETERSEN, O. H. & SUTTON, R. 2008. Direct activation of cytosolic Ca2+ signaling and enzyme secretion by cholecystokinin in human pancreatic acinar cells. *Gastroenterology,* 135**,** 632-41.

MURPHY, J. G., SANDERSON, J. L., GORSKI, J. A., SCOTT, J. D., CATTERALL, W. A., SATHER, W. A. & DELL'ACQUA, M. L. 2014. AKAP-anchored PKA maintains neuronal L-type calcium channel activity and NFAT transcriptional signaling. *Cell Rep,* 7**,** 1577-88.

NAGHDI, S., WALDECK-WEIERMAIR, M., FERTSCHAI, I., POTESER, M., GRAIER, W. F. & MALLI, R. 2010. Mitochondrial Ca2+ uptake and not mitochondrial motility is required for STIM1-Orai1-dependent store-operated Ca2+ entry. *J Cell Sci,* 123**,** 2553-64.

NAKAGAWA, A., SAMOLS, E. & STAGNER, J. I. 1993. Exocrine interstitial insulin and somatostatin in the perfused dog pancreas. *Am J Physiol,* 264**,** G728-34.

NARITA, M., MURATA, T., SHIMIZU, K., NAKAGAWA, T., SUGIYAMA, T., INUI, M., HIRAMOTO, K. & TAGAWA, T. 2007. A role for cyclic nucleotide phosphodiesterase 4 in regulation of the growth of human malignant melanoma cells. *Oncol Rep,* 17**,** 1133-9.

NARITA, M., MURATA, T., SHIMIZU, K., SUGIYAMA, T., NAKAGAWA, T., MANGANIELLO, V. C. & TAGAWA, T. 2003. Phosphodiesterase 4 in osteoblastic osteosarcoma cells as a potential target for growth inhibition. *Anticancer Drugs,* 14**,** 377-81.

NAVAS, C., HERNANDEZ-PORRAS, I., SCHUHMACHER, A. J., SIBILIA, M., GUERRA, C. & BARBACID, M. 2012. EGF receptor signaling is essential for k-ras oncogene-driven pancreatic ductal adenocarcinoma. *Cancer Cell,* 22**,** 318-30.

NEGISHI, M., SUGIMOTO, Y. & ICHIKAWA, A. 1995. Molecular mechanisms of diverse actions of prostanoid receptors. *Biochim Biophys Acta,* 1259**,** 109-19.

NESTEROVA, M., NOGUCHI, K., PARK, Y. G., LEE, Y. N. & CHO-CHUNG, Y. S. 2000. Compensatory stabilization of RIIbeta protein, cell cycle deregulation, and growth arrest in colon and prostate carcinoma cells by antisense-directed down-regulation of protein kinase A RIalpha protein. *Clin Cancer Res,* 6**,** 3434-41.

NETHERTON, S. J. & MAURICE, D. H. 2005. Vascular endothelial cell cyclic nucleotide phosphodiesterases and regulated cell migration: implications in angiogenesis. *Mol Pharmacol,* 67**,** 263-72.

NEVES, S. R., RAM, P. T. & IYENGAR, R. 2002. G protein pathways. *Science,* 296**,** 1636-9.

NI, Q., GANESAN, A., AYE-HAN, N. N., GAO, X., ALLEN, M. D., LEVCHENKO, A. & ZHANG, J. 2011. Signaling diversity of PKA achieved via a Ca2+-cAMP-PKA oscillatory circuit. *Nat Chem Biol,* 7**,** 34-40.

NICOLAS, F. J. & HILL, C. S. 2003. Attenuation of the TGF-beta-Smad signaling pathway in pancreatic tumor cells confers resistance to TGF-beta-induced growth arrest. *Oncogene,* 22**,** 3698-711.
NICOTERA, P., BELLOMO, G. & ORRENIUS, S. 1992. Calcium-mediated mechanisms in chemically induced cell death. *Annu Rev Pharmacol Toxicol,* 32**,** 449-70.
NIIMURA, M., MIKI, T., SHIBASAKI, T., FUJIMOTO, W., IWANAGA, T. & SEINO, S. 2009. Critical role of the N-terminal cyclic AMP-binding domain of Epac2 in its subcellular localization and function. *J Cell Physiol,* 219**,** 652-8.
NIINO, Y., HOTTA, K. & OKA, K. 2010. Blue fluorescent cGMP sensor for multiparameter fluorescence imaging. *PLoS One,* 5**,** e9164.
NISHI, A., KUROIWA, M., MILLER, D. B., O'CALLAGHAN, J. P., BATEUP, H. S., SHUTO, T., SOTOGAKU, N., FUKUDA, T., HEINTZ, N., GREENGARD, P. & SNYDER, G. L. 2008. Distinct roles of PDE4 and PDE10A in the regulation of cAMP/PKA signaling in the striatum. *J Neurosci,* 28**,** 10460-71.
NIU, W., LIU, X., ZHANG, Z., XU, K., CHEN, R., LIU, E., WANG, J., PENG, C. & NIU, J. 2010. Effects of alphavbeta6 gene silencing by RNA interference in PANC-1 pancreatic carcinoma cells. *Anticancer Res,* 30**,** 135-42.
NOLAN, M. F., MALLERET, G., DUDMAN, J. T., BUHL, D. L., SANTORO, B., GIBBS, E., VRONSKAYA, S., BUZSAKI, G., SIEGELBAUM, S. A., KANDEL, E. R. & MOROZOV, A. 2004. A behavioral role for dendritic integration: HCN1 channels constrain spatial memory and plasticity at inputs to distal dendrites of CA1 pyramidal neurons. *Cell,* 119**,** 719-32.
NOLAN, M. F., MALLERET, G., LEE, K. H., GIBBS, E., DUDMAN, J. T., SANTORO, B., YIN, D., THOMPSON, R. F., SIEGELBAUM, S. A., KANDEL, E. R. & MOROZOV, A. 2003. The hyperpolarization-activated HCN1 channel is important for motor learning and neuronal integration by cerebellar Purkinje cells. *Cell,* 115**,** 551-64.
NURNBERG, A., KITZING, T. & GROSSE, R. 2011. Nucleating actin for invasion. *Nat Rev Cancer,* 11**,** 177-87.
O'CONNOR, K. L., CHEN, M. & TOWERS, L. N. 2012. Integrin alpha6beta4 cooperates with LPA signaling to stimulate Rac through AKAP-Lbc-mediated RhoA activation. *Am J Physiol Cell Physiol,* 302**,** C605-14.
O'CONNOR, K. L. & MERCURIO, A. M. 2001. Protein kinase A regulates Rac and is required for the growth factor-stimulated migration of carcinoma cells. *J Biol Chem,* 276**,** 47895-900.
O'CONNOR, K. L., SHAW, L. M. & MERCURIO, A. M. 1998. Release of cAMP gating by the alpha6beta4 integrin stimulates lamellae formation and the chemotactic migration of invasive carcinoma cells. *J Cell Biol,* 143**,** 1749-60.
OESTREICH, E. A., MALIK, S., GOONASEKERA, S. A., BLAXALL, B. C., KELLEY, G. G., DIRKSEN, R. T. & SMRCKA, A. V. 2009. Epac and phospholipase Cepsilon regulate Ca2+ release in the heart by activation of protein kinase Cepsilon and calcium-calmodulin kinase II. *J Biol Chem,* 284**,** 1514-22.
OFFERMANNS, S., MANCINO, V., REVEL, J. P. & SIMON, M. I. 1997. Vascular system defects and impaired cell chemokinesis as a result of Galpha13 deficiency. *Science,* 275**,** 533-6.
OHGA, K., TAKEZAWA, R., ARAKIDA, Y., SHIMIZU, Y. & ISHIKAWA, J. 2008. Characterization of YM-58483/BTP2, a novel store-operated Ca2+ entry blocker, on T cell-mediated immune responses in vivo. *Int Immunopharmacol,* 8**,** 1787-92.
OKUMURA, S., KAWABE, J., YATANI, A., TAKAGI, G., LEE, M. C., HONG, C., LIU, J., TAKAGI, I., SADOSHIMA, J., VATNER, D. E., VATNER, S. F. & ISHIKAWA, Y. 2003. Type 5 adenylyl cyclase disruption alters not only sympathetic but also parasympathetic and calcium-mediated cardiac regulation. *Circ Res,* 93**,** 364-71.
OMI, H., OKAYAMA, N., SHIMIZU, M., FUKUTOMI, T., NAKAMURA, A., IMAEDA, K., OKOUCHI, M. & ITOH, M. 2004. Cilostazol inhibits high glucose-mediated endothelial-neutrophil adhesion by decreasing adhesion molecule expression via NO production. *Microvasc Res,* 68**,** 119-25.

ONG, H. L., JANG, S. I. & AMBUDKAR, I. S. 2012. Distinct contributions of Orai1 and TRPC1 to agonist-induced [Ca(2+)](i) signals determine specificity of Ca(2+)-dependent gene expression. *PLoS One,* 7**,** e47146.

OZAKI, N., SHIBASAKI, T., KASHIMA, Y., MIKI, T., TAKAHASHI, K., UENO, H., SUNAGA, Y., YANO, H., MATSUURA, Y., IWANAGA, T., TAKAI, Y. & SEINO, S. 2000. cAMP-GEFII is a direct target of cAMP in regulated exocytosis. *Nat Cell Biol,* 2**,** 805-11.

PALMER, D., TSOI, K. & MAURICE, D. H. 1998. Synergistic inhibition of vascular smooth muscle cell migration by phosphodiesterase 3 and phosphodiesterase 4 inhibitors. *Circ Res,* 82**,** 852-61.

PANNEKOEK, W. J., KOOISTRA, M. R., ZWARTKRUIS, F. J. & BOS, J. L. 2009. Cell-cell junction formation: the role of Rap1 and Rap1 guanine nucleotide exchange factors. *Biochim Biophys Acta,* 1788**,** 790-6.

PAREKH, A. B. 2011. Decoding cytosolic Ca2+ oscillations. *Trends Biochem Sci,* 36**,** 78-87.

PARK, C. Y., HOOVER, P. J., MULLINS, F. M., BACHHAWAT, P., COVINGTON, E. D., RAUNSER, S., WALZ, T., GARCIA, K. C., DOLMETSCH, R. E. & LEWIS, R. S. 2009. STIM1 clusters and activates CRAC channels via direct binding of a cytosolic domain to Orai1. *Cell,* 136**,** 876-90.

PARSONS, J. T., HORWITZ, A. R. & SCHWARTZ, M. A. 2010. Cell adhesion: integrating cytoskeletal dynamics and cellular tension. *Nat Rev Mol Cell Biol,* 11**,** 633-43.

PARVEZ, S., BECK, A., PEINELT, C., SOBOLOFF, J., LIS, A., MONTEILH-ZOLLER, M., GILL, D. L., FLEIG, A. & PENNER, R. 2008. STIM2 protein mediates distinct store-dependent and store-independent modes of CRAC channel activation. *FASEB J,* 22**,** 752-61.

PATRUCCO, E., NOTTE, A., BARBERIS, L., SELVETELLA, G., MAFFEI, A., BRANCACCIO, M., MARENGO, S., RUSSO, G., AZZOLINO, O., RYBALKIN, S. D., SILENGO, L., ALTRUDA, F., WETZKER, R., WYMANN, M. P., LEMBO, G. & HIRSCH, E. 2004. PI3Kgamma modulates the cardiac response to chronic pressure overload by distinct kinase-dependent and -independent effects. *Cell,* 118**,** 375-87.

PAULUCCI-HOLTHAUZEN, A. A., VERGARA, L. A., BELLOT, L. J., CANTON, D., SCOTT, J. D. & O'CONNOR, K. L. 2009. Spatial distribution of protein kinase A activity during cell migration is mediated by A-kinase anchoring protein AKAP Lbc. *J Biol Chem,* 284**,** 5956-67.

PEKKINEN, M., AHLSTROM, M. E., RIEHLE, U., HUTTUNEN, M. M. & LAMBERG-ALLARDT, C. J. 2008. Effects of phosphodiesterase 7 inhibition by RNA interference on the gene expression and differentiation of human mesenchymal stem cell-derived osteoblasts. *Bone,* 43**,** 84-91.

PEPPIATT, C. M., COLLINS, T. J., MACKENZIE, L., CONWAY, S. J., HOLMES, A. B., BOOTMAN, M. D., BERRIDGE, M. J., SEO, J. T. & RODERICK, H. L. 2003. 2-Aminoethoxydiphenyl borate (2-APB) antagonises inositol 1,4,5-trisphosphate-induced calcium release, inhibits calcium pumps and has a use-dependent and slowly reversible action on store-operated calcium entry channels. *Cell Calcium,* 34**,** 97-108.

PERINO, A., GHIGO, A., FERRERO, E., MORELLO, F., SANTULLI, G., BAILLIE, G. S., DAMILANO, F., DUNLOP, A. J., PAWSON, C., WALSER, R., LEVI, R., ALTRUDA, F., SILENGO, L., LANGEBERG, L. K., NEUBAUER, G., HEYMANS, S., LEMBO, G., WYMANN, M. P., WETZKER, R., HOUSLAY, M. D., IACCARINO, G., SCOTT, J. D. & HIRSCH, E. 2011. Integrating cardiac PIP3 and cAMP signaling through a PKA anchoring function of p110gamma. *Mol Cell,* 42**,** 84-95.

PETERSEN, O. H. & UEDA, N. 1976. Pancreatic acinar cells: the role of calcium in stimulus-secretion coupling. *J Physiol,* 254**,** 583-606.

PETRIE, R. J., DOYLE, A. D. & YAMADA, K. M. 2009. Random versus directionally persistent cell migration. *Nat Rev Mol Cell Biol,* 10**,** 538-49.

PICCART, E., GANTOIS, I., LAEREMANS, A., DE HOOGT, R., MEERT, T., VANHOOF, G., ARCKENS, L. & D'HOOGE, R. 2011. Impaired appetitively as well as aversively motivated behaviors and learning in PDE10A-deficient mice suggest a role for striatal signaling in evaluative salience attribution. *Neurobiol Learn Mem,* 95**,** 260-9.

PIDOUX, G. & TASKEN, K. 2010. Specificity and spatial dynamics of protein kinase A signaling organized by A-kinase-anchoring proteins. *J Mol Endocrinol,* 44**,** 271-84.

PODDA, M. V. & GRASSI, C. 2014. New perspectives in cyclic nucleotide-mediated functions in the CNS: the emerging role of cyclic nucleotide-gated (CNG) channels. *Pflugers Arch,* 466**,** 1241-57.

PODZUWEIT, T., NENNSTIEL, P. & MULLER, A. 1995. Isozyme selective inhibition of cGMP-stimulated cyclic nucleotide phosphodiesterases by erythro-9-(2-hydroxy-3-nonyl) adenine. *Cell Signal,* 7**,** 733-8.

PONSIOEN, B., GLOERICH, M., RITSMA, L., REHMANN, H., BOS, J. L. & JALINK, K. 2009. Direct spatial control of Epac1 by cyclic AMP. *Mol Cell Biol,* 29**,** 2521-31.

POSTEA, O. & BIEL, M. 2011. Exploring HCN channels as novel drug targets. *Nat Rev Drug Discov,* 10**,** 903-14.

POZZAN, T., RIZZUTO, R., VOLPE, P. & MELDOLESI, J. 1994. Molecular and cellular physiology of intracellular calcium stores. *Physiol Rev,* 74**,** 595-636.

PULLAMSETTI, S. S., BANAT, G. A., SCHMALL, A., SZIBOR, M., POMAGRUK, D., HANZE, J., KOLOSIONEK, E., WILHELM, J., BRAUN, T., GRIMMINGER, F., SEEGER, W., SCHERMULY, R. T. & SAVAI, R. 2013. Phosphodiesterase-4 promotes proliferation and angiogenesis of lung cancer by crosstalk with HIF. *Oncogene,* 32**,** 1121-34.

PYLAYEVA-GUPTA, Y., LEE, K. E., HAJDU, C. H., MILLER, G. & BAR-SAGI, D. 2012. Oncogenic Kras-induced GM-CSF production promotes the development of pancreatic neoplasia. *Cancer Cell,* 21**,** 836-47.

RAAIJMAKERS, J. H. & BOS, J. L. 2009. Specificity in Ras and Rap signaling. *J Biol Chem,* 284**,** 10995-9.

RAHRMANN, E. P., COLLIER, L. S., KNUTSON, T. P., DOYAL, M. E., KUSLAK, S. L., GREEN, L. E., MALINOWSKI, R. L., ROETHE, L., AKAGI, K., WAKNITZ, M., HUANG, W., LARGAESPADA, D. A. & MARKER, P. C. 2009. Identification of PDE4D as a proliferation promoting factor in prostate cancer using a Sleeping Beauty transposon-based somatic mutagenesis screen. *Cancer Res,* 69**,** 4388-97.

RAMSEY, I. S., DELLING, M. & CLAPHAM, D. E. 2006. An introduction to TRP channels. *Annu Rev Physiol,* 68**,** 619-47.

RASHEVA, V. I. & DOMINGOS, P. M. 2009. Cellular responses to endoplasmic reticulum stress and apoptosis. *Apoptosis,* 14**,** 996-1007.

REHMANN, H. 2013. Epac-inhibitors: facts and artefacts. *Sci Rep,* 3**,** 3032.

REHMANN, H., DAS, J., KNIPSCHEER, P., WITTINGHOFER, A. & BOS, J. L. 2006. Structure of the cyclic-AMP-responsive exchange factor Epac2 in its auto-inhibited state. *Nature,* 439**,** 625-8.

REHMANN, H., WITTINGHOFER, A. & BOS, J. L. 2007. Capturing cyclic nucleotides in action: snapshots from crystallographic studies. *Nat Rev Mol Cell Biol,* 8**,** 63-73.

RHIM, A. D., MIREK, E. T., AIELLO, N. M., MAITRA, A., BAILEY, J. M., MCALLISTER, F., REICHERT, M., BEATTY, G. L., RUSTGI, A. K., VONDERHEIDE, R. H., LEACH, S. D. & STANGER, B. Z. 2012. EMT and dissemination precede pancreatic tumor formation. *Cell,* 148**,** 349-61.

RICCARDI, D. & KEMP, P. J. 2012. The calcium-sensing receptor beyond extracellular calcium homeostasis: conception, development, adult physiology, and disease. *Annu Rev Physiol,* 74**,** 271-97.

RICHTER, W., DAY, P., AGRAWAL, R., BRUSS, M. D., GRANIER, S., WANG, Y. L., RASMUSSEN, S. G., HORNER, K., WANG, P., LEI, T., PATTERSON, A. J., KOBILKA, B. & CONTI, M. 2008. Signaling from beta1- and beta2-adrenergic receptors is defined by differential interactions with PDE4. *EMBO J,* 27**,** 384-93.

RIDLEY, A. J. 2013. RhoA, RhoB and RhoC have different roles in cancer cell migration. *J Microsc,* 251**,** 242-9.

RIENTO, K. & RIDLEY, A. J. 2003. Rocks: multifunctional kinases in cell behaviour. *Nat Rev Mol Cell Biol,* 4**,** 446-56.

RISSEL, C. E., RICHTERS, J., GRULICH, A. E., DE VISSER, R. O. & SMITH, A. M. 2003. Sex in Australia: first experiences of vaginal intercourse and oral sex among a representative sample of adults. *Aust N Z J Public Health,* 27**,** 131-7.

ROTHBERG, B. S., WANG, Y. & GILL, D. L. 2013. Orai channel pore properties and gating by STIM: implications from the Orai crystal structure. *Sci Signal,* 6**,** pe9.

ROUBILLE, F. & TARDIF, J. C. 2013. New therapeutic targets in cardiology: heart failure and arrhythmia: HCN channels. *Circulation,* 127**,** 1986-96.

ROZE, C., DE LA TOUR, J., CHARIOT, J., SOUCHARD, M., VAILLE, C., DUPONT, C., JEAN, E. & WEPIERRE, J. 1976. Isoproterenol induced pancreatic secretion in rats. A comparison with secretin. *Biomedicine,* 24**,** 410-7.

RUELLAN, C., SCEMAMA, J. L., CLERC, P., FAGOT-REVURAT, P., CLEMENTE, F. & RIBET, A. 1986. VIP regulation of a human pancreatic cancer cell line: Capan-1. *Peptides,* 7 Suppl 1**,** 267-71.

RYBALKIN, S. D., RYBALKINA, I., BEAVO, J. A. & BORNFELDT, K. E. 2002. Cyclic nucleotide phosphodiesterase 1C promotes human arterial smooth muscle cell proliferation. *Circ Res,* 90**,** 151-7.

SABBATINI, M. E., D'ALECY, L., LENTZ, S. I., TANG, T. & WILLIAMS, J. A. 2013. Adenylyl cyclase 6 mediates the action of cyclic AMP-dependent secretagogues in mouse pancreatic exocrine cells via protein kinase A pathway activation. *J Physiol,* 591**,** 3693-707.

SAITO, M., YAGUCHI, T., YASUDA, Y., NAKANO, T. & NISHIZAKI, T. 2010. Adenosine suppresses CW2 human colonic cancer growth by inducing apoptosis via A(1) adenosine receptors. *Cancer Lett,* 290**,** 211-5.

SAKURAI-YAGETA, M., RECCHI, C., LE DEZ, G., SIBARITA, J. B., DAVIET, L., CAMONIS, J., D'SOUZA-SCHOREY, C. & CHAVRIER, P. 2008. The interaction of IQGAP1 with the exocyst complex is required for tumor cell invasion downstream of Cdc42 and RhoA. *J Cell Biol,* 181**,** 985-98.

SALDANA, C., DIAZ-MUNOZ, M., ANTARAMIAN, A., GONZALEZ-GALLARDO, A., GARCIA-SOLIS, P. & MORALES-TLALPAN, V. 2009. MCF-7 breast carcinoma cells express ryanodine receptor type 1: functional characterization and subcellular localization. *Mol Cell Biochem,* 323**,** 39-47.

SALIDO, G. M., SAGE, S. O. & ROSADO, J. A. 2009. TRPC channels and store-operated Ca(2+) entry. *Biochim Biophys Acta,* 1793**,** 223-30.

SAMTLEBEN, S., JAEPEL, J., FECHER, C., ANDRESKA, T., REHBERG, M. & BLUM, R. 2013. Direct imaging of ER calcium with targeted-esterase induced dye loading (TED). *J Vis Exp***,** e50317.

SANTAMARIA, L. F., TORRES, R., GIMENEZ-ARNAU, A. M., GIMENEZ-CAMARASA, J. M., RYDER, H., PALACIOS, J. M. & BELETA, J. 1999. Rolipram inhibits staphylococcal enterotoxin B-mediated induction of the human skin-homing receptor on T lymphocytes. *J Invest Dermatol,* 113**,** 82-6.

SANTANA, L. F., CHASE, E. G., VOTAW, V. S., NELSON, M. T. & GREVEN, R. 2002. Functional coupling of calcineurin and protein kinase A in mouse ventricular myocytes. *J Physiol,* 544**,** 57-69.

SANTORO, B. & BARAM, T. Z. 2003. The multiple personalities of h-channels. *Trends Neurosci,* 26**,** 550-4.

SANTOS-SILVA, A. J., CAIRRAO, E., MORGADO, M., ALVAREZ, E. & VERDE, I. 2008. PDE4 and PDE5 regulate cyclic nucleotides relaxing effects in human umbilical arteries. *Eur J Pharmacol,* 582**,** 102-9.

SANTOS, A. I., CARREIRA, B. P., NOBRE, R. J., CARVALHO, C. M. & ARAUJO, I. M. 2014. Stimulation of neural stem cell proliferation by inhibition of phosphodiesterase 5. *Stem Cells Int,* 2014**,** 878397.

SANZ-MORENO, V., GADEA, G., AHN, J., PATERSON, H., MARRA, P., PINNER, S., SAHAI, E. & MARSHALL, C. J. 2008. Rac activation and inactivation control plasticity of tumor cell movement. *Cell,* 135**,** 510-23.

SAVAI, R., PULLAMSETTI, S. S., BANAT, G. A., WEISSMANN, N., GHOFRANI, H. A., GRIMMINGER, F. & SCHERMULY, R. T. 2010. Targeting cancer with phosphodiesterase inhibitors. *Expert Opin Investig Drugs,* 19**,** 117-31.

SAVDIE, C., FERGUSON, S. S., VINCENT, J., BEAUDET, A. & STROH, T. 2006. Cell-type-specific pathways of neurotensin endocytosis. *Cell Tissue Res,* 324**,** 69-85.

SAYED, K. A., KHANFAR, M. A., SHALLAL, H. M., MURALIDHARAN, A., AWATE, B., YOUSSEF, D. T., LIU, Y., ZHOU, Y. D., NAGLE, D. G. & SHAH, G. 2008. Latrunculin A and its C-17-O-carbamates inhibit prostate tumor cell invasion and HIF-1 activation in breast tumor cells. *J Nat Prod,* 71**,** 396-402.

SCHAEFER, M. L., WONG, S. T., WOZNIAK, D. F., MUGLIA, L. M., LIAUW, J. A., ZHUO, M., NARDI, A., HARTMAN, R. E., VOGT, S. K., LUEDKE, C. E., STORM, D. R. & MUGLIA, L. J. 2000. Altered stress-induced anxiety in adenylyl cyclase type VIII-deficient mice. *J Neurosci,* 20**,** 4809-20.

SCHAFFER, L., BRAND, C. L., HANSEN, B. F., RIBEL, U., SHAW, A. C., SLAABY, R. & STURIS, J. 2008. A novel high-affinity peptide antagonist to the insulin receptor. *Biochem Biophys Res Commun,* 376**,** 380-3.

SCHINDL, R., BERGSMANN, J., FRISCHAUF, I., DERLER, I., FAHRNER, M., MUIK, M., FRITSCH, R., GROSCHNER, K. & ROMANIN, C. 2008. 2-aminoethoxydiphenyl borate alters selectivity of Orai3 channels by increasing their pore size. *J Biol Chem,* 283**,** 20261-7.

SCHLEIFER, H., DOLESCHAL, B., LICHTENEGGER, M., OPPENRIEDER, R., DERLER, I., FRISCHAUF, I., GLASNOV, T. N., KAPPE, C. O., ROMANIN, C. & GROSCHNER, K. 2012. Novel pyrazole compounds for pharmacological discrimination between receptor-operated and store-operated Ca(2+) entry pathways. *Br J Pharmacol,* 167**,** 1712-22.

SCHMID, R. M. 2002. Acinar-to-ductal metaplasia in pancreatic cancer development. *J Clin Invest,* 109**,** 1403-4.

SCHMIDT, A. L., DE FARIAS, C. B., ABUJAMRA, A. L., KAPCZINSKI, F., SCHWARTSMANN, G., BRUNETTO, A. L. & ROESLER, R. 2010. BDNF and PDE4, but not the GRPR, regulate viability of human medulloblastoma cells. *J Mol Neurosci,* 40**,** 303-10.

SCHMIDT, M., DEKKER, F. J. & MAARSINGH, H. 2013. Exchange protein directly activated by cAMP (epac): a multidomain cAMP mediator in the regulation of diverse biological functions. *Pharmacol Rev,* 65**,** 670-709.

SCHNEIDER, C. A., RASBAND, W. S. & ELICEIRI, K. W. 2012. NIH Image to ImageJ: 25 years of image analysis. *Nat Methods,* 9**,** 671-5.

SCHROR, K. 2002. The pharmacology of cilostazol. *Diabetes Obes Metab,* 4 Suppl 2**,** S14-9.

SCHULLER, H. M. & AL-WADEI, H. A. 2010. Neurotransmitter receptors as central regulators of pancreatic cancer. *Future Oncol,* 6**,** 221-8.

SCHUNKE, S. & STOLDT, M. 2013. Structural snapshot of cyclic nucleotide binding domains from cyclic nucleotide-sensitive ion channels. *Biol Chem,* 394**,** 1439-51.

SCHWETZ, T. A., USTIONE, A. & PISTON, D. W. 2013. Neuropeptide Y and somatostatin inhibit insulin secretion through different mechanisms. *Am J Physiol Endocrinol Metab,* 304**,** E211-21.

SCOTT, J. D., GLACCUM, M. B., ZOLLER, M. J., UHLER, M. D., HELFMAN, D. M., MCKNIGHT, G. S. & KREBS, E. G. 1987. The molecular cloning of a type II regulatory subunit of the cAMP-dependent protein kinase from rat skeletal muscle and mouse brain. *Proc Natl Acad Sci U S A,* 84**,** 5192-6.

SENGUPTA, R., SUN, T., WARRINGTON, N. M. & RUBIN, J. B. 2011. Treating brain tumors with PDE4 inhibitors. *Trends Pharmacol Sci,* 32**,** 337-44.

SETTE, C. & CONTI, M. 1996. Phosphorylation and activation of a cAMP-specific phosphodiesterase by the cAMP-dependent protein kinase. Involvement of serine 54 in the enzyme activation. *J Biol Chem,* 271**,** 16526-34.

SHABB, J. B. 2001. Physiological substrates of cAMP-dependent protein kinase. *Chem Rev,* 101**,** 2381-411.

SHAKUR, Y., HOLST, L. S., LANDSTROM, T. R., MOVSESIAN, M., DEGERMAN, E. & MANGANIELLO, V. 2001. Regulation and function of the cyclic nucleotide phosphodiesterase (PDE3) gene family. *Prog Nucleic Acid Res Mol Biol,* 66**,** 241-77.

SHEN, B., DELANEY, M. K. & DU, X. 2012. Inside-out, outside-in, and inside-outside-in: G protein signaling in integrin-mediated cell adhesion, spreading, and retraction. *Curr Opin Cell Biol,* 24**,** 600-6.

SHEN, J. X. & COOPER, D. M. 2013. AKAP79, PKC, PKA and PDE4 participate in a Gq-linked muscarinic receptor and adenylate cyclase 2 cAMP signalling complex. *Biochem J,* 455**,** 47-56.
SHEN, W. W., FRIEDEN, M. & DEMAUREX, N. 2011. Local cytosolic Ca2+ elevations are required for stromal interaction molecule 1 (STIM1) de-oligomerization and termination of store-operated Ca2+ entry. *J Biol Chem,* 286**,** 36448-59.
SHI, G., DIRENZO, D., QU, C., BARNEY, D., MILEY, D. & KONIECZNY, S. F. 2013. Maintenance of acinar cell organization is critical to preventing Kras-induced acinar-ductal metaplasia. *Oncogene,* 32**,** 1950-8.
SHIMIZU-ALBERGINE, M., TSAI, L. C., PATRUCCO, E. & BEAVO, J. A. 2012. cAMP-specific phosphodiesterases 8A and 8B, essential regulators of Leydig cell steroidogenesis. *Mol Pharmacol,* 81**,** 556-66.
SHIMIZU, K., MURATA, T., OKUMURA, K., MANGANIELLO, V. C. & TAGAWA, T. 2002. Expression and role of phosphodiesterase 3 in human squamous cell carcinoma KB cells. *Anticancer Drugs,* 13**,** 875-80.
SHUTTLEWORTH, T. J. 2012a. Orai3--the 'exceptional' Orai? *J Physiol,* 590**,** 241-57.
SHUTTLEWORTH, T. J. 2012b. Orai channels - new insights, new ideas. *J Physiol,* 590**,** 4155-6.
SIUCIAK, J. A., CHAPIN, D. S., HARMS, J. F., LEBEL, L. A., MCCARTHY, S. A., CHAMBERS, L., SHRIKHANDE, A., WONG, S., MENNITI, F. S. & SCHMIDT, C. J. 2006. Inhibition of the striatum-enriched phosphodiesterase PDE10A: a novel approach to the treatment of psychosis. *Neuropharmacology,* 51**,** 386-96.
SIUCIAK, J. A., MCCARTHY, S. A., CHAPIN, D. S., REED, T. M., VORHEES, C. V. & REPASKE, D. R. 2007. Behavioral and neurochemical characterization of mice deficient in the phosphodiesterase-1B (PDE1B) enzyme. *Neuropharmacology,* 53**,** 113-24.
SKALHEGG, B. S. & TASKEN, K. 2000. Specificity in the cAMP/PKA signaling pathway. Differential expression,regulation, and subcellular localization of subunits of PKA. *Front Biosci,* 5**,** D678-93.
SMITH, F. D., LANGEBERG, L. K., CELLURALE, C., PAWSON, T., MORRISON, D. K., DAVIS, R. J. & SCOTT, J. D. 2010. AKAP-Lbc enhances cyclic AMP control of the ERK1/2 cascade. *Nat Cell Biol,* 12**,** 1242-9.
SMITH, J. P., SHIH, A., WU, Y., MCLAUGHLIN, P. J. & ZAGON, I. S. 1996. Gastrin regulates growth of human pancreatic cancer in a tonic and autocrine fashion. *Am J Physiol,* 270**,** R1078-84.
SMITH, P. G., WANG, F., WILKINSON, K. N., SAVAGE, K. J., KLEIN, U., NEUBERG, D. S., BOLLAG, G., SHIPP, M. A. & AGUIAR, R. C. 2005. The phosphodiesterase PDE4B limits cAMP-associated PI3K/AKT-dependent apoptosis in diffuse large B-cell lymphoma. *Blood,* 105**,** 308-16.
SMITH, S. J., CIESLINSKI, L. B., NEWTON, R., DONNELLY, L. E., FENWICK, P. S., NICHOLSON, A. G., BARNES, P. J., BARNETTE, M. S. & GIEMBYCZ, M. A. 2004. Discovery of BRL 50481 [3-(N,N-dimethylsulfonamido)-4-methyl-nitrobenzene], a selective inhibitor of phosphodiesterase 7: in vitro studies in human monocytes, lung macrophages, and CD8+ T-lymphocytes. *Mol Pharmacol,* 66**,** 1679-89.
SMYTH, E. M., AUSTIN, S. C., REILLY, M. P. & FITZGERALD, G. A. 2000. Internalization and sequestration of the human prostacyclin receptor. *J Biol Chem,* 275**,** 32037-45.
SOBOLOFF, J., MADESH, M. & GILL, D. L. 2011. Sensing cellular stress through STIM proteins. *Nat Chem Biol,* 7**,** 488-92.
SOBOLOFF, J., ROTHBERG, B. S., MADESH, M. & GILL, D. L. 2012. STIM proteins: dynamic calcium signal transducers. *Nat Rev Mol Cell Biol,* 13**,** 549-65.
SONG, M., CHEN, D. & YU, S. P. 2014. The TRPC channel blocker SKF 96365 inhibits glioblastoma cell growth by enhancing reverse mode of the Na(+) /Ca(2+) exchanger and increasing intracellular Ca(2+). *Br J Pharmacol,* 171**,** 3432-47.
SONI, S., SCHOLTEN, A., VOS, M. A. & VAN VEEN, T. A. 2014. Anchored protein kinase A signalling in cardiac cellular electrophysiology. *J Cell Mol Med*.

SOUZA, M. A., MAGNI, D. V., GUERRA, G. P., OLIVEIRA, M. S., FURIAN, A. F., PEREIRA, L., MARQUEZ, S. V., FERREIRA, J., FIGHERA, M. R. & ROYES, L. F. 2012. Involvement of hippocampal CAMKII/CREB signaling in the spatial memory retention induced by creatine. *Amino Acids,* 43**,** 2491-503.

SPRANG, S. R. 1997. G protein mechanisms: insights from structural analysis. *Annu Rev Biochem,* 66**,** 639-78.

SPRENGER, J. U. & NIKOLAEV, V. O. 2013. Biophysical Techniques for Detection of cAMP and cGMP in Living Cells. *Int J Mol Sci,* 14**,** 8025-46.

STANGHERLIN, A. & ZACCOLO, M. 2012. Phosphodiesterases and subcellular compartmentalized cAMP signaling in the cardiovascular system. *Am J Physiol Heart Circ Physiol,* 302**,** H379-90.

STANISLAUS, D., PONDER, S., JI, T. H. & CONN, P. M. 1998. Gonadotropin-releasing hormone receptor couples to multiple G proteins in rat gonadotrophs and in GGH3 cells: evidence from palmitoylation and overexpression of G proteins. *Biol Reprod,* 59**,** 579-86.

STEEGBORN, C. 2014. Structure, mechanism, and regulation of soluble adenylyl cyclases - similarities and differences to transmembrane adenylyl cyclases. *Biochim Biophys Acta*.

STOCK, A. M., HAHN, S. A., TROOST, G., NIGGEMANN, B., ZANKER, K. S. & ENTSCHLADEN, F. 2014. Induction of pancreatic cancer cell migration by an autocrine epidermal growth factor receptor activation. *Exp Cell Res,* 326**,** 307-14.

STOCK, A. M., POWE, D. G., HAHN, S. A., TROOST, G., NIGGEMANN, B., ZANKER, K. S. & ENTSCHLADEN, F. 2013. Norepinephrine inhibits the migratory activity of pancreatic cancer cells. *Exp Cell Res,* 319**,** 1744-58.

STRYER, L. 1983. Transducin and the cyclic GMP phosphodiesterase: amplifier proteins in vision. *Cold Spring Harb Symp Quant Biol,* 48 Pt 2**,** 841-52.

SUN, H. Q., YAMAMOTO, M., MEJILLANO, M. & YIN, H. L. 1999. Gelsolin, a multifunctional actin regulatory protein. *J Biol Chem,* 274**,** 33179-82.

SUZUKI, N., HAJICEK, N. & KOZASA, T. 2009. Regulation and physiological functions of G12/13-mediated signaling pathways. *Neurosignals,* 17**,** 55-70.

SWEENEY, E. A., SAKAKURA, C., SHIRAHAMA, T., MASAMUNE, A., OHTA, H., HAKOMORI, S. & IGARASHI, Y. 1996. Sphingosine and its methylated derivative N,N-dimethylsphingosine (DMS) induce apoptosis in a variety of human cancer cell lines. *Int J Cancer,* 66**,** 358-66.

TAGLIERI, D. M., JOHNSON, K. R., BURMEISTER, B. T., MONASKY, M. M., SPINDLER, M. J., DESANTIAGO, J., BANACH, K., CONKLIN, B. R. & CARNEGIE, G. K. 2014. The C-terminus of the long AKAP13 isoform (AKAP-Lbc) is critical for development of compensatory cardiac hypertrophy. *J Mol Cell Cardiol,* 66**,** 27-40.

TAKEHARA, A., HOSOKAWA, M., EGUCHI, H., OHIGASHI, H., ISHIKAWA, O., NAKAMURA, Y. & NAKAGAWA, H. 2007. Gamma-aminobutyric acid (GABA) stimulates pancreatic cancer growth through overexpressing GABAA receptor pi subunit. *Cancer Res,* 67**,** 9704-12.

TANG, J., LI, Z., LU, L. & CHO, C. H. 2013. beta-Adrenergic system, a backstage manipulator regulating tumour progression and drug target in cancer therapy. *Semin Cancer Biol,* 23**,** 533-42.

TANG, T., GAO, M. H., LAI, N. C., FIRTH, A. L., TAKAHASHI, T., GUO, T., YUAN, J. X., ROTH, D. M. & HAMMOND, H. K. 2008. Adenylyl cyclase type 6 deletion decreases left ventricular function via impaired calcium handling. *Circulation,* 117**,** 61-9.

TANG, W. J. & HURLEY, J. H. 1998. Catalytic mechanism and regulation of mammalian adenylyl cyclases. *Mol Pharmacol,* 54**,** 231-40.

TASKEN, K. & AANDAHL, E. M. 2004. Localized effects of cAMP mediated by distinct routes of protein kinase A. *Physiol Rev,* 84**,** 137-67.

TAYLOR, C. W. & TOVEY, S. C. 2010. IP(3) receptors: toward understanding their activation. *Cold Spring Harb Perspect Biol,* 2**,** a004010.

TAYLOR, S. S., ILOUZ, R., ZHANG, P. & KORNEV, A. P. 2012. Assembly of allosteric macromolecular switches: lessons from PKA. *Nat Rev Mol Cell Biol,* 13**,** 646-58.

TAYLOR, S. S., KIM, C., CHENG, C. Y., BROWN, S. H., WU, J. & KANNAN, N. 2008. Signaling through cAMP and cAMP-dependent protein kinase: diverse strategies for drug design. *Biochim Biophys Acta,* 1784**,** 16-26.

TAYLOR, S. S., KIM, C., VIGIL, D., HASTE, N. M., YANG, J., WU, J. & ANAND, G. S. 2005. Dynamics of signaling by PKA. *Biochim Biophys Acta,* 1754**,** 25-37.

TAYLOR, S. S., YANG, J., WU, J., HASTE, N. M., RADZIO-ANDZELM, E. & ANAND, G. 2004. PKA: a portrait of protein kinase dynamics. *Biochim Biophys Acta,* 1697**,** 259-69.

TAYLOR, S. S., ZHANG, P., STEICHEN, J. M., KESHWANI, M. M. & KORNEV, A. P. 2013. PKA: lessons learned after twenty years. *Biochim Biophys Acta,* 1834**,** 1271-8.

TEIXEIRA, M. M., GRISTWOOD, R. W., COOPER, N. & HELLEWELL, P. G. 1997. Phosphodiesterase (PDE)4 inhibitors: anti-inflammatory drugs of the future? *Trends Pharmacol Sci,* 18**,** 164-71.

TESMER, J. J. & SPRANG, S. R. 1998. The structure, catalytic mechanism and regulation of adenylyl cyclase. *Curr Opin Struct Biol,* 8**,** 713-9.

THOMMESEN, L., HOFSLI, E., PAULSSEN, R. H., ANTHONSEN, M. W. & LAEGREID, A. 2001. Molecular mechanisms involved in gastrin-mediated regulation of cAMP-responsive promoter elements. *Am J Physiol Endocrinol Metab,* 281**,** E1316-25.

THU, K. L., RADULOVICH, N., BECKER-SANTOS, D. D., PIKOR, L. A., PUSIC, A., LOCKWOOD, W. W., LAM, W. L. & TSAO, M. S. 2014. SOX15 is a candidate tumor suppressor in pancreatic cancer with a potential role in Wnt/beta-catenin signaling. *Oncogene,* 33**,** 279-88.

TIAN, G., SAGETORP, J., XU, Y., SHUAI, H., DEGERMAN, E. & TENGHOLM, A. 2012. Role of phosphodiesterases in the shaping of sub-plasma-membrane cAMP oscillations and pulsatile insulin secretion. *J Cell Sci,* 125**,** 5084-95.

TIAN, G., SANDLER, S., GYLFE, E. & TENGHOLM, A. 2011a. Glucose- and hormone-induced cAMP oscillations in alpha- and beta-cells within intact pancreatic islets. *Diabetes,* 60**,** 1535-43.

TIAN, X., VROOM, C., GHOFRANI, H. A., WEISSMANN, N., BIENIEK, E., GRIMMINGER, F., SEEGER, W., SCHERMULY, R. T. & PULLAMSETTI, S. S. 2011b. Phosphodiesterase 10A upregulation contributes to pulmonary vascular remodeling. *PLoS One,* 6**,** e18136.

TIWARI, S., DONG, H., KIM, E. J., WEINTRAUB, L., EPSTEIN, P. M. & LERNER, A. 2005. Type 4 cAMP phosphodiesterase (PDE4) inhibitors augment glucocorticoid-mediated apoptosis in B cell chronic lymphocytic leukemia (B-CLL) in the absence of exogenous adenylyl cyclase stimulation. *Biochem Pharmacol,* 69**,** 473-83.

TSAI, F. C. & MEYER, T. 2012. Ca2+ pulses control local cycles of lamellipodia retraction and adhesion along the front of migrating cells. *Curr Biol,* 22**,** 837-42.

TSAI, F. C., SEKI, A., YANG, H. W., HAYER, A., CARRASCO, S., MALMERSJO, S. & MEYER, T. 2014a. A polarized Ca2+, diacylglycerol and STIM1 signalling system regulates directed cell migration. *Nat Cell Biol,* 16**,** 133-44.

TSAI, L. C. & BEAVO, J. A. 2012. Regulation of adrenal steroidogenesis by the high-affinity phosphodiesterase 8 family. *Horm Metab Res,* 44**,** 790-4.

TSAI, M. K., HSIEH, C. C., KUO, H. F., LEE, M. S., HUANG, M. Y., KUO, C. H. & HUNG, C. H. 2014b. Effect of prostaglandin I analogs on monocyte chemoattractant protein-1 in human monocyte and macrophage. *Clin Exp Med*.

TSUNODA, T., ISHIKURA, S., DOI, K., MATSUZAKI, H., IWAIHARA, Y. & SHIRASAWA, S. 2014. Resveratrol induces luminal apoptosis of human colorectal cancer HCT116 cells in three-dimensional culture. *Anticancer Res,* 34**,** 4551-5.

TSUNODA, T., OTA, T., FUJIMOTO, T., DOI, K., TANAKA, Y., YOSHIDA, Y., OGAWA, M., MATSUZAKI, H., HAMABASHIRI, M., TYSON, D. R., KUROKI, M., MIYAMOTO, S. & SHIRASAWA, S. 2012. Inhibition of phosphodiesterase-4 (PDE4) activity triggers luminal apoptosis and AKT dephosphorylation in a 3-D colonic-crypt model. *Mol Cancer,* 11**,** 46.

TUCKER, O. N., DANNENBERG, A. J., YANG, E. K., ZHANG, F., TENG, L., DALY, J. M., SOSLOW, R. A., MASFERRER, J. L., WOERNER, B. M., KOKI, A. T. & FAHEY, T. J., 3RD 1999. Cyclooxygenase-2 expression is up-regulated in human pancreatic cancer. *Cancer Res,* 59**,** 987-90.

UBERSAX, J. A. & FERRELL, J. E., JR. 2007. Mechanisms of specificity in protein phosphorylation. *Nat Rev Mol Cell Biol,* 8**,** 530-41.
UENO, H., SHIBASAKI, T., IWANAGA, T., TAKAHASHI, K., YOKOYAMA, Y., LIU, L. M., YOKOI, N., OZAKI, N., MATSUKURA, S., YANO, H. & SEINO, S. 2001. Characterization of the gene EPAC2: structure, chromosomal localization, tissue expression, and identification of the liver-specific isoform. *Genomics,* 78**,** 91-8.
UMEMURA, M., BALJINNYAM, E., FESKE, S., DE LORENZO, M. S., XIE, L. H., FENG, X., ODA, K., MAKINO, A., FUJITA, T., YOKOYAMA, U., IWATSUBO, M., CHEN, S., GOYDOS, J. S., ISHIKAWA, Y. & IWATSUBO, K. 2014. Store-operated Ca2+ entry (SOCE) regulates melanoma proliferation and cell migration. *PLoS One,* 9**,** e89292.
VAN DEN BRINK, G. R., BLOEMERS, S. M., VAN DEN BLINK, B., TERTOOLEN, L. G., VAN DEVENTER, S. J. & PEPPELENBOSCH, M. P. 1999. Study of calcium signaling in non-excitable cells. *Microsc Res Tech,* 46**,** 418-33.
VAN PETEGEM, F. 2012. Ryanodine receptors: structure and function. *J Biol Chem,* 287**,** 31624-32.
VANE, J. R. & BOTTING, R. M. 1995. Pharmacodynamic profile of prostacyclin. *Am J Cardiol,* 75**,** 3A-10A.
VARNAI, P., TOTH, B., TOTH, D. J., HUNYADY, L. & BALLA, T. 2007. Visualization and manipulation of plasma membrane-endoplasmic reticulum contact sites indicates the presence of additional molecular components within the STIM1-Orai1 Complex. *J Biol Chem,* 282**,** 29678-90.
VATNER, S. F., PARK, M., YAN, L., LEE, G. J., LAI, L., IWATSUBO, K., ISHIKAWA, Y., PESSIN, J. & VATNER, D. E. 2013. Adenylyl cyclase type 5 in cardiac disease, metabolism, and aging. *Am J Physiol Heart Circ Physiol,* 305**,** H1-8.
VATNER, S. F., YAN, L., ISHIKAWA, Y., VATNER, D. E. & SADOSHIMA, J. 2009. Adenylyl cyclase type 5 disruption prolongs longevity and protects the heart against stress. *Circ J,* 73**,** 195-200.
VAZQUEZ, G., WEDEL, B. J., AZIZ, O., TREBAK, M. & PUTNEY, J. W., JR. 2004. The mammalian TRPC cation channels. *Biochim Biophys Acta,* 1742**,** 21-36.
VENKATACHALAM, K. & MONTELL, C. 2007. TRP channels. *Annu Rev Biochem,* 76**,** 387-417.
VIGIL, D., BLUMENTHAL, D. K., HELLER, W. T., BROWN, S., CANAVES, J. M., TAYLOR, S. S. & TREWHELLA, J. 2004. Conformational differences among solution structures of the type Ialpha, IIalpha and IIbeta protein kinase A regulatory subunit homodimers: role of the linker regions. *J Mol Biol,* 337**,** 1183-94.
VONA-DAVIS, L. & MCFADDEN, D. W. 2007. PYY and the pancreas: inhibition of tumor growth and inflammation. *Peptides,* 28**,** 334-8.
VORONINA, S., OKEKE, E., PARKER, T. & TEPIKIN, A. 2014. How to win ATP and influence Ca(2+) signaling. *Cell Calcium,* 55**,** 131-8.
WAGNER, B., JAKOBS, S., HABERMEYER, M., HIPPE, F., CHO-CHUNG, Y. S., EISENBRAND, G. & MARKO, D. 2002. 7-Benzylamino-6-chloro-2-piperazino-4-pyrrolidino-pteridine, a potent inhibitor of cAMP-specific phosphodiesterase, enhancing nuclear protein binding to the CRE consensus sequence in human tumour cells. *Biochem Pharmacol,* 63**,** 659-68.
WAHL-SCHOTT, C. & BIEL, M. 2009. HCN channels: structure, cellular regulation and physiological function. *Cell Mol Life Sci,* 66**,** 470-94.
WANG, J. G., LI, N. N., LI, H. N., CUI, L. & WANG, P. 2011. Pancreatic cancer bears overexpression of neurotensin and neurotensin receptor subtype-1 and SR 48692 counteracts neurotensin induced cell proliferation in human pancreatic ductal carcinoma cell line PANC-1. *Neuropeptides,* 45**,** 151-6.
WANG, W., KANG, W., TANG, Q., YAO, G., CHEN, Y., CHENG, B. & KONG, K. 2014. Cilostazol prevents the degradation of collagen type II in human chondrocytes. *Biochem Biophys Res Commun,* 451**,** 352-5.
WANG, Z., LI, V., CHAN, G. C., PHAN, T., NUDELMAN, A. S., XIA, Z. & STORM, D. R. 2009. Adult type 3 adenylyl cyclase-deficient mice are obese. *PLoS One,* 4**,** e6979.

WARRINGTON, N. M., GIANINO, S. M., JACKSON, E., GOLDHOFF, P., GARBOW, J. R., PIWNICA-WORMS, D., GUTMANN, D. H. & RUBIN, J. B. 2010. Cyclic AMP suppression is sufficient to induce gliomagenesis in a mouse model of neurofibromatosis-1. *Cancer Res,* 70**,** 5717-27.

WATANABE, Y., MURATA, T., SHIMIZU, K., MORITA, H., INUI, M. & TAGAWA, T. 2012. Phosphodiesterase 4 regulates the migration of B16-F10 melanoma cells. *Exp Ther Med,* 4**,** 205-210.

WAYMAN, C., PHILLIPS, S., LUNNY, C., WEBB, T., FAWCETT, L., BAXENDALE, R. & BURGESS, G. 2005. Phosphodiesterase 11 (PDE11) regulation of spermatozoa physiology. *Int J Impot Res,* 17**,** 216-23.

WEAVER, A. M. 2006. Invadopodia: specialized cell structures for cancer invasion. *Clin Exp Metastasis,* 23**,** 97-105.

WEI, B., ZHANG, Y. P., YAN, H. Z., XU, Y. & DU, T. M. 2014. Cilostazol promotes production of melanin by activating the microphthalmia-associated transcription factor (MITF). *Biochem Biophys Res Commun,* 443**,** 617-21.

WESS, J. 1998. Molecular basis of receptor/G-protein-coupling selectivity. *Pharmacol Ther,* 80**,** 231-64.

WHITE, J. B., THOMPSON, W. J. & PITTLER, S. J. 2004. Characterization of 3',5' cyclic nucleotide phosphodiesterase activity in Y79 retinoblastoma cells: absence of functional PDE6. *Mol Vis,* 10**,** 738-49.

WHITTLE, B. J., SILVERSTEIN, A. M., MOTTOLA, D. M. & CLAPP, L. H. 2012. Binding and activity of the prostacyclin receptor (IP) agonists, treprostinil and iloprost, at human prostanoid receptors: treprostinil is a potent DP1 and EP2 agonist. *Biochem Pharmacol,* 84**,** 68-75.

WILLIAMS, G. S., BOYMAN, L., CHIKANDO, A. C., KHAIRALLAH, R. J. & LEDERER, W. J. 2013. Mitochondrial calcium uptake. *Proc Natl Acad Sci U S A,* 110**,** 10479-86.

WILLOUGHBY, D. & COOPER, D. M. 2007. Organization and Ca2+ regulation of adenylyl cyclases in cAMP microdomains. *Physiol Rev,* 87**,** 965-1010.

WILLOUGHBY, D., EVERETT, K. L., HALLS, M. L., PACHECO, J., SKROBLIN, P., VACA, L., KLUSSMANN, E. & COOPER, D. M. 2012a. Direct binding between Orai1 and AC8 mediates dynamic interplay between Ca2+ and cAMP signaling. *Sci Signal,* 5**,** ra29.

WILLOUGHBY, D., HALLS, M. L., EVERETT, K. L., CIRUELA, A., SKROBLIN, P., KLUSSMANN, E. & COOPER, D. M. 2012b. A key phosphorylation site in AC8 mediates regulation of Ca(2+)-dependent cAMP dynamics by an AC8-AKAP79-PKA signalling complex. *J Cell Sci,* 125**,** 5850-9.

WILLOUGHBY, D., MASADA, N., WACHTEN, S., PAGANO, M., HALLS, M. L., EVERETT, K. L., CIRUELA, A. & COOPER, D. M. 2010a. AKAP79/150 interacts with AC8 and regulates Ca2+-dependent cAMP synthesis in pancreatic and neuronal systems. *J Biol Chem,* 285**,** 20328-42.

WILLOUGHBY, D., WACHTEN, S., MASADA, N. & COOPER, D. M. 2010b. Direct demonstration of discrete Ca2+ microdomains associated with different isoforms of adenylyl cyclase. *J Cell Sci,* 123**,** 107-17.

WILSON, L. S., BAILLIE, G. S., PRITCHARD, L. M., UMANA, B., TERRIN, A., ZACCOLO, M., HOUSLAY, M. D. & MAURICE, D. H. 2011. A phosphodiesterase 3B-based signaling complex integrates exchange protein activated by cAMP 1 and phosphatidylinositol 3-kinase signals in human arterial endothelial cells. *J Biol Chem,* 286**,** 16285-96.

WORLEY, P. F., ZENG, W., HUANG, G. N., YUAN, J. P., KIM, J. Y., LEE, M. G. & MUALLEM, S. 2007. TRPC channels as STIM1-regulated store-operated channels. *Cell Calcium,* 42**,** 205-11.

WU, Z. L., THOMAS, S. A., VILLACRES, E. C., XIA, Z., SIMMONS, M. L., CHAVKIN, C., PALMITER, R. D. & STORM, D. R. 1995. Altered behavior and long-term potentiation in type I adenylyl cyclase mutant mice. *Proc Natl Acad Sci U S A,* 92**,** 220-4.

XIE, Z., ADAMOWICZ, W. O., ELDRED, W. D., JAKOWSKI, A. B., KLEIMAN, R. J., MORTON, D. G., STEPHENSON, D. T., STRICK, C. A., WILLIAMS, R. D. & MENNITI, F. S. 2006. Cellular and

subcellular localization of PDE10A, a striatum-enriched phosphodiesterase. *Neuroscience,* 139**,** 597-607.
XUE, B. & ROBINSON, R. C. 2013. Guardians of the actin monomer. *Eur J Cell Biol,* 92**,** 316-32.
YAN, L., VATNER, D. E., O'CONNOR, J. P., IVESSA, A., GE, H., CHEN, W., HIROTANI, S., ISHIKAWA, Y., SADOSHIMA, J. & VATNER, S. F. 2007. Type 5 adenylyl cyclase disruption increases longevity and protects against stress. *Cell,* 130**,** 247-58.
YANG, H., LEE, C. J., ZHANG, L., SANS, M. D. & SIMEONE, D. M. 2008. Regulation of transforming growth factor beta-induced responses by protein kinase A in pancreatic acinar cells. *Am J Physiol Gastrointest Liver Physiol,* 295**,** G170-G178.
YANG, S., ZHANG, J. J. & HUANG, X. Y. 2009. Orai1 and STIM1 are critical for breast tumor cell migration and metastasis. *Cancer Cell,* 15**,** 124-34.
YANG, X., JIN, H., CAI, X., LI, S. & SHEN, Y. 2012. Structural and mechanistic insights into the activation of Stromal interaction molecule 1 (STIM1). *Proc Natl Acad Sci U S A,* 109**,** 5657-62.
YANIV, Y., JUHASZOVA, M., LYASHKOV, A. E., SPURGEON, H. A., SOLLOTT, S. J. & LAKATTA, E. G. 2011. Ca2+-regulated-cAMP/PKA signaling in cardiac pacemaker cells links ATP supply to demand. *J Mol Cell Cardiol,* 51**,** 740-8.
YAO, H., ZENG, Z. Z., FAY, K. S., VEINE, D. M., STASZEWSKI, E. D., MORGAN, M., WILDER-ROMANS, K., WILLIAMS, T. M., SPALDING, A. C., BEN-JOSEF, E. & LIVANT, D. L. 2011. Role of alpha(5)beta(1) Integrin Up-regulation in Radiation-Induced Invasion by Human Pancreatic Cancer Cells. *Transl Oncol,* 4**,** 282-92.
YAROTSKYY, V. & DIRKSEN, R. T. 2012. Temperature and RyR1 regulate the activation rate of store-operated Ca(2)+ entry current in myotubes. *Biophys J,* 103**,** 202-11.
YARROW, J. C., PERLMAN, Z. E., WESTWOOD, N. J. & MITCHISON, T. J. 2004. A high-throughput cell migration assay using scratch wound healing, a comparison of image-based readout methods. *BMC Biotechnol,* 4**,** 21.
YEO, C. D., KIM, J. W., HA, J. H., KIM, S. J., LEE, S. H., KIM, I. K. & KIM, Y. K. 2014. Chemopreventive effect of phosphodieasterase-4 inhibition in benzo(a)pyrene-induced murine lung cancer model. *Exp Lung Res*.
YOUNG, S. H. & ROZENGURT, E. 2010. Crosstalk between insulin receptor and G protein-coupled receptor signaling systems leads to Ca(2)+ oscillations in pancreatic cancer PANC-1 cells. *Biochem Biophys Res Commun,* 401**,** 154-8.
YUAN, J. P., ZENG, W., DORWART, M. R., CHOI, Y. J., WORLEY, P. F. & MUALLEM, S. 2009. SOAR and the polybasic STIM1 domains gate and regulate Orai channels. *Nat Cell Biol,* 11**,** 337-43.
YUASA, K., KOTERA, J., FUJISHIGE, K., MICHIBATA, H., SASAKI, T. & OMORI, K. 2000. Isolation and characterization of two novel phosphodiesterase PDE11A variants showing unique structure and tissue-specific expression. *J Biol Chem,* 275**,** 31469-79.
ZENG, W., YUAN, J. P., KIM, M. S., CHOI, Y. J., HUANG, G. N., WORLEY, P. F. & MUALLEM, S. 2008. STIM1 gates TRPC channels, but not Orai1, by electrostatic interaction. *Mol Cell,* 32**,** 439-48.
ZHANG, D., MA, Q. Y., HU, H. T. & ZHANG, M. 2010. beta2-adrenergic antagonists suppress pancreatic cancer cell invasion by inhibiting CREB, NFkappaB and AP-1. *Cancer Biol Ther,* 10**,** 19-29.
ZHANG, G., LIU, Y., RUOHO, A. E. & HURLEY, J. H. 1997. Structure of the adenylyl cyclase catalytic core. *Nature,* 386**,** 247-53.
ZHANG, L., MURRAY, F., ZAHNO, A., KANTER, J. R., CHOU, D., SUDA, R., FENLON, M., RASSENTI, L., COTTAM, H., KIPPS, T. J. & INSEL, P. A. 2008a. Cyclic nucleotide phosphodiesterase profiling reveals increased expression of phosphodiesterase 7B in chronic lymphocytic leukemia. *Proc Natl Acad Sci U S A,* 105**,** 19532-7.
ZHANG, M., MOON, C., CHAN, G. C., YANG, L., ZHENG, F., CONTI, A. C., MUGLIA, L., MUGLIA, L. J., STORM, D. R. & WANG, H. 2008b. Ca-stimulated type 8 adenylyl cyclase is required for rapid acquisition of novel spatial information and for working/episodic-like memory. *J Neurosci,* 28**,** 4736-44.

ZHANG, X., CUI, X., CHENG, L., GUAN, X., LI, H., LI, X. & CHENG, M. 2012. Actin stabilization by jasplakinolide affects the function of bone marrow-derived late endothelial progenitor cells. *PLoS One,* 7**,** e50899.

ZHANG, Y., YANG, J., CUI, X., CHEN, Y., ZHU, V. F., HAGAN, J. P., WANG, H., YU, X., HODGES, S. E., FANG, J., CHIAO, P. J., LOGSDON, C. D., FISHER, W. E., BRUNICARDI, F. C., CHEN, C., YAO, Q., FERNANDEZ-ZAPICO, M. E. & LI, M. 2013. A novel epigenetic CREB-miR-373 axis mediates ZIP4-induced pancreatic cancer growth. *EMBO Mol Med,* 5**,** 1322-34.

ZHOU, F. W. & ROPER, S. N. 2014. TRPC3 mediates hyperexcitability and epileptiform activity in immature cortex and experimental cortical dysplasia. *J Neurophysiol,* 111**,** 1227-37.

ZHOU, Y., MANCARELLA, S., WANG, Y., YUE, C., RITCHIE, M., GILL, D. L. & SOBOLOFF, J. 2009. The short N-terminal domains of STIM1 and STIM2 control the activation kinetics of Orai1 channels. *J Biol Chem,* 284**,** 19164-8.

ZIDOVETZKI, R. & LEVITAN, I. 2007. Use of cyclodextrins to manipulate plasma membrane cholesterol content: evidence, misconceptions and control strategies. *Biochim Biophys Acta,* 1768**,** 1311-24.

ZIMMERMAN, N. P., ROY, I., HAUSER, A. D., WILSON, J. M., WILLIAMS, C. L. & DWINELL, M. B. 2013. Cyclic AMP regulates the migration and invasion potential of human pancreatic cancer cells. *Mol Carcinog*.

ZORAGHI, R., BESSAY, E. P., CORBIN, J. D. & FRANCIS, S. H. 2005. Structural and functional features in human PDE5A1 regulatory domain that provide for allosteric cGMP binding, dimerization, and regulation. *J Biol Chem,* 280**,** 12051-63.

ZWEIFACH, A. & LEWIS, R. S. 1995. Rapid inactivation of depletion-activated calcium current (ICRAC) due to local calcium feedback. *J Gen Physiol,* 105**,** 209-26.